

Joe Machinis

CB 0351

903R83003

CHESAPEAKE BAY BASIN MODEL

A Final Report

prepared for

U.S. Environmental Protection Agency
Chesapeake Bay Program
2083 West Street - Suite 5G
Annapolis, Maryland 21401

Prepared by

Northern Virginia Planning District Commission
7630 Little River Turnpike
Annandale, Virginia 22003

January 1983

CHESAPEAKE BAY BASIN MODEL

A Final Report

prepared for

U.S. Environmental Protection Agency
Chesapeake Bay Program
2083 West Street - Suite 5G
Annapolis, Maryland 21401

Prepared by

Northern Virginia Planning District Commission
7630 Little River Turnpike
Annandale, Virginia 22003

January 1983

TABLE OF CONTENTS

CHAPTER		Page
I.	INTRODUCTION	1
	Background	1
	Scope of Report	4
II.	MODELING FRAMEWORK	5
	Introduction	5
	Description of Framework	5
	Description of Model Software	9
III.	BASIN MODEL NETWORK.	11
	Introduction	11
	Sub-basin Network.	11
	Meteorologic Dataset	21
	Idealized Channel Network.	23
	Discharge and Diversion Datasets	27
IV.	PROCESSES REPRESENTED BY BASIN MODEL	29
	Hydrologic Submodel.	29
	Nonpoint Pollution Loading Submodel.	29
	Receiving Water Submodel	32
V.	CALIBRATION/VERIFICATION RESULTS	39
	Introduction	39
	Hydrology Submodel Calibration/Verification.	39
	Methodology	39
	Results	44
	Calibration/Verification of Nonpoint Pollution	
	Loading Submodel.	56
	Introduction.	56
	Data Reduction/Management Requirements for	
	Model Calibration.	59
	EPA/CBP Test Watershed Model Calibration:	
	Site Selection	62
	EPA/CBP Test Watershed Model Calibration:	
	Hydrology Results.	64
	EPA/CBP Test Watershed Model Calibration:	
	Nonpoint Pollution Results	64
	Urban Test Watershed Model Calibration:	
	Northern Virginia and Metropolitan Washington	
	NURP Studies	80
	Verification of Calibrated Nonpoint Pollution	
	Loading Factors.	81

	<u>Page</u>
CHAPTER	
Determination of Representative NPS Loading	
Factors.	89
Dry Weather Flow Concentrations	93
Scale-Up to River Basin Models.	95
Precipitation Loadings on Bay Surface Area.	98
Recommendations for Future Test Watershed Studies	98
Receiving Water Submodel Calibration/Verification.	100
Methodology	100
Fall Line Loading Results	103
Results Based upon Upstream and Fall Line Gages	163
VI. FRAMEWORK FOR MANAGEMENT STUDIES	188
Introduction	188
Periods Selected for Management Studies.	188
Analyses of Long-Term Point/Nonpoint Source	
Impacts.	188
Analyses of "Worst Case" Point Source Impacts	190
Analyses of "Worst Case" Nonpoint Source Impacts.	190
Futher Evaluations of Selected Periods.	196
Intrepretation of Model Output	196
Framework for Model Production Runs.	197
REFERENCES	200
APPENDIX A	A-1
APPENDIX B	B-1

ACKNOWLEDGMENTS

The work described herein was funded through a Cooperative Agreement (No. CR807816-01) with the U.S. Environmental Protection Agency's Chesapeake Bay Program. We gratefully acknowledge the assistance of EPA staff who participated in the project under the direction of Mr. Thomas B. DeMoss, Deputy Director. The project is currently being directed by Ms. Virginia Tippie. Other EPA staff members with whom we worked were Ms. Bess Gillelan, Mr. Joe Macknis, and Mr. Jim Smullen.

The work of the Northern Virginia Planning District Commission was performed under the overall direction of Regional Resources Division Director, John P. Hartigan, P.E. Mr. Hartigan is the primary author of this report. Day to day project management was under the direction of Dr. Elizabeth Southerland. Senior level personnel involved in the modeling activities were Mr. Hugo Bonuccelli, Mr. Alan Cavacas, Mr. John Friedman, Mr. Thomas Quasebarth, Ms. Karen Roffe, Mr. Todd Scott, and Mr. James White. Senior level personnel were assisted by engineer interns Ms. Cynthia Birch, Mr. James Eakin, Ms. Susan Lees, Ms. Mary Jo Rimkus, and Mr. Mark Taylor. Their help during data reduction and model calibration tasks was invaluable. Special thanks go to Ms. Carol Erbe who typed this manuscript and Mrs. Betty Fox who prepared some of the tables. Mr. Steve Kostyal is responsible for the graphics and artwork.

CHESAPEAKE BAY MODEL

INTRODUCTION

Background

The Chesapeake Bay, located in eastern Maryland and Virginia, is one of the largest and most economically important of the 850 estuaries in the United States. In order to determine the sources of eutrophication problems in the upper Bay and major tidal tributaries and to formulate appropriate control strategies, the U.S. EPA Chesapeake Bay Program funded development of the following three computer models to represent the fluvial and estuarine sections of the Bay system:

- A. Basin Model: For the major river basins (e.g., Susquehanna, Potomac, and James) tributary to the Bay, this model simulates streamflow and the transport of point source and nonpoint pollution loadings in the free-flowing streams upstream of the fall lines. For coastal watersheds (e.g., Chester, Choptank, and York river basins) which are drained by major estuaries and the Bay, this model simulates the freshwater streamflows and pollutant loadings delivered to tidal waters.
- B. Major Tidal Tributary Model: This model serves as the interface between the Basin Model and the Bay Model by simulating pollutant transport through the Potomac, James, Rappahannock, York, Patuxent, and Chester estuaries. This model is applied to the portion of the estuary extending from head of tide downstream to the last bridge crossing upstream from the Bay, an area where assumptions of one-dimensional transport are applied. The use of this interface model keeps computer costs from becoming prohibitive and increases the utility of the Bay model package by allowing the more complex Main Bay Model (i.e., two-dimensional model) to be restricted to the lower reaches of the major estuaries and the Main Bay, where more detailed hydrodynamic simulations are required.
- C. Main Bay Model: This two-dimensional, depth-averaged model simulates Baywide water quality impacts of pollutant loadings delivered to the Bay by the Basin Model and the Major Tributary Estuary Model.

A flow chart which outlines the relationships among the three models of the Chesapeake Bay system is shown in Figure 1.

The computer model of the Chesapeake Bay system is designed to simulate a history of water quality conditions for specified streamflows and pollutant loadings. The major purpose of a water quality computer model is to enable the user to look beyond the measured data and establish cause-effect relationships that explain water quality levels at various

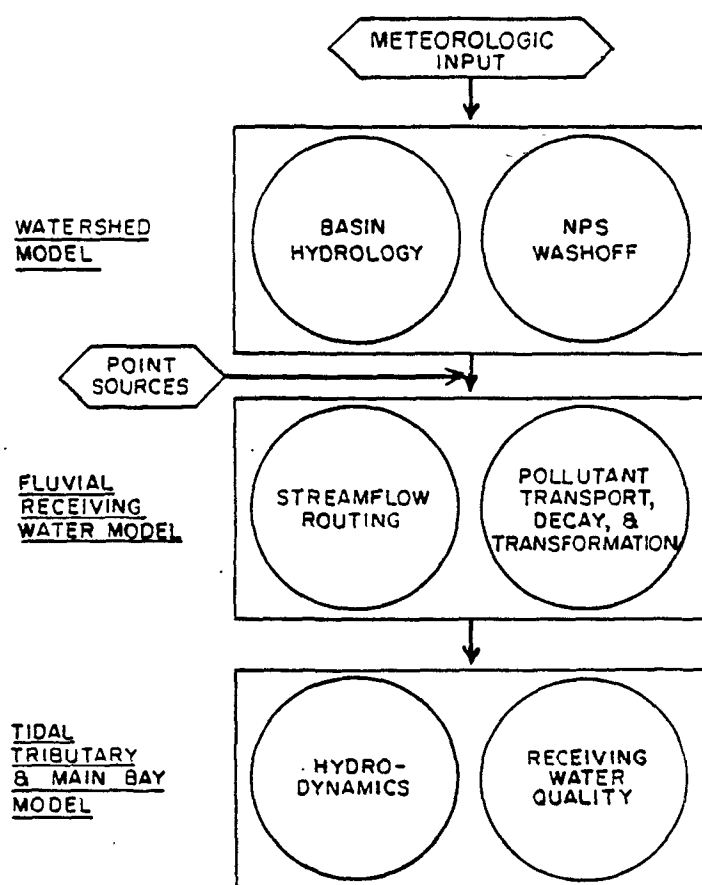


Figure 1. Flow Chart Showing Models Included in Chesapeake Bay Model Package

locations in the system. In a complex system such as the Chesapeake Bay and its major tributaries, it is difficult to develop causal relationships from statistical analyses of water quality monitoring data. This difficulty can be attributed to the limited duration of synoptic records available for the majority of the system, particularly for high flow periods characterized by significant nonpoint pollution loadings. However, even if relatively long water quality records were available, the establishment of cause-effect relationships from analyses of water quality monitoring data would be very difficult. Development of causal relationships would be limited by the inability of the monitoring agency to maintain a constant land use pattern and wastewater treatment plant loadings during a monitoring period which would have to be long enough to cover a wide range of hydrologic conditions. By subjecting the current land use pattern and wastewater treatment plant loadings to a full range of potential hydrologic conditions (e.g., severe drought; wetter than average summer season), a computer model of the Chesapeake Bay system can be used to extend short-term water quality records and to examine the most important processes responsible for water quality levels in various sections of the Bay. Since all the major processes responsible for pollutant discharges and transport are represented by the computer model of the Bay system, it can be used to quantify the sources of pollutant concentrations measured at a water quality monitoring station. For example, a computer model of the major river basins tributary to the Chesapeake Bay can be used to determine the point and nonpoint source contributions to pollutant loadings monitored at the fall lines. Likewise, a computer model of the Chesapeake Bay proper can be used to compare the water quality impacts of river basin pollution loadings and pollutant contributions from other sources such as Bay bottom sediments and the ocean. More important, a computer model of the Bay system can be used to evaluate the water quality impacts of alternate land use patterns and wastewater treatment plant discharges under the same long-term hydrologic conditions.

All three computer models representing the Bay system can be operated for several months at a time to determine the frequency (i.e., number of days) of adverse water quality in the Bay as well as minimum and maximum concentrations during different hydrologic conditions. By operating the three models in series to simulate the entire Bay system, management agencies can for the first time evaluate the Baywide impacts of regional water quality management strategies in terms of the frequency of violations of water quality criteria/standards for different beneficial uses (e.g., fisheries habitat, recreation). For example, the models can be operated with existing and revised regional wastewater treatment standards to evaluate the impacts of regional water quality management programs on the Chesapeake Bay. Locational differences in seasonal pollutant delivery by point and nonpoint sources can be examined with the models to identify sections of the tributary river basins (e.g., Coastal Plain watersheds vs. Piedmont watersheds) where pollution controls promise the greatest benefit in terms of Chesapeake Bay water quality. Since it represents the hydrologic cycle in the tributary area of approximately 64,000 sq mi, the package of computer models can also be used to quantify Baywide water

quality impacts of water resources management strategies such as increased water supply diversions or major flood control impoundments which can have a significant effect on seasonal freshwater inflow to Chesapeake Bay. In short, the Bay model package described herein is a state-of-the-art planning tool which will allow state and regional management agencies to relate upstream water resources management decisions to Chesapeake Bay water quality.

At the outset, it should be emphasized that a computer model is only a tool to assist with the difficult task of comparing and evaluating various alternatives for water quality management. The computer model can neither answer all questions nor solve all problems related to water quality management planning. It provides input to the decision-making process, but it should not be confused with the process by which the management decisions are made. The value of the computer model is its capability to quickly and efficiently analyze the systemwide impacts of management alternatives and provide insights which are not available from measured data alone.

Scope of Report

This report covers the calibration/verification and selected applications of the Basin Model. Chapter II of this report covers the modeling framework, including a summary of the temporal and spatial dimensions of the modeling problem and a discussion of the selected computer software. In order to provide management agencies with an indication of how major sections of river basins were approximated with the Basin Model, Chapter III describes the sub-basin and channel network. Chapter IV provides a description of hydrologic, hydraulic, and water quality processes represented by the Basin Model. Chapter V summarizes calibration/verification results. Chapter VI outlines the types of management studies conducted with the Basin model.

CHAPTER II

MODELING FRAMEWORK

Introduction

A modeling framework includes the identification of the water quality problem to be addressed by the modeling study, the theoretical structure of the computer model software, and guidelines for delineating the network of elements (e.g., sub-basins, reaches) used to describe the prototype water resources system. Development of the modeling framework for the Bay model package required considerations of such factors as temporal and spatial scales of the water quality problem, the availability of field data for model calibration/verification, and the available computer budget.

Of these factors, the temporal and spatial dimensions of the modeling problem figured most prominently in software selection and the configuration of networks for these models. There are two aspects to the determination of time and space scales: (a) the temporal and spatial extent of the water quality problem (For example, in the case of time scales, is the water quality problem short-term or long-term in nature? An example of a short-term problem is the hour-to-hour change in dissolved oxygen, while an example of a long-term problem is several consecutive weeks with dissolved oxygen less than 5.0 mg/l. In the case of space scales, is the water quality problem localized or regional in scope?); and (b) the temporal and spatial interval of model calculations (For example, do water quality calculations have to be made every hour in order to study the condition of the system? Are very detailed spatial grids required to represent the watershed or receiving water?)

This chapter describes the modeling framework for each computer model and presents a summary of the model software selected to fit the framework.

Description of Framework

The principal functions of the Basin Model are to use meteorologic records to calculate the streamflow and nonpoint pollution loadings in the Bay's approximately 64,000 sq mi drainage area (see Figure 2) and to simulate the transport of point source and nonpoint pollution to the Bay's estuarine system. In other words, the water quality problem to be addressed is the transport of streamflow and pollutant loadings to the Bay and its tidal tributaries, rather than localized receiving water problems (e.g., dissolved oxygen sag) within the fluvial river system.

The temporal dimensions of the River Basin modeling framework are as follows:

- a. Since localized water quality problems in the river basins are not the principal focus of the modeling study, simulations of daily or

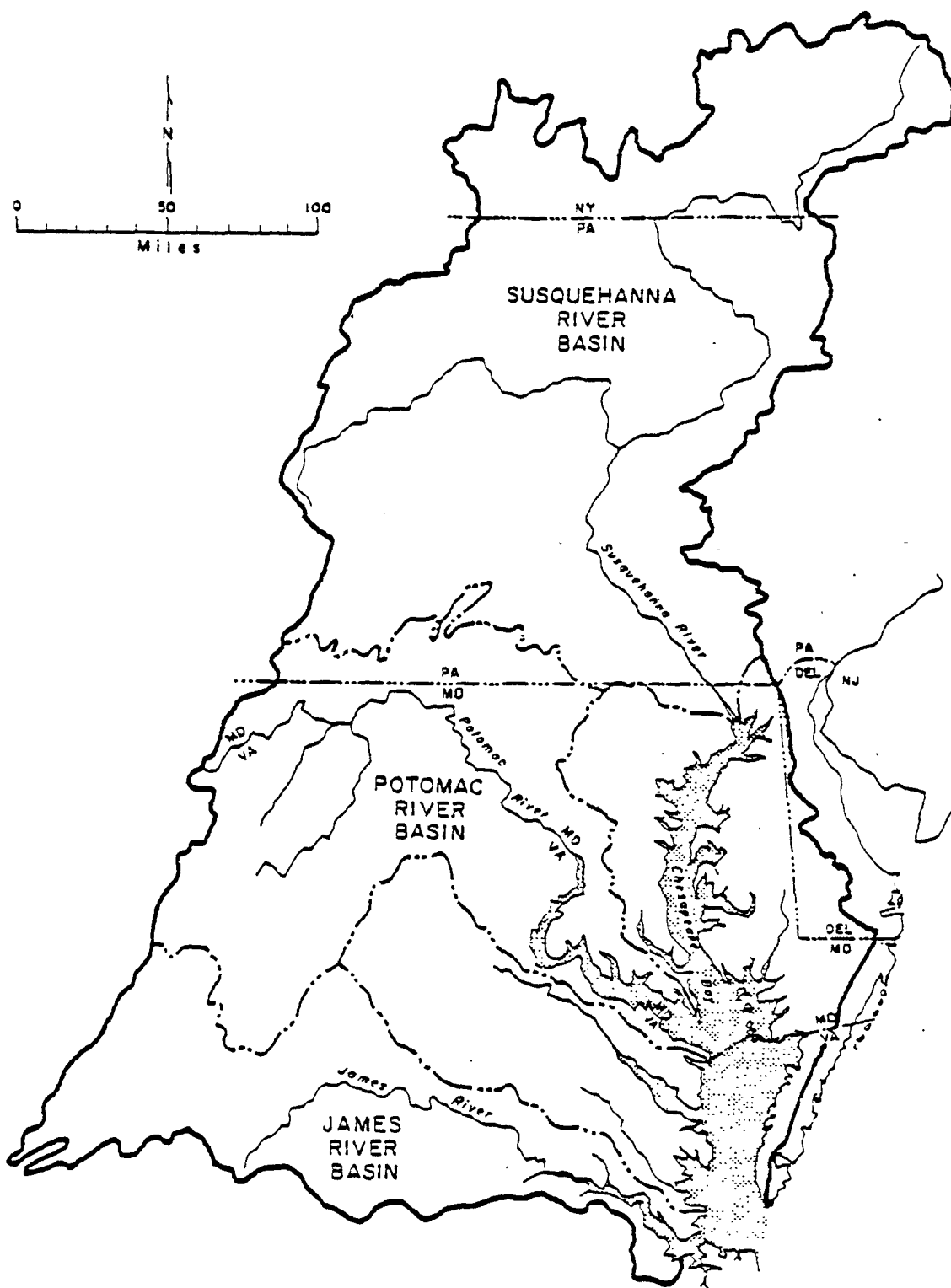


Figure 2. Map of Chesapeake Bay Basin Showing Three Major River Basins

weekly pollutant loadings delivered to the Bay's estuarine system are more important than simulations of hour-to-hour changes in water quality within the tributary rivers.

- b. Surface runoff and nonpoint pollution loadings are generated and delivered to the river system over relatively short time periods (e.g., generally several hours) during and following a rainstorm. Pollutant transport through the river basins to the Chesapeake Bay's estuarine system may require several days, during which time pollutant degradation can occur. In other words, one would not expect all point source and nonpoint pollution loadings to reach the Bay due to physical, chemical, and biological processes which are operating during channel transport. Therefore, the Basin Model must be capable of accounting for pollutant degradation enroute to the Bay, although detailed simulations of localized water quality problems due to pollutant decay and transformations are not required.
- c. The Basin Model should be capable of producing a long-term record of streamflow and pollutant loadings which reach the Bay from a long-term record of precipitation and evaporation. This will permit analyses of the frequency of water quality criteria violations in the Bay system.
- d. In order to properly simulate river basin hydrology, soil erosion, and nonpoint pollution loadings, the Basin Model should be capable of accounting for long-term changes in watershed state variables (e.g., soil moisture, seasonal variations in vegetative cover, soil disturbance due to cropland tillage, and pollutant loading factors).
- e. Since runoff and soil loss equations in most computer models require short-term rainfall intensity data in order to accurately calculate the amount of rainfall which does not infiltrate into the soil profile and soil erosion due to the kinetic energy of raindrops, precipitation records should be input to the Basin Model at intervals of one hour or less.
- f. Since localized water quality impacts in the river basins are not the principal focus of the modeling study, idealized channel reaches with relatively high travel times (e.g., 1-3 days) and lengthy computations time-steps (e.g., 12 hrs) for flow routing and water quality processes can be used to ensure that computer costs for long-term simulations do not become prohibitive. If local water quality problems were of interest, (e.g., dissolved oxygen sag in certain segments of a river), shorter channel travel times and computational time-steps would be required and the computer costs for model operation would be significantly higher.
- g. April 1st through October 31st is the critical period for studies of eutrophication management in the Bay system.

The spatial dimensions of the modeling framework are as follows:

- a. The number and size of elements (e.g., sub-basins, channels) in the model network should reflect the fact that the Basin Model is primarily intended for the calculation of nonpoint pollution loadings on the fluvial channel system and pollutant transport to the Bay's estuarine system, rather than localized water quality problems.
- b. So long as a sufficiently short rainfall intensity interval (e.g., 1-hr) is used for model input, relatively large sub-basins (e.g., 1,000-2,000 sq mi) can be used to accurately simulate nonpoint pollution loadings and point and nonpoint pollution transport to the Bay. The factors limiting sub-basin size are homogeneity of hydrologic characteristics (e.g., soils, geology) and similarities in rainfall characteristics (i.e., clusters of raingages are used to develop a single rainfall record for each sub-basin).
- c. The Basin Model's channel reaches can be relatively long (e.g., 30-50 mi depending upon slope) so long as the network provides a reasonable representation of transport from the river basin to the Bay's estuarine system and also maintains computational stability. In general, a single channel reach can be assigned to each sub-basin and still satisfy this criterion.
- d. Since localized receiving water quality problems are not addressed by the modeling study, a one-dimensional model assuming complete mixing conditions in each channel reach should suffice for most receiving waters in the major river basins. For a one-dimensional representation, channel system geometry is represented by a linear network of volume elements (i.e., reaches), each of which is assumed to be completely mixed so that there is no water quality variation laterally or with depth. Water quality variation occurs longitudinally (in the x-direction) as flows are transported out of one volume element into the next.
- e. In order to minimize computer costs for model executions, the series of major reservoirs (i.e., Lake Aldred and Lake Clarke) located near the mouth of the Susquehanna River may be aggregated and represented as a single impoundment which has similar pollutant trap efficiencies.

In summary, the major components of the Basin Model framework are as follows:

- o Capability to simulate pollutant decay and transformations during channel transport which requires a time scale on the order of several days

- o Capability to simulate long-term records of streamflow and pollutant loadings reaching the Bay in order to permit frequency analyses
- o Capability to simulate continuous changes in river basin soil moisture and seasonal changes in other important land surface features
- o Use of long-term rainfall records with intensity data at relatively short intervals
- o Use of a level of detail in sub-basin and channel reach network which reflects the focus of the Basin Model on the calculation of nonpoint pollution loading and transport to the Bay's estuarine system: relatively large sub-basins (e.g., 1,000-2,000 sq mi) and relatively long channel reaches (e.g., 30-50 mi)
- o Use of one-dimensional representation for fluvial channel system
- o Reliance on relatively high channel travel times (e.g., 1-3 days) and relatively long computational times (e.g., 0.5 day)
- o Where feasible, aggregation of reservoirs in series into a single idealized impoundment
- o The total number of sub-basin/channel reach elements should not exceed about 100, to ensure that long-term simulations are affordable

Description of Model Software

The software (1) selected for the Basin Model is a version of the U.S. Environmental Protection Agency's HSPF model (2), which is currently being disseminated by EPA as the state-of-the-art nonpoint pollution simulation model. The Model falls into the classification of "continuous simulation" watershed engineering models (3) because it calculates a continuous record of soil moisture levels, streamflow, nonpoint pollution loadings, and receiving water quality from time series input data consisting of continuous meteorologic records. Therefore, the selected Basin Model can be used to produce the long-term streamflow and water quality records required for frequency analyses. The watershed components of the selected model are capable of providing a reasonable simulation of a sub-basin on the order of 1,000 to 2,000 sq mi so long as a representative record of mean hourly rainfall is used as input. Likewise, the receiving water components of the selected model can provide an acceptable one-dimensional representation of pollutant transport and decay in relatively long channel reaches with travel times on the order of 1-3 days for high flow conditions.

The selected Basin Model consists of three submodels:

- o Hydrologic submodel: Based upon a modified version of the Stanford Watershed Model (4), this submodel is operated with hourly rainfall records and daily evaporation records. It calculates the amount of rainfall converted to runoff, a continuous record of soil moisture, and subsurface recharge of stream channels. The hydrologic submodel was calibrated/verified with daily streamflow records from U.S.G.S. streamgages on the major tributaries and main stems of river basins.
- o Nonpoint pollution loading submodel: This submodel, which is a version of the U.S. Environmental Protection Agency's NPS model (5), calculates pollutant loadings on a stream channel from rainfall intensity records (i.e., to simulate soil erosion due to raindrop detachment) and the hydrologic submodel's output records of surface runoff and subsurface flows. Nonpoint pollution loading factors were calibrated with monitoring data from the EPA/Chesapeake Bay Program (EPA/CBP) test watershed study (6) and other recent nonpoint pollution loading studies (7,8,9,10) and were verified with monitoring data from the EPA/CBP fall line monitoring study (11).
- o Receiving water submodel: This submodel (e.g., see receiving water algorithms in 2) routes streamflow and pollutant loadings through the river and lake system. The major physical, chemical, and biological processes which cause pollutant decay and transformations in the Chesapeake Bay Basin are included. Input includes the sum of runoff and subsurface flows output by the hydrologic submodel, the sum of nonpoint pollution loadings output by the nonpoint pollution loading model, and point source pollution loadings. This submodel also accounts for major water supply diversions that reduce flows in the river basin channel system. Rate coefficients (e.g., BOD decay rate) and parameters for other water quality processes were calibrated with monitoring data at U.S.G.S. monitoring stations on river basin main stems.

The selected software has been used for several modeling studies in the metropolitan Washington, D.C. region during the past five years. It has been applied most extensively to the 580 sq mi Occoquan River Basin of Northern Virginia for studies ranging from nonpoint pollution management assessments (10,12,13) to evaluations of advanced wastewater treatment (AWT) needs (14,15). The model has also been interfaced with estuary models for studies of AWT standards for embayments of the Potomac Estuary (16). Versions of the model have also been used by the Maryland-National Capital Park and Planning Commission as a basis for flood management and nonpoint pollution management plans for several watersheds in Montgomery County, Maryland (17,18) and by the Metropolitan Washington Council of Governments for nonpoint pollution modeling studies in the Maryland suburbs of Washington, D.C. (19).

CHAPTER III

BASIN MODEL NETWORK

Introduction

As shown in Figure 3, the Basin Model network for the major river basins consists of 35 sub-basins on the order of 1,000-2,000 sq mi, 28 idealized channels with lengths ranging from 21 to 184 mi, and six reservoirs. In addition, 29 Coastal Plain watersheds are included in the Basin Model network to provide detailed representations of direct inflows to the major tidal tributaries and embayments of the Main Bay. The sub-basin network for Coastal Plain watersheds is shown in Figure 4.

Each sub-basin is characterized by relatively homogeneous hydrologic characteristics, while each channel or reservoir accepts inflows from a single sub-basin. This network is more generalized than networks used for previous regional studies in the respective river basins, since pollutant transport to the Chesapeake Bay is of greater interest than localized water quality problems.

Sub-basin Network

The methodology for delineating the sub-basin network is based upon an analysis of geographic variations in the following characteristics, which are listed in the assumed order of consideration:

1. Physiographic province
2. Topography
3. Hydrologic soil group
4. Total water holding capacity of soil

1:500,000 scale map overlays were developed for each of the aforementioned datasets for purposes of hydrologic segment delineation. In the case of the physiographic province dataset, the actual boundaries of each province are shown on the overlay. A map of the physiographic provinces in the Chesapeake Bay Basin is shown in Figure 5. In the case of datasets 2, 3, and 4, the overlays display the predominant or average characteristic in a 100 sq mi grid cell network which is used to manage and aggregate basinwide physical features data (i.e., each cell has dimensions of 10 mi x 10 mi). The 100 sq mi grid size was selected as a reasonable level of detail for a 64,000 sq mi drainage area. The author's previous modeling experiences in the Northern Virginia region suggest that localized variations in physical features tend to have a relatively insignificant effect on the development of lumped parameter model datasets for sub-basins on the order of a few hundred square miles. Therefore, 100 sq mi grids should provide an adequate indication of geographic variations in predominant or average characteristics within the Chesapeake Bay basin. Confidence in the representativeness of the 100 sq mi grid cell datasets was gained through

CHESAPEAKE BAY BASIN

MODEL SUB-BASINS ABOVE FALL LINE

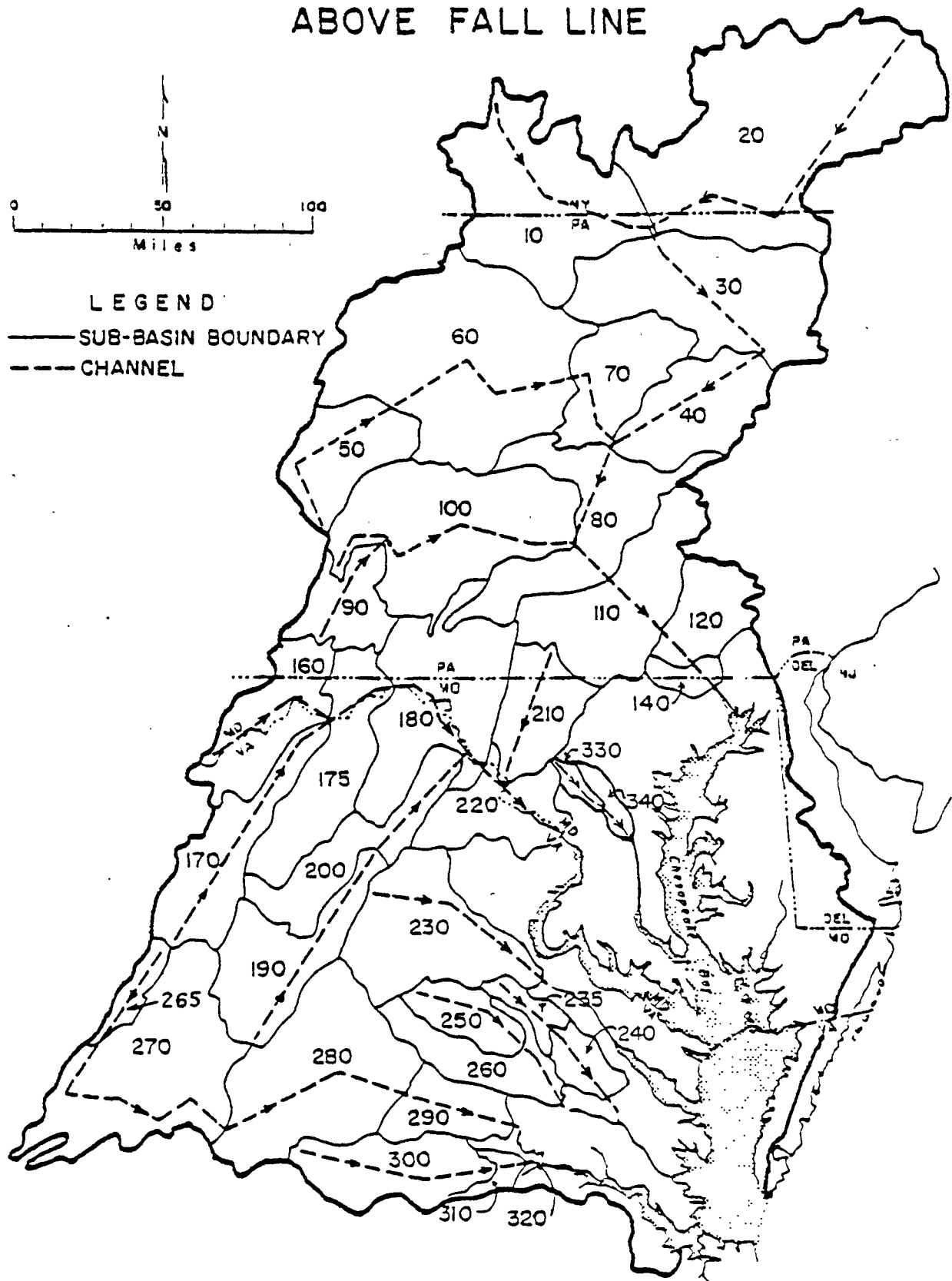


Figure 3

CHESAPEAKE BAY BASIN

MODEL SUB-BASINS BELOW FALL LINE

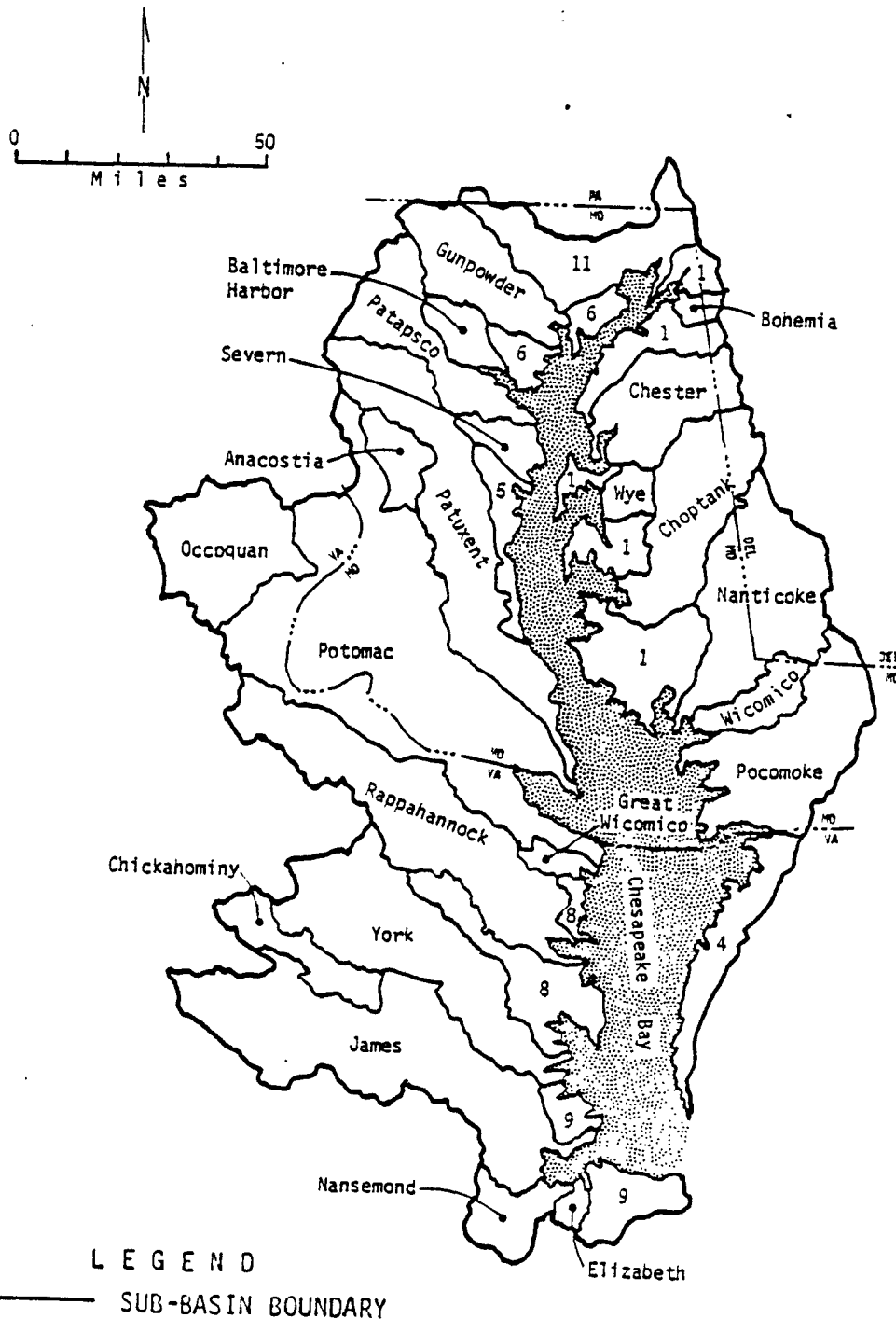


Figure 4

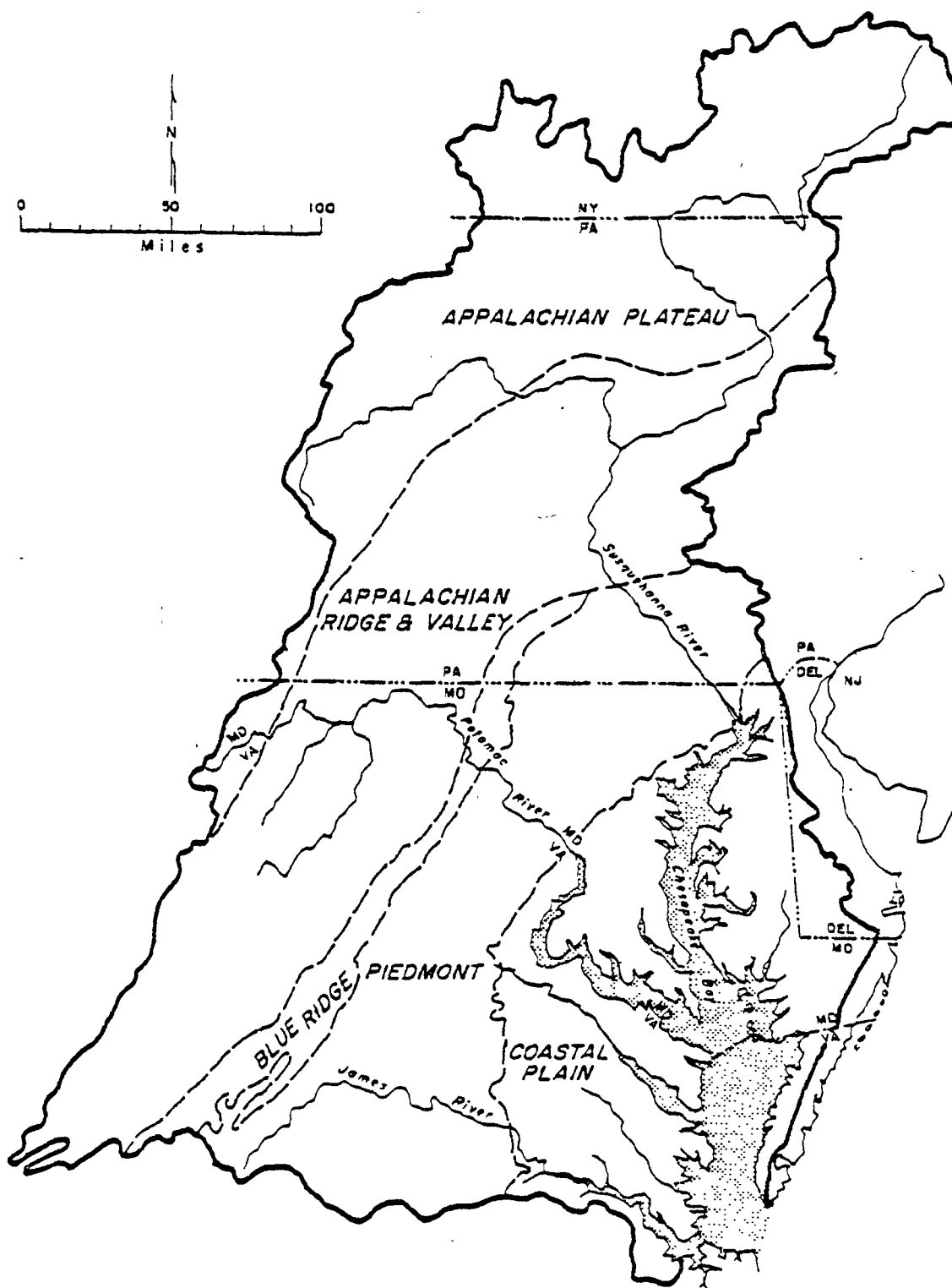


Figure 5. Physiographic Provinces in Chesapeake Bay Basin

sensitivity studies based upon County soils maps and 1:24,000 scale topographic maps for Howard and Kent Counties in Maryland and the Occoquan River Basin in Northern Virginia (20).

The results of the sensitivity studies for Howard and Kent counties were as follows: (a) average soils characteristics derived by overlaying a Statewide soil association map with a 100 sq mi grid cell network agreed very closely with average characteristics derived by planimetering a County soil association map; and (b) average slopes derived by overlaying the 100 sq mi grid cell network on a 1:250,000 scale topographic map (100-ft and 50-ft contour intervals) agreed reasonably well with average slopes derived by overlaying a 25 sq mi grid cell network on a 1:24,000 scale topographic map (20-ft contour intervals). In the case of the sensitivity studies for the 580 sq mi Occoquan River Basin, a five-year simulation of weekly runoff volumes (cu ft/week) and nonpoint pollution loads (lbs/week) based upon a 100-sq mi grid cell dataset of soils and topographic characteristics correlated very well with a five-year simulation based upon a 23-ac grid cell dataset (21) that had been previously derived for a detailed modeling study (12). The results of these sensitivity studies tend to support the selected data reduction methodologies for soils and slope datasets.

Due to the size of the Chesapeake Bay basin, the assessment of soils characteristics were based upon "soil associations." This decision was based on previous modeling experiences which indicated that localized variations in soils characteristics, as indicated by a "soil series" dataset for example, tend to have a relatively insignificant effect on the development of lumped parameter values for very large sub-basins. Soil association characterizations were carried out on a state-by-state basis. The distribution of the Chesapeake Bay basin's 135 soil associations among the five states in the drainage area is as follows: Virginia: 54; Maryland: 27; West Virginia: 12; Pennsylvania: 34; and New York: 8. Each soil association consists of one-to-four soil series which are listed in order of dominance. Composite characteristics for each association are typically developed by weighting the characteristics of the individual soil series according to the fraction of the association that is typically attributed to the series. Unfortunately, statewide data on the fraction of each association that is attributed to each series is available only for the State of Pennsylvania and the Northern Virginia region. The only source of such data in other sections of the basin are the soil surveys prepared by the individual counties in each state. Based on a review of typical soil series distributions attributed to Pennsylvania and Northern Virginia soil associations, the following relative distributions were assumed for use in analyzing soil association characteristics throughout the Chesapeake Bay basin:

<u>Soil Series Order</u>	<u>Total Number of Soil Series in Association</u>		
	<u>Two Soil Series</u>	<u>Three Soil Series</u>	<u>Four Soil Series</u>
1st Series	60%	60%	50%
2nd Series	40%	30%	30%
3rd Series		10%	10%
4th Series			10%

The "soil series order" refers to the hierarchy implicit in the soil association name, with the first series always being the most predominant and subsequent series exhibiting less predominance depending upon the order of appearance. These assumed distributions were used to weight the hydrologic characteristics of each series to derive a composite characteristic for each soil association. The results of the sensitivity studies of Howard and Kent Counties and the Occoquan River Basin support the use of these distributions (20).

Average values of the following characteristics were derived for each soil association by applying the assumed distributions to the soil series data presented in State SCS-5 reports: permeability; hydrologic soil group; total water holding capacity; soil texture; soil depth; and erodibility factor (K). Using the 100 sq mi grid cell network, 1:500,000 scale map overlays showing the average value for the predominant soil association in each grid cell were developed for each of these characteristics.

The first step in the delineation of homogeneous hydrologic segments was to overlay the physiographic province map with the 100 sq mi grid map of average slopes. Areas with relatively uniform slopes within physiographic provinces were selected as the first segment approximation. The next step was to overlay this intermediate segment network with the grid maps of hydrologic soil group and total water holding capacity. More detailed segments were derived from these last two overlays since they delineated areas with relatively similar infiltration rates and soil moisture storage capacities. Particular attention was given to defining more detailed segments in the Coastal Plain where surface runoff and nonpoint pollution loads have a greater chance of reaching the Bay's estuarine system due to the relatively short travel times. This analysis of basinwide physical features resulted in the delineation of a preliminary hydrologic unit network consisting of 23 hydrologic segments.

This preliminary segment network was further refined by analyzing areal variations in rainfall patterns within each segment. National Weather Service (NWS) tapes with hourly/daily raingage records for the period 1966-1978 were used for this analysis.* A total of 93 raingages were included in this study. A generalized map of this raingage network is shown in Figure 6. The distribution of these hourly and daily raingages among the major physiographic provinces is as follows:

*NWS rainfall tapes were only available through 1978 at the time this study was initiated. Since budget constraints prevented the acquisition of tapes of rainfall data for the full period of record at each gage, the period 1966-1978 was selected for use in calibration/verification and production runs because it included a good mix of wet, dry, and average years. As indicated in a later section, analyses of streamflow records for the 30-year period (1949-1978) covered by NWS hourly raingages indicate that 1966 through 1978 is an excellent surrogate for the longer period of record.

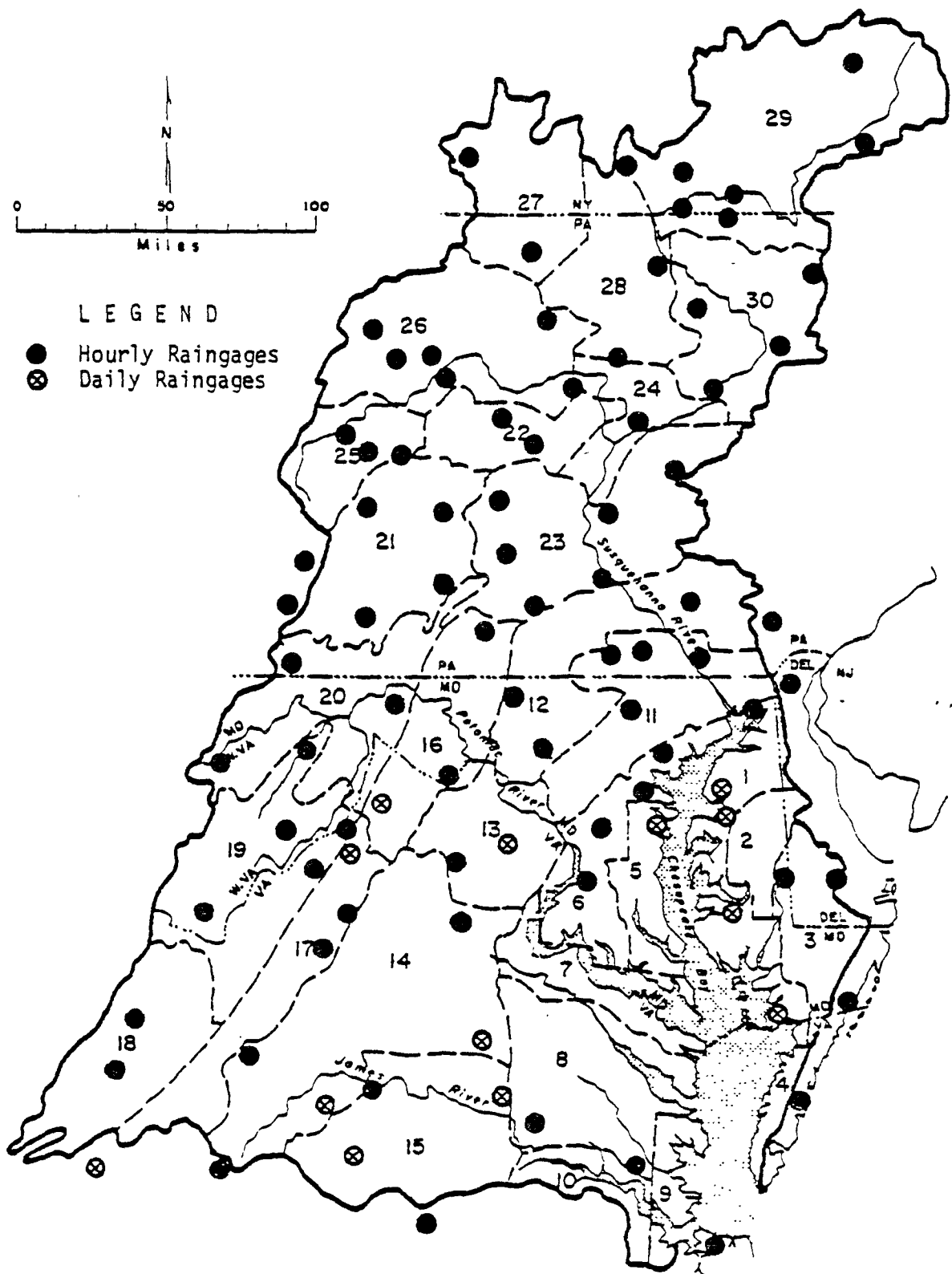


Figure 6. Map Showing Distribution of Hourly and Daily Raingages

<u>PHYSIOGRAPHIC PROVINCE</u>	<u>NO. OF HOURLY GAGES</u>	<u>NO. OF DAILY GAGES</u>
Appalachian Plateau	23	0
Appalachian Ridge & Valley	31	3
Piedmont	14	5
Coastal Plain	<u>12</u>	<u>5</u>
TOTAL:	80	13

Statistics such as mean annual volume, standard deviation, and coefficient of variation were calculated for each raingage and compared with surrounding gages to identify groups of gages that have similar characteristics. Raingage groupings were further refined through intercorrelation analyses based upon daily rainfall totals. Basinwide isohyetal maps and Thiessen polygons constructed for the final raingage groupings (e.g., Figure 7) were used to further subdivide seven hydrologic segments, resulting in the final network of 30 segments shown in Figure 8. Maps showing the NWS raingages assigned to each hydrologic segment are shown in Appendix A. As may be seen from a comparison with the major physiographic province map (Figure 5), many hydrologic segment boundaries correspond to the physiographic boundaries as might be expected for a generalized network representing a 64,000 sq mi drainage area. Segments 1-10 represent Coastal Plain province areas, segments 11-15 represent Piedmont province areas, segments 16 and 17 represent the Blue Ridge and Great Valley province, segments 18-24 represent Appalachian Ridge and Valley province areas, and segments 25-30 represent Appalachian Plateau province areas. Average soils characteristics and topography data used in the hydrologic submodel were tabulated for each segment by weighting the values stored in the 100 sq mi grid cell dataset.

Since the hydrologic segments often overlapped river basin boundaries, a network of sub-basins was delineated to represent each river basin. In order to maximize homogeneity, the sub-basins were sized to ensure that the majority of the drainage area was located within a single hydrologic segment. In addition, an effort was made to maintain a bankfull channel travel time on the order of 24-72 hrs in establishing the outflow of each sub-basin. The resulting sub-basin network for the major river basins represented by Basin Model is shown in Figure 3. The hydrologic characteristics assigned to the segments traversed by each sub-basin were weighted for input to the hydrologic submodel.

In light of the size of the study area, sophisticated remote-sensing techniques offered the only feasible method for defining land cover data for each sub-basin. Existing land use summaries for each sub-basin are based upon interpretations of LANDSAT satellite images from the period 1977-1979 with state-of-the-art software available at the Goddard Space Flight Center in Greenbelt, Maryland. The majority of the LANDSAT scenes used in this study are based upon 1979 conditions. The following land use classifications were available from the LANDSAT dataset for all sub-basins:

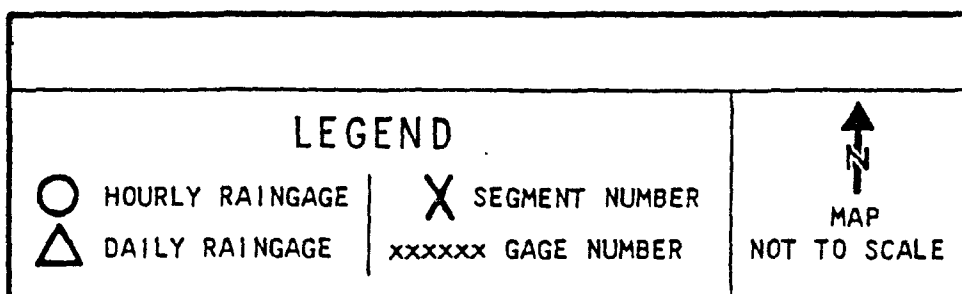
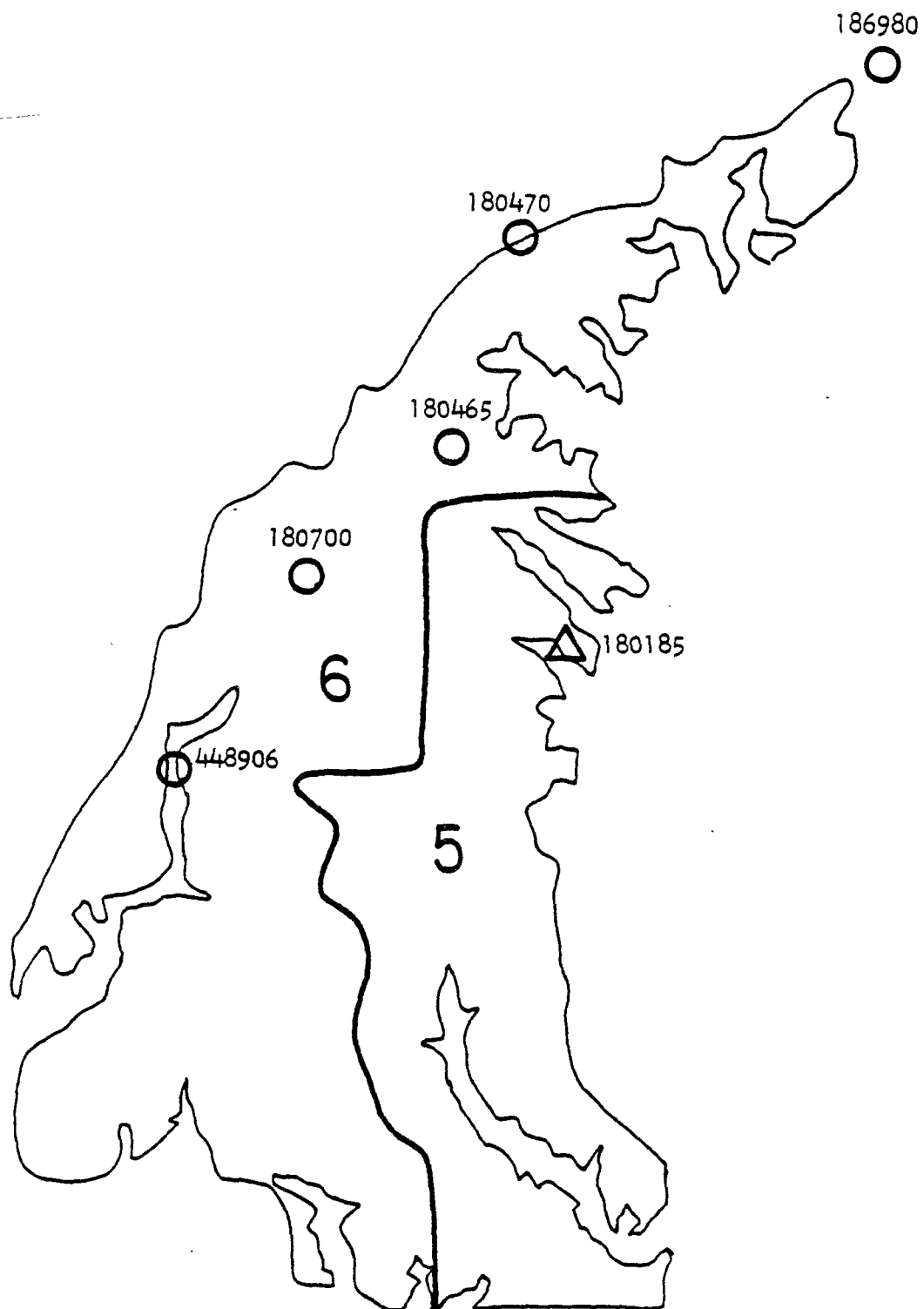


Figure 7. Sample Raingage Grouping

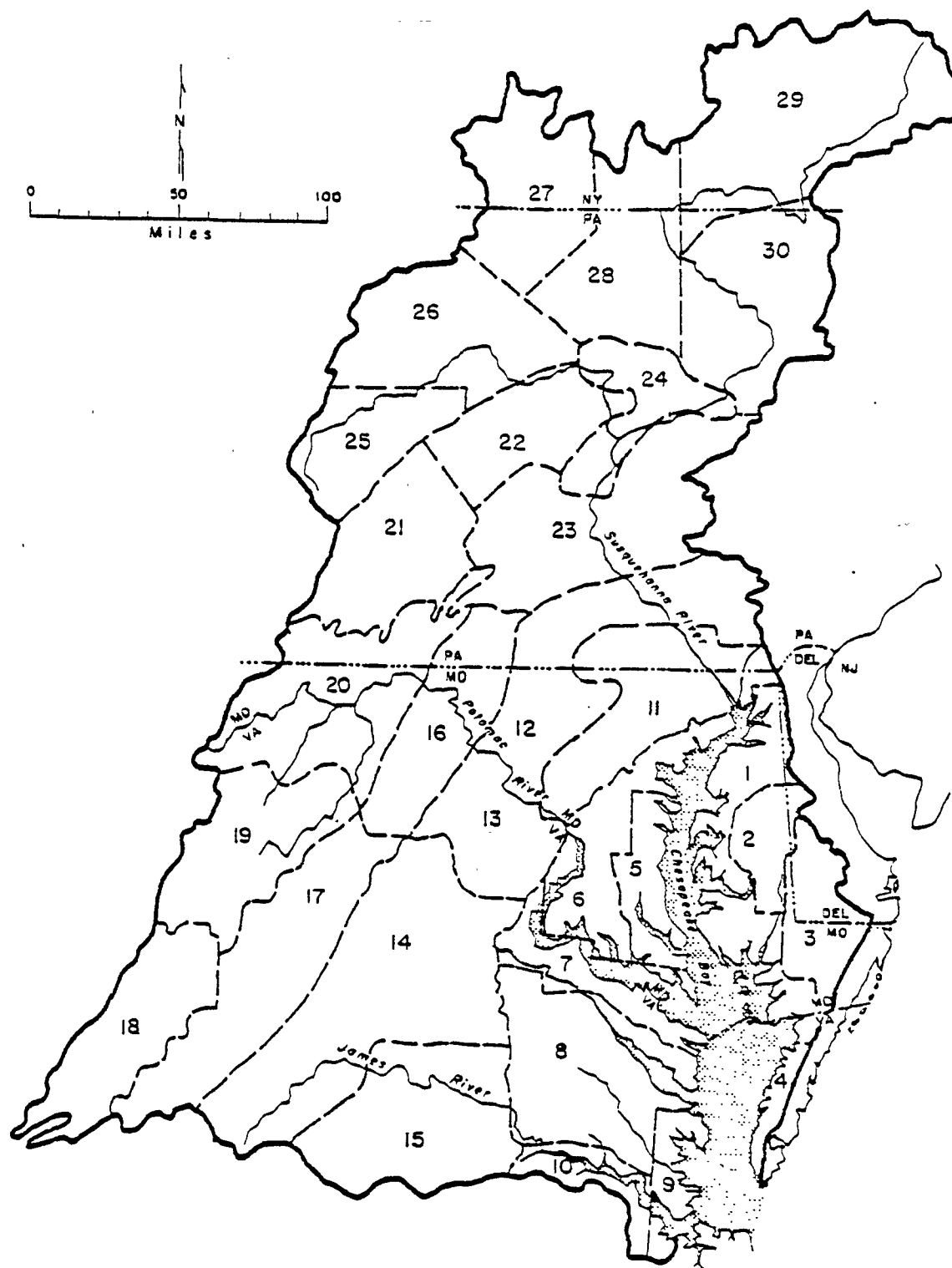


Figure 8. Map of Hydrologic Segments in Basin Model

- o Forest and idle land
- o Pasture land
- o High tillage cropland
- o Low tillage cropland
- o Urban land

In the major metropolitan areas in the approximately 64,000 sq mi drainage area, urban land is broken down into residential and commercial categories. A total of 15 LANDSAT scenes were required to cover the entire Chesapeake Bay basin. For each quadrant of a LANDSAT scene, "ground-truth" sites identified on available low altitude aerial photographs were used to interpret statistical groupings of ground cover signatures. Based upon the ground-truth checks, each ground cover signature was assigned to a land use classification and the total area in each classification was tabulated by sub-basin for model input. Based upon follow-up accuracy checks in areas which were not used for ground-truth sites and comparisons of river basin data with published data, it is felt that the sub-basin LANDSAT database provides a very reasonable representation of existing land use in the Chesapeake. A summary of the LANDSAT analysis and results is presented in Appendix B.

Meteorologic Dataset

To produce a single hourly rainfall record for each hydrologic segment, for the period 1966-1978, the Thiessen polygon method was used. Special software was designed to produce an hourly rainfall record which was based on a representative area-weighted daily rainfall volume, preserved hourly rainfall intensities, and compensated for missing records. The excellent hydrologic calibration results described later in this report indicate that the segment rainfall records generated in this manner provide a reasonable representation of total rainfall volumes and distributions within the relatively large river basins.

Other daily meteorologic data (e.g., evaporation, air temperature, solar radiation, wind speed) required for the hydrologic and water quality submodels were derived for the eight meteorologic regions shown in Figure 9, in comparison with the thirty precipitation regions which were designated. Eight regions for non-precipitation data were felt to be adequate because the gages for these records are fewer in number than the rainfall gages, areal variations in these meteorologic indicators tend to be easier to characterize, and hydrologic responses in the river basins tend to be more sensitive to month-to-month fluctuations in these data in comparison with the day-to-day fluctuations in rainfall which are so important.

For the hydrologic sub-model, the predominant hydrologic segment and meteorologic region determine the hourly rainfall dataset and general meteorologic dataset, respectively, which are assigned to each sub-basin.

CHESAPEAKE BAY BASIN METEOROLOGIC REGIONS

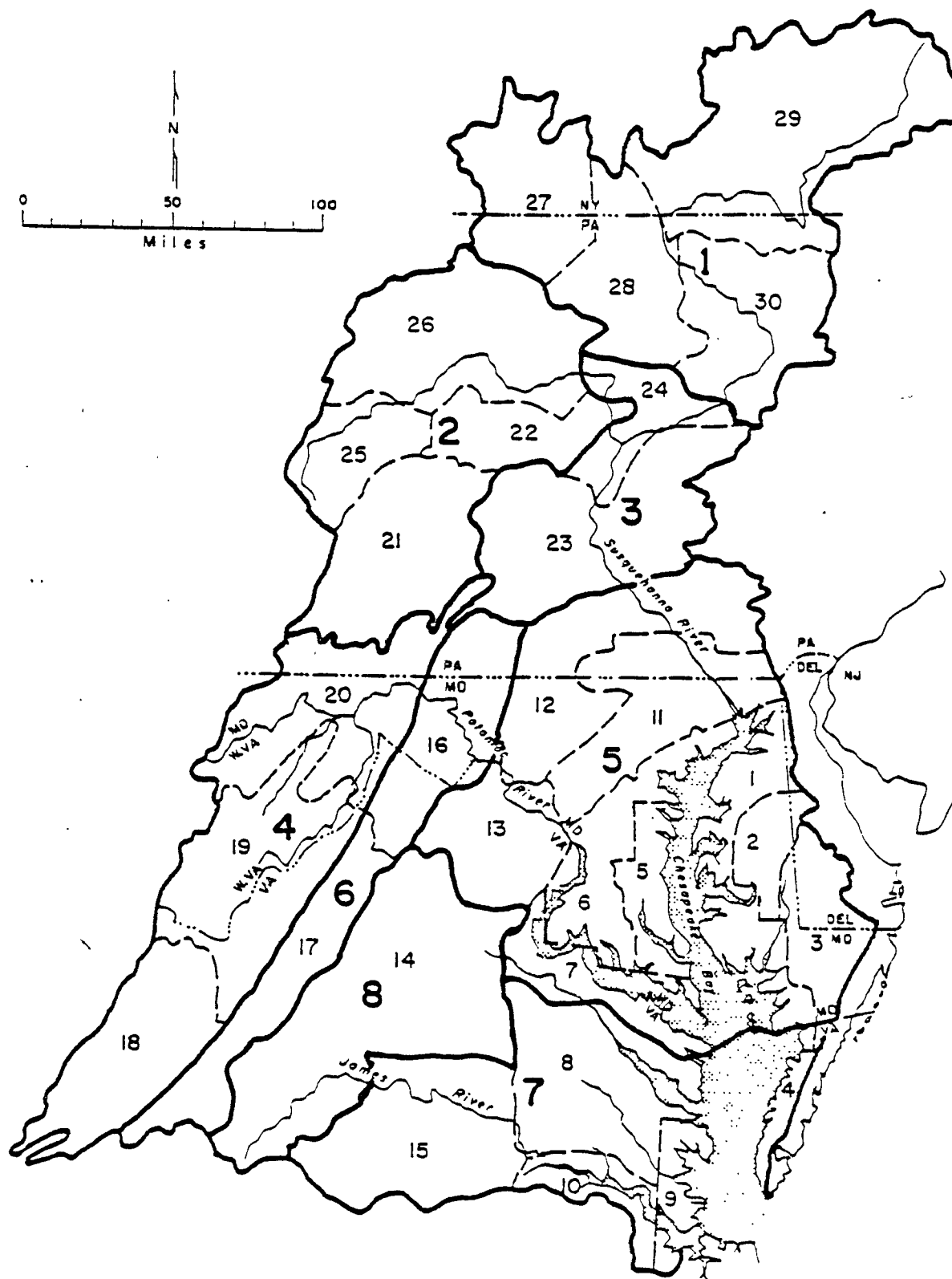


Figure 9

Idealized Channel Network

A single idealized trapezoidal channel with constant cross-sectional geometry is assigned to each sub-basin. To facilitate the development of idealized cross-sections, all channels are terminated at U.S.G.S. streamgaging stations, with the exception of tributary channels which are extended to their confluence points, where data on channel geometry is available from the table (Form 9-207) used to construct the stage-discharge relationship for the gage. As indicated above, idealized channel length was established in conjunction with the determination of sub-basin size in order to maintain bankfull travel times on the order of 1 to 3 days for each channel reach. Flood plain slopes for each idealized channel were determined from 1:24,000 scale topographic maps for the sub-basin. A sketch of the Basin Model's channel reach system is shown in Figure 3. As may be seen, the idealized channel system is restricted to the main stems of the major river basins, since the focus of Basin Model applications is the transport of pollutant loadings to the Chesapeake Bay rather than localized receiving water problems. It should also be noted that channels are generally not included in the Basin Model to transport streamflows and pollutant loads from Coastal Plain sub-basins to the tidal waters that drain these areas. In limiting the idealized channel system to the main stems of major river basins, it has been assumed for purposes of this pollutant transport study that the time lag and pollutant transformations achieved by channel storage in minor tributaries and small Coastal Plain watersheds is relatively insignificant and can be neglected. It should be noted that such an assumption may not be appropriate for modeling studies focussing on local flooding problems or local receiving water quality impacts. Such an assumption would be particularly inappropriate for local point source management studies since the tributaries which must assimilate the waste load during low flow periods would not be included in the model.

To calculate the slope of each idealized channel, the Basin Model relies upon channel length and the channel bottom elevation at the upstream and downstream end. Since the idealized channel reaches begin and end at U.S.G.S. streamgaging stations, the channel invert elevations reported for each streamgage were assigned to the respective channels. Downstream invert elevations for tributary channels were extrapolated from the next two upstream U.S.G.S. streamgaging stations.

Data on channel roughness coefficients was collected from State and regional agencies which had performed local studies in the Chesapeake Bay basin. An average value was derived for each idealized channel reach based upon the arithmetic means of roughness coefficient values at several representative cross-sections.

For purposes of pollutant transport studies with the Basin Model, the assumption of a uniform change in cross-section geometry between selected U.S.G.S. gaging stations provides a reasonable approximation of average cross-sectional area and hydraulic radius within the idealized channel network. Since the Basin Model is not intended for assessments of localized

Table 1

CHANNEL NETWORK PARAMETERS

RCH #	TYPE*	TRIB TO	LENGTH (mi.)	UPSTREAM ELEVATION (ft)	DOWNSTREAM ELEVATION (ft)	BOTTOM WIDTH (ft)	TOP WIDTH (ft)	DEPTH (ft)	FL PL SLOPE	CHANNEL n	FL PL n
10	S	30	108.0	1527.1	727.9	94	509	6.4	0.027	0.040	0.060
20	S	30	184.4	1278.7	727.9	270	565	12.8	0.026	0.037	0.073
30	S	40	94.9	727.9	512.1	650	1130	19.1	0.053	0.040	0.075
40	S	80	68.4	512.1	408.6	760	1990	20.1	0.050	0.030	0.061
50	S	60	91.0	1348.2	830.6	74	291	8.1	0.050	0.036	0.063
60	S	70	88.2	830.6	495.0	403	977	15.1	0.072	0.041	0.074
70	S	80	42.1	495.0	413.5	550	1880	18.8	0.050	0.040	0.070
80	S	110	50.6	408.6	290.0	2092	3494	16.5	0.050	0.031	0.068
90	R	100	27.0	731.1	597.4	2536	2536	61.9	0.069	0.034	0.072
100	S	110	111.9	831.8	326.8	200	730	9.5	0.031	0.036	0.073
110	S	120	24.2	290.0	200.6	2118	5895	14.4	0.028	0.034	0.081
120	R	140	19.6	200.6	86.5	4108	4108	18.9	0.031	0.034	0.081
140	R	150**	14.0	86.5	5.0	5280	5280	35.9	0.057	0.034	0.081

* S = Stream

R = Reservoir

**Dummy reach below Conowingo Dam

NOTE: RCH # conforms to sub-basin no. in Figure 3.

Table 1 (continued)

CHANNEL NETWORK PARAMETERS

RCH #	TYPE*	TRIB TO	LENGTH (mi.)	UPSTREAM ELEVATION (ft)	DOWNSTREAM ELEVATION (ft)	BOTTOM WIDTH (ft)	TOP WIDTH (ft)	DEPTH (ft)	FL PL SLOPE	CHANNEL n	FL PL n
160	S	175	92.3	2951.2	516.9	77	354	5.3	0.061	0.034	0.085
170	S	175	127.6	2120.4	516.9	74	260	5.8	0.061	0.034	0.085
175	S	180	43.3	516.9	383.7	115	549	19.8	0.061	0.040	0.090
180	S	220	78.6	383.7	200.6	433	972	19.6	0.064	0.050	0.098
190	S	200	139.0	1544.8	469.4	154	246	6.8	0.061	0.048	0.080
200	S	220	57.8	469.4	241.3	378	628	9.4	0.064	0.048	0.080
210	S	220	64.5	384.8	175.5	99	214	6.8	0.200	0.036	0.072
220	S	---	41.0	200.6	38.0	512	1833	19.6	0.001	0.050	0.098
230	S	---	73.0	382.2	55.2	90	418	5.7	0.042	0.040	0.079
235	S	240	27.6	141.4	85.1	2	111	5.7	0.023	0.058	0.105
240	S	---	35.7	85.1	12.4	15	30	6.0	0.005	0.085	0.180
250	R	260	16.3	118.4	90.6	6479	6479	26.7	0.008	0.058	0.105
260	S	---	44.5	90.6	14.7	42	268	13.2	0.005	0.058	0.105

* S = Stream

R = Reservoir

NOTE: RCH # conforms to sub-basin no. in Figure 3.

Table 1 (continued)

CHANNEL NETWORK PARAMETERS

RCH #	TYPE*	TRIB TO	LENGTH (mi.)	UPSTREAM ELEVATION (ft)	DOWNSTREAM ELEVATION (ft)	BOTTOM WIDTH (ft)	TOP WIDTH (ft)	DEPTH (ft)	FL PL SLOPE	CHANNEL n	FL PL n
265	R	270	12.0	2925	2698	1741	1741	48.9	0.130	0.048	0.079
270	S	280	114.0	2698	548.5	102	673	7.1	0.044	0.048	0.079
280	S	290	107.3	548.5	164.0	420	825	13.3	0.108	0.036	0.067
290	S	---	39.0	164.0	98.8	348	2910	12.0	0.006	0.030	0.050
300	S	310	108.4	371.6	195.2	93	138	14.0	0.006	0.054	0.125
310	R	320	13.8	195.2	71.7	2027	2027	10.8	0.008	0.054	0.125
320	S	---	2.9	71.7	68.3	207	266	19.4	0.006	0.054	0.125
330	R	340	12.0	311.9	153.5	1017	1017	24.5	0.063	0.055	0.100
340	S	---	21.0	153.5	13.1	35	300	6.2	0.010	0.055	0.100

* S = Stream

R = Reservoir

NOTE: RCH # conforms to sub-basin no. in Figure 3.

flooding problems or local receiving water quality impacts, fluctuations in channel geometry between the U.S.G.S. gaging station nodes can generally be ignored without introducing significant error into the simulations of pollutant travel time within each idealized reach. Likewise, local variations in the channel roughness coefficient can be neglected for the same reason so long as the value assigned to each idealized reach provides an adequate approximation of average conditions between the upstream and downstream ends of each channel.

A summary of the characteristics of Basin Model channel reaches is presented in Table 1. Reading from left to right, the entries in Table 1 are as follows: Reach number; type of channel (i.e., either stream or reservoir); the downstream reach number (i.e., "TRIB TO"); reach length; upstream invert elevation (ft above m.s.l.); downstream invert elevation; bottom width of incised channel; top width of incised channel; depth of incised channel; average slope (ft/ft) of floodplain; Mannings n for channel; and Mannings n for floodplain.

The following major reservoirs are represented by the Basin Model as single-layer lakes: Lake Anna (York River Basin); Lake Chesdin (Appomattox River Basin); Raystown Reservoir (Juniata River Basin); the two Patuxent River reservoirs; the Lake Aldred/Lake Clarke reservoir system (Susquehanna River Basin); and Conowingo Reservoir (Susquehanna River Basin). In the case of the two Patuxent reservoirs and the Lake Aldred/Lake Clarke system, the two reservoirs in series are combined into a single idealized impoundment with appropriate aggregate characteristics. For the Conowingo hydroelectric reservoir, a separate operating rule computer program (22) is used to calculate daily spills from simulated daily streamflows entering the reservoir. The procedure for simulating flows and pollutant transport through Conowingo Reservoir is as follows: (1) execution of the Basin Model is stopped immediately upstream of Conowingo Reservoir and simulated daily streamflows are stored for input to the Conowingo operating rule program; (2) the operating rule program calculates daily Conowingo spills for the simulation period; and (3) the calculated daily spills are input to the Basin Model's representation of Conowingo Reservoir, and the model is operated with the simulated flows and loads entering the impoundment.

Discharge and Diversion Datasets

Industrial and municipal wastewater treatment plants located upstream of the fall line are included in the Basin Model, while discharges below the fall line are included in either the Tidal Tributary Model or the Main Bay model. Only treatment plants with existing discharges in excess of 0.5 MGD are explicitly represented, under the assumption that smaller discharges represent a negligible fraction of the pollutant load delivered to the Bay's estuarine system. Since both point and nonpoint source loadings from a sub-basin are evenly distributed along the length of an idealized channel, wastewater treatment plant flows and loadings are aggregated into a single dataset for each sub-basin. Wastewater treatment plant flows and treatment levels are based upon a survey of recent NPDES monitoring records. Since

most NPDES records do not include data on nitrogen and phosphorus discharges, effluent levels are assigned to each plant to reflect the reported treatment level. Constant average daily flows and effluent levels are assumed for each treatment plant for each day of the simulation period.

Major water supply diversions are also represented by the Basin Model. Since the model evenly distributes the diversions along an idealized reach or reservoir, average daily withdrawals are summed by reach for Basin Model input.

CHAPTER IV

PROCESSES REPRESENTED BY BASIN MODEL

Hydrologic Submodel

Based upon a modified version (1,5) of the Stanford Watershed Model (4), which was developed in 1960, this submodel can be operated with 5-minute, 15-minute, or hourly rainfall records and daily evaporation records. A flow chart summarizing the hydrologic processes represented by the submodel is shown in Figure 10. It calculates the amount of rainfall converted to runoff, a continuous record of soil moisture during and after rainstorms, and subsurface recharge of stream channels. For hydrologic simulations of the 63 sub-basins in the Chesapeake Bay drainage area, continuous records of hourly rainfall (i.e., 24 values per day) were used. For hydrologic simulations of the small test watersheds used to develop nonpoint pollution loading factors, a continuous record of either 5-minute (i.e. 288 values per day) or 15-minute (i.e., 96 values per day) data were used because of the shorter times-of-concentration.

During storm periods, rainfall is distributed among surface runoff and soil moisture storage compartments based upon adjusted infiltration rates and the nominal storage capacities assigned to different sections of the soil profile. Between rainstorms, water storage in soil moisture zones is depleted by mechanisms such as evapotranspiration and subsurface recharge of streams, thereby freeing up soil moisture storage capacity for rainfall inputs from the next storm.

The most sensitive parameters in the submodel are the infiltration rate and the soil moisture storage capacities (i.e., lower zone and upper zone). The model's infiltration rates are based upon sub-basin soils characteristics such as hydrologic soil group, permeability, total water holding capacity and depth to restrictive layer. Both the infiltration rate and soil moisture storage capacities are estimated from sub-basin data and refined by calibrating the model with observed streamflow records. Parameters governing subsurface recharge of streams are generally estimated from analyses of observed hydrographs and refined during calibration.

Nonpoint Pollution Loading Submodel

The nonpoint pollution loading submodel is a slightly modified version (1,9) of the U.S. Environmental Protection Agency's NPS model (5). It operates on rainfall intensity records and on the hydrologic submodel's output of surface runoff and subsurface flow records. All constituents are treated conservatively (i.e., no degradation or transformations) during overland flow transport to a stream channel, whereupon instream processes are applied through the receiving water submodel. Nonpoint pollution loading processes represented by the submodel are summarized in Figure 11.

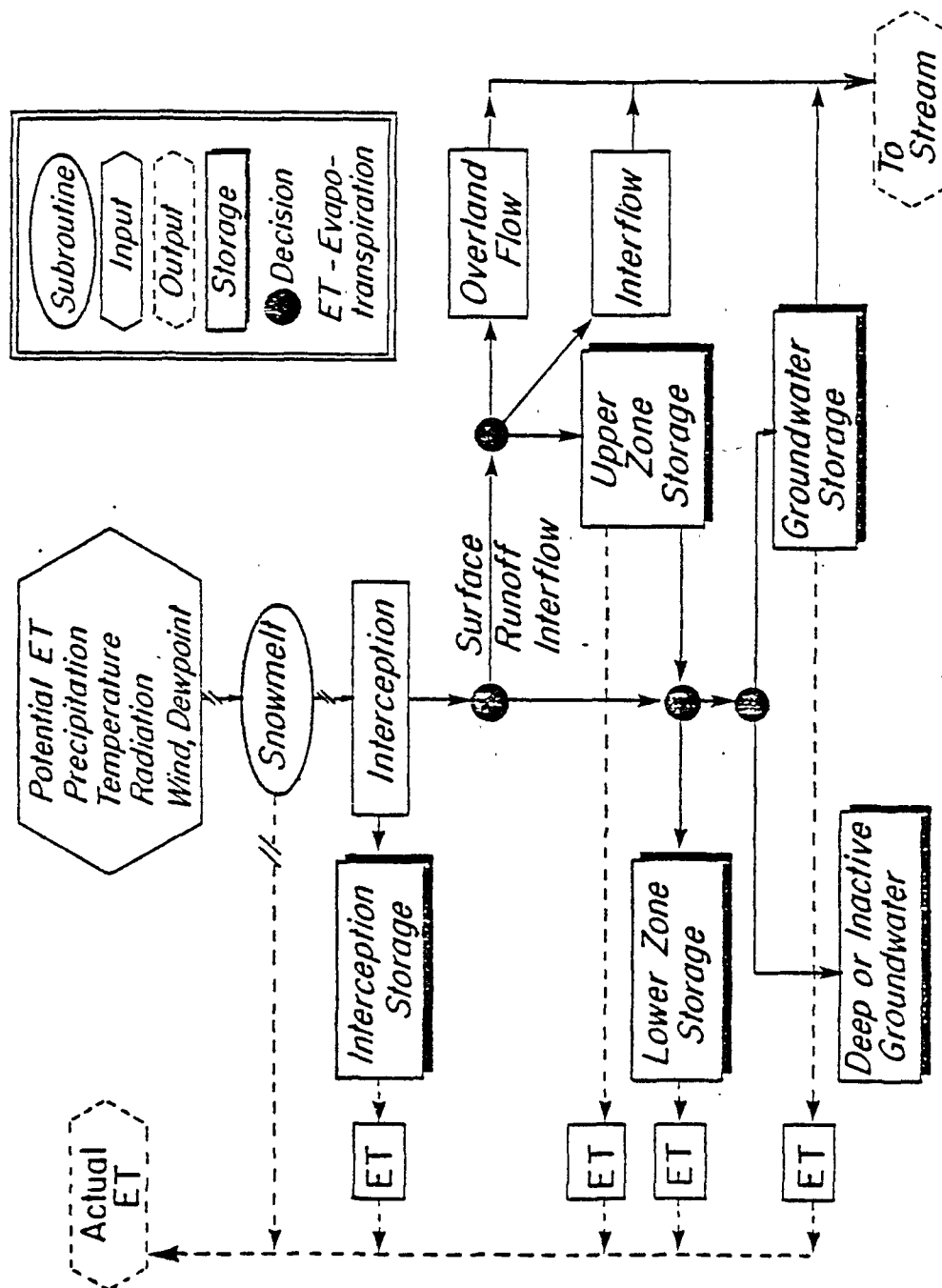


Figure 10. Hydrologic Model Flow Chart

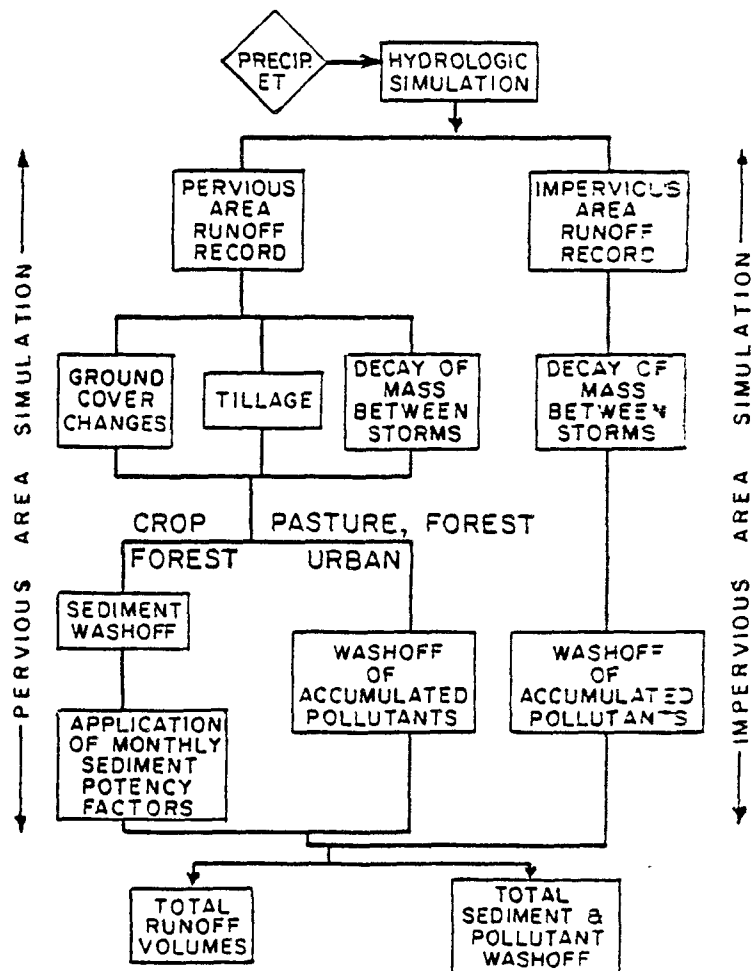


Figure 11. Nonpoint Pollution Loading Processes Represented by NPS Model

For cropland, the model assumes that sediment generation and washoff (i.e., soil loss) are the driving forces for loadings of all pollutants. Cropland loadings of sediment, which are calculated from rainfall records with a soil loss algorithm related to the Universal Soil Loss Equation (23), are assigned sediment "potency factors" (i.e., ratio of pollutant mass to sediment mass) to calculate loadings of other pollutants. The representation of cropland areas is enhanced by several model features such as the capability to assign monthly vegetative cover percentages that represent seasonal variations in exposed ground cover resulting from crop growth and harvest and the capability to simulate soil disturbance on user-specified dates to account for tillage practices. For urban and pasture land uses, nonpoint pollution washoff algorithms relate the washoff of accumulated pollutant loads to the simulated runoff rate in each time-step. Accumulated pollutant loads at the start of a rainstorm are calculated from the "daily pollutant accumulation rates" (lbs/ac/day) assigned to each land use classification to represent the buildup of pollutants on the land surface and in the atmosphere (i.e., air pollution between rainstorms). For the forestland category, pollutant loading calculations are based upon soil loss/potency factors as well as daily pollutant accumulations, with the former more prominent during periods of low leaf cover (i.e., fall and winter) and the latter more prominent during periods of high leaf cover (i.e., spring and summer).

Nonpoint pollution loading factors such as sediment potency factors and daily pollutant accumulation rates have been developed for the Chesapeake Bay Basin from model calibration studies with EPA/CBP test watershed data (6) and with other monitoring studies (7,8,9,10), as described in a later section of this report. Given the state-of-the-art of nonpoint pollution loading models, loading factors such as sediment potency factors and daily pollutant accumulation rates are probably best viewed as empirical factors which can provide a reasonable approximation of a land use's nonpoint pollution loading potential, much like the C coefficient in the "rational formula" is viewed as an empirical factor that relates rainfall intensity to peak runoff. The model has the capability to use monthly variations in pollutant loading factors. This feature permits a representation of variations in the pollutant loading potential of cropland areas due to such factors as fertilizer/manure applications, crop growth, crop harvest, etc. Subsurface flow loadings based upon user-specified concentrations are added to hourly runoff pollution loadings and delivered to the outlet of each sub-basin.

Receiving Water Submodel

The hydrologic and nonpoint pollution loading submodels are used to calculate hourly runoff, subsurface flow, and pollutant loadings delivered to a stream channel or reservoir by the tributary sub-basin. The receiving water submodel (1,2,24) combines the hourly streamflow and pollutant loadings from the sub-basin models with daily point source loadings, subtracts out water supply diversions, and calculates daily pollutant transport and concentrations throughout the stream and reservoir system.

While all pollutant loading calculations in the nonpoint pollution loading submodel assume no pollutant decay or transformation, the receiving water model simulates the major physical, chemical, and biological processes that change the magnitude and form of pollutants being transported downstream. The one-dimensional receiving water model is operated on an hourly computation interval with the streamflow and pollutant loading records produced by the hydrologic and nonpoint pollution loading submodels as well as daily records of solar radiation, cloud cover, maximum/minimum daily air temperature, dewpoint temperature, average wind velocity, and precipitation/evaporation. Streamflow transport is handled with a form of kinematic wave routing, while pollutant transport out of a given channel reach into a downstream channel reach is based upon advection (i.e., transport of a pollutant by movement of the parcel of water containing it). Since the travel time through any reach is significantly greater than the one-hour computational interval, plug flow conditions and negligible dispersion are assumed for pollutant transport calculations.

Included among the water quality processes calculated on a one-hour interval for each channel reach or reservoir are: heat transfer processes used to calculate water temperature which affects a range of water quality processes; BOD changes due to decay, sedimentation, sediment releases and decomposition of dead algae; nitrification (i.e., conversion of ammonia and nitrite to nitrate) when sufficient dissolved oxygen is available; denitrification under oxygenless conditions; sedimentation of organic nitrogen and organic phosphorus; transformation of nitrogen and phosphorus from organic to inorganic forms and back again; phytoplankton growth, respiration and sinking; sediment oxygen demand and bottom sediment releases of BOD, nitrogen, and phosphorus; and dissolved oxygen changes due to BOD decay, nitrification, reaeration, phytoplankton photosynthesis and sediment oxygen demand. The receiving water submodel relies upon standard sanitary engineering equations to represent the water quality processes summarized above. For most BOD, phosphorus, and nitrogen decay mechanisms, the standard first-order differential equations are used.

The first-order differential equations assume that the amount of constituent decayed in each time interval is a function of: (1) the amount of constituent present at the start of the time interval; and (2) the rate constant for the reaction being considered. The differential equation can be integrated to yield the following equation for water quality processes involving pollutant decay (i.e., reduction in concentration due to physical, chemical or biological mechanisms) during each time interval:

$$C_t = C_o e^{-K_D(t-t_o)}$$

where

C_t = concentration at time t (i.e., at end of time interval)

C_o = concentration at time t_o (i.e., at start of time interval)

K_D = decay rate constant for water quality process (hr^{-1})

$(t-t_o)$ = time interval for calculation

Decay processes represented by this equation in the Basin Model include the following: nitrification (i.e., conversion of ammonia N to nitrite N and ultimately to nitrate N); hydrolysis of organic N (i.e., conversion of organic N to ammonia N); conversion of organic P to inorganic P; and oxidation of carbonaceous BOD reaeration.

For phytoplankton (i.e., chlorophyll-a), both growth and decay are simulated:

$$C_t = C_o e^{(K_G - K_D)(t - t_o)}$$

where

K_G = growth rate factor representing increase in phytoplankton concentration due to uptake of nitrogen and phosphorus (hr^{-1})

K_D = decay rate factor representing reduction in phytoplankton concentration due to respiration and zooplankton feeding (hr^{-1})

Following the calculation of the net change in phytoplankton concentration, the model calculates algal death with rate factors that reflect the availability of nutrients in the water column.

The representation of algal growth, which is based upon Michaelis-Menton kinetics with a limiting condition (e.g., light, temperature, phosphorus, or nitrogen) assigned to each computation interval, merits some elaboration. Given the scale of the modeling problem, chlorophyll-a simulations are used to approximate the aggregate effects of three processes that probably would be treated separately for a smaller-scale receiving water modeling study:

1. Uptake and removal of N and P through growth and settling of free-floating phytoplankton: free-floating chlorophyll-a is subject to removal by sedimentation while being advected from one channel reach to the next;
2. Uptake and removal of N and P through growth of benthic algae: uptake and removal by attached algae and rooted aquatic plants differs from free-floating phytoplankton processes in that the former typically remains within its channel reach while the latter is advected downstream; and
3. Removal of suspended inorganic P and inorganic N through sedimentation: since the Basin Model does not provide an explicit representation of phosphorus sorption/desorption reactions with suspended sediment,* chlorophyll-a growth assists with the approximation of inorganic P and N removal.

*Such a model would not only have to represent sorption/desorption kinetics, but it would also have to provide a more rigorous representation of sediment transport mechanisms than is available in most models used for management studies today.

The representation of benthic algae and sedimentation of inorganic N and P must be approximated through free-floating phytoplankton simulations, since this is the only type of phytoplankton that the Basin Model is capable of representing. Since upstream concentrations are not of interest for the Basin Model study (i.e., the Model is not calibrated to represent localized receiving water quality problems), the tendency of this procedure to overestimate chlorophyll-a concentrations in the upstream sections of the river basins is not of serious consequence. What is critical is that the Basin Model must provide a reasonable representation of pollutant transport through the main stem river system to the fall line.

This approach to chlorophyll-a simulation is quite reasonable for calculations of benthic algae growth, since other models (2,25) use the same equations for both free-floating phytoplankton and attached phytoplankton/rooted aquatic plants. However, care must be taken with such a representation to ensure that the simulated advection of free-floating phytoplankton does not result in a significant overestimate of organic P and N delivery to the fall line. Comparisons of simulated and recorded N and P concentrations at upstream gages during dry weather flow periods were used to identify growth rate parameters that satisfied this criterion.

As for the inclusion of inorganic P and N adsorption to sediments in the calculation of chlorophyll-a, this Michaelis-Menton approximation parallels first-order decay terms in other models (26), and probably provides a more deterministic representation since it accounts for adsorption (i.e., conversion to settleable organic form) and sedimentation through a two-step process. The representation of these processes is most important for simulations of nonpoint pollution transport during high flow periods, since adsorption of point source ortho-P loadings onto suspended sediment during dry weather periods is likely to be a relatively insignificant instream process due to the relatively low TSS concentrations in comparison with wet-weather periods. In the prototype river basins, high percentages of the inorganic P and N loadings delivered to a stream channel and adsorbed to suspended sediment are likely to be delivered through unimpounded channel systems to the fall line during the well-distributed storms that produce the overwhelming majority of seasonal and annual fall line loadings. The relatively high transport rates for well-distributed storms can be attributed to such factors as: (a) much greater significance of sediment fines in washload (i.e., rather than coarse grained particles in bedload) in any sorption-desorption reactions for inorganic P and N; and (b) relatively high fall line delivery ratios for sediment fines due to turbulent flow conditions and relatively high channel velocities throughout the river basin channel system. Given these assumptions, the Basin Model's treatment of inorganic P and N transport should be a very good approximation of the prototype for well-distributed storms, in that both the prototype and the model should exhibit relatively high fall line delivery ratios. For storms which are not uniformly distributed throughout the river basin, the model relies upon chlorophyll-a growth and settling under quiescent conditions in downstream channel reaches to achieve the required reductions in the delivery of upstream inorganic P and N loads to the fall line (i.e., NPS

loads of inorganic P and N produced by a localized storm upstream of the fall line are reduced through algal growth in a downstream reach where detention times are considerably higher and flow conditions are relatively quiescent). Thus, comparisons of simulated and recorded loads to check on this mechanism for inorganic P and N removal focussed on rainstorms which were not uniformly distributed throughout the river basin.

Additional details on the Model's approximation of phytoplankton growth are presented below:

- A. Representation of Phytoplankton: To quantitatively describe the dynamic behavior of phytoplankton populations, assumptions must be made concerning their behavior. In the Chesapeake Bay Basin Model, the entire phytoplankton population is considered as one species, and the mean behavior of the population is described through a series of generalized equations. While such an approach obscures the behavior of individual species, the overall effect of the phytoplankton population on water quality can be modeled with reasonable accuracy. Observed and simulated phytoplankton concentrations are based upon the concentration of "chlorophyll-a," which is a widely accepted measure of the overall phytoplankton population. The mean phytoplankton composition simulated by the model is defined by the carbon:nitrogen:phosphorus ratio, the percent of algae dry weight as carbon, and the ratio of chlorophyll-a to algal phosphorus. Based upon a review of typical literature values (2,25,26), the representation of phytoplankton growth in each channel and reservoir reach is based upon a C:N:P ratio of 106:16:1 (i.e., Redfield ratio), 49% of algae dry weight as carbon, and 0.6 ug/L chlorophyll-a per 1.0 ug/L of algal phosphorus.
- B. Determination of Limiting Conditions for Phytoplankton Growth: The growth of phytoplankton is dependent upon temperature, plant nutrient concentrations, light, minerals, and vitamins. In most waters, the necessary concentrations of minerals and vitamins are available for phytoplankton growth; consequently, the variables which generally determine phytoplankton growth rate are temperature, plant nutrients, and light. During each hourly time step in which the water temperature will support algal growth, the Model compares the phytoplankton growth rates associated with each of these parameters and assigns the smallest of the growth rates to phytoplankton in the upper layer of the Reservoir.
 1. Temperature Control: The Model relies upon a linear smoothing function to adjust algal growth rates to account for temperature effects. The smoothing function is typically based upon a low temperature threshold which triggers the start of growth and a high temperature threshold for optimal growth, with the smoothing factor ranging from 0.0 at the low threshold to 1.0 at the high threshold. For the

representation of the channel system in the Chesapeake Bay drainage area, the temperature endpoints of the smoothing functions were set at levels that permitted the necessary levels of phytoplankton growth in all four seasons.

2. Phosphorus-Limited Growth: Phytoplankton are dependent upon uptake of orthophosphorus to provide the continual supply of phosphorus necessary for ordinary cellular metabolism and reproductive processes. In phosphorus limited situations, the resultant growth rate has been shown to be dependent not only on the concentration of phosphate ions, but on the nitrate concentration as well. In the model, the phosphorus-limited growth rate factor is computed in accordance with Michaelis-Menton kinetics:

$$GROP = VMAXP * \frac{PO4}{CMM P + PO4} * \frac{NO3}{CMMNP + NO3}$$

where GROP is the algal growth rate factor (hr^{-1}) under phosphorus-limiting conditions, VMAXP is the maximum growth rate (hr^{-1}) under phosphorus-limiting conditions, CMM P and CMMNP are Michaelis-Menton constants, PO4 is the orthophosphorus concentration in mg/l as P and NO3 is the nitrate-N concentration in mg/l as N. VMAXP is the most sensitive parameter for phosphorus-limited growth calculations. VMAXP values for each reach were based upon typical literature values (26) which were refined during model calibration to produce acceptable mean chlorophyll-a concentrations in each river basin. In general, the river systems with the highest wastewater discharges exhibited the highest VMAXP values, and vice versa. River values ranged from 0.16 hr^{-1} in the James River system, to approximately 0.25 hr^{-1} in the Potomac River system, to approximately 0.30 in the Susquehanna and Patuxent river systems. After accounting for the fact that the Model does not permit algal growth during periods of darkness (i.e., 9-12 hrs per day depending upon the season), the calibrated VMAXP values for river systems are equivalent to $1.9-2.4 \text{ day}^{-1}$ for the James River, $3.2-3.5 \text{ day}^{-1}$ for the Potomac River and $3.6-4.2 \text{ day}^{-1}$ for the Patuxent River. These maximum growth rates are within the range reported by Baca and Arnett (1976) and are typically less than default values recommended for continuous simulation models (2,25) which rely upon non-multiplicative Michaelis-Menton formulations. However, they do fall outside the range of several other literature values for free-floating phytoplankton. It should be emphasized, as indicated above, that these algal growth representations are intended to account for both free-floating and benthic algae as well as adsorption/sedimentation mechanisms for reducing inorganic P and N during instream

transport. Therefore, it is not unusual that the calibrated VMAXP values are in excess of some literature values, because the Basin Model represents two different types of phytoplankton and overall partitioning between organic and inorganic nutrient fractions whereas the literature values typically represent only free-floating phytoplankton.

3. Nitrogen-Limited Growth: Nitrogen is essential to phytoplankton for assimilation of cellular proteins and enzymes. The sum of ammonia-N and nitrate-N concentrations represent the pool of inorganic nitrogen available to support algal growth. The ratio of ammonia-N uptake to nitrate-N uptake is based upon an ammonia preference factor specified by the Model user. In nitrogen-limited situations, the model uses a Michaelis-Menton expression to determine the growth rate factor as a function of the total inorganic nitrogen concentration:

$$GRON = VMAXN * \frac{(NO3 + NH3)}{CMMN + (NO3 + NH3)}$$

where GRON is the algal growth rate factor (hr^{-1}) under nitrogen-limiting conditions, VMAXN is the maximum growth rate (hr^{-1}) under nitrogen limiting conditions, and CMMN is the Michaelis-Menton constant. Simulations of nitrogen-limited conditions typically occurred during extreme low flow periods in reaches with significant wastewater discharges, where ambient inorganic N:inorganic P ratios were less than 10.0. Based upon calibration studies for low flow periods, maximum growth rates (VMAXN) which were typically similar to or slightly higher than VMAXP values were derived.

4. Light-Limited Growth: During each hourly time step, the Model computes the amount of radiation available to phytoplankton in the upper layer of the idealized reservoir by applying computed light adsorption rates to the amount of radiation entering the water. The Model then applies the Michaelis-Menton equation for light-limited growth of phytoplankton:

$$GROL = VMAXLT * \frac{LIGHT}{CMML + LIGHT}$$

where GROL is the phytoplankton growth rate factor (hr^{-1}) under less than optimal light conditions, LIGHT is the light intensity available for algal growth in langley's per minute, and CMML is the Michaelis-Menton constant for light-limited growth. As previously indicated, the Model does not permit growth to occur during night-time hours when solar radiation is set to zero. In general, VMAXLT values were set at levels that restricted light-limiting conditions in river reaches to night-time hours.

CHAPTER V

CALIBRATION/VERIFICATION RESULTS

Introduction

Before the Basin Model could be used to evaluate management strategies, it had to be "fine-tuned" or calibrated to ensure that the model accurately represents the prototype river basins. Following calibration, the model had to be verified by operating it for conditions which are different from the calibration conditions. Three levels of calibration were required for the Basin Model: Basinwide hydrology calibration; nonpoint pollution loading factor calibration for single land use watersheds; and receiving water calibration to set subsurface flow concentrations and rate coefficients for water quality processes.

Hydrology Submodel Calibration/Verification

Methodology. As indicated in Table 2, a total of 14 streamgage records were used for hydrology calibration. The locations of streamgages used for calibration/verification are shown in Figure 12. The period April 1971 through October 1976 was used for model calibration, since this period included a good mixture of relatively wet, dry, and average years. Model verification was based upon the periods April 1966 through June 1970 and November 1976 through December 1978, which were generally somewhat drier than the calibration period. During calibration, the models were operated with meteorologic records for the entire 5.75-yr period and a single set of parameter values. Based on comparisons of simulated and observed streamflows, the most sensitive parameter values were iteratively adjusted to establish the final parameter sets. After acceptable agreement was achieved on a seasonal and annual basis, simulated and observed daily streamflows were compared for each storm event to set hydrograph shape factors and for dry weather flow periods to set baseflow recession constants. Following calibration, the models were operated for the 6.4 year verification period without any adjustment to the calibrated parameter values to determine how well the models represented conditions different from the calibration period.

Since only 3% of the Chesapeake Bay Basin is currently covered by urban development, the calibration activities focused on soils parameters that determine an undeveloped area's hydrologic characteristics. Due to the distribution of raingages and streamgages, it was not possible to calibrate the Basin Model for every major watershed in the 64,000 sq mi drainage area. Therefore, one objective of hydrology calibration was to derive relationships between river basin physical features and model parameter values which could be applied to major watersheds that could not be calibrated separately. In other words, rather than indiscriminately adjusting the model's parameter values to produce the best possible comparisons between simulated and recorded streamflows at each streamgage,

Table 2
USGS Gages Used for Calibration/Verification of Basin Model

MAP KEY ¹	U S G S G A G E		DRAINAGE AREA (KM ²)	CALIBRATION/VERIFICATION	
	NUMBER	NAME		HYDROLOGY	WATER QUALITY
A	02033000	James River at Cartersville, Va.	16,206	X	X
B	01668000	Rappahannock River near Fredericksburg, Va.	4,134	x	X
C	01613000	Potomac River at Hancock, Md.	10,550	X	X
D	01631100	So. Fork Shenandoah River at Front Royal, Va.	4,253		X
E	01636500	Shenandoah River at Millville, WV	7,374	X	X
F	0161800	Potomac River at Shepherdstown, WV	15,374		X
G	01638500	Potomac River at Point of Rocks, MD	24,996		X
H	01646500	Potomac River nr. Washington, D.C.	29,942	X	X
I	01551500	West Branch Susquehanna River at Williamsport, Pa.	14,716	X	
J	01553500	West Branch Susquehanna River at Lewisburg, PA	17,734		X
K	01536500	Susquehanna River at Wilkes- Barre, PA	25,800	X	
L	01540500	Susquehanna River at Danville, PA	29,060		X
M	01567000	Juniata River at Newport, Pa.	8,687	X	X
N	01570500	Susquehanna River at Harrisburg, PA	62,400		X
O	01576000	Susquehanna River at Marietta, PA	67,313	X	
P	01578310	Susquehanna River at Conowingo, MD	70,193	X	X
Q	02042500	Chickahominy River at Providence Forge, VA	642	X	
R	01674000	Mattaponi River at Bowling Green, VA	666	X	
S	01674500	Mattaponi River at Beulahville, VA	1,357	X	
T	EASTERN SHORE GAGES (SUM OF FLOWS)		644	X	
	01491000	Choptank River nr. Greensboro, MD	(293)		
	01487000	Nanticoke River nr. Bridgeville, DE	(194)		
	01485000	Pocomoke River nr. Willards, MD	(157)		

¹ Gage locations are shown in Figure 12.

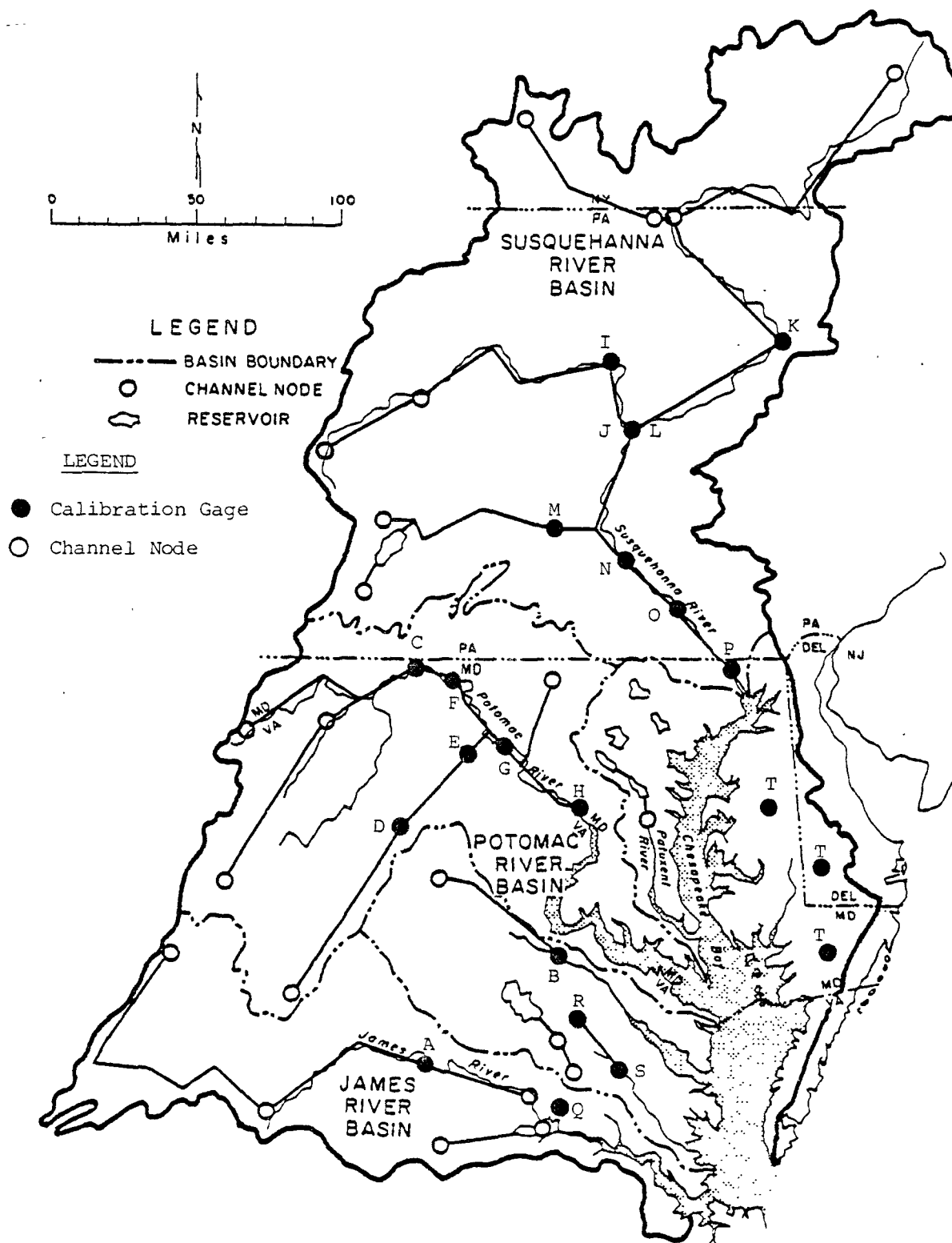


Figure 12. Map Showing Basin Model Channel Network and Calibration/Verification Gages

NOTE: See Table 2 for Map Key

hydrology calibration focused on developing parameter estimation methods that could be applied to ungaged watersheds. This approach has previously been used to calibrate hydrologic models of several watersheds in the Northern Virginia portion of the Chesapeake Bay Basin (27,28).

A summary of the major model parameters which were related to river basin physical features is shown in Table 3. LZSN (lower zone soil moisture storage capacity) and INFIL (infiltration rate) are the most important parameters for simulations of annual streamflow volumes. An increase in LZSN will increase the storage of water in the idealized lower zone of the soil, thereby lowering seasonal and annual streamflows by increasing the depletion of soil moisture through evapotranspiration and by reducing the frequency of saturated soil conditions. An increase in INFIL will likewise lower annual streamflows by reducing direct runoff due to higher infiltration and increasing soil moisture depletion through evapotranspiration. INFIL is most often used to modify seasonal streamflows after LZSN and a reasonable range of INFIL values which achieve acceptable annual streamflows have been identified. As has been the case in previous studies (1,9,27,28,29,30,31), LZSN in the Chesapeake Bay Basin was found to generally be directly related to average total water holding capacity and depth of soil above the restrictive layer. Calibrated LZSN values ranged from approximately 2.0 to 4.0 in. in the Appalachian Plateau and mountainous areas of the Appalachian Ridge and Valley to approximately 6.0 to 8.0 in. in the Coastal Plain, lower Piedmont, and portions of the Appalachian Ridge and Valley. INFIL was found to be related to indicators of surface runoff potential such as hydrologic soil group, soil permeability, and soil texture. Calibrated INFIL values ranged from approximately 0.01 to 0.015 in./hr in the Appalachian Plateau and sections of the Coastal Plain and lower Piedmont with "D" hydrologic soil groups to 0.06 to 0.07 in./hr in sections of the Coastal Plain with "B" hydrologic soil groups. K3 is an evapotranspiration index that is generally set at reasonable levels to reflect vegetative cover, and then held constant while LZSN and INFIL are calibrated. K3 values on the order of 0.3-0.45 were used throughout the Chesapeake Bay Basin, with the higher values typically associated with areas characterized by high forest cover to account for the effect of vegetative cover on evapotranspiration. Although it is not as sensitive a parameter as either LZSN or INFIL, UZSN (i.e., soil moisture storage near the soil surface most closely related to depression storage) can have some effect on seasonal and annual streamflow volumes because of its impact on individual storm events. UZSN is most often related to the calibrated LZSN value and in the Chesapeake Bay Basin was typically found to be 5%-15% of LZSN. After acceptable agreement between simulated and observed streamflows is achieved on an annual and seasonal basis, the interflow coefficient INTER is adjusted to redistribute streamflows between surface runoff and subsurface flows in order to match the shapes of the recession limbs of observed hydrographs. Relatively low INTER values assign more of the streamflows to surface runoff, thereby resulting in higher peak flows and steep recession limbs. Like previous studies (1,9,27,28), Chesapeake Bay Basin calibration results indicated that INTER could be related to average land slopes, with values ranging from 1.0 in relatively flat Coastal Plain areas to 1.5 in

TABLE 3

RELATIONSHIPS BETWEEN HYDROLOGY MODEL
PARAMETERS AND SUB-BASIN PHYSICAL FEATURES

<u>MODEL PARAMETER</u>	<u>DEFINITION</u>	<u>RELATIONSHIPS</u>
LZSN	Nominal capacity of idealized compartment for lower zone soil moisture storage	LZSN is related to Total Water Holding Capacity
INFIL	Infiltration rate parameter	INFIL is related to Hydrologic Soil Group, Soil permeability, and Soil Texture of Upper Layers
K3	Index to actual evapotranspiration	K3 is related to vegetative cover
UZSN	Nominal capacity of idealized compartment for upper zone soil moisture storage	UZSN is related to LZSN
INTER	Interflow coefficient	INTER is related to topography

mountainous areas. After INTER had been set, the baseflow recession coefficient (KK24) was fine tuned to improve the agreement between simulated and observed dry weather flows.

Results. Calibration/verification runs were terminated for each streamgage when it was determined that the differences between simulated and observed streamflows could not be improved with further parameter set adjustment and a sufficient number of model runs had been completed to develop reasonable regional parameter sets. The calibrated parameter values for the sub-basins located above the fall line are summarized in Table 4. The hydrology parameter sets produced by these calibration/verification runs are quite reasonable based upon some previous continuous simulation modeling studies in the Chesapeake Basin (1,9,16,17,27,28) and other literature values (5,30,32).

Comparisons of simulated and observed streamflow data based upon streamflow volumes (annual and seasonal), daily streamflow time series, and daily flow-duration plots (period of record and seasonal) generally indicate very good calibration and verification results. Table 5 summarizes comparisons of simulated and observed annual streamflow volumes for 14 streamgages. As may be seen, differences between simulated and observed annual volumes are typically within the range of observation errors (e.g., $\pm 20\%$) associated with meteorologic and streamflow data collection activities (33). In general, the greatest differences between simulated and observed streamflow were associated with winter periods and drought periods. Winter periods, which were typically somewhat undersimulated by the Model, tend to be characterized by frozen ground conditions which are not simulated by the River Basin Model as well as the highest raingage errors due to freezing conditions. Since winter periods are not expected to be used for water quality assessments due to the relatively high assimilative capacities of most receiving waters, the higher errors in winter flow simulations are not of serious concern. Streamflow errors during drought periods, which were typically oversimulated by the River Basin Model, can be attributed in large part to the tendency of the Thiessen-weighting procedure to exaggerate the areal distribution of localized storms which tend to be more significant during droughts.

Comparisons of simulated and observed daily flow-duration curves are shown in Figures 13 through 21 for both calibration and verification periods at nine major river streamgages. As may be seen, the agreement between simulated and observed curves is typically quite good, with goodness-of-fit for the verification period typically almost as good as for the calibration period. In general, the calibration period exhibits better agreement for low flow periods than does the verification period, which was characterized by drought periods that presented difficulties with the development of a representative mean segment rainfall record.

As another indication of goodness-of-fit, Table 6 summarizes statistics on the correlation between simulated and observed weekly streamflows at the nine gages covered by Figures 13 through 21. Correlation coefficients are

Table 4

HYDROLOGY PARAMETERS

SUB-BASIN	AREA ⁴ (x 10 ⁴ acres)	LZSN	UZSN	INFIL	INTER	K3	NN	L	SS	KRER
RCH 10	166.27	2.500	0.210	0.015	1.444	0.40	0.35	400.	0.117	0.260
RCH 20	317.06	2.200	0.210	0.012	1.370	0.40	0.35	400.	0.080	0.300
RCH 30	154.11	2.263	0.210	0.015	1.446	0.40	0.35	400.	0.118	0.252
RCH 40	89.408	3.857	0.382	0.0208	1.422	0.40	0.35	338.	0.108	0.241
RCH 50	93.568	2.000	0.150	0.015	1.390	0.40	0.35	300.	0.090	0.300
RCH 60	270.08	2.282	0.161	0.0126	1.515	0.40	0.35	300.	0.161	0.266
RCH 70	80.704	3.742	0.319	0.0192	1.433	0.40	0.35	340.	0.113	0.248
RCH 80	152.70	4.216	0.3947	0.0268	1.405	0.40	0.35	300.	0.098	0.240
RCH 90	61.44	3.640	0.220	0.024	1.450	0.40	0.35	300.	0.120	0.230
RCH 100	157.06	3.814	0.287	0.0258	1.429	0.40	0.35	300.	0.109	0.234
RCH 110	120.96	5.582	0.557	0.031	1.302	0.40	0.35	360.	0.063	0.295
RCH 120	51.456	6.455	0.645	0.0349	1.250	0.40	0.35	400.	0.047	0.327
RCH 140	19.584	7.165	0.716	0.0162	1.203	0.40	0.35	400.	0.031	0.358
RCH 160	85.696	5.000	0.500	0.024	1.390	0.40	0.35	300.	0.126	0.250
RCH 170	95.552	5.000	0.500	0.040	1.460	0.40	0.35	300.	0.146	0.230
RCH 175	79.424	5.000	0.500	0.0298	1.415	0.40	0.35	300.	0.133	0.243
RCH 180	161.15	7.010	1.002	0.0233	1.377	0.33	0.35	300.	0.0952	0.283

Table 4 (continued)

HYDROLOGY PARAMETERS

SUB-BASIN	AREA (x 10 acres)	LZSN	UZSN	INFIL	INTER	K3	NN	L	SS	KRER
RCH 190	105.09	7.280	1.070	0.0301	1.452	0.32	0.35	300.	0.126	0.283
RCH 200	90.752	7.224	1.056	0.0293	1.430	0.33	0.35	300.	0.116	0.282
RCH 210	63.488	6.300	0.630	0.039	1.260	0.40	0.35	400.	0.050	0.320
RCH 220	59.328	5.560	0.560	0.015	1.190	0.40	0.35	400.	0.030	0.320
RCH 230	102.14	6.150	0.620	0.026	1.300	0.45	0.35	400.	0.060	0.310
RCH 235	16.448	6.362	0.727	0.0245	1.253	0.45	0.35	425.	0.050	0.303
RCH 240	22.016	6.817	0.958	0.0213	1.151	0.45	0.35	478.	0.029	0.286
RCH 250	21.952	6.150	0.620	0.026	1.300	0.45	0.35	400.	0.060	0.310
RCH 260	47.232	6.810	0.686	0.026	1.210	0.45	0.35	400.	0.036	0.322
RCH 265,270	208.58	5.830	0.689	0.058	1.496	0.42	0.35	300.	0.143	0.269
RCH 280	191.87	6.293	0.634	0.026	1.280	0.45	0.35	400.	0.055	0.313
RCH 290	32.064	7.250	0.730	0.026	1.150	0.45	0.35	400.	0.020	0.330
RCH 300,310,320	86.019	7.250	0.730	0.026	1.150	0.45	0.35	400.	0.020	0.330
RCH 330,340	22.269	6.760	0.769	0.017	1.163	0.40	0.35	436.	0.026	0.368

Table 4 (continued)

HYDROLOGY PARAMETERS
Coastal Basins

SUB-BASIN	AREA (x 10 ⁴ acres)	LZSN	UZSN	INFIL	INTER	K3	NN	L	SS	KRER
ANACOSTIA	8.136	6.212	0.842	0.016	1.120	0.40	0.35	475.	0.021	0.375
BALT. HARBOR	10.103	6.650	0.788	0.016	1.155	0.40	0.35	442.	0.025	0.368
BOHEMIA	3.624	4.390	0.440	0.012	1.0	0.40	0.35	500.	0.010	0.370
CHESTER	26.274	5.034	0.504	0.035	1.148	0.35	0.35	500.	0.010	0.331
CHICKAHOMINY	15.952	7.052	0.984	0.021	1.118	0.45	0.35	479.	0.020	0.290
CHOPTANK	37.937	5.559	0.556	0.054	1.268	0.31	0.35	500.	0.010	0.299
ELIZABETH	1.616	5.660	0.566	0.056	1.0	0.40	0.35	500.	0.010	0.250
GREAT WILCOM.	4.149	6.930	1.040	0.022	1.084	0.40	0.35	500.	0.017	0.290
GUNPOWDER	27.912	6.926	0.714	0.020	1.204	0.40	0.35	408.	0.033	0.353
JAMES	83.576	6.854	0.910	0.032	1.075	0.42	0.35	471.	0.016	0.293
LOWER PATUX.	34.303	6.430	0.708	0.049	1.103	0.40	0.35	500.	0.019	0.384
NANSEMOND	13.481	6.405	0.884	0.043	1.016	0.40	0.35	500.	0.011	0.272
NANTICOKE	51.552	5.212	0.521	0.068	1.270	0.31	0.35	500.	0.010	0.298
OCCOQUAN	38.634	5.579	0.566	0.015	1.191	0.40	0.35	401.	0.030	0.320
PATAPSCO	27.084	6.607	0.733	0.023	1.192	0.40	0.35	425.	0.033	0.353
POCOMOKE	44.79	5.029	0.503	0.056	1.211	0.33	0.35	500.	0.010	0.314
POTOMAC	117.30	6.274	0.852	0.021	1.121	0.40	0.35	477.	0.023	0.339

Table 4 (continued)

HYDROLOGY PARAMETERS
Coastal Basins

SUB-BASIN	AREA ⁴ (x 10 ⁴ acres)	LZSN	UZSN	INFIL	INTER	K3	NN	L	SS	KRER
RAPPAHANNOCK	59.161	6.954	1.035	0.021	1.106	0.43	0.35	497.	0.020	0.284
SEVERN	3.764	6.324	0.722	0.045	1.102	0.40	0.35	500.	0.019	0.387
WICOMICO	12.758	5.086	0.509	0.060	1.230	0.32	0.35	500.	0.010	0.309
WYE	8.095	5.199	0.520	0.041	1.185	0.34	0.35	500.	0.010	0.321
YORK	58.66	6.956	1.034	0.021	1.106	0.45	0.35	500.	0.020	0.279
COASTAL 1	40.465	4.464	0.447	0.015	1.017	0.39	0.35	500.	0.010	0.365
COASTAL 4	19.055	5.700	0.571	0.056	1.035	0.39	0.35	500.	0.010	0.263
COASTAL 5	13.217	6.450	0.659	0.056	1.106	0.40	0.35	500.	0.020	0.390
COASTAL 6	3.082	5.880	0.882	0.017	1.094	0.40	0.35	500.	0.018	0.380
COASTAL 8	27.757	6.990	1.049	0.020	1.106	0.44	0.35	500.	0.020	0.281
COASTAL 9	19.337	6.083	0.719	0.045	1.035	0.42	0.35	500.	0.013	0.259
COASTAL 11	46.580	6.972	0.741	0.015	1.181	0.40	0.35	416.	0.028	0.363

COMPARISON OF STREAMFLOW VOLUMES FOR CALIBRATION/VERIFICATION PERIODS

STREAMGAGE	DRAINAGE AREA (SQ. MI.)	"LANDS" SEGMENTS	RATIO OF SIMULATED TO OBSERVED WATER YEAR FLOW VOLUMES			
			CALIBRATION PERIOD		VERIFICATION PERIOD	
			MEAN	NO. OF WATER YEARS WITH 0.8 ≤ RATIO ≤ 1.2	MEAN	NO. OF WATER YEARS WITH 0.8 ≤ RATIO ≤ 1.2
JAMES RIVER AT CARTERSVILLE, VA. (#02035000)	6,257	14,15,17,18	0.96 ±0.17	5 out of 6	0.96 ±0.2	4 out of 5
RAPPAHANNOCK RIVER NEAR FREDERICKSBURG, VA. (#01668000)	1,596	14	1.0 ±0.22	5 out of 6	0.93 ±0.15	4 out of 5
POTOMAC RIVER AT HANCOCK, MD. (#01613000)	4,073	19,20	0.88 ±0.06	6 out of 6	0.95 ±0.13	5 out of 5
SIEMANDON RIVER AT MILLVILLE, W.VA. (#01636500)	3,040	16,17,19	1.1 ±0.13	5 out of 6	1.07 ±0.27	3 out of 5
POTOMAC RIVER NEAR WASHINGTON, D.C. (#01646500)	11,560	12,13,16,17,19,20	0.94 ±0.06	6 out of 6	0.94 ±0.10	5 out of 5
SUSQUEHANNA RIVER AT WILKES-BARRE, PA. (#01536500)	9,960	27,28,29,30	0.94 ±0.05	6 out of 6	1.0 ±0.04	5 out of 5
WEST BR. SUSQUEHANNA RIVER AT WILLIAMSPORT, PA. (#01551500)	5,682	22,25,26	0.93 ±0.03	6 out of 6	1.01 ±0.07	5 out of 5
JUNIATA RIVER AT NEWPORT, PA. (#01567000)	3,354	21,23	0.93 ±0.05	6 out of 6	1.15 ±0.2	4 out of 5
SUSQUEHANNA RIVER AT MARIETTA, PA. (#01570500)	25,990	21-30	0.90 ±0.04	6 out of 6	0.99 ±0.04	5 out of 5
SUSQUEHANNA RIVER AT CONWINGO, MD. (#01578310)	27,100	21-30,11,12	0.91 ±0.04	6 out of 6	0.97 ±0.05	4 out of 4
EASTERN SHORE A. CHOPTANK R. NR. GREENSBORO, MD. (#01491000)	113					
B. NANTICOKE R. NR. BRIDGEVILLE, DELAWARE (#01487000)	75					
C. POCOMOKE R. NR. WILLARDS, MD. (#01485000)	60.5					
D. TOTAL	248.5	2,3	0.99 ±0.06	6 out of 6	0.9 ±0.19 (1.04 ±0.06 for WY 68-69, 76-77, 77-78)	3 out of 5
CHICKAHOMINY RIVER AT PROVIDENCE FORGE, VA. (#02042500)	248	8	0.98 ±0.12	5 out of 6	1.31 ±0.12	2 out of 5
MATTAPONI RIVER AT BOWLING GREEN, VA. (#01674000)	257	8,14	1.00 ±0.17	5 out of 6	1.23 ±0.17	2 out of 5
MATTAPONI RIVER AT BEULAHVILLE, VA. (#01674500)	601	8,14	0.94 ±0.15	6 out of 6	1.23 ±0.07	3 out of 5

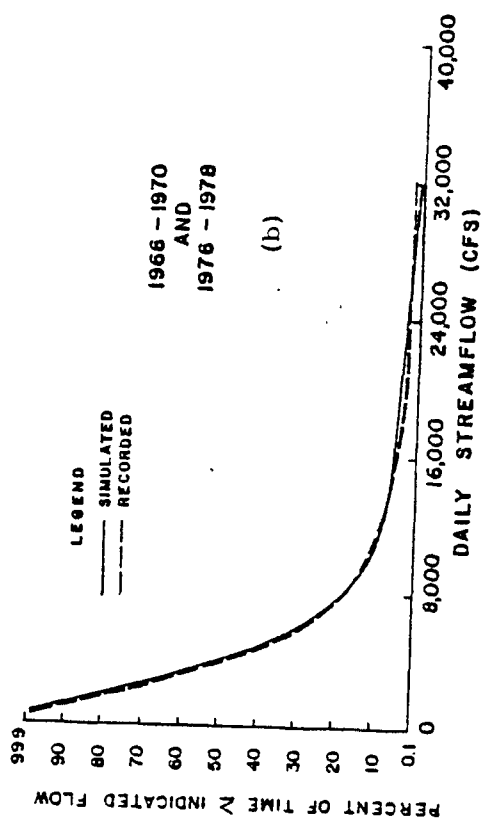
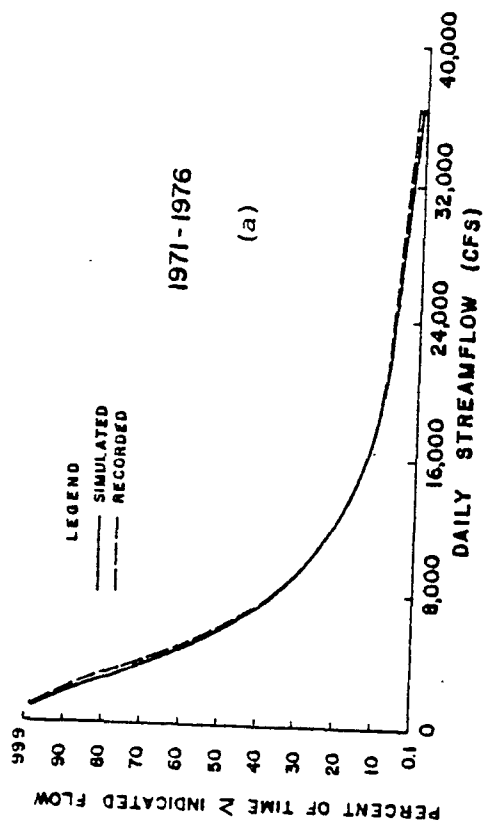


Figure 13. Flow-Duration Curves for
Calibration (a) and Verification (b)
Periods: James River at Cartersville,
VA (6,257 sq mi)

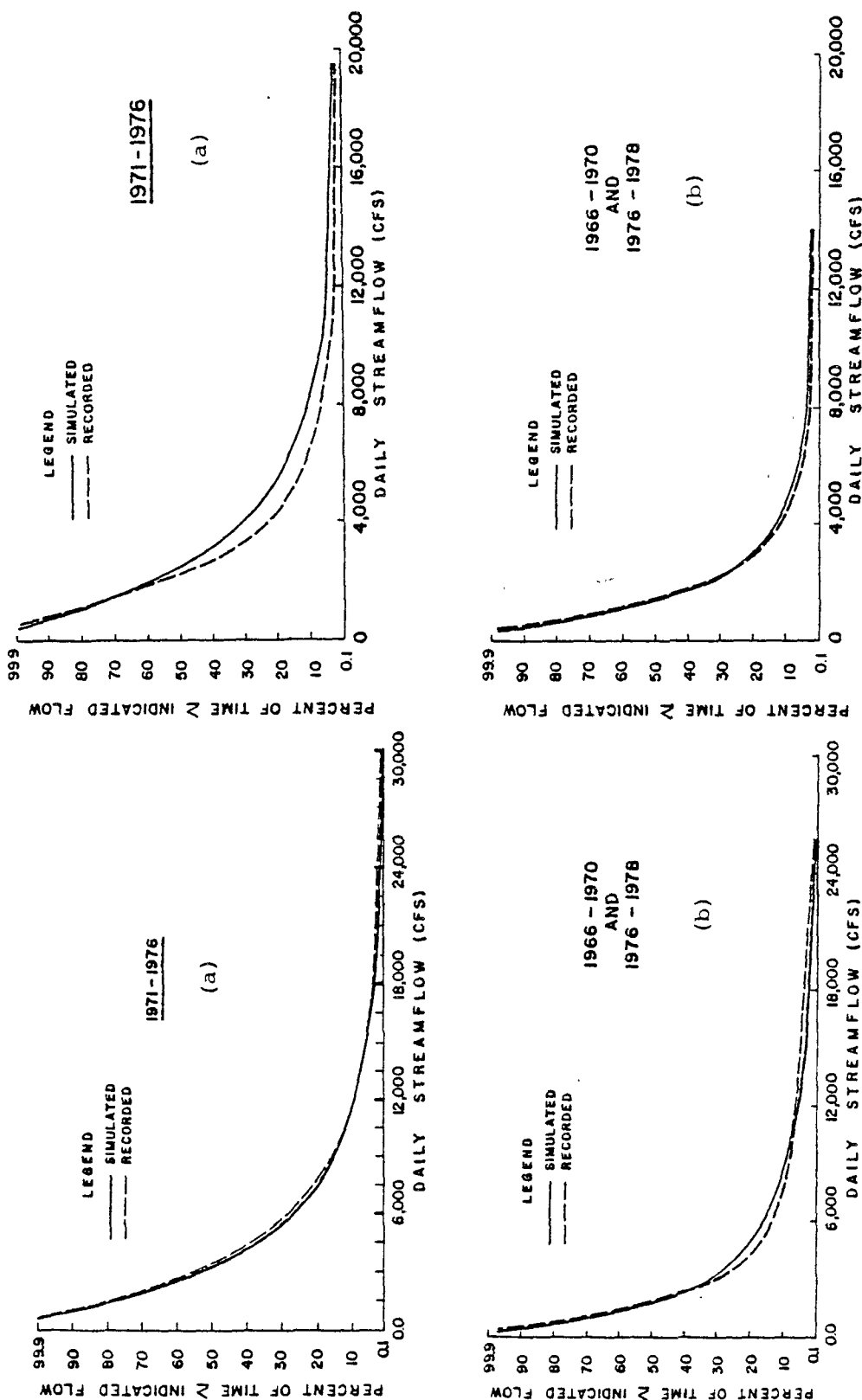


Figure 15. Flow-Duration Curves for
 Calibration (a) and Verification (b)
 Periods: Shenandoah River at
 Millville, W.VA. (3,040 sq mi)

Figure 14. Flow-Duration Curves for
 Calibration (a) and Verification (b)
 Periods: Potomac River at Hancock,
 MD (4,073 sq mi)

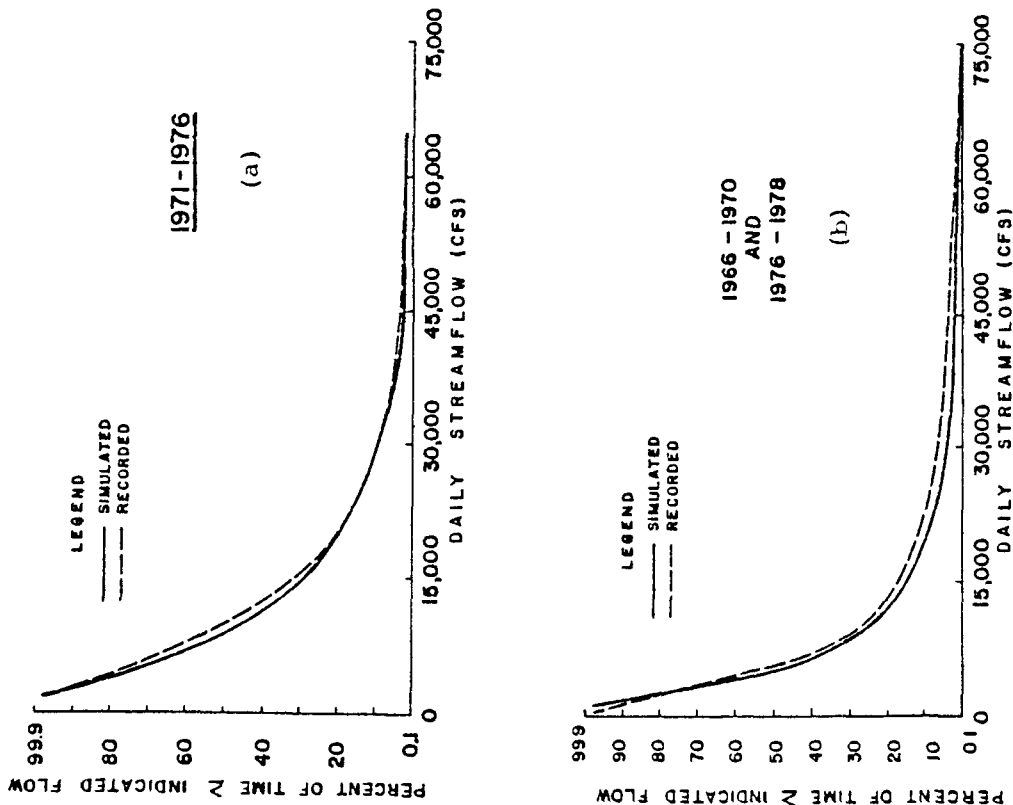


Figure 16. Flow-Duration Curves for
Calibration (a) and Verification (b)
Periods: Potomac River near
Washington, D.C. (11,560 sq mi)

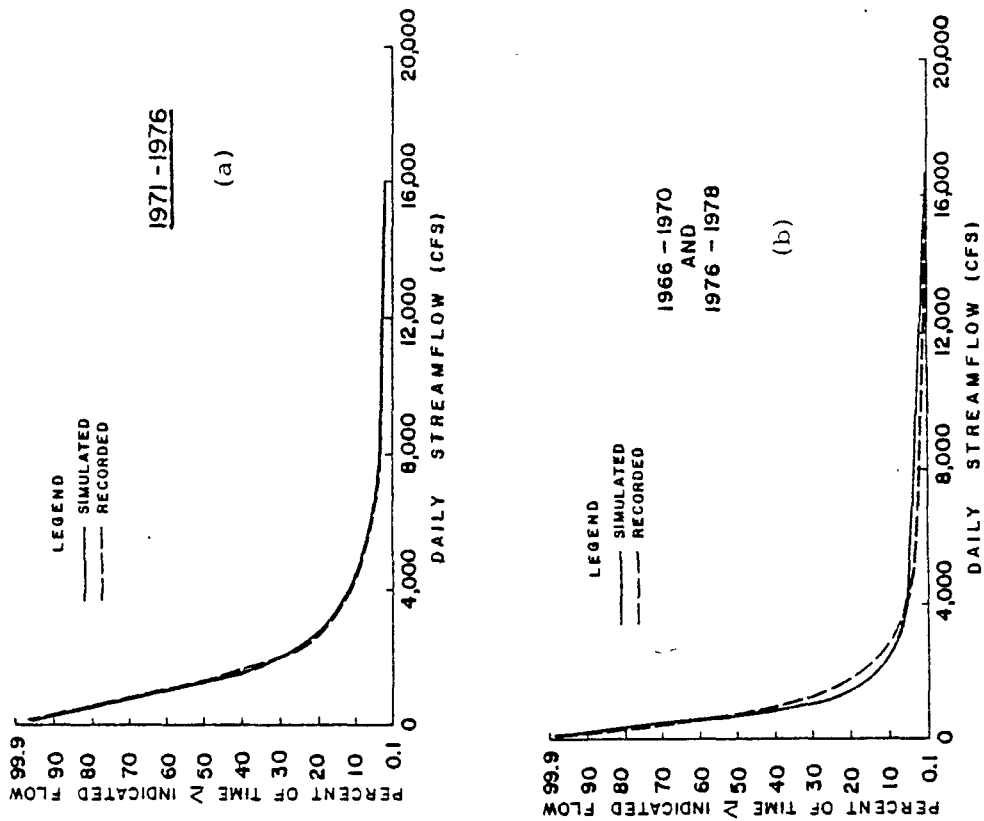


Figure 17. Flow-Duration Curves for
Calibration (a) and Verification (b)
Periods: Rappahannock River at
Fredericksburg, VA (1,596 sq mi)

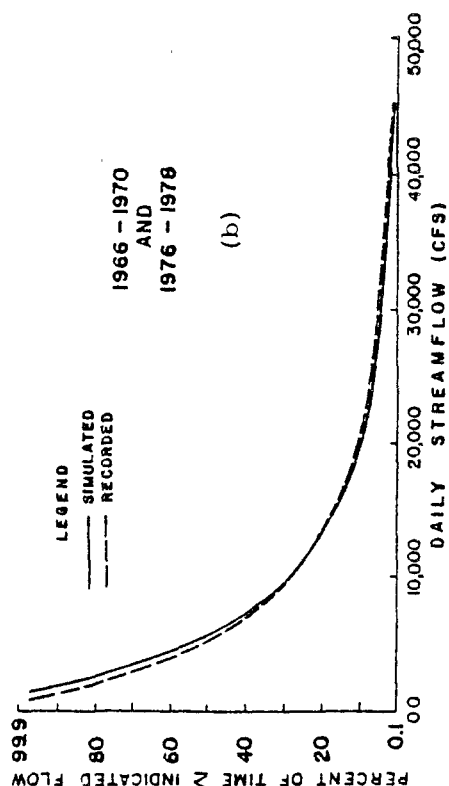
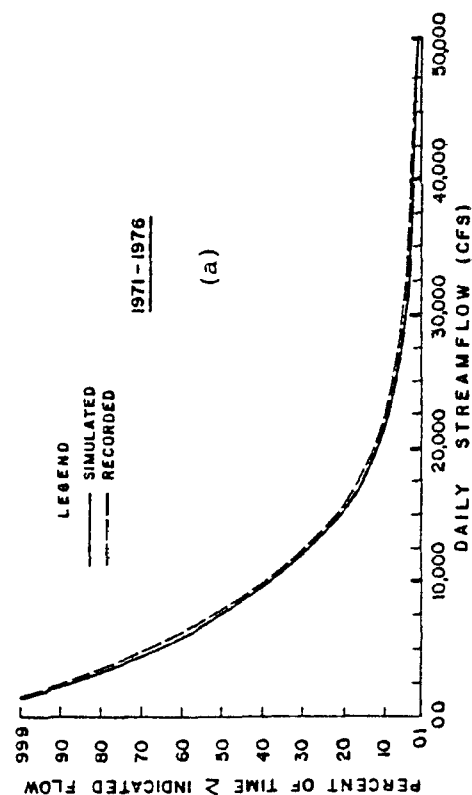


Figure 18. Flow-Duration Curves for
Calibration (a) and Verification (b)
Periods: West Branch Susquehanna
River at Williamsport, PA
(5,682 sq mi)

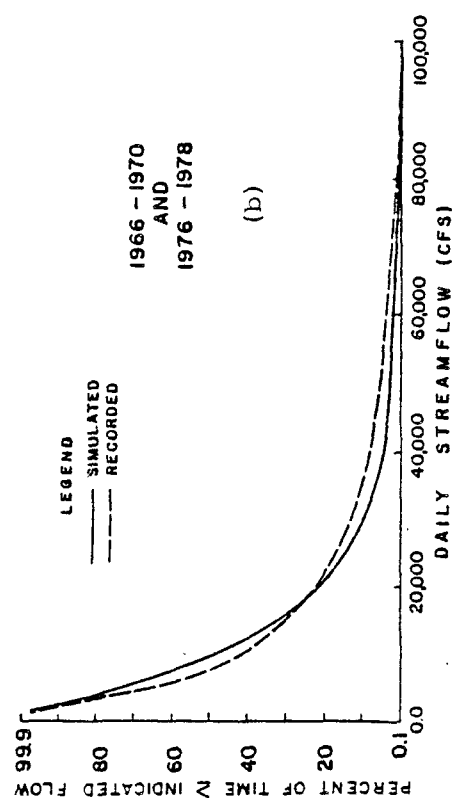
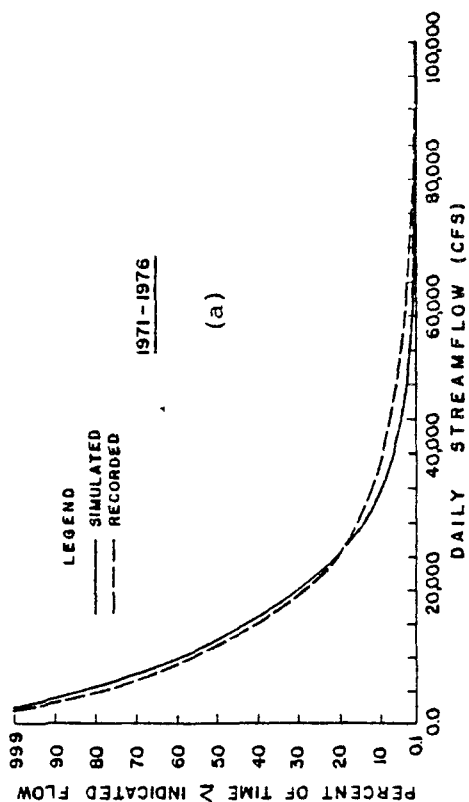


Figure 19. Flow-Duration Curves for
Calibration (a) and Verification (b)
Periods: Susquehanna River at
Wilkes-Barre, PA (9,960 sq mi)

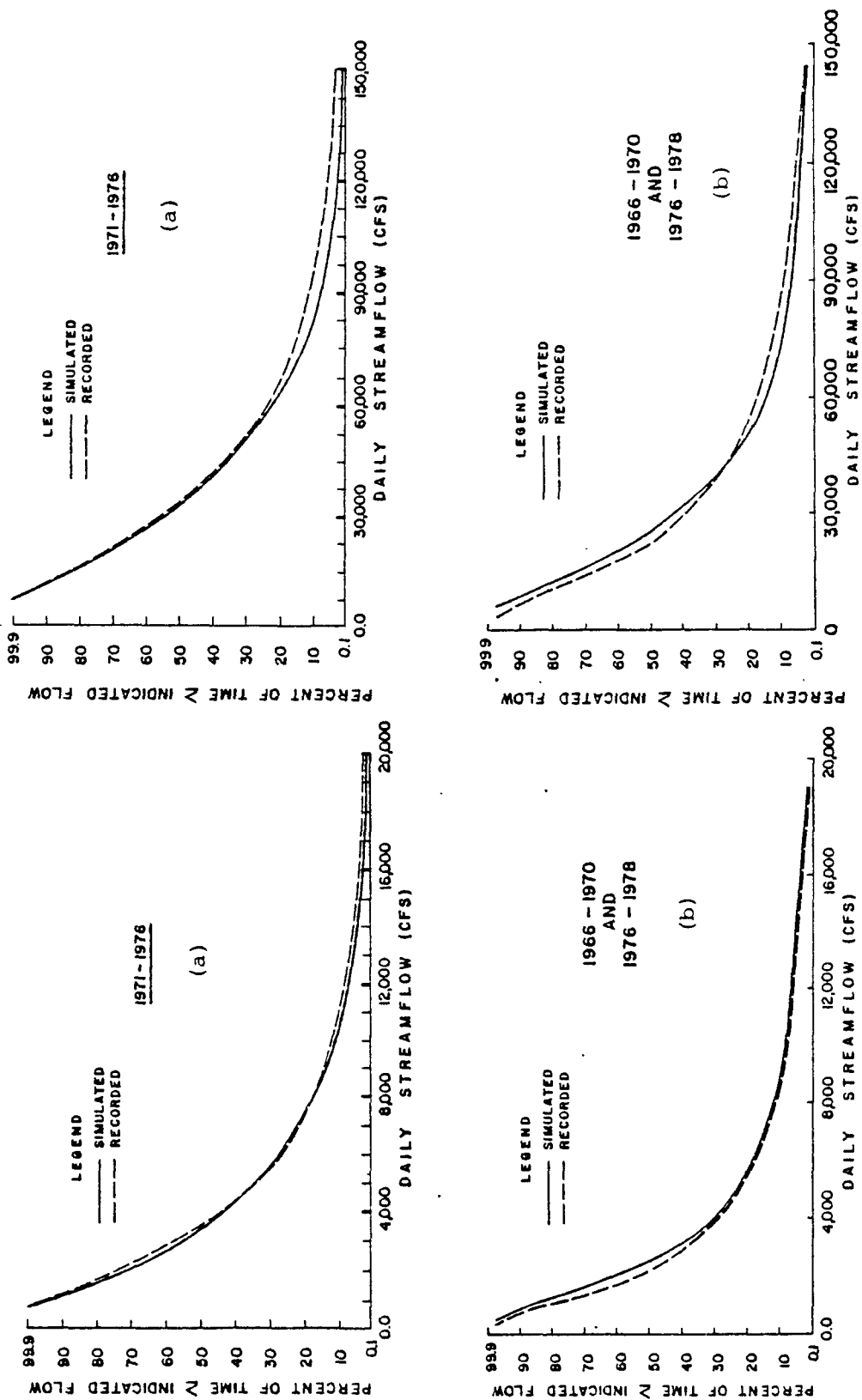


Figure 20. Flow-Duration Curves for Calibration (a) and Verification (b) Periods: Juniata River at Newport, PA (3,354 sq mi)

Figure 21. Flow-Duration Curves for Calibration (a) and Verification (b) Periods: Susquehanna River at Marietta, PA (25,990 sq mi)

Table 6

Correlation Coefficients for Weekly Streamflows at Major River Gages

STREAMGAGE	CORRELATION COEFFICIENT (WEEKLY STREAMFLOWS)	
	CALIBRATION PERIOD	VERIFICATION PERIOD
James River at Cartersville, VA	0.94	0.84
Potomac River at Hancock, MD	0.91	0.78
Shenandoah River at Millville, WV	0.92	0.74
Potomac River near Washington, D.C.	0.95	0.80
Rappahannock River near Fredericksburg, VA	0.85	0.81
West Branch Susquehanna River at Williamsport, PA	0.85	0.71
Susquehanna River at Wilkes-Barre, PA	0.88	0.74
Juniata River at Newport, PA	0.86	0.81
Susquehanna River at Marietta, PA	0.92	0.80

based upon weekly streamflows because weekly-to-monthly flows were of greatest interest for the pollutant transport study. As may be seen in Table 6, correlation coefficients for the calibration period are somewhat higher than for the verification period, although coefficients for both periods are within acceptable ranges. The gages at the mouths of the three largest river basins are characterized by the highest correlation coefficients.

Comparisons of simulated and observed hydrographs for Hurricane Agnes (late June 1972) and Tropical Storm Eloise (late September 1975) reveal that the Model appears to handle these relatively infrequent events rather well at some gages. Sample comparisons are presented in Figure 22 for the gages on the West Branch Susquehanna River at Williamsport, Pennsylvania and on the Potomac River at Hancock, Maryland. It is felt that the River Basin Model handled infrequent storm events better than some earlier models (1,27) of smaller watersheds in large part because the rainfall during these storms tends to be rather uniformly distributed over sub-basins with areas on the order of 2,000 sq mi.

In summary, both calibration and verification results are very good particularly, in light of the very large rainfall segments (e.g., approximately 2,100 sq mi on the average). Most of the remaining error can probably be attributed to factors such as frozen ground conditions which were not explicitly represented by the Model and errors in the mean segment rainfall record due to localized rainstorms, low raingage densities in some areas, missing rainfall records, and freezing conditions (34).

Calibration/Verification of Nonpoint Pollution Loading Submodel

Introduction. Nonpoint pollution loading factors were developed for urban and rural-agricultural land use categories by calibrating the nonpoint pollution loading submodel with monitoring data collected by intensive test watershed studies. Approximately 70 years of nonpoint pollution monitoring data collected at more than 50 test watersheds was analyzed to develop the nonpoint pollution loading factors used in the Basin Model.

A total of 27 test watersheds suitable for nonpoint pollution loading characterizations were monitored from late 1979 through mid-1981 under a \$2.5 million study funded by the EPA Chesapeake Bay Program (EPA/CBP). These EPA/CBP testing sites were distributed among the Occoquan River Basin (6 sites) in northern Virginia, the Pequea Creek Watershed (3 sites) in southern Pennsylvania, the Ware River Basin (4 sites) in southeastern Virginia, and the Patuxent (5 sites) and Chester River (9 sites) basins in Maryland. As may be seen in Figure 23, the test watersheds were located in Coastal Plain and Piedmont river basins in the vicinity of the Bay's estuarine system. In the majority of cases, the test watershed sites covered only one land use category. Nonpoint pollution loading data collected at the EPA/CBP test watershed sites was used to develop loading factors for the following rural-agricultural land use categories: forestland, pasture land, high tillage cropland, and low tillage cropland.

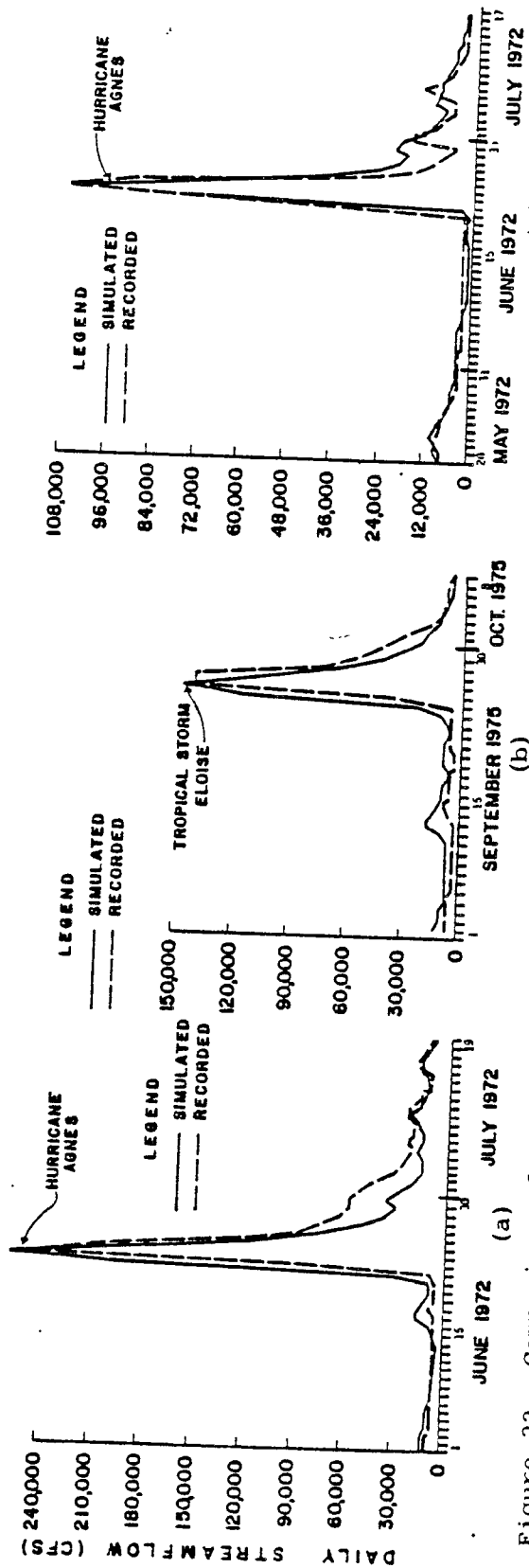


Figure 22. Comparison of Simulated and Recorded Hydrographs: (a) and (b) West Br. Susquehanna River at Williamsport, PA; and (c) Potomac River at Hancock, MD

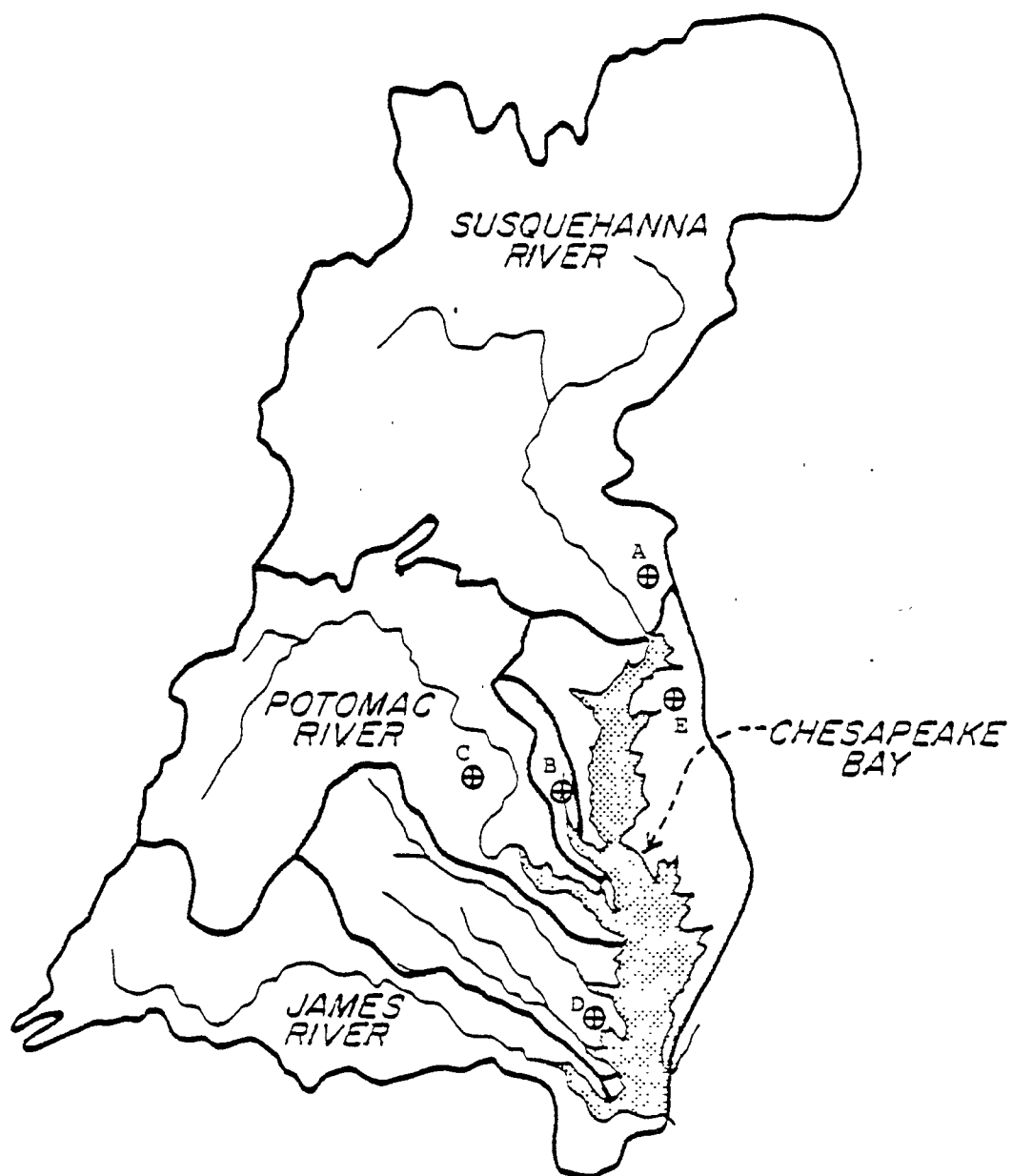


Figure 23. Map Showing Location of River Basins Subjected to EPA/CBP Test Watershed Studies: Pequea Creek (A), Patuxent River (B), Occoquan River (C), Ware River (D), and Chester River (E)

Urban nonpoint pollution loading factors developed by a previous twelve-month (1976-1977) test watershed monitoring study in northern Virginia were the principal sources of data for characterizing total P and total N loadings from different urban land use categories (7,8,9). The urban loading factors developed from northern Virginia testing site data were verified at three urban test watersheds covered by the EPA/CBP monitoring study. In addition, nonpoint pollution loading data collected at 10 urban testing sites in the Metropolitan Washington region under the 1980-1981 Nationwide Urban Runoff Program (NURP) was used to refine the distribution between organic and inorganic nutrient fractions for nitrogen and phosphorus loadings in urban runoff.

Each test watershed site was equipped with a flowmeter, automatic sampler, and was served by a continuous recording raingauge located within or nearby the site. Either a natural (e.g., ephemeral stream) or artificial (e.g., H-flume, Parshall flume, storm sewer) drainage control was typically used to establish stage-discharge relationships at the outlet of each watershed. The sampling interval was generally automatically initiated by the flowmeter at the start of a runoff event. For studies which relied upon flow-composite sampling methods, the flowmeter activated the sampler at preselected increments of runoff volume. For studies which relied upon sequential-discrete sampling methods (i.e., collection of discrete samples at numerous points along the runoff hydrograph), the flowmeter activated the sampler at preselected stage increments. At the larger sites which exhibited dry weather flow, baseflow samples were periodically collected. Runoff and baseflow samples were analyzed for plant nutrients and total suspended solids, with periodic analyses for organics.

At the time the EPA/CBP test watershed monitoring studies were designed and implemented, a work program for data management and model calibration had not yet been developed, although a follow-up modeling study was under consideration. The absence of a modeling study work program at the start of the monitoring studies tended to significantly complicate data reduction/management activities during the modeling effort and to reduce the amount of monitoring data that was suitable for model calibration studies. A later section of this chapter discusses specific problems and recommendations for coordinating future test watershed monitoring and modeling investigations.

Data Reduction/Management Requirements for Model Calibration. This section focusses on the data reduction/management requirements for the EPA/CBP testing sites. Requirements for the earlier studies of urban test watersheds in northern Virginia and the metropolitan Washington region were similar and are summarized elsewhere (REFS).

The test watershed monitoring investigators reduced the data required to characterize the runoff pollution loadings from each runoff and baseflow sample. Investigators who relied upon flow-composite sampling techniques reported mean flow rate and mean concentration data for the runoff or baseflow sampling interval, while investigators who relied upon

sequential-discrete sampling methods reported instantaneous flow rate and instantaneous concentration for each runoff or baseflow sample. All other meteorologic and hydrologic data required for model calibration typically had to be reduced by the modeling investigator.

Since the test watersheds were relatively small, a 15-minute time step was required for the continuous rainfall record to ensure that the rainfall interval was not significantly greater than the watershed's time of concentration. Drum raingage stripcharts used at the Pequea Creek and Ware River basin sites were manually reduced, while other rainfall stripcharts were reduced with a Numonics digitizer equipped with software to create files with the appropriate time-step. Approximately 1.0-1.5 yrs of stripchart record was reduced for the modeling studies. Since the monitoring investigators were only required to report and analyze water quality monitoring data, raingage maintenance appeared to receive the lowest priority of all equipment checks and considerable gaps were found in the onsite records. During periods when the sampling station was shut down due to a breakdown of either the flowmeter or automatic sampler, the raingage was sometimes shut down until water quality sampling was resumed. Since a continuous simulation model requires rainfall records covering the periods between monitored runoff events in order to calculate antecedent soil moisture and sediment accumulations for each monitored storm, missing rainfall records for periods when the onsite raingage was shut down had to be constructed from a nearby raingage. Separate software was developed to create a continuous rainfall file for input to the NPS model.

The other meteorologic input file required for the NPS model calibration study is a time series of daily potential evapotranspiration for the test watershed monitoring period. A continuous potential ET record was developed for each river based upon meteorologic data at the nearest NWS station.

Since it is advisable to use a long-term runoff record to calibrate a continuous simulation model, the reported flow records for runoff events with water quality samples were expanded to include all flow records collected during the monitoring period. Although all monitoring sites were equipped with continuous recording flowmeters, the Pequea Creek test watersheds were the only sites with a complete daily streamflow record. The flow records at some sites were restricted to those runoff events with water quality samples. Stripcharts with additional flow records were reduced with the same digitizer software used to construct rainfall records.

Since the quality control programs of most monitoring investigators concentrated on laboratory analyses, the modeling investigator was required to perform most of the quality assurance checks on the hydrometeorologic datasets. The digitized rainfall and runoff records were integrated for each storm event and rainfall and runoff volumes were compared to identify potential water balance problems due to such factors as backwater, an incorrect stage-discharge relationship or an error in the reported flowmeter setting. Flow stripcharts for monitored storms were also checked for "flat-top" hydrographs which indicated that the maximum stage exceeded the

full-scale setting of the flowmeter. In cases of spurious rainfall/runoff ratios or "flat-top" hydrographs, the runoff and water quality data were deleted from the observed dataset for model calibration.

Software was developed to calculate total storm loads from datasets with mean or instantaneous flow rates and concentrations for each runoff sample. For test watersheds with flow-composite samples, the product of mean flow rate and mean concentration was multiplied by the storm duration to calculate total load. For test watersheds with sequential discrete samples, the time series of instantaneous loading rates (i.e., product of instantaneous flow rate and concentration) was numerically integrated between the first and last sample time to calculate total loads for each storm. Mean storm concentrations were also calculated for the sequential discrete sampling datasets. Dry weather flow concentration statistics were calculated for test watersheds with significant amounts of baseflow.

Land use and drainage area data was typically based upon maps, drawings, and tables compiled by the monitoring investigator, which were checked through site inspections and with available aerial photographs and topographic maps. At one test watershed where a check of rainfall/runoff ratios revealed a serious water balance problem, the authors performed a plane-table survey which produced a significant increase in the drainage area and more reasonable rainfall/runoff relationships. For urban test watersheds, percent imperviousness was determined by planimetry of aerial photographs or site plans.

Soils characteristics for each test watershed were derived from county soil series maps and surveys. The predominant hydrologic soil group was determined and average values of permeability, total water holding capacity, and erodibility were calculated for use in deriving hydrologic and nonpoint pollution model parameters.

Average overland flow slope was typically reported by the monitoring investigator. Reported values were checked with 1:24,000 scale maps of the test watershed and surrounding areas.

For cropland sites, data on monthly vegetative cover and the timing and extent of tillage activities are required to accurately model soil loss. Based upon discussions with local SCS staff and information on the timing and extent of harvest and tillage operations at the test watershed, a time series of monthly ground cover was derived for each cropland site. Since the NPS model does not permit the user to alter ground cover time series from year-to-year, two different input datasets were sometimes required to model cropland watersheds with more than one year of monitoring data due to changes in harvest and or tillage dates from one year to the next. The monthly ground cover time series and tillage parameter values were refined during model calibration to help achieve acceptable agreement between simulated and observed sediment loadings.

Although the monitoring investigators made an effort to select test watersheds which included only one land use, finding an acceptable catchment

with a single land use was not always possible. For test watersheds with a mixed land use pattern, aerial photographs of the test watershed were checked to determine the character and extent of any secondary land uses. In cases where nonpoint pollution loading rates from the secondary land use were significantly higher than the loading rates for the primary land use, the complexity of the model calibration study was significantly greater. An example is the forestland test watershed (Site #2) in the Pequea Creek basin which included a high-tillage cropping site (approximately 13% of drainage area) that contributed the majority of the nonpoint pollution loads during major storm events. In such a case, loading factors for the secondary land use had to be set based on model calibration for a similar test watershed prior to model calibration at the mixed land use site. Also, the monitoring dataset had to be screened to identify those storm events (e.g., minor runoff events in the case of Pequea #2) which are least likely to be characterized by major nonpoint pollution loading contributions from the secondary land use.

EPA/CBP Test Watershed Model Calibration: Site Selection. Not all of the test watersheds were characterized by sufficient land use homogeneity and hydrometeorologic data to permit NPS model calibration. Sufficient hydrometeorologic and water quality data was available to calibrate the NPS model to 11 of the 12 acceptable sites in the Occoquan River, Ware River, and Pequea Creek basins. A summary of the sites with monitoring records suitable for model calibration is shown in Table 7. Due to the late start of the Maryland test watershed studies, insufficient hydrometeorologic data was available for model calibration of the single land use sites in the Patuxent and Chester basin sites. Therefore, only statistical analyses could be performed on the Maryland testing site database prior to the initiation of Basin Model calibration/verification runs in the Fall of 1981. Following completion of Basin Model production runs in the Spring of 1982, nonpoint pollution loading factors calibrated for the Virginia and Pennsylvania testing sites were successfully verified at two Maryland testing sites:

1. Browntown Rd. Low Tillage Cropland (Chester River Basin): 331 ac
2. Chestertown B Single Family Residential/Commercial (Chester River Basin): 49 ac

For most EPA/CBP test watersheds, the nonpoint pollution monitoring records were not extensive enough to permit subdividing the dataset into separate calibration/verification periods. Consequently, the entire test watershed monitoring dataset was used for NPS model calibration. The calibrated NPS loading factors were verified through applications to mixed land use river basins in the Chesapeake Bay drainage area. Even in the absence of verification in the Chesapeake Bay river basins, it is felt that the risk of producing biased calibration results from the test watershed modeling studies are significantly reduced by the use of continuous simulation calibration techniques which involve long-term simulations and parameter adjustments that are not keyed to individual storm events.

Table 7

Summary of Test Watershed Characteristics and Hydrology Calibration Results (1.00 ha = 2.47 ac)

LAND USE/SITE	AREA (acres)	REGRESSIONS OF SIMULATED AND OBSERVED FLOW VOLUMES					
		MONITORED STORMS			DAILY STREAMFLOWS		
		N	SLOPE	R ²	N	SLOPE	R ²
A. HIGH TILLAGE CROPLAND							
A. PEQUEA #3	115.2	15	0.76	0.88	492 ^a	0.98	0.70
B. WARE #7	16.2	7	0.72	0.99	--	--	--
B. LOW TILLAGE CROPLAND							
A. OCCOQUAN #2	26.6	8	0.98	0.98	--	--	--
B. OCCOQUAN #10	25.8	7	1.03	0.99	--	--	--
C. PASTURE							
A. OCCOQUAN #1	31.3	5	0.81	0.95	--	--	--
B. OCCOQUAN #5	18.8	5	1.07	0.90	--	--	--
D. FOREST							
A. PEQUEA #2	128.0	18	0.70	0.62	222 ^b	0.7	0.79
B. OCCOQUAN #9	75.8	7	1.11	0.95	--	--	--
C. WARE #8	17.4	9	1.15	0.97	--	--	--
E. RESIDENTIAL							
A. PEQUEA #4	147.2	26	0.86	0.98	374 ^c	0.96	0.84
B. WARE #5	6.2	17	0.80	0.92	--	--	--

^aMay 23, 1979 - September 26, 1980

^bMay 23, 1979 - December 31, 1979

^cMay 23, 1979 - May 31, 1980

EPA/CBP Test Watershed Model Calibration: Hydrology Results. Due to the relatively small size of the test watersheds, the majority of the subsurface flows were often not detectable at the monitoring stations and therefore, baseflow and interflow components of runoff had to be suppressed in hydrologic model calibrations for most sites. Typically, baseflow and interflow were only included in models of forested watersheds where the dry weather flow component represented a significant fraction of monitored flows.

For most test watersheds, hydrologic calibration focused on achieving acceptable agreement between simulated and observed storm volumes. Each test watershed model was iteratively executed with a continuous rainfall record which bracketed the 1-2 year monitoring period and agreement with monitored flows checked for each model parameter set. A 3-6 month antecedent rainfall period was used for most test watersheds to minimize the impacts of the assumed soil moisture conditions at the start of the simulation period. Scatterplots and simple linear regressions of simulated and observed runoff volumes were generated for each calibration run to guide parameter adjustments. Sample comparisons of the final simulated and observed runoff volumes for monitored storm events are shown in Figure 24. Based on the goodness-of-fit regression statistics for monitored storms presented in Table 7, it was concluded that acceptable hydrology calibration had been achieved at the 11 test watersheds. For the three Pequea Creek test watersheds, continuous daily flow records were also available for calibration. As shown in Table 7, acceptable regression statistics were achieved for all three Pequea Creek test watersheds, with the lower slope term for the forested watershed (Pequea #2) probably due in large part to the underlying Conestoga Valley limestone formations which appeared to contribute subsurface flows that originated outside the drainage area.

EPA/CBP Test Watershed Model Calibration: Nonpoint Pollution Results. After achieving an acceptable hydrologic calibration, nonpoint pollution loading factors were calibrated for each test watershed by iteratively executing the NPS model with continuous meteorologic records for the entire monitoring period and checking model projections for monitored storms. The calibration of nonpoint pollution loading factors for total P and total N focused on the agreement of simulated loadings with monitored storms which exhibited acceptable hydrologic simulations. Goodness-of-fit evaluations were based upon conventional and nonparametric statistical analyses.

For urban land uses, daily pollutant accumulation rates developed by the 1976-1977 northern Virginia study (8,9) for pervious and impervious fractions were tested with the Chesapeake Bay Program monitoring data. The calibration techniques used to derive separate loading factors for the pervious and impervious fractions are described below. These urban loading factors were held constant in the models for Pequea #4 and Ware #5 to see how well they represented loadings in different regions under different meteorologic conditions. As was the case in the previous urban modeling study, the daily pollutant accumulation rates were held constant from month to month.

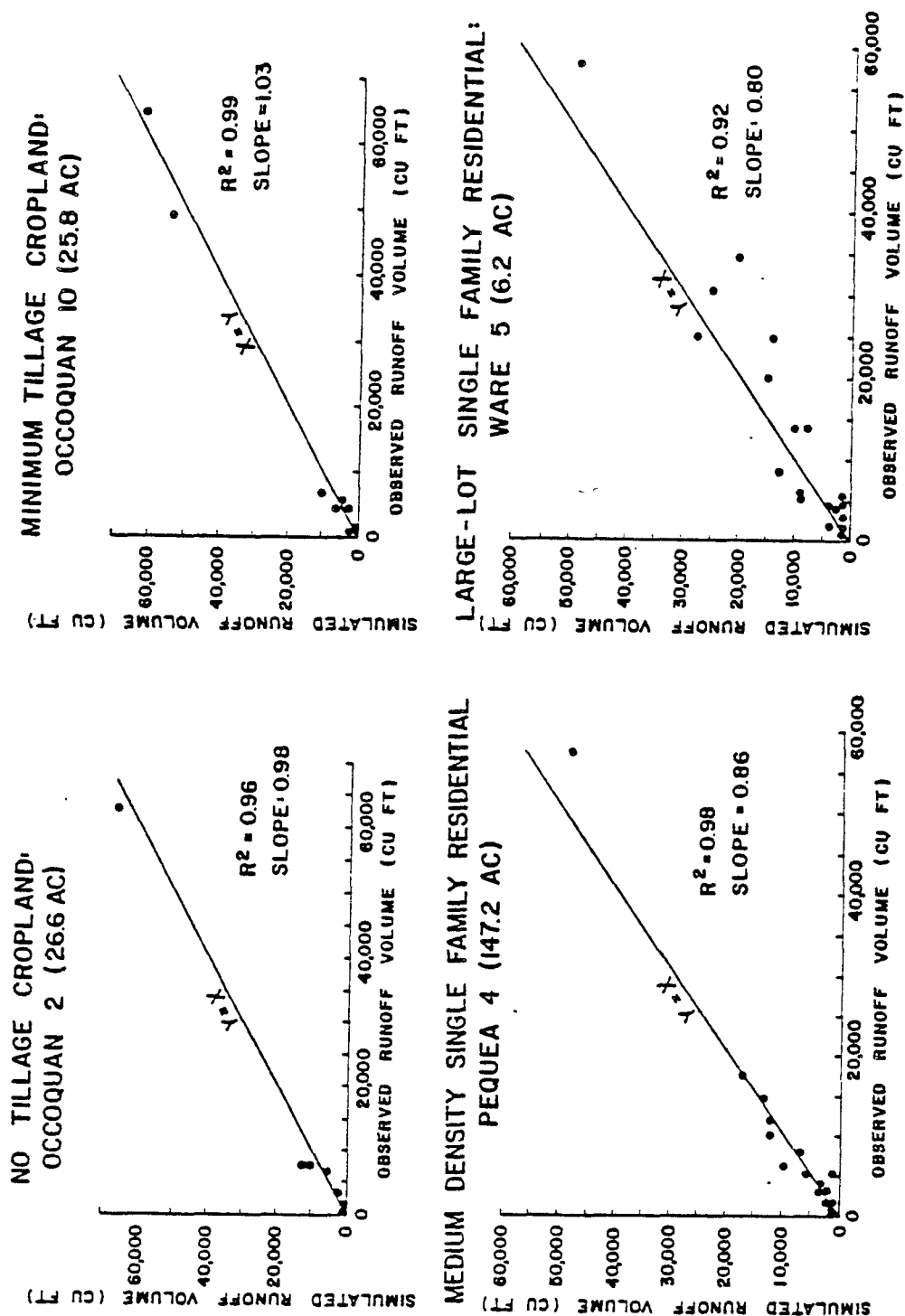


Figure 24. Sample Regressions of Simulated and Observed Runoff Volumes for Monitored Storm Events: Occoquan #2, Occoquan #10, Pequea #4, and Ware #5

For cropland test watersheds, monthly variations in sediment potency factors were required to account for such factors as fertilizer/manure applications and crop harvest, with the higher potencies generally associated with the months characterized by highest percentages of vegetative cover and vice versa. The monthly distribution of potency factors is established during model calibration by deriving the upper limit for the summer months of high ground cover and the lower limit for the winter months of low ground cover. For forestland test watersheds, monthly variations in sediment potency factors and daily pollutant accumulation rates were required to account for the variations in ground cover and leaf litter. Table 8 illustrates the relationship between monthly potency factor and monthly ground cover for cropland and forest land uses. For pasture test watersheds, monthly variations in sediment potency factors were generally not required to achieve an acceptable calibration.

The conventional goodness-of-fit evaluations included scatterplots and linear regressions of simulated and observed storm loads and comparisons of simulated and observed volume-weighted mean concentrations for the entire monitoring period. The simulated volume-weighted mean concentration was calculated by summing the loads and runoff volumes for all storm events within the simulation period, including storms which were not covered by the monitoring study. The protocol for NPS loading factor adjustment after each calibration placed greater emphasis on the agreement of volume-weighted mean concentrations, since long-term loading trends were felt to provide the best indication of the need for and direction of further loading factor adjustments. In other words, whenever a parameter adjustment decision involved choosing between improving volume-weighted mean concentration vs. improving the storm load scatterplots and linear regression statistics, the former usually governed.

Comparisons of simulated and observed volume-weighted mean concentrations for the calibrated NPS loading factors are shown in Table 9. As may be seen, the ratios of simulated to observed mean concentrations typically fell within the range 0.75-1.25 which is comparable to the typical errors inherent in hydrometeorologic gaging and laboratory analyses (33,35,36). Thus, Table 9 indicates that the calibrated NPS loading factors provide a good representation of long-term nonpoint pollution loads per unit volume during the monitoring period.

Some of the better scatterplots and regression results for storm loads are shown in Figure 25. As may be seen, agreement between simulated and observed storm loads was quite good for selected sites. However, regression statistics for several other test watersheds were insufficient to demonstrate goodness-of-fit for storm loads. It is felt that much of the difficulty in achieving acceptable regression statistics for storm load comparisons can be attributed to the lower power of conventional normal statistics for evaluations of small sample sizes characterized by skewed (i.e., non-normal) distributions.

TABLE 8

NONPOINT POLLUTION LOADING FACTORS APPLIED TO CHESAPEAKE BAY DRAINAGE AREA

LAND USE/PARAMETER	<div> <div>2.41</div> <div>8.11</div> <div>3.69</div> <div>3.07</div> <div>5.61</div> <div>3.77</div> <div>4.58</div> <div>4.21</div> <div>3.12</div> <div>2.11</div> <div>4.13</div> <div>5.26</div> </div>											
	JAN	FEB	MAR	APR	MAY	JUN	JUL	AUG	SEP	OCT	NOV	DEC
A. FOREST												
1. GROUND COVER (%)	99.1	99.1	99.7	100	100	100	100	100	100	100	100	99.4
2. SEDIMENT POTENCY: TOTAL-N (%)	1.06	1.06	1.06	1.06	1.06	1.88	1.88	1.88	1.88	1.06	1.06	1.06
3. SEDIMENT POTENCY: ORGANIC-N (%)	0.99	0.99	0.99	0.99	0.99	1.75	1.75	1.75	1.75	0.99	0.99	0.99
4. SEDIMENT POTENCY: AMMONIA-N (%)	0.01	0.01	0.01	0.01	0.01	0.02	0.02	0.02	0.02	0.01	0.01	0.01
5. SEDIMENT POTENCY: NITRATE-N (%)	0.06	0.06	0.06	0.06	0.06	0.11	0.11	0.11	0.11	0.06	0.06	0.06
6. SEDIMENT POTENCY: TOTAL-P (%)	0.15	0.15	0.15	0.15	0.15	0.26	0.26	0.26	0.26	0.15	0.15	0.15
7. SEDIMENT POTENCY: ORGANIC-P (%)	0.14	0.14	0.14	0.14	0.14	0.24	0.24	0.24	0.24	0.14	0.14	0.14
8. SEDIMENT POTENCY: ORTHO-P (%)	0.01	0.01	0.01	0.01	0.01	0.02	0.02	0.02	0.02	0.01	0.01	0.01
B. HIGH TILLAGE CROPLAND												
1. GROUND COVER (%)	0	0	0	0	20	50	85	90	95	20	0	0
2. SEDIMENT POTENCY: TOTAL-N (%)	1.76	1.76	2.32	2.32	2.32	2.32	3.34	3.34	3.34	1.76	1.76	1.76
3. SEDIMENT POTENCY: ORGANIC-N (%)	1.52	1.52	2.02	2.02	2.02	2.02	2.89	2.89	2.89	1.52	1.52	1.52
4. SEDIMENT POTENCY: AMMONIA-N (%)	0.03	0.03	0.04	0.04	0.04	0.04	0.06	0.06	0.06	0.03	0.03	0.03
5. SEDIMENT POTENCY: NITRATE-N (%)	0.21	0.21	0.26	0.26	0.26	0.26	0.39	0.39	0.39	0.21	0.21	0.21
6. SEDIMENT POTENCY: TOTAL-P (%)	0.30	0.30	0.40	0.40	0.40	0.40	0.57	0.57	0.57	0.30	0.30	0.30
7. SEDIMENT POTENCY: ORGANIC-P (%)	0.21	0.21	0.28	0.28	0.28	0.28	0.40	0.40	0.40	0.21	0.21	0.21
8. SEDIMENT POTENCY: ORTHO-P (%)	0.09	0.09	0.12	0.12	0.12	0.12	0.17	0.17	0.17	0.09	0.09	0.09

TABLE 8
(continued)

NONPOINT POLLUTION LOADING FACTORS APPLIED TO CHESAPEAKE BAY DRAINAGE AREA

2.91 2.81 3.69 3.07 3.61 3.77 4.57 4.21 3.12 2.81 3.13 3.26 40.46

LAND USE/PARAMETER

JAN FEB MAR APR MAY JUN JUL AUG SEP OCT NOV DEC

C. LOW TILLAGE CROPLAND

1. GROUND COVER (%)

40

60

75

85

92

99

99

99

99

97

97

94

2. SEDIMENT POTENCY: TOTAL-N (%)

2.06

2.06

2.06

2.52

3.21

3.44

3.44

3.44

2.06

2.06

2.06

3. SEDIMENT POTENCY: ORGANIC-N (%)

0.99

0.99

0.99

1.21

1.54

1.65

1.65

1.65

0.99

0.99

0.99

4. SEDIMENT POTENCY: AMMONIA-N (%)

0.08

0.08

0.08

0.10

0.13

0.14

0.14

0.14

0.08

0.08

0.08

5. SEDIMENT POTENCY: NITRATE-N (%)

0.99

0.99

0.99

1.21

1.54

1.65

1.65

1.65

0.99

0.99

0.99

6. SEDIMENT POTENCY: TOTAL-P (%)

0.17

0.17

0.17

0.21

0.26

0.29

0.29

0.29

0.17

0.17

0.17

7. SEDIMENT POTENCY: ORGANIC-P (%)

0.14

0.14

0.14

0.17

0.21

0.23

0.23

0.23

0.14

0.14

0.14

8. SEDIMENT POTENCY: ORTHO-P (%)

0.03

0.03

0.03

0.04

0.05

0.06

0.06

0.06

0.03

0.03

0.03

D. PASTURE

1. GROUND COVER (%)

100

100

100

100

100

100

100

100

100

100

2. SEDIMENT POTENCY: TOTAL-N (%)

1.52

1.52

1.52

1.52

1.52

1.52

1.52

1.52

1.52

1.52

1.52

3. SEDIMENT POTENCY: ORGANIC-N (%)

1.17

1.17

1.17

1.17

1.17

1.17

1.17

1.17

1.17

1.17

1.17

4. SEDIMENT POTENCY: AMMONIA-N (%)

0.18

0.18

0.18

0.18

0.18

0.18

0.18

0.18

0.18

0.18

0.18

5. SEDIMENT POTENCY: NITRATE-N (%)

0.17

0.17

0.17

0.17

0.17

0.17

0.17

0.17

0.17

0.17

0.17

6. SEDIMENT POTENCY: TOTAL-P (%)

0.26

0.26

0.26

0.26

0.26

0.26

0.26

0.26

0.26

0.26

0.26

7. SEDIMENT POTENCY: ORGANIC-P (%)

0.16

0.16

0.16

0.16

0.16

0.16

0.16

0.16

0.16

0.16

0.16

8. SEDIMENT POTENCY: ORTHO-P (%)

0.10

0.10

0.10

0.10

0.10

0.10

0.10

0.10

0.10

0.10

0.10

TABLE 8
(continued)

NONPOINT POLLUTION LOADING FACTORS APPLIED TO CHESAPEAKE BAY DRAINAGE AREA

LAND USE/PARAMETER	JAN	FEB	MAR	APR	MAY	JUN	JUL	AUG	SEP	OCT	NOV	DEC
B. SINGLE FAMILY RESIDENTIAL												
1. GROUND COVER (%)	99	99	99	99	99	99	99	99	99	99	99	99
2. PERVIOUS AREA ACCUMULATION RATE: TOTAL-N (lbs/ac/day)	0.020	0.020	0.020	0.020	0.020	0.020	0.020	0.020	0.020	0.020	0.020	0.020
3. PERVIOUS AREA ACCUMULATION RATE: ORGANIC-N (lbs/ac/day)	0.013	0.013	0.013	0.013	0.013	0.013	0.013	0.013	0.013	0.013	0.013	0.013
4. PERVIOUS AREA ACCUMULATION RATE: AMMONIA-N (lbs/ac/day)	0.0019	0.0019	0.0019	0.0019	0.0019	0.0019	0.0019	0.0019	0.0019	0.0019	0.0019	0.0019
5. PERVIOUS AREA ACCUMULATION RATE: NITRATE-N (lbs/ac/day)	0.0051	0.0051	0.0051	0.0051	0.0051	0.0051	0.0051	0.0051	0.0051	0.0051	0.0051	0.0051
6. PERVIOUS AREA ACCUMULATION RATE: TOTAL-P (lbs/ac/day)	0.0035	0.0035	0.0035	0.0035	0.0035	0.0035	0.0035	0.0035	0.0035	0.0035	0.0035	0.0035
7. PERVIOUS AREA ACCUMULATION RATE: ORGANIC-P (lbs/ac/day)	0.0018	0.0018	0.0018	0.0018	0.0018	0.0018	0.0018	0.0018	0.0018	0.0018	0.0018	0.0018
8. PERVIOUS AREA ACCUMULATION RATE: ORTHO-P (lbs/ac/day)	0.0017	0.0017	0.0017	0.0017	0.0017	0.0017	0.0017	0.0017	0.0017	0.0017	0.0017	0.0017

TABLE 8
(continued)

NONPOINT POLLUTION LOADING FACTORS APPLIED TO CHESAPEAKE BAY DRAINAGE AREA

LAND USE/PARAMETER	JAN	FEB	MAR	APR	MAY	JUN	JUL	AUG	SEP	OCT	NOV	DEC
B. SINGLE FAMILY RESIDENTIAL (cont.)												
1. IMPERVIOUS AREA ACCUMULATION RATE:												
TOTAL-N (lbs/ac/day)	0.08	0.08	0.08	0.08	0.08	0.08	0.08	0.08	0.08	0.08	0.08	0.08
2. IMPERVIOUS AREA ACCUMULATION RATE:												
ORGANIC-N (lbs/ac/day)	0.036	0.036	0.036	0.036	0.036	0.036	0.036	0.036	0.036	0.036	0.036	0.036
3. IMPERVIOUS AREA ACCUMULATION RATE:												
AMMONIA-N (lbs/ac/day)	0.012	0.012	0.012	0.012	0.012	0.012	0.012	0.012	0.012	0.012	0.012	0.012
4. IMPERVIOUS AREA ACCUMULATION RATE:												
NITRATE-N (lbs/ac/day)	0.032	0.032	0.032	0.032	0.032	0.032	0.032	0.032	0.032	0.032	0.032	0.032
5. IMPERVIOUS AREA ACCUMULATION RATE:												
TOTAL-P (lbs/ac/day)	0.01	0.01	0.01	0.01	0.01	0.01	0.01	0.01	0.01	0.01	0.01	0.01
6. IMPERVIOUS AREA ACCUMULATION RATE:												
ORGANIC-P (lbs/ac/day)	0.005	0.005	0.005	0.005	0.005	0.005	0.005	0.005	0.005	0.005	0.005	0.005
7. IMPERVIOUS AREA ACCUMULATION RATE:												
ORTHO-P (lbs/ac/day)	0.005	0.005	0.005	0.005	0.005	0.005	0.005	0.005	0.005	0.005	0.005	0.005

TABLE 8
(continued)

NONPOINT POLLUTION LOADING FACTORS APPLIED TO CHESAPEAKE BAY DRAINAGE AREA

LAND USE/PARAMETER	JAN	FEB	MAR	APR	MAY	JUN	JUL	AUG	SEP	OCT	NOV	DEC
F. COMMERCIAL												
1. GROUND COVER (%)	99	99	99	99	99	99	99	99	99	99	99	99
2. PERVIOUS AREA ACCUMULATION RATE: TOTAL N (lbs/ac/day)	0.011	0.011	0.011	0.011	0.011	0.011	0.011	0.011	0.011	0.011	0.011	0.011
3. PERVIOUS AREA ACCUMULATION RATE: ORGANIC-N (lbs/ac/day)	0.0023	0.0023	0.0023	0.0023	0.0023	0.0023	0.0023	0.0023	0.0023	0.0023	0.0023	0.0023
4. PERVIOUS AREA ACCUMULATION RATE: AMMONIA-N (lbs/ac/day)	0.0070	0.0070	0.0070	0.0070	0.0070	0.0070	0.0070	0.0070	0.0070	0.0070	0.0070	0.0070
5. PERVIOUS AREA ACCUMULATION RATE: NITRATE-N (lbs/ac/day)	0.0017	0.0017	0.0017	0.0017	0.0017	0.0017	0.0017	0.0017	0.0017	0.0017	0.0017	0.0017
6. PERVIOUS AREA ACCUMULATION RATE: TOTAL-P (lbs/ac/day)	0.0017	0.0017	0.0017	0.0017	0.0017	0.0017	0.0017	0.0017	0.0017	0.0017	0.0017	0.0017
7. PERVIOUS AREA ACCUMULATION RATE: ORGANIC-P (lbs/ac/day)	0.0011	0.0011	0.0011	0.0011	0.0011	0.0011	0.0011	0.0011	0.0011	0.0011	0.0011	0.0011
8. PERVIOUS AREA ACCUMULATION RATE: ORTHO-P (lbs/ac/day)	0.0006	0.0006	0.0006	0.0006	0.0006	0.0006	0.0006	0.0006	0.0006	0.0006	0.0006	0.0006

TABLE 8
(continued)

NONPOINT POLLUTION LOADING FACTORS APPLIED TO CHESAPEAKE BAY DRAINAGE AREA

LAND USE/PARAMETER	JAN	FEB	MAR	APR	MAY	JUN	JUL	AUG	SEP	OCT	NOV	DEC
F. COMMERCIAL (cont.)												
1. IMPERVIOUS AREA ACCUMULATION RATE:												
TOTAL-N (lbs/ac/day)	0.050	0.050	0.050	0.050	0.050	0.050	0.050	0.050	0.050	0.050	0.050	0.050
2. IMPERVIOUS AREA ACCUMULATION RATE:												
ORGANIC-N (lbs/ac/day)	0.030	0.030	0.030	0.030	0.030	0.030	0.030	0.030	0.030	0.030	0.030	0.030
3. IMPERVIOUS AREA ACCUMULATION RATE:												
AMMONIA-N (lbs/ac/day)	0.006	0.006	0.006	0.006	0.006	0.006	0.006	0.006	0.006	0.006	0.006	0.006
4. IMPERVIOUS AREA ACCUMULATION RATE:												
NITRATE-N (lbs/ac/day)	0.014	0.014	0.014	0.014	0.014	0.014	0.014	0.014	0.014	0.014	0.014	0.014
5. IMPERVIOUS AREA ACCUMULATION RATE:												
TOTAL-P (lbs/ac/day)	0.006	0.006	0.006	0.006	0.006	0.006	0.006	0.006	0.006	0.006	0.006	0.006
6. IMPERVIOUS AREA ACCUMULATION RATE:												
ORGANIC-P (lbs/ac/day)	0.0041	0.0041	0.0041	0.0041	0.0041	0.0041	0.0041	0.0041	0.0041	0.0041	0.0041	0.0041
7. IMPERVIOUS AREA ACCUMULATION RATE:												
ORTHO-P (lbs/ac/day)	0.0019	0.0019	0.0019	0.0019	0.0019	0.0019	0.0019	0.0019	0.0019	0.0019	0.0019	0.0019

Table 9

Comparison of Simulated and Observed Volume-Weighted Mean Concentrations

SITE (LAND USE)	OBS. N	SEDIMENT			TOTAL P			TOTAL N		
		SIM. (MG/L)	OBS. (MG/L)	RATIO	SIM. (MG/L)	OBS. (MG/L)	RATIO	SIM. (MG/L)	OBS. (MG/L)	RATIO
PEQUEA 3 (H.T. CROP)	17	783	829	0.94	4.53	4.70	0.96	18.7	19.2	0.98
WARE 7 (H.T. CROP)	10	272	222	1.23	0.70	0.62	1.13	1.6	1.30	1.20
OCC. 2 (L.T. CROP)	16	370	361	1.02	1.96	1.67	1.17	6.8	6.6	1.03
OCC. 10 (L.T. CROP)	13	138	121	1.14	0.47	0.40	1.18	4.6	3.8	1.22
OCC. 9 (FOREST)	15	83	70	1.19	0.13	0.13	1.0	1.1	0.9	1.22
PEQUEA 2 (FOREST)	21	99	169	0.58	0.1	0.13	0.74	3.8	3.6	1.05
WARE 8 (FOREST)	34	64	71	0.90	0.05	0.06	0.83	0.37	0.4	0.93
OCC. 1 (PASTURE)	27	561	670	0.84	0.94	1.12	0.84	5.3	6.2	0.86
OCC. 5 (PASTURE)	11	166	145	1.14	0.43	0.38	1.13	2.5	2.2	1.15
PEQUEA 4 (RESID.)	52	115	194	0.56	0.24	0.30	0.80	1.8	2.4	0.75
WARE 5 (RESID.)	30	50	38	1.32	0.12	0.10	1.23	0.95	0.70	1.36

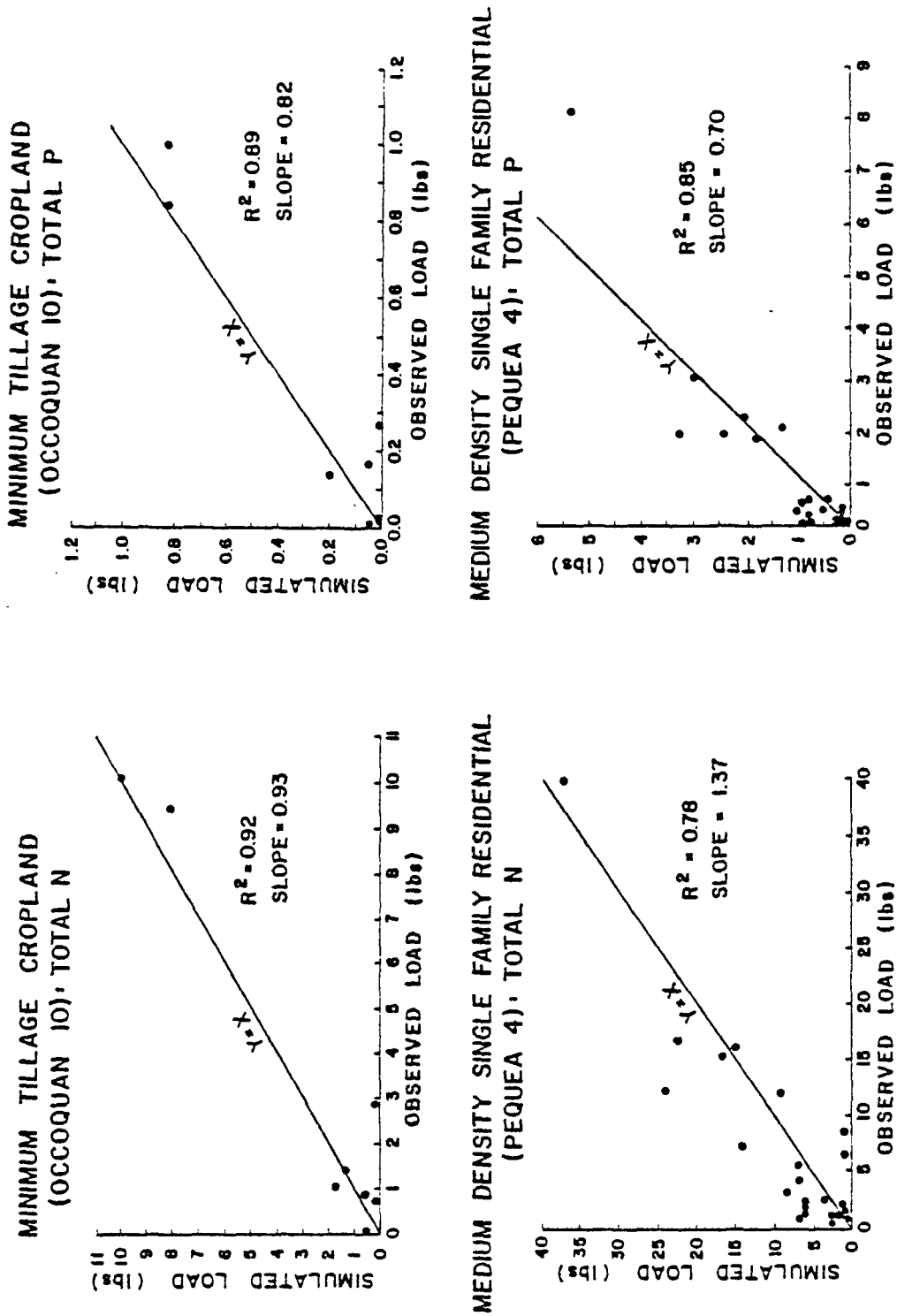


Figure 25. Sample Regressions of Simulated and Observed Loadings for Monitored Storms: Occoquan #10 and Pequea #4

To provide a visual check of agreement between simulated and observed frequency distributions, box and whisker plots were developed for the simulated and observed storm load datasets for each test watershed. As illustrated in Figure 26, the box and whisker plot displays the 25th, 50th, and 75th percentile values in the frequency distribution as well as the upper and lower extremes. The departure of the 25th and 75th percentile lines from the median line provides an indication of skewness of the distribution. The mean value is sometimes plotted on the box and whisker diagram to highlight departure from the median value and the non-normality of the distribution. Box and whisker plots for the calibrated NPS loading factors are shown in Figures 27, 28, and 29 for cropland, forest/pasture, and urban land uses, respectively. To provide an indication of non-normality, the location of the mean in each diagram is indicated by an "o". Since it is the driving force for simulated cropland loadings, sediment data is presented for the cropland test watersheds in Figure 27.

As was the case with the simulated volume-weighted mean concentrations reported in Table 9, the simulated box and whisker plots are based on all storms which occurred during the test watershed monitoring period, including those which were not monitored. The inclusion of all storms tended to automatically skew the simulated distribution in the direction of minor storms which typically were not monitored in the field due to the very small runoff volumes. This skewness can be attributed to the fact that whereas the mathematical model will calculate runoff volumes and loads from minor storms, the test watershed monitoring studies relied upon runoff volume thresholds associated with more significant rainfall events. Since similar runoff volume distributions are required to ensure meaningful statistical comparisons of storm loading datasets, minor storms were generally deleted from the simulated dataset prior to the development of the box and whisker plots shown in Figures 27-29. The establishment of the cutoff for minor storms was based upon iterative analyses of box and whisker plots and nonparametric statistics for the simulated and observed runoff volume datasets. The storm runoff volume thresholds which resulted in box and whisker plots and nonparametric statistics that indicated acceptable agreement between the simulated and observed runoff volume distributions and median values are summarized in the "runoff interval" column of Table 10. A check of the total runoff volume and nonpoint pollution load produced by storm events which fall within the specified runoff interval indicates that typically 90% or more of the total volume or load produced during the monitoring period was generated by these storms. This check suggests that the minor storms deleted from the simulated and observed datasets were relatively insignificant in terms of seasonal or annual loads.

The runoff intervals shown in Table 10 were used as the basis for the box and whisker plots of simulated and observed datasets in Figures 27-29. Inspection of these box and whisker plots confirms the highly skewed distributions of the runoff and nonpoint pollution loading datasets. The similarities between the simulated and observed plots, in terms of distribution and median value, also serves as graphical evidence of model goodness-of-fit.

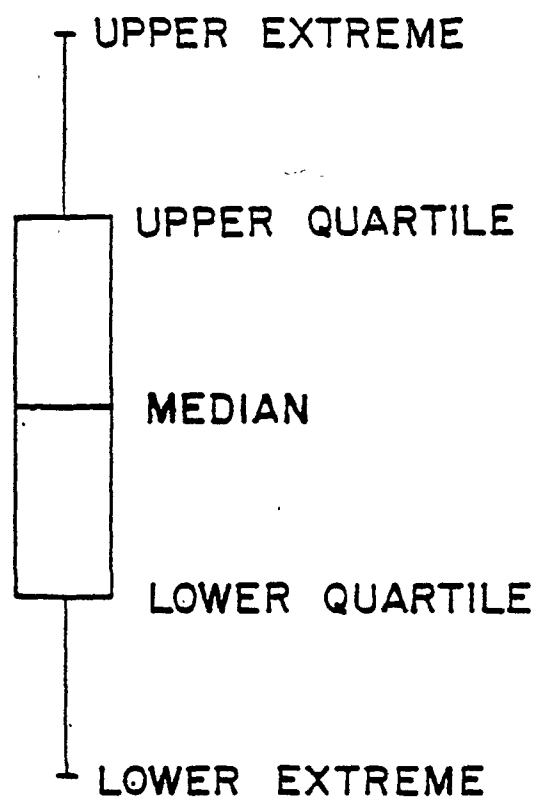


Figure 26. Configuration of a
Box and Whisker Plot

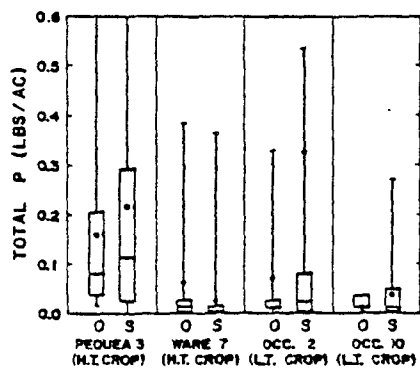
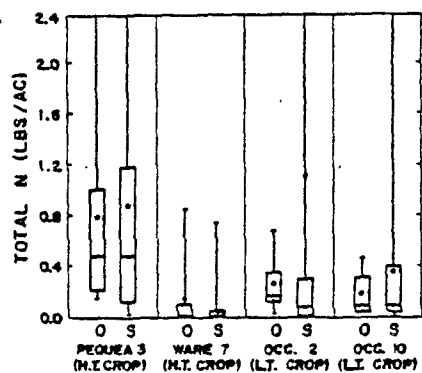
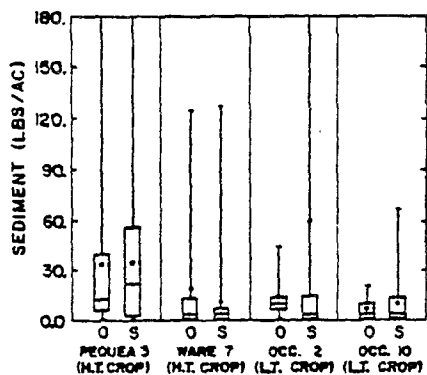
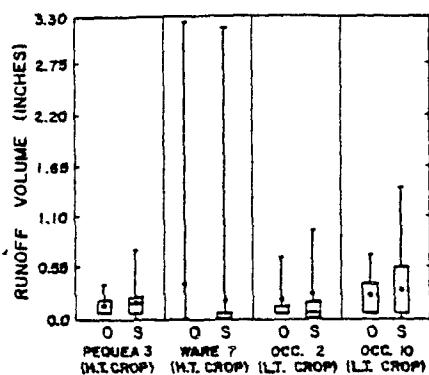


Figure 27. Comparison of Simulated (S) and Observed (O) Box and Whisker Plots for Cropland Watersheds

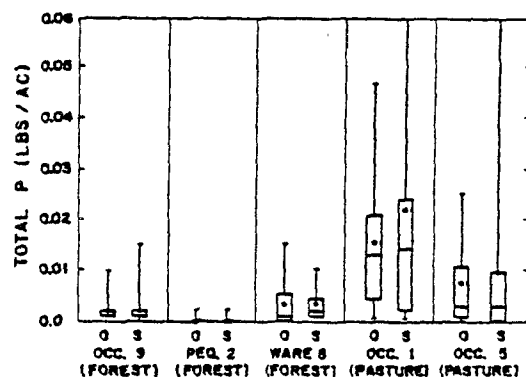
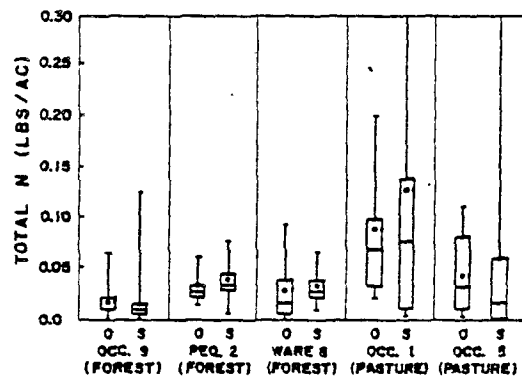
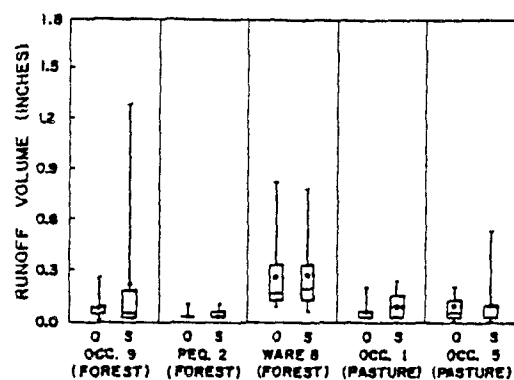


Figure 28. Comparison of Simulated (S) and Observed (O) Box and Whisker Plots for Forest and Pasture Watersheds

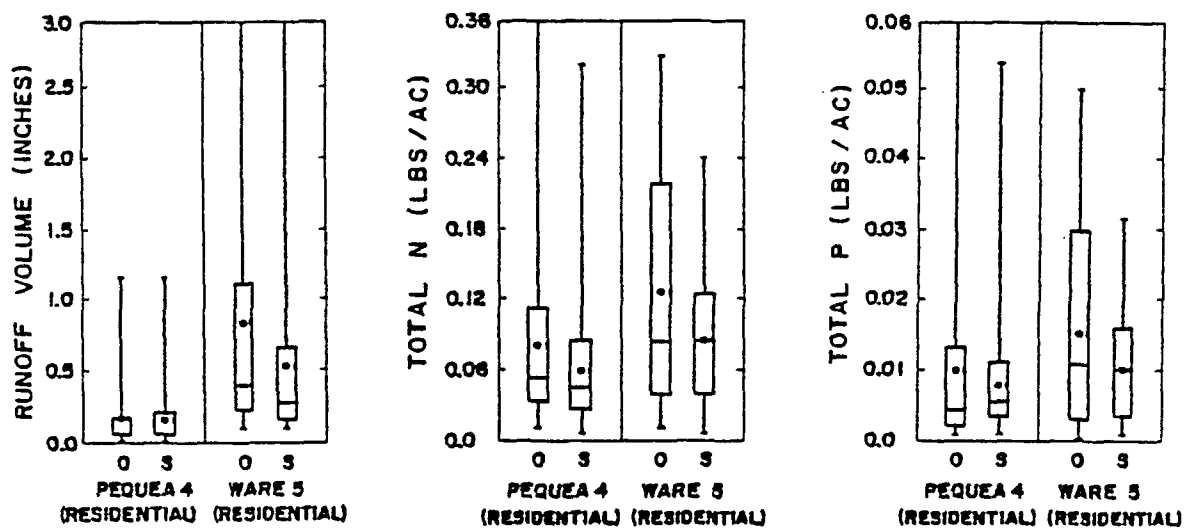


Figure 29. Comparisons of Simulated (S) and Observed (O) Box and Whisker Plots for Single-Family Residential Watersheds

Table 10

Nonparametric Goodness-of-Fit Statistics for Test Watershed Model
 Calibration: Runoff Volumes (R.O.) and Total Phosphorus (TP),
 Total Nitrogen (TN), and Sediment (SED) Loadings (lbs)

SITE (LAND USE)	RUNOFF INTERVAL (IN.)	SIM. STORMS	OBS. STORMS	TWO-SIDED K-S TEST				WILCOXON RANK SUM TEST			
				LEVEL OF SIGNIFICANCE				LEVEL OF SIGNIFICANCE			
				R.O.	TP	TN	SED	R.O.	TP	TN	SED
PEQUEA 3 (H.T. CROP)	>0.025	28	13	0.20	>0.20*	>0.20*	>0.20*	0.58	0.96	0.65	0.83
WARE 7 (H.T. CROP)	(0.01-0.125 + HURR.)	26	9	0.10	>0.20*	>0.20*	>0.20*	0.17	0.23	0.42	0.84
OCC. 2 (L.T. CROP)	>0.015	29	6	>0.20*	>0.20*	0.10	>0.20*	0.71	0.91	0.20	0.39
OCC. 10 (L.T. CROP)	>0.025	19	8	>0.11*	>0.11*	>0.11*	>0.11*	0.65	0.97	0.94	0.98
OCC. 9 (FOREST)	>0.03	30	9	>0.20*	>0.20*	>0.20*	N/A	0.56	0.45	0.80	N/A
PEQUEA 2 (FOREST)	<0.09	91	16	0.42	0.34	0.26	N/A	0.30	0.61	0.18	N/A
WARE 8 (FOREST)	(0.075-0.9)	20	24	>0.20*	0.10	0.10	N/A	0.86	0.31	0.13	N/A
OCC. 1 (PASTURE)	(0.025-0.5)	15	9	>0.10*	>0.10*	>0.10*	N/A	0.40	0.95	0.81	N/A
OCC. 5 (PASTURE)	>0.01	21	8	>0.20*	>0.20*	0.20	N/A	0.37	0.54	0.25	N/A
PEQUEA 4 (RESID.)	>0.025	86	25	0.94	0.39	0.44	N/A	0.76	0.70	0.48	N/A
WARE 5 (RESID.)	>0.09	43	24	0.58	0.22	0.29	N/A	0.31	0.64	0.34	N/A

*EXCEEDS MAXIMUM PROBABILITY VALUE CURRENTLY REPORTED IN STATISTICAL TABLES FOR SAMPLE SIZES

Nonparametric statistical tests (37) were performed for a quantitative assessment of the goodness-of-fit for the datasets plotted in Figures 6-8. Nonparametric statistics assume no shape for the population distribution and therefore are valid for both normal and skewed distributions. Consequently, nonparametric statistical techniques have a much higher power than normal statistical techniques for analyses of datasets, such as the monitored storm load dataset, which are characterized by small sample sizes and skewed distributions. The results of two-sided Kolmogorov-Smirnov (K-S) and Wilcoxon Rank Sum tests are summarized in Table 10. The K-S analysis is a test for any significant deviation of the simulated distribution from the observed distribution. The analysis involves checking the maximum difference between simulated and observed distributions to determine if it exceeds a critical value. Since it is a broad alternative test, the K-S test has lower power for any specific alternative, such as a difference in median values. The Wilcoxon Rank Sum analysis compensates for this deficiency since it is designed to test for differences in median values, under the assumption that the simulated and observed distributions may differ only with respect to this value. The Wilcoxon Rank Sum test assigns ranks to the combined dataset of simulated and observed values and calculates the sum of the data ranks for each dataset. If the simulated median value differs significantly from the observed median value, the sum of the simulated data ranks will be higher or lower than the sum of the observed data ranks.

Based on a 0.05 probability cutoff for the 95% confidence interval, the level of significance statistics in Table 10 indicate that the simulated runoff volumes and nutrient loads do not vary significantly from those monitored in each test watershed. The high significance levels of the nonparametric tests summarized in Table 10 meet the primary objective of a goodness-of-fit evaluation by indicating a low probability of accepting a false model as true (Type II error).

Urban Test Watershed Model Calibration: Northern Virginia and Metropolitan Washington NURP Studies. Sixteen small watersheds (26 ac average) characterized by a homogeneous urban land use pattern were monitored from June 1976 through May 1977 to develop the required database for loading factor calibration. The distribution of monitoring sites among urban land use classifications was as follows: 2 large-lot single family (0.5-2.0 DU/AC) residential watersheds; 3 medium density single family (2.0-8.0 DU/AC) residential watersheds, 4 townhouse-garden apartment (8-22 DU/AC) watersheds, 3 high-rise residential (greater than 22 DU/AC) watersheds, 3 shopping center watersheds, and 1 central business district watershed. Separate daily pollutant accumulation rates (lbs/ac/day) were calibrated for the pervious and impervious fractions of each test watershed, with the same loading factors found to provide an acceptable representation of all test watersheds within a particular land use category (9). The calibrated urban loading factors were found to provide acceptable loading simulations without altering the factors from month to month. Five-minute rainfall records collected within each test watershed were used for NPS model calibration.

In order to derive separate pollutant accumulation rates for pervious and impervious fractions of each urban testing site, observed nonpoint pollution loadings were separated into pervious and impervious area components. Although the monitoring data collected in each test watershed did not provide such a breakdown of land surface loadings, the contribution of each fraction can be inferred from the projections of pervious and impervious area runoff volumes developed with a watershed model which has previously undergone hydrology calibration. The first step in the calibration procedure was the execution of a separate model of the test watershed's pervious fraction to identify those monitored storm events which produced runoff from pervious areas. Those storms which do not produce pervious area runoff were designated for the calibration of a separate model of the test watershed's impervious fraction. The impervious fraction model was then executed with the rainfall record for the entire monitoring period and pollutant accumulation rates were iteratively adjusted until there was acceptable agreement between simulated and observed loadings for those storms which did not generate any runoff from the test watershed's pervious fraction. Differences between observed pollutant loads and simulated impervious fraction loadings were used as calibration data for iterative executions of the pervious fraction model. Following the determination of pervious fraction accumulation rates with the pervious fraction model, simulated pervious and impervious area loadings for each storm event were summed and compared with composite loading observations for goodness-of-fit assessments which are reported elsewhere (9,10).

During calibration of daily pollutant accumulation rates, care was taken to develop an approximate equilibrium or balance between the accumulation of loads on the one hand and pollutant washoff and transport on the other. Extended dry periods produced noticeable increases in surface pollutants and extended wet periods produced decreases. However, accumulation rates and other model parameters were adjusted to assure that the overall trend was relatively stable so that accumulated pollutant loads were not continually increasing or decreasing during the calibration period. This equilibrium was developed for both the pervious and impervious fractions in each urban watershed. It was found that daily pollutant decay factors, which approximate reductions in pollutant loading potential within the pervious (REPER) and impervious (REIMP) fractions resulting from wind and biochemical processes, should be set at 5%/day to 8%/day to prevent pollutant accumulations from becoming unstable during extended dry periods. The results of test watershed model calibration study also indicate that the necessary accumulation-washoff balance during periods of average rainfall can be maintained with transport parameters set at about 0.4 for the pervious fraction (KSER) and 0.5 in./hr for the impervious fraction (RIMPX).

Verification of Calibrated Nonpoint Pollution Loading Factors. As previously indicated, the risk of producing biased calibration results are significantly reduced by the use of continuous simulation calibration techniques involving long-term simulations and parameter adjustments that are not keyed to individual storm events. Nonetheless, four different modeling studies have been performed to verify the NPS loading factors developed from the aforementioned test watershed model calibration studies.

One of the verification studies involved testing the urban nonpoint pollution loading factors from the 1976-1977 northern Virginia study (9) at two of the EPA/CBP test watersheds covered by the aforementioned calibration study: Pequea #4 and Ware #5, both of which are characterized by single family residential land use patterns. As indicated in Figure 29 and Table 10, the total P and total N loading factors developed by the earlier study achieved a satisfactory representation of monitored loadings at these two EPA/CBP residential testing sites.

A second verification study involved applying calibrated nonpoint pollution loading factors to two of the EPA/CBP testing sites located in Maryland: Chestertown B (single family residential) and Browntown Road (low tillage cropland). Due to the timing of the Maryland test watershed monitoring studies, the schedule and budget for the modeling study could accommodate model verification work at only a few sites. Based upon a review of available monitoring data for the Maryland testing sites with a relatively homogeneous land use pattern, Chestertown B and Browntown Road were selected for the verification study.* The NPS loading factors developed by the 1976-1977 northern Virginia test watershed study (9) for single family residential land uses produced a satisfactory representation of monitored loadings at Chestertown B. As may be seen in Table 11 which presents nonparametric goodness-of-fit statistics, there is no significant difference between the simulated and recorded datasets at the 95% confidence interval. The Chestertown B results represent a third level of verification of the total P and total N loading factors used for single family residential land uses. For the Browntown Road site, the monthly total N loading factors which produced an acceptable agreement between simulated and recorded (see Table 11) values were only 15% higher than the Basin Model factors shown in Table 8 for low tillage cropland land uses. This represents an acceptable verification of total N loading factors for

*The following Patuxent River testing sites were not modeled for this study because of mixed agricultural land use patterns: Deale A (131 ac); Deale B (606 ac); Zepp Farm (55 ac); and Grey Farm (34 ac). Even if these sites were characterized by homogeneous land use patterns, the unavailability of reduced rainfall and streamflow records for this study would have prevented modeling analyses as was the case with the Patuxent Park forest site (144 ac) which also lacked a land use breakdown. Although reduced rainfall and streamflow records were available for all Chester River testing sites, the following were not modeled for this study because of mixed land use patterns and/or excessive drainage areas for a testing site modeling study: Sutton Farm mixed agricultural site (804 ac); Millington A forest/pasture site (1,295 ac); and Chestertown A residential/institutional site (46 ac). Of the 5 Chester River sites with relatively homogeneous land use patterns and acceptable drainage areas, Still Pond Road minimum tillage cropland site (29 ac) and Harris Farm no till cropland site (14 ac) were not modeled due to the limited number of storm loading observations (i.e., 1 to 3 storms), while the Millington B forest site (271 ac) was not modeled due to difficulties encountered in characterizing the hydrologic responses (e.g., flat, swampy watershed with high water table conditions) at this site.

Table 11

Nonparametric Goodness-of-Fit Statistics for Maryland Test Watershed Verification Sites
Runoff Volumes (R.O.) and Total Phosphorus (TP), Total Nitrogen (TN),
and Sediment (SED) Loadings (lbs)

SITE (LAND USE)	RUNOFF INTERVAL (IN)	SIM. STORMS	OBS. STORMS	TWO-SIDED K-S TEST		WILCOXON RANK SUM TEST	
				LEVEL OF SIGNIFICANCE R.O.	TP	LEVEL OF SIGNIFICANCE R.O.	TP
CHESTERTOWN B (RESIDENTIAL)	None	52	19	0.86	0.35	0.56	0.49
BROWNTOWN ROAD (L.T. CROP)	.001 ≤ INCHRO ≤ 0.14	25	9	>0.20	*	0.20	*
						0.88	0.21

*Only one total P observation available for Browntown Road site.

low tillage cropland. Total N was the only constituent which could be verified for Browntown Road, due to the availability of only one total P observation and exaggerated sediment loads caused by plowing of the stream channel in the vicinity of the monitoring station.

A third verification study involved testing the NPS loading factors used in the Basin Model (see Table 8) in two mixed land use watersheds within northern Virginia's Occoquan River Basin: Occoquan Creek Watershed (343 sq mi) and Bull Run Watershed (185 sq mi). The wet-weather monitoring stations used for this verification study were located at the outlets of these two watersheds. These two watersheds, which are located in the Piedmont physiographic province, are tributary to the upper Potomac Estuary. As may be seen in Table 12, which summarizes the land use patterns in the two watersheds, pasture and cropland land uses are more predominant (i.e., 43% of total area) in Occoquan Creek Watershed while urban land uses are more predominant (i.e., 15% of total area) in Bull Run Watershed. The model used in this verification study is the same one referred to in this report as the Basin Model. A two-year period was used for NPS loading factor testing: January 1, 1978 - December 31, 1979. The year 1978 was characterized by average to slightly below average streamflows while 1979 was characterized by relatively high streamflows. These two years were selected because they bracket the start-up of an advanced wastewater treatment plant in the Bull Run Watershed which essentially eliminated point source loadings of total P. Due to the AWT operations, the pollution loadings monitored at the outlets of Occoquan Creek and Bull Run watersheds can be attributed primarily to nonpoint sources, particularly the former which includes no major wastewater discharges. After reverifying previous hydrology calibration/verification results (38), simulated and recorded pollution loadings delivered to the outlets of these two watersheds were compared on an annual and storm event basis. Table 13 summarizes comparisons between simulated and recorded annual loads for total P, total N, nitrate-N and TKN. After accounting for errors in streamflow simulations, errors in the annual load simulations for total P and total N are approximately $\pm 20\%$ or less for both 1978 and 1979. Since observation errors of 10%-20% are not unreasonable for N and P measurements (34,35), these comparisons indicate satisfactory agreement on an annual basis. To provide a visual check of agreement between simulated and recorded storm load datasets, box and whisker plots of runoff and loading frequency distributions are presented in Figure 30 for the Occoquan Creek and Bull Run monitoring stations. A total of 38 monitored storm events were available for the Occoquan Creek watershed for 1978-1979, while 24 monitored storm events were available for the Bull Run watershed. Visual inspection of the box-and-whisker plots in Figure 30 indicates that there is good agreement between the simulated and recorded distributions for storm flow volumes and N and P loads. Table 14 summarizes the results of the two nonparametric statistical tests used to provide a quantitative assessment of the goodness-of-fit for the NPS loading datasets plotted in Figure 30. Based on a 0.05 probability cutoff for the 95% confidence interval, the high level of significance statistics in Table 14 indicate that the simulated storm flow volumes and pollutant loads do not vary significantly from those monitored in each watershed. Thus, the

Table 12

SUMMARY OF EXISTING LAND USE
IN OCCOQUAN CREEK AND BULL RUN WATERSHEDS

<u>LAND USE</u>	<u>% OF TOTAL WATERSHED AREA</u>	
	<u>OCCOQUAN CREEK</u>	<u>BULL RUN</u>
Urban Residential	5.3%	10.3%
Urban Commercial & Industrial	0.7%	2.7%
Other Urban	0.7%	1.9%
Forest & Idle Land	50.0%	58.1%
Pasture Land	31.3%	15.9%
High Tillage Cropland	2.0%	1.6%
Low Tillage Cropland	<u>10.0%</u>	<u>9.5%</u>
TOTAL:	100%	100%

Table 13

Comparison of Annual Total Flows and Loads
for Calendar Years 1978 and 1979: Occoquan Creek
and Bull Run Watersheds
(1.0 in. = 2.54 cm; 1.0 lb = 0.453 kg)

	<u>FLOW</u> <u>(in.)</u>	<u>TOTAL P</u> <u>(lbs.)</u>	<u>TOTAL N</u> <u>(lbs.)</u>	<u>NITRATE-N</u> <u>(lbs.)</u>	<u>TKN</u> <u>(lbs.)</u>
A. OCCOQUAN CREEK					
1978 Simulated	16.0	97,130	1.31×10^6	529,750	779,950
1978 Recorded	14.2	71,628	1.35×10^6	680,020	669,980
1978 Error	12.7%	35.6%	-3.0%	-22.1%	16.4%
1979 Simulated	28.1	201,100	2.48×10^6	914,000	1.56×10^6
1979 Recorded	29.3	180,000	2.12×10^6	870,740	1.24×10^6
1979 Error	-4.1%	11.7%	17%	5.0%	25.5%
B. BULL RUN*					
1978 Simulated	17.6	89,540	1.26×10^6	489,400	775,000
1978 Recorded	16.2	115,060	1.32×10^6	525,000	793,980
1978 Error	8.6%	-22.2%	-4.2%	-6.8%	-2.4%

*Insufficient monitoring data for calculations of 1979 annual loads

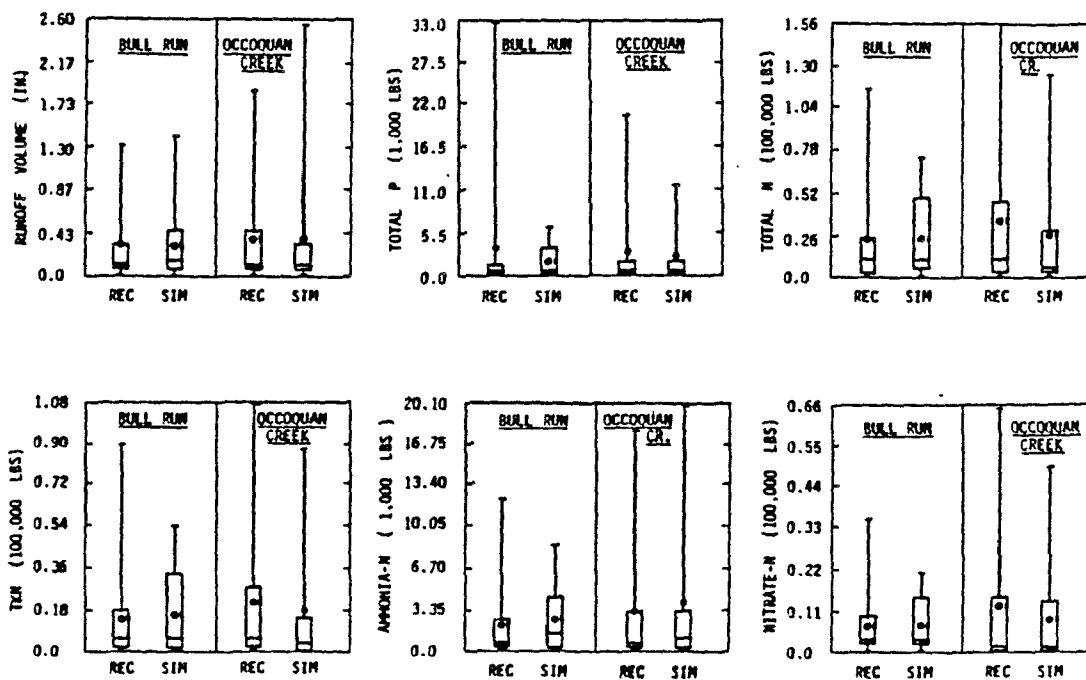
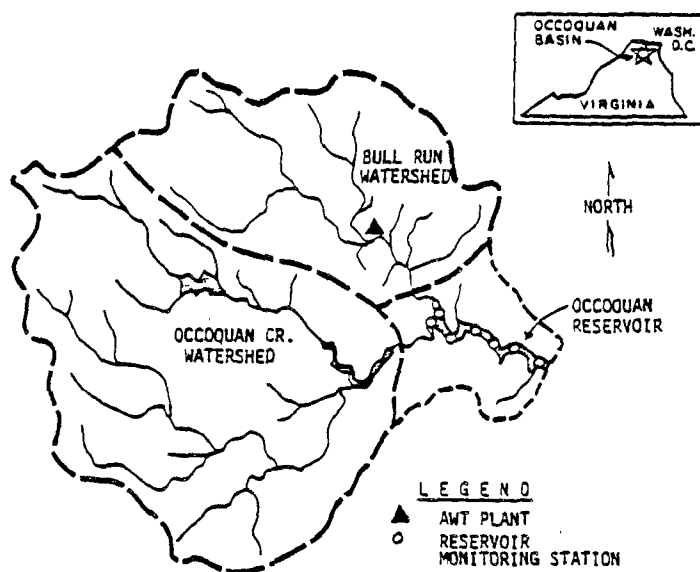


Figure 30. Comparison of Simulated (SIM) and Recorded (REC) Box and Whisker Plots for Storm Volumes and Loads at Outlets of Bull Run (185 sq mi) and Occoquan Creek (343 sq mi) Watersheds: 1978 - 1979

Table 14

LEVEL OF SIGNIFICANCE FOR NONPARAMETRIC
GOODNESS-OF-FIT TESTS: OCCOQUAN CREEK AND BULL RUN
WATERSHED SIMULATIONS OF STORM LOADS FOR 1978-1979

<u>CONSTITUENT</u>	<u>TWO-SIDED K-S</u> <u>DISTRIBUTION TEST</u>		<u>WILCOXON RANK SUM</u> <u>MEDIAN TEST</u>	
	<u>OCCOQUAN CREEK</u>	<u>BULL RUN</u>	<u>OCCOQUAN CREEK</u>	<u>BULL RUN</u>
Flow (cu. ft)	0.15	>0.20*	0.13	0.39
Total P (lbs)	0.54	>0.20*	0.40	0.41
Total N (lbs)	0.44	>0.20*	0.25	0.34
Ammonia-N (lbs)	0.92	>0.20*	0.75	0.15
TKN (lbs)	0.54	>0.20*	0.19	0.28
Nitrate-N (lbs)	0.70	>0.20*	0.79	0.49

*Exceeds maximum probability value currently reported in statistical tables for sample sizes.

NOTE: N = 38 storm events for Occoquan Creek Watershed
N = 24 storm events for Bull Run Watershed

calibrated NPS loading factors used in the Basin Model provided a very good representation of nonpoint pollution loadings in two mixed land use watersheds with drainage areas on the order of a few hundred sq mi.

A fourth verification study relied upon streamflow-loading relationships developed by the U.S.G.S. fall line monitoring study (11) funded by EPA/CBP. The U.S.G.S. monitoring study covered wet-weather loadings at the Susquehanna, Potomac, and James river fall lines from January 1979 through April 1981. Unfortunately, since sufficient NWS rainfall records were not available for the period corresponding to the U.S.G.S. monitoring period, the Basin Model could not be operated for direct loads. Instead, regression equations (11,39) relating daily streamflow to database, were used to synthesize a daily loading database for a period with available NWS rainfall records: January 1974 - December 1978. The Basin Model was then operated for the 1974-1978 period with the NPS loading factors derived from the test watershed statistics (e.g., Table 8) and simulated daily loading records at the Susquehanna, Potomac, and James river fall lines were compared with the daily records synthesized from the fall line regression equations. The period 1974-1978 was selected for model verification because its streamflow statistics (i.e., flow-duration curves) at the three fall line gages are reasonably similar to the streamflow statistics during the period covering the U.S.G.S. monitoring study. The results of these fall line comparisons, which are summarized in a later section on receiving water submodel calibration/verification, provide further evidence of the reliability of the NPS loading factors developed from the testing site studies.

Determination of Representative NPS Loading Factors. The purpose of the test watershed studies was the development of nonpoint pollution loading factors for application throughout the 64,000 sq mi drainage area of Chesapeake Bay. Of the 30 modeled test watersheds, only the urban sites relied upon a single set of loading factors for each land use category. Since the urban loading factors developed from test watershed studies provided a good representation of urban loadings in four different sections of the study area (i.e., metropolitan Washington, D.C., southeastern Pennsylvania, eastern Maryland, and southeastern Virginia), it was decided that these loading factors would be used for all residential and commercial land uses in the Chesapeake Bay Basin. The transferability of urban nonpoint pollution loading factors is not surprising because impervious cover is such an important contributor to urban nonpoint pollution loadings (8,9) and an urban land use tends to exhibit similar impervious cover patterns regardless of location.

Differences in calibrated loading factors at the test watersheds in each rural-agricultural land use category can be attributed to variations in management practices and in the significance of sediment loadings. For each land use category, volume-weighted mean concentrations for modeled and unmodeled (i.e., Patuxent and Chester rivers) test watersheds were compared to ascertain long-term loading differences among the testing sites. Volume-weighted mean concentrations for forest, pasture, and cropping land uses are shown in Table 15. For the forest land use category, a review of

Table 15

Volume Weighted Mean Concentrations: Chesapeake Bay Test Watersheds

LANDUSE=FOREST							
SITE	BASIN	ACRES	MNINCHRO	NTN	MNTN	NTP	MNTP
MILLINGTON A	CHESTER	1178.0	0.08	24	0.86	24	0.07
MILLINGTON B	CHESTER	271.0	0.33	29	1.05	23	0.10
OCCC9 (FOREST)	OCCOQUAN	75.8	0.33	15	0.91	15	0.13
PATUXENT PARK	PATUXENT	144.0	0.11	20	1.11	28	0.22
PEQ2 (FOREST)	PEQUEA	123.0	0.04	19	3.32	19	0.19
WARE B (FOREST)	WARE	17.4	0.51	27	0.43	34	0.06
LANDUSE=HIGHTILL							
SITE	BASIN	ACRES	MNINCHRO	NTN	MNTN	NTP	MNTP
PEQ3 (CONTILL)	PEQUEA	115.20	0.22	13	22.22	13	3.96
WARE 2 (CROP)	WARE	43.20	0.52	6	1.35	7	0.72
WARE 7 (CROP)	WARE	16.16	0.30	7	1.33	10	0.62
LANDUSE=LOWTILL							
SITE	BASIN	ACRES	MNINCHRO	NTN	MNTN	NTP	MNTP
BROWNTOWN ROAD	CHESTER	352.0	0.11	12	22.53	5	0.57
OCCC10 (MINTILL)	OCCOQUAN	25.8	0.34	13	3.31	11	0.40
STILL POND ROAD	CHESTER	29.0	0.10	3	3.01	3	1.65
LANDUSE=MIXED-AG							
SITE	BASIN	ACRES	MNINCHRO	NTN	MNTN	NTP	MNTP
CEALE A	PATUXENT	300	0.09	32	4.21	29	1.41
CEALE B	PATUXENT	1300	0.09	27	4.00	25	1.02
GREY FARM	PATUXENT	40	0.16	3	3.94	3	2.13
SUTTON FARM	CHESTER	804	0.14	35	4.81	34	0.82
USGS GAGE	CHESTER	8704	0.11	40	3.50	30	1.74
ZEPP FARM	PATUXENT	50	0.05	17	3.90	17	1.91
LANDUSE=NOTILL							
SITE	BASIN	ACRES	MNINCHRO	NTN	MNTN	NTP	MNTP
HARRIS FARM	CHESTER	14.1	0.19	2	2.72	1	4.50
OCCC2 (NO-TILL)	OCCOQUAN	26.6	0.33	15	9.00	15	1.28
LANDUSE=PASTURE							
SITE	BASIN	ACRES	MNINCHRO	NTN	MNTN	NTP	MNTP
OCCC1 (POOR-PAST)	OCCOQUAN	31.3	0.16	25	5.97	25	1.06
OCCC5 (GOOD-PAST)	OCCOQUAN	18.8	0.12	10	2.12	9	0.35
LANDUSE=RESIDENTIAL							
SITE	BASIN	ACRES	MNINCHRO	NTN	MNTN	NTP	MNTP
CHESTERTOWN A	CHESTER	46.40	0.11	26	2.61	25	1.08
CHESTERTOWN B	CHESTER	50.00	0.12	21	3.23	22	0.91
PEQ4 (RESID)	PEQUEA	147.20	0.43	57	2.40	57	0.30
WARE 5 (RESID)	WARE	6.18	1.68	22	0.65	30	0.10

KEY: ACRES = Test Watershed Area (ac)
 MNINCHRO = Mean Runoff Volume (in)
 NTN = # Events Sampled For TN
 MNTN = Volume Weighted Mean TN (mg/L)
 NTP = # Events Sampled for TP
 MNTP = Volume Weighted Mean TP (mg/L)

long-term loading statistics for 3 modeled and 3 unmodeled sites indicates that Occoquan #9 is characterized by mean concentrations which are similar to the mean concentrations at most other forest sites. Therefore, the calibrated total P and total N loading factors for Occoquan #9 were selected as the most representative forest loading factors for application throughout the Chesapeake Bay drainage area.

The selection of representative pastureland loading factors was influenced by the limitations of the land use database for the Chesapeake Bay Basin which is based upon interpretations of LANDSAT satellite images from the period 1977-1979. The LANDSAT data interpretations tend to emphasize reasonably well-managed pasture (e.g., Occoquan #5) rather than poorly-managed pastureland (e.g., Occoquan #1) since the latter is difficult to distinguish from low-tillage cropland. Therefore, the calibrated total P and total N loading factors for Occoquan #5 were felt to be most appropriate for application to the Chesapeake Bay Basin.

For the cropland land use categories, variations in management practices such as manure applications produced different monthly and average annual potency factors for each watershed. Because sediment is modeled as the driving force for nonpoint pollution loadings, comparisons of test watersheds to identify representative loading factors were based upon average annual sediment potency factors. Monitored total P and total N loads were regressed with monitored sediment loads for each site, and the slope of the regression line was designated as an average annual sediment potency factor (i.e., pollutant mass/sediment mass) which could be used to compare site loading factors with factors for the high tillage or low tillage cropland datasets. The monitored storm load datasets were then pooled by land use category, and separate pollutant load vs. sediment load regressions were performed for the high-tillage cropland and low-tillage cropland datasets. In this manner, total P and total N loading factors for test watersheds which were not suited to model calibration could be compared with factors for modeled watersheds. Likewise, average annual sediment potency factors for calibrated watersheds could be compared with average annual values for the entire high tillage cropland or low tillage cropland datasets. For the high tillage cropland category, the average annual sediment potency factors for total P and total N resulting from the pooled regressions fell approximately midway between the relatively high values for Pequea #3 and the relatively low values for Ware #7. For the low tillage cropland category, the average annual loading factors resulting from the pooled regressions are felt to represent an approximate midpoint between no tillage and minimum tillage values. Having identified average annual total P and total N loading factors for basinwide application, monthly factors were based upon the relationship between the average annual values for the cropland category and a selected calibration site. The "land use:site" ratios of the regressed sediment potency factors were multiplied by the calibrated average annual sediment potency factors for Pequea #3 and Occoquan #10 to develop average annual sediment potency factors for high-tillage cropland and low-tillage cropland, respectively. The average annual potency factor was then distributed to monthly values based upon the distributions calibrated for Pequea #3 and Occoquan #10.

The resulting NPS loading factors for each land use are shown in Table 8. The loading factors for the organic and inorganic fractions of phosphorus and nitrogen are based upon mean fractions (%) calculated from monitoring data for each land use category. For each land use, the percentage of P and N in each organic or inorganic form was multiplied by the composite total P and total N loading factors to obtain the monthly values for organic-N, ammonia-N, nitrate-N, organic P, and ortho-P shown in Table 8. In other words, this approach relied upon the test watershed model calibration studies to derive NPS loading factors for total P and total N, which are then distributed between organic and inorganic fractions based upon statistical analyses. It ensures that the sum of each land use's NPS loading factors for P and N fractions is equivalent to the composite total P and total N loading factors derived for each land use category. Consequently, this procedure was felt to be preferable to calibrating separate loading factors for P and N fractions monitored at each testing site and then trying to establish composite loading factors for each land use.

Comparisons of simulated and recorded loading data at the river basin gages, as described in a later section, permitted some verification of the P and N fractions assigned to each land use category.

The P and N fractions for rural-agricultural land use categories are based upon monitoring data from the EPA/CBP test watersheds, while the fractions for urban land use categories were based upon monitoring data collected at the NURP testing sites in the metropolitan Washington, D.C. region (38). As may be seen in Table 8, the organic fraction typically predominates in runoff from most land use categories.

Based on test watershed model calibration results, monthly ground cover (COVVEC) for urban and pasture land uses was set at 100% so that pervious area loadings are governed entirely by the calibrated pollutant accumulation rate rather than soil loss. For the other land use categories, ground cover was based upon the calibrated values for the test watershed used to derive the representative loading factors: Occoquan #9 for forestland, Pequea #3 for high-tillage cropland, and Occoquan #10 for low tillage cropland. The forestland and cropland ground cover values shown in Table 8 were used to model the river basins in the southern half of the Chesapeake Bay drainage area (e.g., Potomac and James river basins). For the Susquehanna River Basin, which occupies the northern half of the Bay's drainage area, the ground cover and corresponding sediment potency factors for forestland and cropland were shifted one month to represent the shorter growing season and earlier crop harvest.

Based upon discussions with State SCS staff and some initial Basin Model test runs, cropland tillage dates were assigned to each major river basin. On the specified tillage date, the accumulated sediment load on the soil surface is reset to a user-specified value to account for the tillage operation. Based upon the specified daily decay rate (REPERV), the accumulated sediment load becomes less available for direct washoff with

each day that passes following the tillage operation. The accumulated sediment value assigned to each tillage practice is based upon the test watershed model calibration studies described above. Based upon the testing site studies, accumulated sediment is reset to 1.0 ton/acre on each tillage date for high tillage cropland and to 0.25 ton/acre on the single tillage date for low tillage cropland. For the river basins in the southern half of the Chesapeake Bay drainage area, the Basin Model assumed that high tillage cropland areas are tilled on April 20th and September 23rd of each year (September 24 for 1976). For the Susquehanna River Basin, the Basin Model assumes high tillage cropland areas are tilled on May 10th and October 15th (May 11 and October 16 for 1976), while low tillage cropland areas are tilled on October 15th (October 16 for 1976). Obviously, every farm field is not tilled on the same date in each river basin. However, it is felt that assumed tillage dates and accumulated sediment reset values provide a reasonable representation of average changes in soil disturbance during the 2-3 week period when tillage practices typically occur in each river basin. While the selected tillage dates are felt to be adequate for general planning studies of the 64,000 sq mi drainage area of Chesapeake Bay, these values can be changed for any follow-up modeling studies by modifying the TIMTIL parameter in the nonpoint pollution loading submodel.

In order to compare annual nonpoint pollution loadings from the various land use categories, the NPS model was set up on a hypothetical single-land use watershed with silt loam soils typical of the Piedmont Province and a 2% overland flow slope. The NPS model was executed with hourly rainfall records from the Virginia suburbs of Washington, D.C. to simulate annual loadings for each land use based upon the NPS loading factors in Table 8 and in Hartigan et al. (9). Annual loadings were developed for a year of average wetness (1967) characterized by 40.6 in of rainfall, and a relatively wet year (1975), characterized by 54.1 in of rainfall. The simulated annual unit area loadings of total N and total P are summarized in Table 16. As may be seen, high tillage cropland produces the highest unit area loads of total N and total P while forestland produces the lowest unit area loads. Also of note are the higher loadings for wet year conditions. For example, Table 16 shows significantly higher cropland loadings for wet year conditions which can be attributed to percentage increases in soil loss that are much greater than runoff increases, while urban land uses exhibit increases proportional to runoff increases.

Dry Weather Flow Concentrations. As previously indicated, the relatively small size of the test watersheds tended to reduce the detection of subsurface flow contributions at the testing site monitoring stations. Based upon hydrology calibrations, it appears that the majority of the baseflow/interflow from the small test watersheds is delivered to a stream channel downstream of the testing site outlet where the monitoring station was located. Consequently, baseflow/interflow contributions either were not considered or were suppressed in the model calibration studies for most test watersheds. As discussed in a later section of this chapter, concentrations of baseflow/interflow for the Basin Model were calibrated to large sub-basins without regard for land use breakdown. However, concentration

Table 16

Simulated Annual Surface Washoff of Total N (as N) and Total P (as P) for
Average and Wet Years: Silt Loam Soils Typical of Piedmont Province in
Northern Virginia (1.0 lb/ac/yr = 0.89 kg/ha/yr)

LAND USE	TOTAL N LOAD (lbs-N/acre/yr)		TOTAL P LOAD (lbs-P/acre/yr)	
	AVG. YR.	WET YR.	AVG. YR.	WET YR.
FOREST	0.6	0.8	0.08	0.12
PASTURE	2.6	3.0	0.45	0.52
SINGLE FAMILY RESIDENTIAL (18% impervious)	6.0	6.8	0.86	0.97
COMMERCIAL (90% impervious)	10.7	12.2	1.29	1.46
LOW TILLAGE CROPLAND	5.0	9.0	0.42	0.74
HIGH TILLAGE CROPLAND	12.0	51.2	2.05	8.72

NOTE: Based on rainfall for Northern Virginia gages

o AVG. YR. (1967) = 40.6 in (104.1 cm)

o WET YR. (1975) = 54.1 in (138.7 cm)

statistics on the dry weather flow which was monitored at some of the EPA/CBP testing sites should be of some assistance in interpreting the average sub-basin concentrations reported later in this chapter. As may be seen in Table 17, the highest P and N concentrations in dry weather flow are typically associated with cropland sites, the lowest values with forest sites, and the midrange values with pasture and urban sites.

Also of interest in Table 17 are the much higher concentrations at the Pequea Creek sites, particularly in the case of nitrate-N. For example, the mean nitrate-N concentration for the Pequea Creek forest site (Pequea #2) is 37 and 329 times greater than the dry weather flow means for the Occoquan and Ware forest sites, respectively. Likewise, the mean nitrate-N concentration for the Pequea Creek residential site (Pequea #4) is on the order of 30 times greater than the mean concentration for the other residential sites. It is felt that the much higher dry weather flow concentrations associated with the Pequea sites, particularly for a readily reached constituent like nitrate-N, can be attributed in large part to the underlying limestone formations in the Pequea Creek basin. In addition to increasing monitored streamflow volumes at the outlets of most Pequea Creek testing sites, it is conceivable that the limestone formations can accelerate the delivery of leachate to streams at certain times of the year and also cause highly concentrated leachate from other land uses to be delivered to the outlet of a particular test watershed.

Scale-Up to River Basin Models. A five-step procedure was followed to scale-up from the test watershed models to the Chesapeake Bay river basin models.

First, the river basin models were subjected to the independent hydrology calibration/verification study which was described earlier in this chapter. Hydrologic parameter sets developed from the test watershed model calibration could not be applied directly to the river basin models because the subsurface flow component was often not detectable at the testing sites. Further, the independent hydrology calibration for the river basin model permits an accurate simulation of overland flow transport to the stream channel system. An accurate representation of overland flow transport eliminates the need for application of a "sediment delivery ratio" to simulated sediment and sediment-related loads. Based upon test watershed model sensitivity studies, the river basin models relied upon a transport coefficient (KSER) equal to 0.4 which provides a stable representation of runoff transport of detached pollutants.

Second, an erodibility factor (KRER) based upon the "K" factors presented in the State SCS-5 reports was assigned to each sub-basin based upon average soils characteristics. Since the NPS loading factors for each land use category are the same in each river basin, the erodibility factor is one of the most important parameters to represent locational differences in cropland nonpoint pollution loadings. For example, high tillage cropland in a sub-basin with highly erodible soils will produce higher NPS loads of total N and total P than the same land use in a sub-basin with less erodible

Table 17

Statistics on Dry Weather Flow Concentrations (mg/L)

LAND USE	MONITORING SITE	TOTAL P			ORTHO-P			TOTAL N		
		N	MEAN	DEVIATION	N	MEAN	DEVIATION	N	MEAN	DEVIATION
FOREST	OCCOQUAN 9	52	0.05	0.03	52	0.01	0.01	52	0.39	0.16
	PEQUEA 2	26	0.03	0.03	25	0.01	0.01	26	3.57	1.11
	WARE 8	10	0.01	0.02	10	0.0	0.0	9	0.12	0.06
PASTURE	OCCOQUAN 1	72	0.05	0.03	72	0.01	0.01	71	3.34	1.39
	OCCOQUAN 3	4	0.10	0.09	5	0.22	0.01	4	2.18	0.17
	OCCOQUAN 4	38	0.16	0.10	38	0.02	0.02	38	3.32	1.17
	OCCOQUAN 5	8	0.05	0.02	9	0.01	0.01	8	1.12	0.61
	PEQUEA 5	22	0.48	0.34	22	0.33	0.25	21	7.75	1.76
	PEQUEA 6	22	0.30	0.24	22	0.22	0.20	22	7.27	1.37
LOW-TILL CROPLAND	OCCOQUAN 2	49	0.11	0.20	49	0.01	0.01	48	5.10	2.19
HIGH-TILL CROPLAND	PEQUEA 3	21	0.16	0.05	21	0.12	0.06	21	21.2	2.41
	WARE 2	11	0.07	0.08	11	0.04	0.07	11	0.44	0.25
SINGLE FAMILY RESIDENTIAL	OCCOQUAN 7	68	0.08	0.22	70	0.01	0.02	69	0.69	0.82
	OCCOQUAN 8	65	0.05	0.03	67	0.01	0.01	65	0.64	0.40
	PEQUEA 4	22	0.04	0.04	22	0.01	0.01	22	3.74	1.16
	WARE 5	10	0.02	0.04	10	0.01	0.01	9	0.27	0.15
MIXED	PEQUEA 1	22	0.10	0.05	22	0.06	0.03	21	6.53	1.03

NOTE: No baseflow recorded at Ware 7 (High-Till Crop) & Occoquan 10 (Low-Till Crop)

Table 17 (continued)
Statistics on Dry Weather Flow Concentrations (mg/L)

LAND USE	MONITORING SITE	TKN			AMMONIA-N			NITRATE-N		
		N	MEAN	DEVIATION	N	MEAN	DEVIATION	N	MEAN	DEVIATION
FOREST	OCCOQUAN 9	52	0.30	0.15	51	0.05	0.02	53	0.09	0.05
	PEQUEA 2	26	0.28	0.20	26	0.03	0.03	26	3.29	1.12
	WARE 8	9	0.10	0.06	10	0.0	0.0	10	0.01	0.02
PASTURE	OCCOQUAN 1	72	0.48	0.26	72	0.10	0.14	71	2.86	1.40
	OCCOQUAN 3	4	0.75	0.73	5	0.18	0.22	5	1.56	0.81
	OCCOQUAN 4	38	1.95	1.43	38	0.36	0.40	38	1.37	0.94
	OCCOQUAN 5	8	0.81	0.47	9	0.17	0.21	9	0.35	0.30
	PEQUEA 5	21	1.34	1.14	22	0.16	0.13	21	6.43	1.18
	PEQUEA 6	22	0.62	0.47	22	0.09	0.08	22	6.65	1.27
LOW-TILL CROPLAND	OCCOQUAN 2	49	0.74	0.74	49	0.11	0.14	48	4.35	1.95
HIGH-TILL CROPLAND	PEQUEA 3	21	0.28	0.30	21	0.06	0.06	21	21.1	2.51
	WARE 2	11	0.32	0.13	11	0.0	0.0	11	0.12	0.14
SINGLE FAMILY RESIDENTIAL	OCCOQUAN 7	69	0.46	0.66	70	0.09	0.07	70	0.23	0.26
	OCCOQUAN 8	65	0.51	0.30	67	0.17	0.15	67	0.13	0.16
	PEQUEA 4	22	0.42	0.20	22	0.05	0.04	22	3.31	1.15
	WARE 5	9	0.19	0.12	10	0.0	0.0	10	0.10	0.12
MIXED	PEQUEA 1	22	0.41	0.16	22	0.04	0.03	21	6.13	1.02

NOTE: No baseflow recorded at Ware 7 (High-Till Crop) & Occoquan 10 (Low-Till Crop)

soils, even though the sediment potency factors are the same in both sub-basins.

Third, the NPS loading factors shown in Table 8 were assigned to the land use categories in each sub-basin.

Fourth, a receiving water model with point source discharge files was iteratively executed in a quasi-steady state mode for a typical low flow condition (i.e., 25th percentile flow). Simulated baseflow concentrations were compared to low flow monitoring data to establish an initial estimate of baseflow/interflow concentrations.

Fifth, the sub-basin/receiving water models of each river basin were calibrated for a two-year period (January 1974-December 1975) and verified for a three-year period (January 1976-December 1978). The models were iteratively executed for the two-year calibration period with the NPS loading factors assigned in Step 3 to set instream process parameters and to derive a final set of baseflow/interflow concentrations for each sub-basin. The NPS loading factors were not adjusted during the calibration/verification of the river basin models. The results of the receiving water model calibration/verification are presented in a later section of this chapter.

Precipitation Loadings on Bay Surface Area. The wetfall dataset developed by EPA/CBP. (39) was analyzed to derive the following mean annual concentrations of precipitation falling on the surface area of Chesapeake Bay:

Organic N:	0.67 mg/L
Ammonia-N:	0.35 mg/L
Nitrate-N:	0.57 mg/L
Organic P:	0.048 mg/L
Inorganic P:	0.016 mg/L
BOD ₂₀ :	13.0 mg/L

These mean concentrations were then combined with the hourly rainfall records for segments 5 and 6 (upper Bay) and segments 9 and 10 (lower Bay) to develop daily "per acre" loading records for precipitation. Daily precipitation loading records were developed for 1966, 1974, and 1975 (i.e., production run periods) in a format suitable for input to each node in the Main Bay water quality model.

Recommendations for Future Test Watershed Studies. Outlined below are recommendations for improved coordination between the monitoring and modeling efforts to ensure maximum usefulness of the test watershed database (6). The recommendations address problems with site selection and certain elements in the monitoring work program which were encountered during the modeling study described herein.

A. Site Selection: One problem which reduced the applications of monitoring data from certain test watersheds was the selection of mixed land use catchments with significantly different loading factors. Secondary land uses which represent a relatively small percentage of the total catchment area can distort monitoring characterizations of the primary land use if runoff concentrations for the secondary land use are significantly higher. While it may not always be possible to identify single land use watersheds for monitoring studies, mixed land use catchments with a secondary land use that is characterized by much higher NPS loading factors than the primary land use should not be designated as test watersheds.

Two of the test watersheds in the Pequea Creek basin were located over limestone formations that affected the quantity and probably the quality of monitored baseflow during dry weather and storm periods. Since the purpose of test watershed monitoring studies is to collect nonpoint pollution loading data that are representative of larger basins, care should be taken during site selection to ensure that underlying geology as well as land use and upper soils characteristics are representative of the river basins in which the data is to be applied.

B. Monitoring Work Program: As previously indicated, the test watershed monitoring studies were designed and initiated in the absence of a specific watershed modeling work program. The earlier start-up of the monitoring study was intended to ensure sufficient time for modeling studies of the monitoring data. However, if the monitoring and modeling work program had been developed and implemented concurrently, it is likely that: some different site selection decisions would have been made; collection of the continuous rainfall and runoff records required for model calibration would have received a higher priority in order to increase the amount of data available for model calibration; data reduction requirements could have been reduced considerably; and the results of model calibration studies would be improved due to the expanded database. After the monitoring studies have started, periodic interactions between the modeling and monitoring investigators can facilitate any mid-course corrections necessary to enhance the applications of the monitoring database. While it is often necessary to initiate test watershed monitoring studies at the earliest possible date to ensure the maximum amount of monitoring data and/or a sufficient amount of time for data analysis, the advantages of better coordination between the monitoring and modeling efforts from start to finish merits consideration.

The majority of the hydrometeorologic data reduction required for model calibration was performed by the modeling investigator. The monitoring investigators were not required to reduce rainfall stripcharts and reductions of flow stripcharts were generally restricted to the storms which produced water quality samples. Consequently, the modeling investigator was required to perform most of the quality assurance checks on hydrometeorologic data for the majority of the test watersheds. These checks included assessments of rainfall-runoff relationships and comparisons of runoff volumes recorded at the test watersheds in each river basin. Due to the later start-up of the modeling study and delayed transmittal of

monitoring data to the modeling investigator, initial quality assurance checks on the hydrometeorologic dataset were not completed until most test watershed monitoring studies had ended. As a result, onsite experiments to resolve hydrometeorologic data problems could not be performed, and mid-course corrections involving additional instrumentation, further instrument calibration, or the selection of substitute testing sites could not be considered. Further, an earlier quality assurance effort focusing on model calibration needs probably would have flagged the significant gaps in the hydrometeorologic records required for model calibration in time to produce an expanded database. Therefore, it is recommended that extensive quality assurance checks be performed on the hydrometeorologic data very early in the test watershed monitoring study so that problems and anomalies can be identified in time for mid-course corrections.

For certain test watersheds, relatively long sampling periods (e.g., 24-72 hrs) resulted in the inclusion of excessive baseflow volumes in the flow-composite samples for monitored storm events. As a result, the separation of baseflow volumes and loadings from the reported storm volumes and loadings was very difficult for these test watersheds, and model calibration studies were significantly complicated. To ensure the development of a reliable nonpoint pollution loading dataset by test watershed monitoring studies, it is recommended that the sample collection/retrieval schedule be designed to minimize baseflow contributions during monitored storms.

For test watershed monitoring studies in four of the five river basins, separate raingage and flowmeter recorders were used for the majority of the monitoring period. The use of separate recorders generally resulted in unsynchronized rainfall and flow records due to inevitable differences in chart speeds. Consequently, one of the more time-consuming data reduction tasks involved scanning the individual stripcharts to match rainfall and flow records for monitored storms. The use of a dual-pen recorder for the raingage and the flowmeter would not only reduce data reduction requirements for continuous simulation studies but would also facilitate the quality assurance checks of hydrometeorologic data recommended above.

Receiving Water Submodel Calibration/Verification

Methodology. A total of 13 major U.S.G.S. water quality gages with extensive monitoring records were selected for the receiving water model calibration/verification study. These gages are listed in Table 2 and shown in Figure 12. Comparisons of simulated and recorded data were performed at 10 of these gages. Due to a limited number of observations for most constituents of interest, water quality data for the following five gages was used only to develop subsurface flow concentrations, not for goodness-of-fit assessments: Rappahannock River near Fredericksburg, VA (#01668000); South Fork Shenandoah River at Front Royal, VA (#0163100); Shenandoah River at Millville, WV (#01636500); Potomac River at Hancock, MD (#01613000); and Potomac River at Shepherdstown, WV (#01618000).

Calibration of the receiving water submodel involved: setting the rate coefficients for instream water quality processes; setting baseflow/interflow concentrations which account for pollutant loadings from subsurface flows as well as the relatively small wastewater discharges (i.e., less than 0.5 MGD) that are not included in the wastewater treatment plant dataset and for net flux from stream channel bottom sediments; and quality control checks on wastewater discharge files based upon instream monitoring data. To minimize calibration costs, the receiving water submodel was initially operated in a quasi-steady state mode for a typical low flow condition to develop initial estimates for baseflow/interflow concentrations and chlorophyll-a growth parameters. It was felt that a low flow period would be most appropriate for setting initial receiving water model parameters, since it would be very difficult to distinguish runoff loadings from subsurface and wastewater loads under high flow conditions. Because the test watershed data could not be used to establish subsurface flow concentrations for each land use category (i.e., since baseflow/interflow contributions were not detectable at the test watershed monitoring station), average baseflow/interflow concentrations were calibrated for each sub-basin without regard for land use breakdown. While it would have been preferable to establish subsurface flow concentrations for each land use category, the selected approach does provide a reasonably accurate representation of the magnitude of subsurface flow contributions upstream from each calibration gage as well as locational differences within the Chesapeake Bay drainage area.

The 25th percentile daily streamflow (i.e., streamflow which is exceeded 75% of the time) at each gage for the period 1966-1978 was selected for use in the steady-state model applications. Starting at the upstream gages and working downstream, the receiving water model was operated with the 25th percentile daily streamflow, reported wastewater discharges, and typical daily meteorologic data for May through October to set instream process parameters and tributary baseflow/interflow concentrations. It should be emphasized that the baseflow/interflow concentrations are intended to approximate small wastewater discharges and errors in the wastewater discharge input files (e.g., treatment plant bypasses) as well as subsurface flow concentrations. Simulated concentrations for the quasi-steady state model executions were compared with the observed median concentrations for low flow periods at each major gaging station. Following the refinement of initial parameter estimates and baseflow/interflow concentrations with the steady-state model, the Basin Model was calibrated in a continuous simulation mode for the period January 1974-December 1975.

The receiving water model was executed for the two-year calibration period and the following parameters were adjusted in conjunction with the baseflow/interflow concentrations for each river basin: chlorophyll-a growth parameters; BOD sinking rate; chlorophyll-a sinking rate; and sinking rates for organic N and P. Rate coefficients for BOD decay and nitrification were derived from stream channel geometry relationships developed by Wright and McDonnell (41) and Bansal (42). With the exception of nitrification rates in a few reaches, no further adjustment to these

coefficients was made during calibration. Likewise, nonpoint pollution loading factors developed from the test watershed modeling study were not adjusted during receiving water model calibration to provide a verification of the previous loading factor calibration work.

Parameter adjustments were based upon comparisons between simulated and observed water quality data at two different levels:

1. Inspection of time series plots of simulated and observed concentrations at USGS monitoring stations and comparison of statistics for the simulated and observed concentration datasets.
2. Comparison of simulated loading records delivered to the mouths of the Susquehanna, Potomac, and James river basins with synthesized pollutant loading records developed from regression equations for the USGS fall line monitoring dataset.

In other words, calibration focussed on balancing the goodness-of-fit for upstream reaches with the match of pollutant loading relationships for the three major river basins. Comparisons of simulated loadings with "flow-loading" relationships from the USGS fall line monitoring study were made on a daily, monthly, and annual basis. Daily loading comparisons provided an excessively rigorous test of the nonpoint pollution loading factors derived from the test watershed modeling studies, while the monthly and annual loading comparisons were used to guide adjustments to receiving water model parameters and baseflow/interflow calibrations.

Following calibration, the receiving water model was verified by operating it for the period January 1976-December 1978 with constant parameter sets and baseflow/interflow concentrations. Since nonpoint pollution loading factors were not adjusted during the two-year calibration period, the verification of the test watershed model calibration results actually totalled five years.

The 1974-1978 period was selected for receiving water submodel calibration/verification for five reasons. First, in order to perform a meaningful model verification, the wastewater flows and effluent levels used in the model must be reasonably close to the actual wastewater discharges which produced the monitored receiving water quality. Since wastewater treatment levels changed significantly throughout the Basin during the early 1970's (i.e., prior to 1974) and sufficient data on actual discharges is not available for model input, it was advisable to use a verification period (1974-1978) with available wastewater discharge records and relatively constant wastewater flows and effluent levels. Second, the period selected for model verification should also have a defined land use pattern that is consistent with the available water quality monitoring records in order to ensure a meaningful verification of nonpoint pollution loading factors. Since the existing land use data for the Basin Model was based upon LANDSAT data from the period 1977-1979, it was appropriate to select a verification period that does not predate the LANDSAT scenes by a significant amount,

particularly in light of the significant switchover from high tillage to low tillage cropland practices that occurred in mid- to late-1970's. Third, only a limited amount of plant nutrient data is available for U.S.G.S. monitoring stations prior to 1974. Thus, even if an earlier verification period was acceptable from the standpoint of wastewater discharges and the Basin land use pattern, an insufficient amount of water quality data would be available for comparison with Basin Model simulations. Fourth, the 1974-1978 period includes a good mix of normal and above-normal streamflow periods which should provide a good test for parameter sets and baseflow/interflow concentrations based upon low flow periods. Finally, as previously indicated, the 1974-1978 period could be used to verify nonpoint pollution loading factors because its streamflow statistics are reasonably similar to the streamflow statistics (e.g., flow-duration curves and annual/seasonal streamflow volumes) during the 1979-1981 U.S.G.S. fall line monitoring study.

Fall Line Loading Results. Monthly, daily, and annual fall line loads were compared to measure agreement between the Basin Model simulations and the USGS flow-loading relationships. The simulated values represent the loads the total point and nonpoint pollution loads delivered to the fall line from the tributary river basin. In all cases, USGS loads were based upon daily loads calculated from simulated daily streamflows at the mouth of each river basin, which were then aggregated to produce either monthly or annual totals.

Scatterplots and regression statistics for the calibration and verification periods that indicate goodness-of-fit for monthly and daily loads are presented in Figures 31 through 48 for the Susquehanna River fall line, Figures 49 through 66 for the Potomac River fall line, and Figures 67 through 84 for the James River fall line. For each set of river basin figures, the first six cover the two-year calibration period (January 1, 1974 - December 31, 1975), the second six cover the three-year verification period (January 1, 1976 - December 31, 1978), and the final six cover both the calibration and verification periods (January 1, 1974 - December 31, 1978). Each group of six scatterplots covers monthly loads of total P, inorganic P, total N, and nitrate-N and daily loads of total P and total N. The "line of equal values" in each scatterplot is indicated by a "**". Therefore, a visual inspection of the scatterplots to assess departure from the line of equal values can serve as one measure of goodness-of-fit. The month associated with each point in the scatterplot can be determined from the following key:

- 1 = January
- 2 = February
- 3 = March
- 4 = April
- 5 = May
- 6 = June
- 7 = July
- 8 = August

9 = September
O = October
N = November
D = December

Therefore, it is easy to determine whether any months consistently exhibit significant errors from a visual inspection of each scatterplot.

In order to quantify goodness-of-fit, a least-square regression line was fit to each scatterplot, and the R^2 and slope terms associated with the regression are reported in each figure. The coefficient of determination (R^2) indicates the percent of total variance which is accounted for by the regression line or how well the simulated and USGS-based loads are fit by a least-squares regression line with the reported slope. Acceptable goodness-of-fit is demonstrated by regressions with a relatively high R^2 and a slope that is reasonably close to 1.0. Calculations of t-statistics on the significance of the slope and intercept terms in the linear regression equations covered by Figures 31 through 84 revealed that the slope term was always significantly different from zero while the intercept term was generally not. Consequently, for regressions exhibiting relatively high R^2 values, a reasonable indication of simulation error is provided by the following relationship:

$$\text{Average \% Error} = (\text{Slope} - 1.0) * (100\%)$$

Based upon both visual inspection of Figures 31 through 84 and the reported regression statistics, all three river basins typically exhibit satisfactory goodness-of-fit for all three periods. Most R^2 values are in excess of 0.85 and many are 0.90 or higher. Many regression line slope terms are between 0.9 and 1.1 while most slopes are between 0.75 and 1.25, which represents an acceptable range of error in light of errors on the order of 20% that can be encountered in water quality monitoring studies (REF). In general, inorganic P tends to exhibit the least satisfactory goodness-of-fit in all three river basins, probably because of factors such as: (a) sewage treatment plant upgrading during the calibration/verification period that is not reflected in the constant wastewater discharge values used in the model; and (b) the approximations required to model transport through the large river basins. However, because total P loads are accurately simulated and organic P is the predominant phosphorus form delivered to the fall line, the poorer fits associated with inorganic P are not of serious concern. The potential role of wastewater discharge errors in the James River Basin simulations is discussed in a later section. Some of the other general conclusions about goodness-of-fit that can be based upon the fall line loading comparisons are the following:

- o While all three river basins exhibit goodness-of-fit for critical constituents, the Susquehanna River Basin appears to exhibit the best agreement between simulated and USGS-based loads, followed by the Potomac River Basin and the James River Basin in that order.

Figure 31. Comparison of Simulated Monthly Loads and Loads Based upon USGS Flow-Loading Relationships:
SUSQUEHANNA RIVER FALL LINE (1/1/74 - 12/31/75): MONTHLY TOTAL P

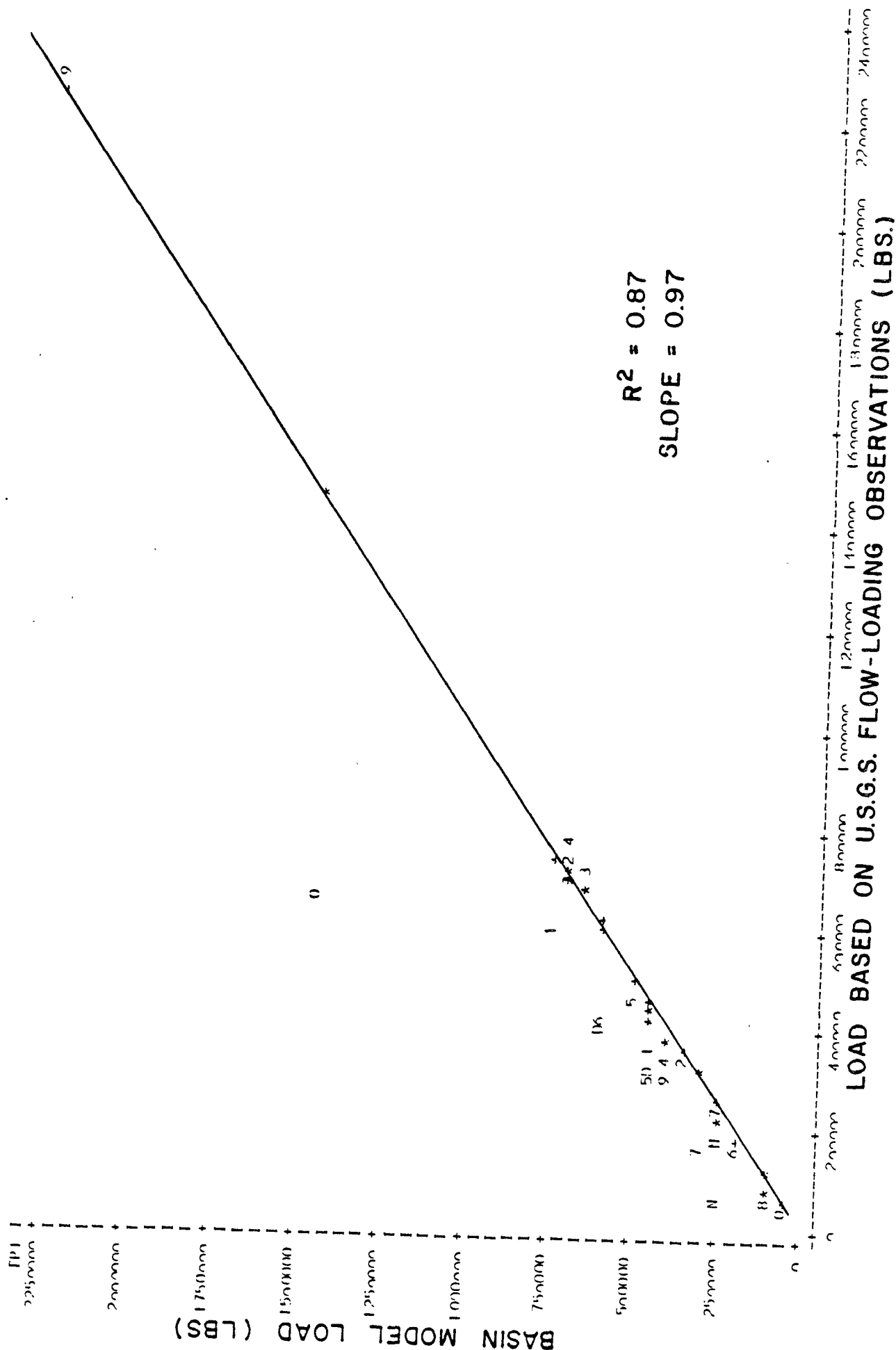


Figure 32. Comparison of Simulated Monthly Loads and Loads Based upon USGS Flow-Loading Relationships:
SUSQUEHANNA RIVER FALL LINE (1/1/74 - 12/31/75) MONTHLY INORGANIC P

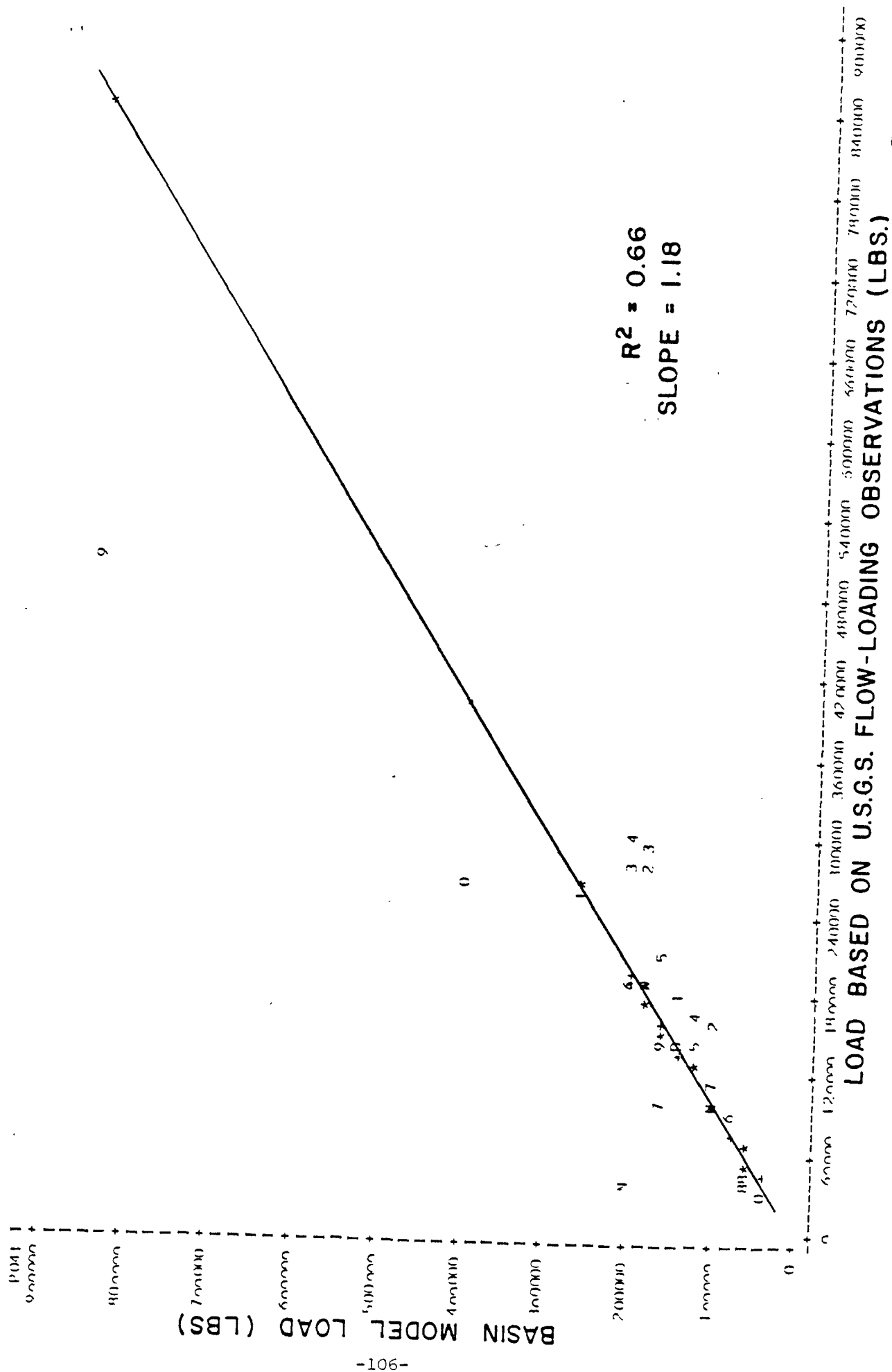


Figure 33. Comparison of Simulated Monthly Loads and Loads Based upon USGS Flow-Loading Relationships:
SUSQUEHANNA RIVER FALL LINE (1/1/74 - 12/31/75): MONTHLY TOTAL N

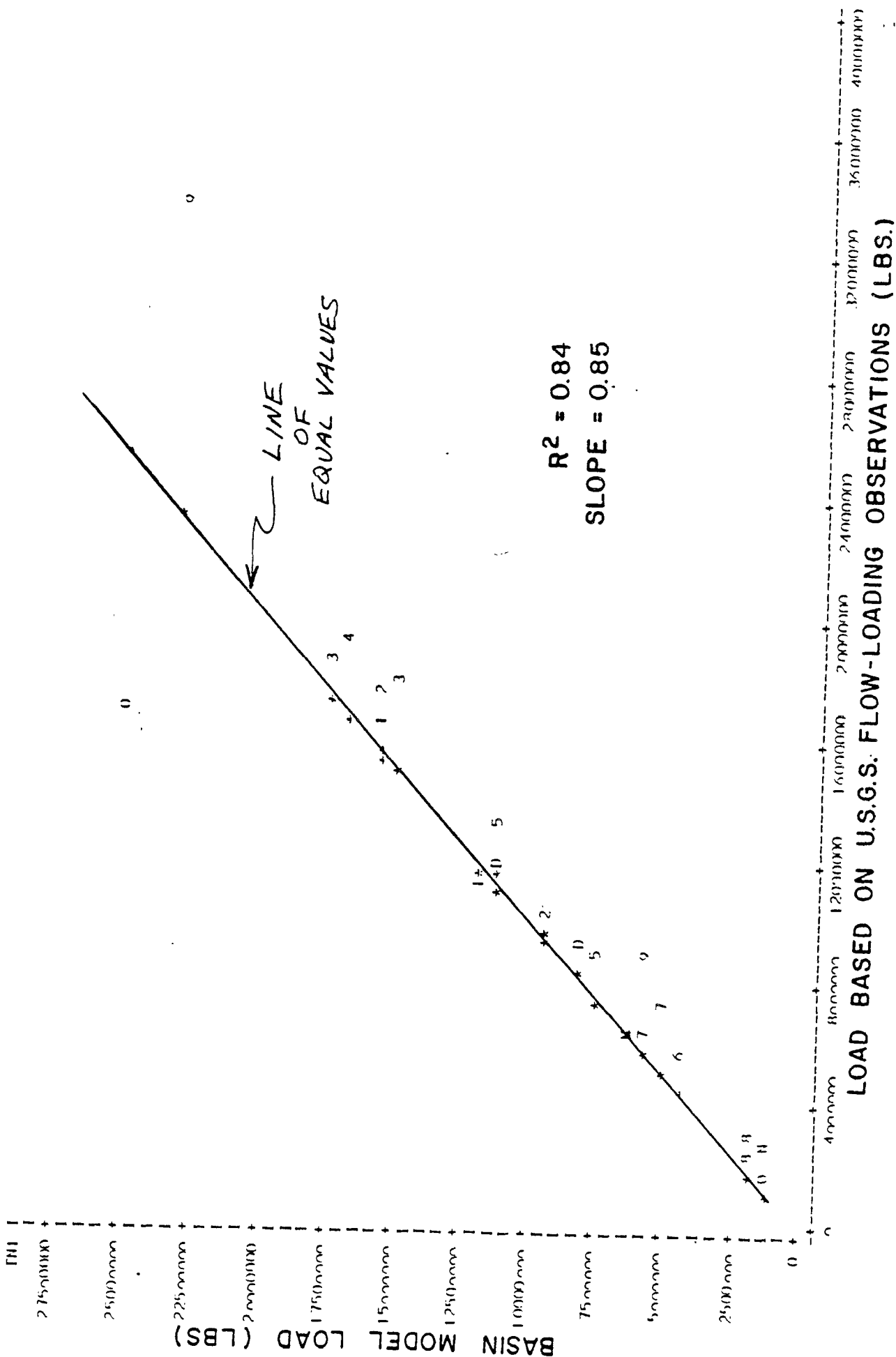


Figure 34. Comparison of Simulated Monthly Loads and Loads Based upon USGS Flow-Loading Relationships:
**SUSQUEHANNA RIVER FALL LINE (1/1/74 - 12/31/75): MONTHLY NITRITE
 + NITRATE -N**

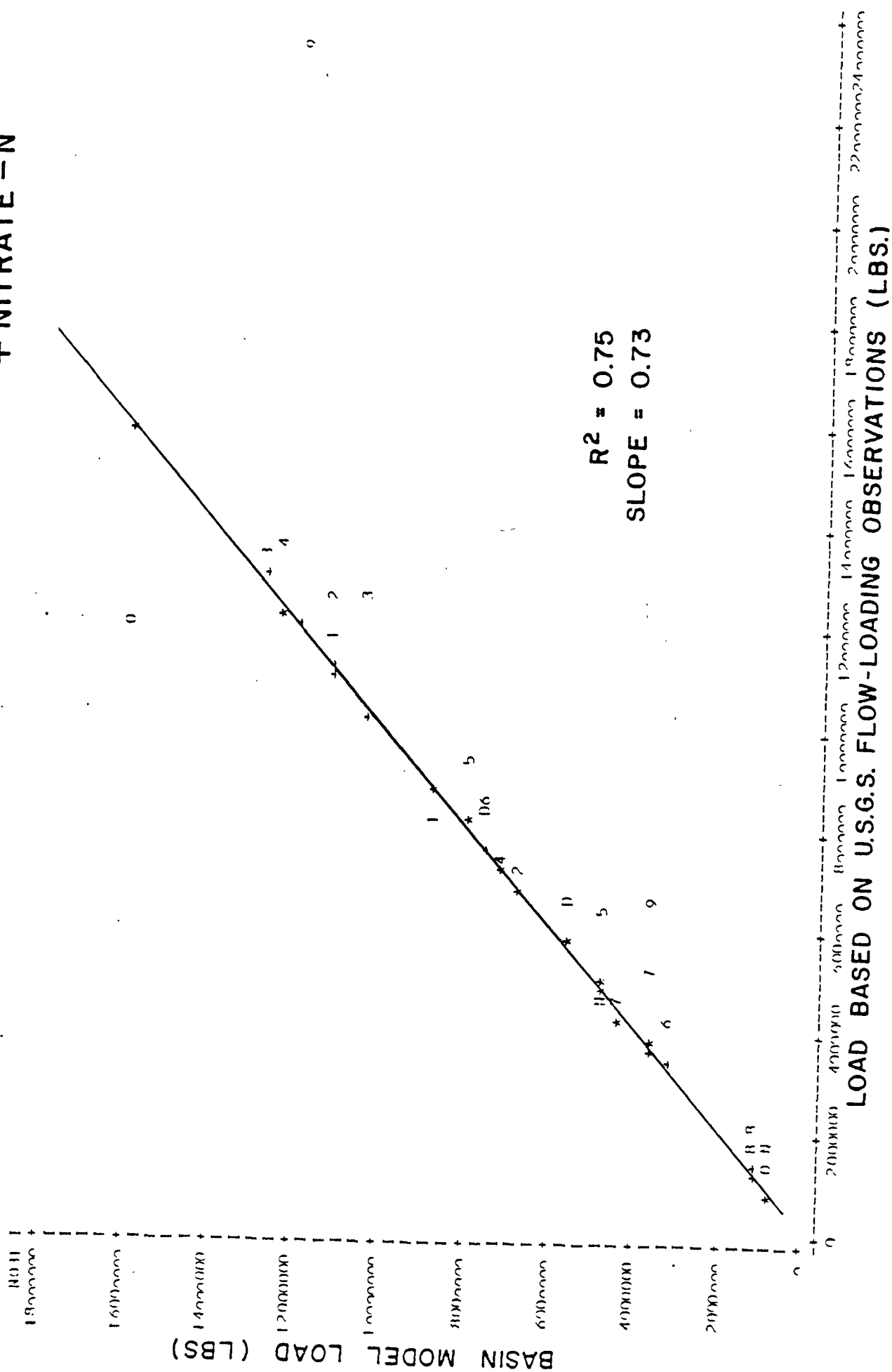


Figure 35. Comparison of Simulated Daily Loads and Loads Based upon USGS Flow-Loading Relationships:
SUSQUEHANNA RIVER FALL LINE (1/1/74 - 12/31/75): DAILY TOTAL P

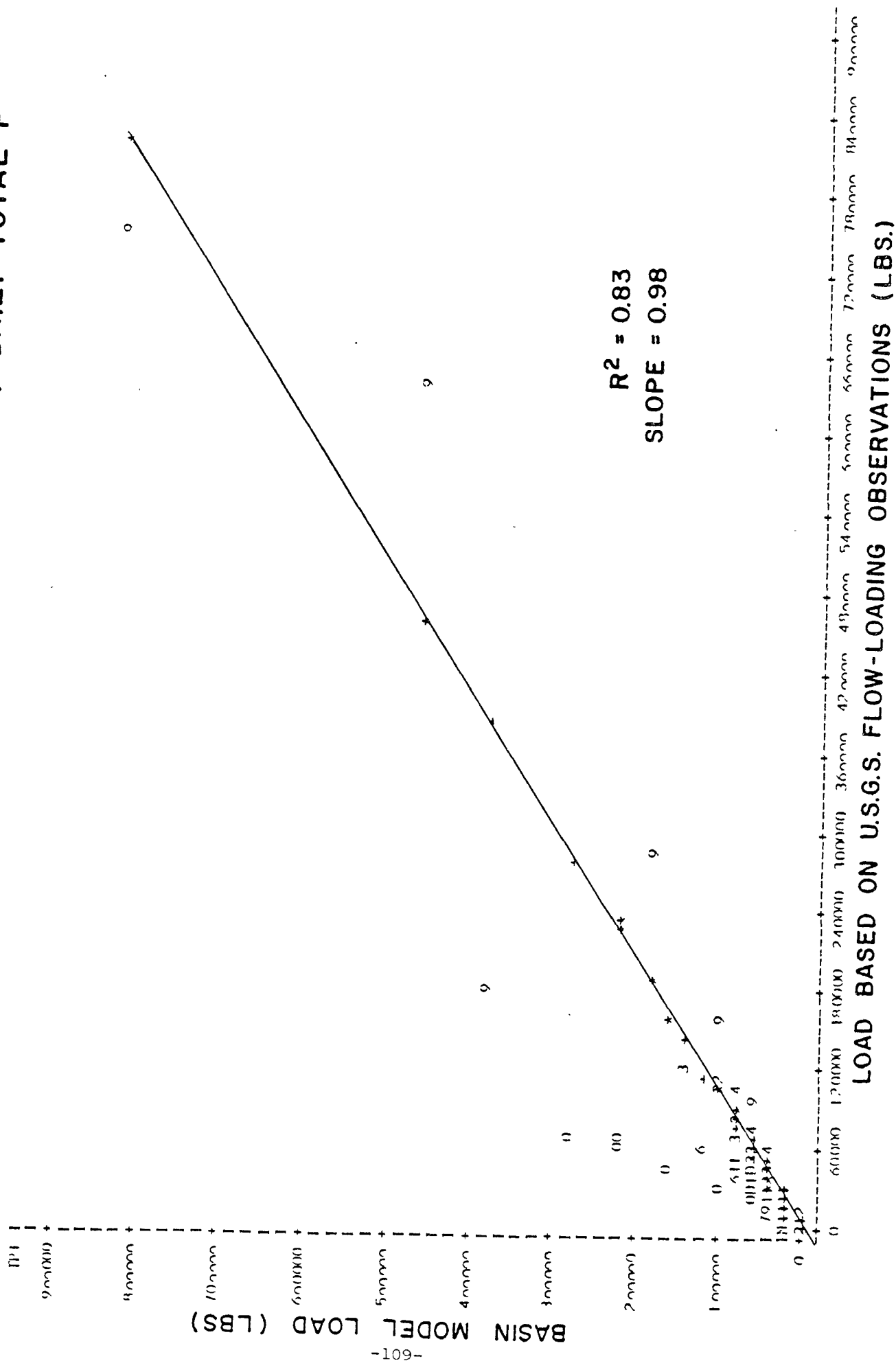


Figure 36. Comparison of Simulated Daily Loads and Loads Based upon USGS Flow-Loading Relationships:
SUSQUEHANNA RIVER FALL LINE (1/1/74 - 12/31/75): DAILY TOTAL N

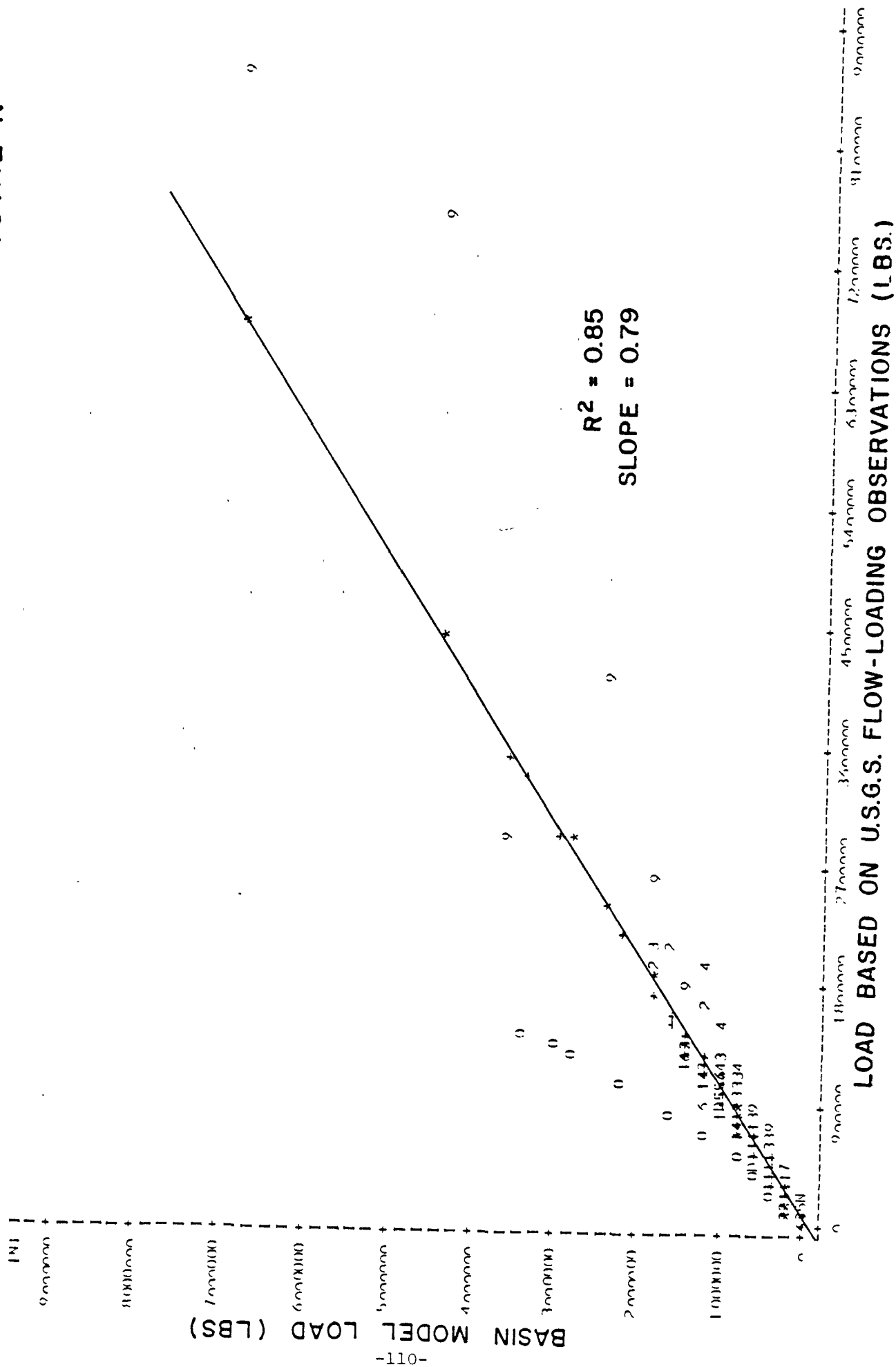


Figure 37. Comparison of Simulated Monthly Loads and Loads Based upon USGS Flow-Loading Relationships:
SUSQUEHANNA RIVER FALL LINE (1/1/76 - 12/31/78): MONTHLY TOTAL P

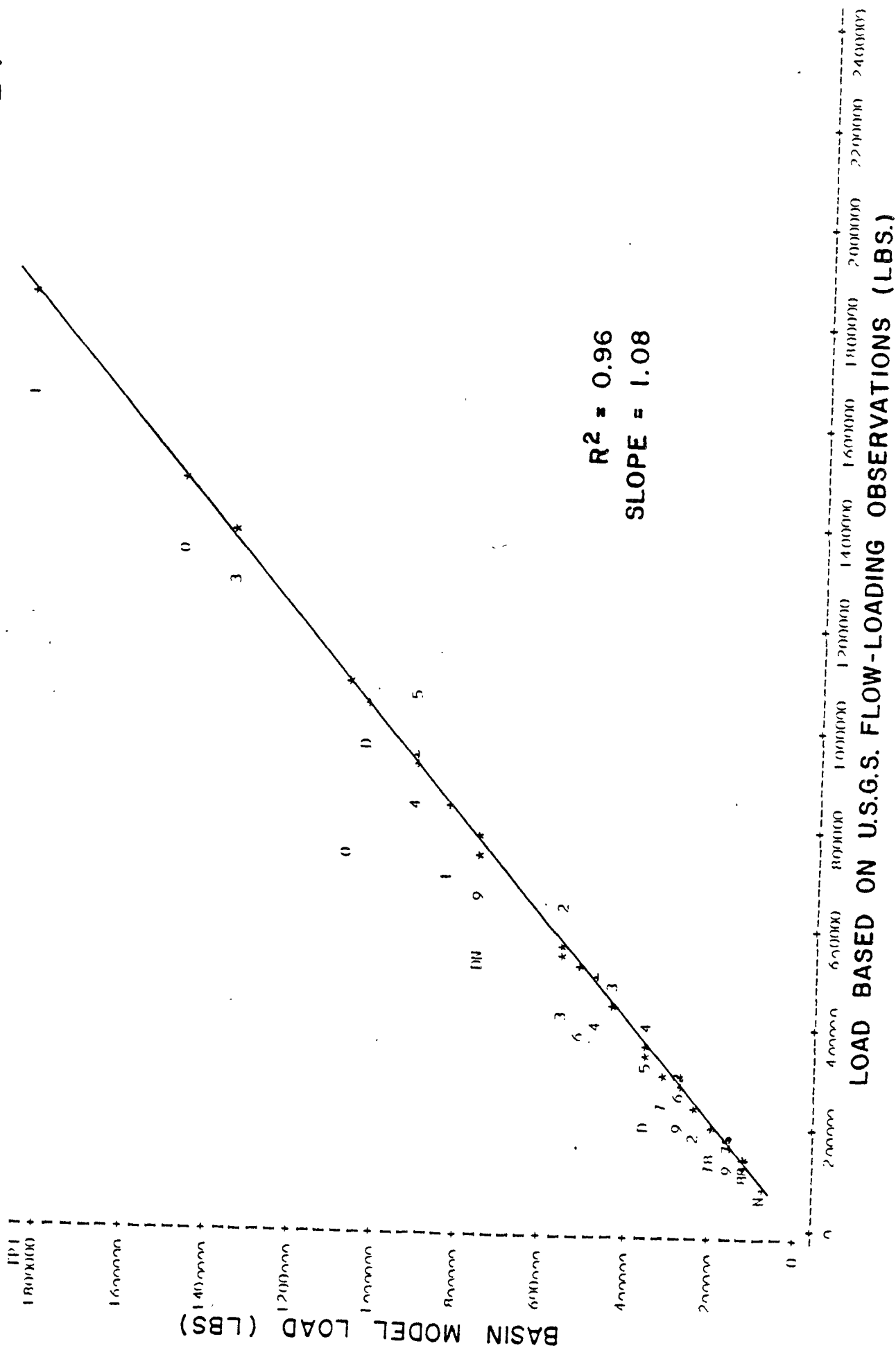


Figure 38. Comparison of Simulated Monthly Loads and Loads Based upon USGS Flow-Loading Relationships:
SUSQUEHANNA RIVER FALL LINE (1/1/76 - 12/31/78) MONTHLY INORGANIC P

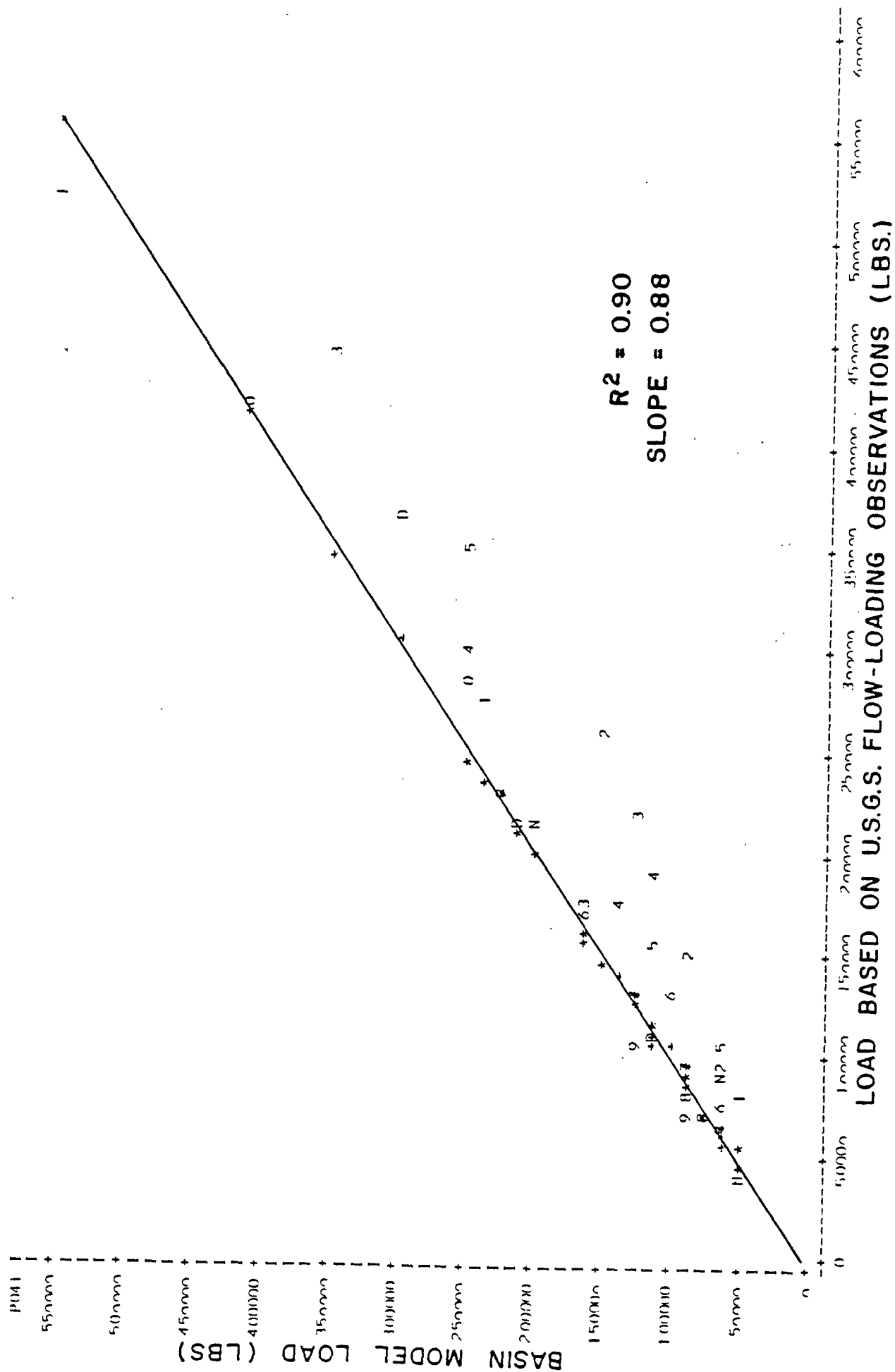


Figure 39. Comparison of Simulated Monthly Loads and Loads Based upon USGS Flow-Loading Relationships:
SUSQUEHANNA RIVER FALL LINE (1/1/76 - 12/31/78): MONTHLY TOTAL N

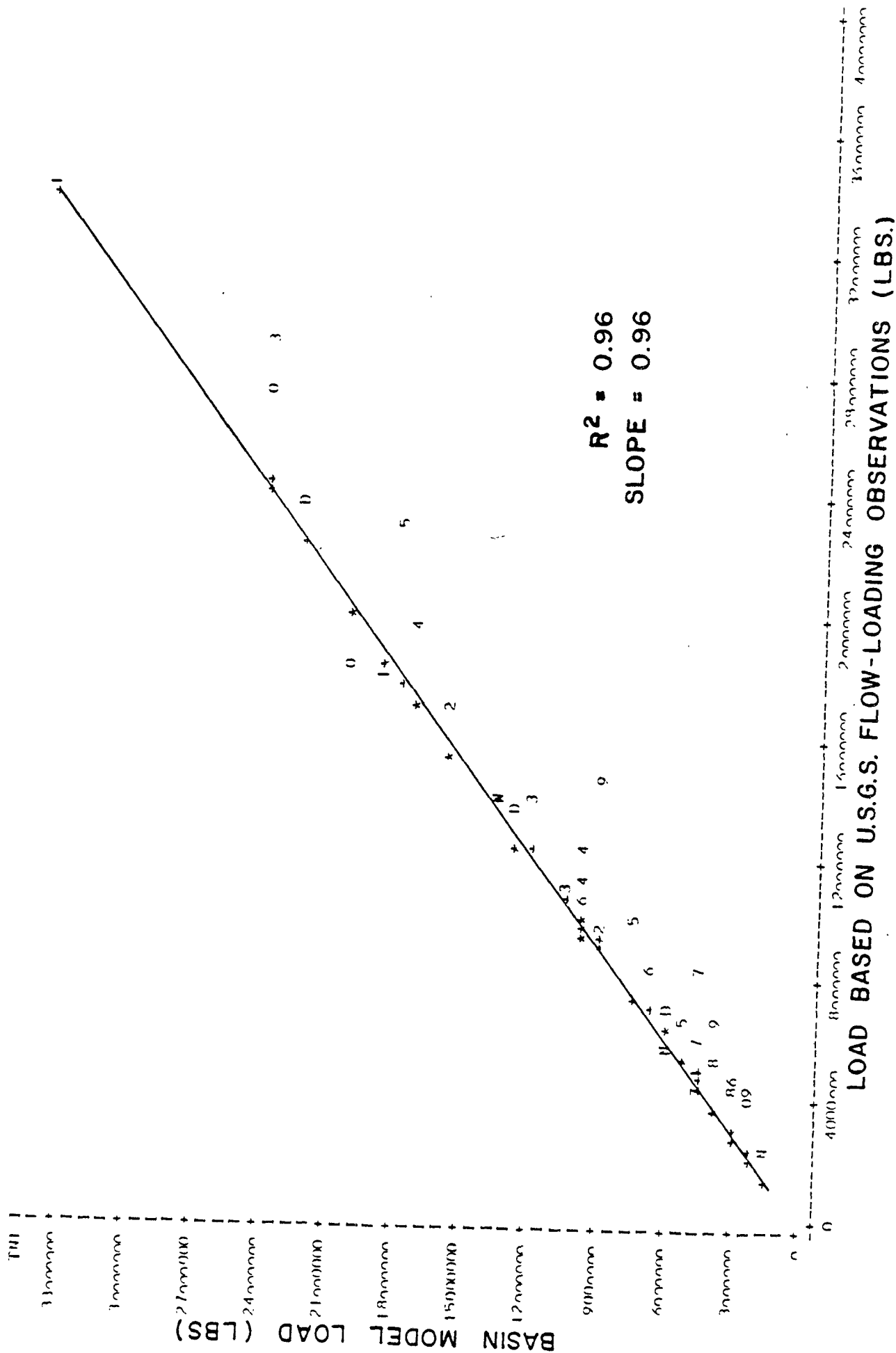


Figure 40. Comparison of Simulated Monthly Loads and Loads Based upon USGS Flow-Loading Relationships:

**SUSQUEHANNA RIVER FALL LINE (1/1/76 - 12/31/78): MONTHLY NITRITE
+ NITRATE - N**

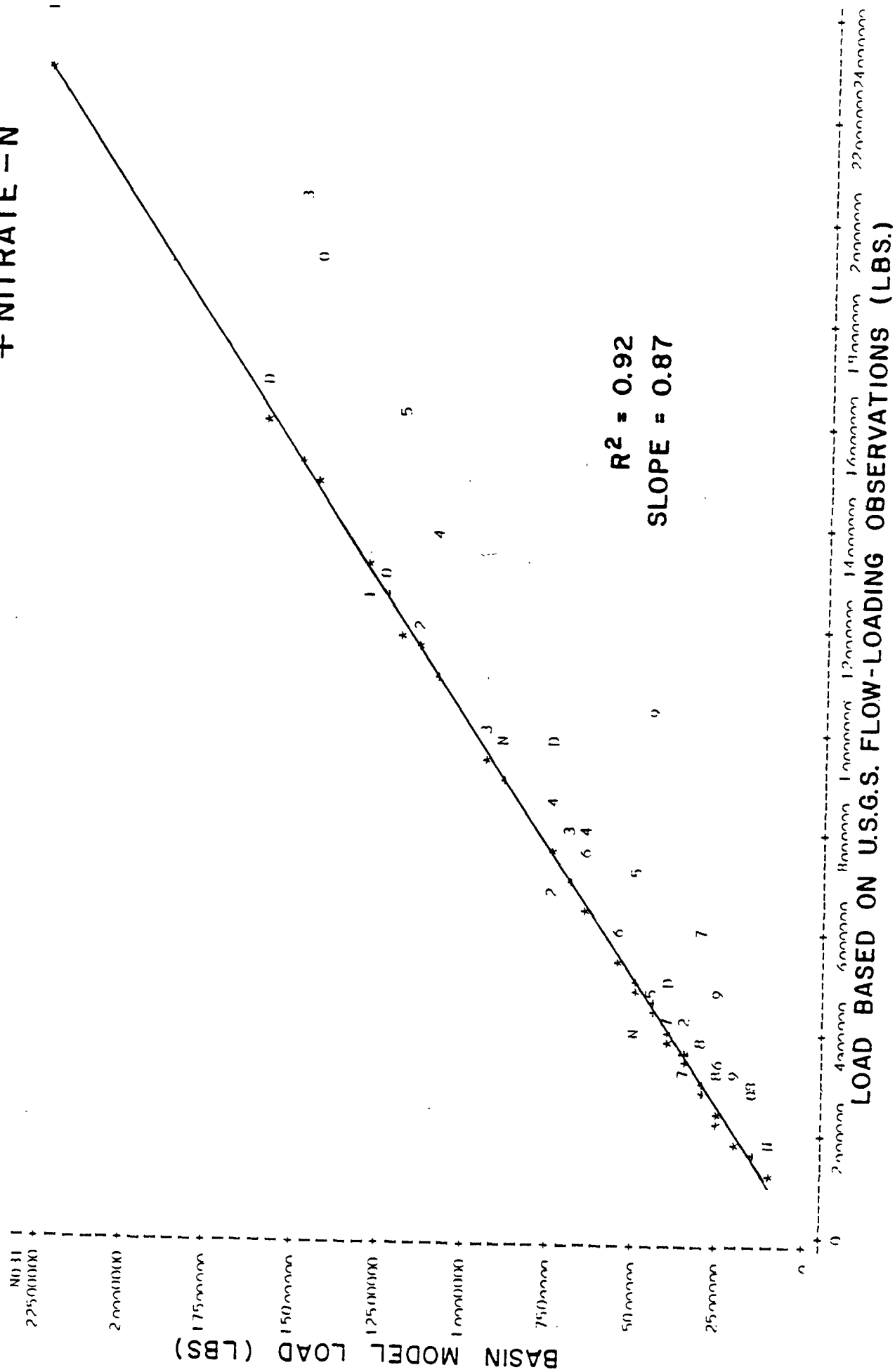


Figure 41. Comparison of Simulated Daily Loads and Loads Based upon USGS Flow-Loading Relationships:
SUSQUEHANNA RIVER FALL LINE (1/1/76 - 12/31/78): DAILY TOTAL P

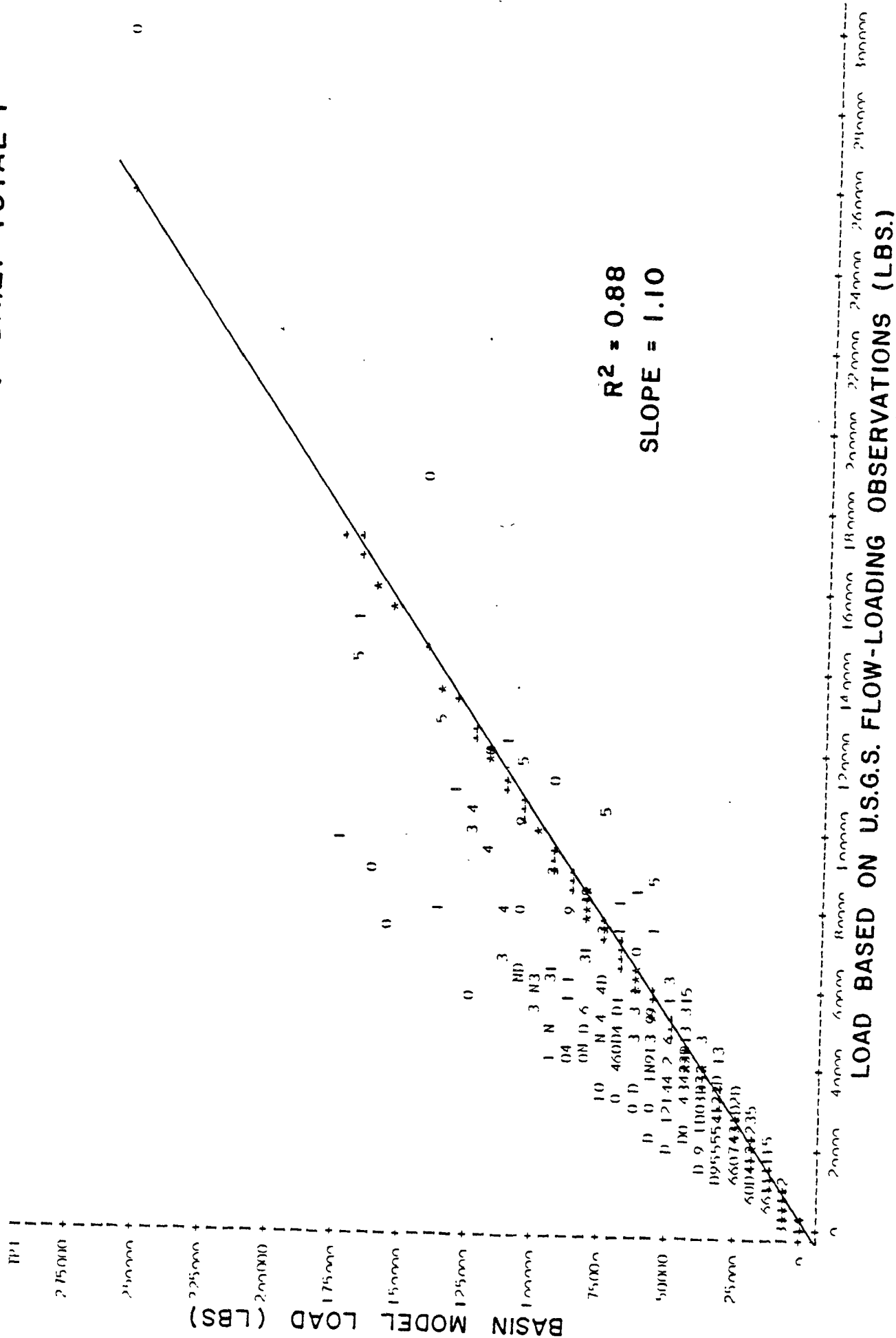


Figure 42. Comparison of Simulated Daily Loads and Loads Based upon USGS Flow-Loading Relationships:

SUSQUEHANNA RIVER FALL LINE (1/1/76 - 12/31/78): DAILY TOTAL N

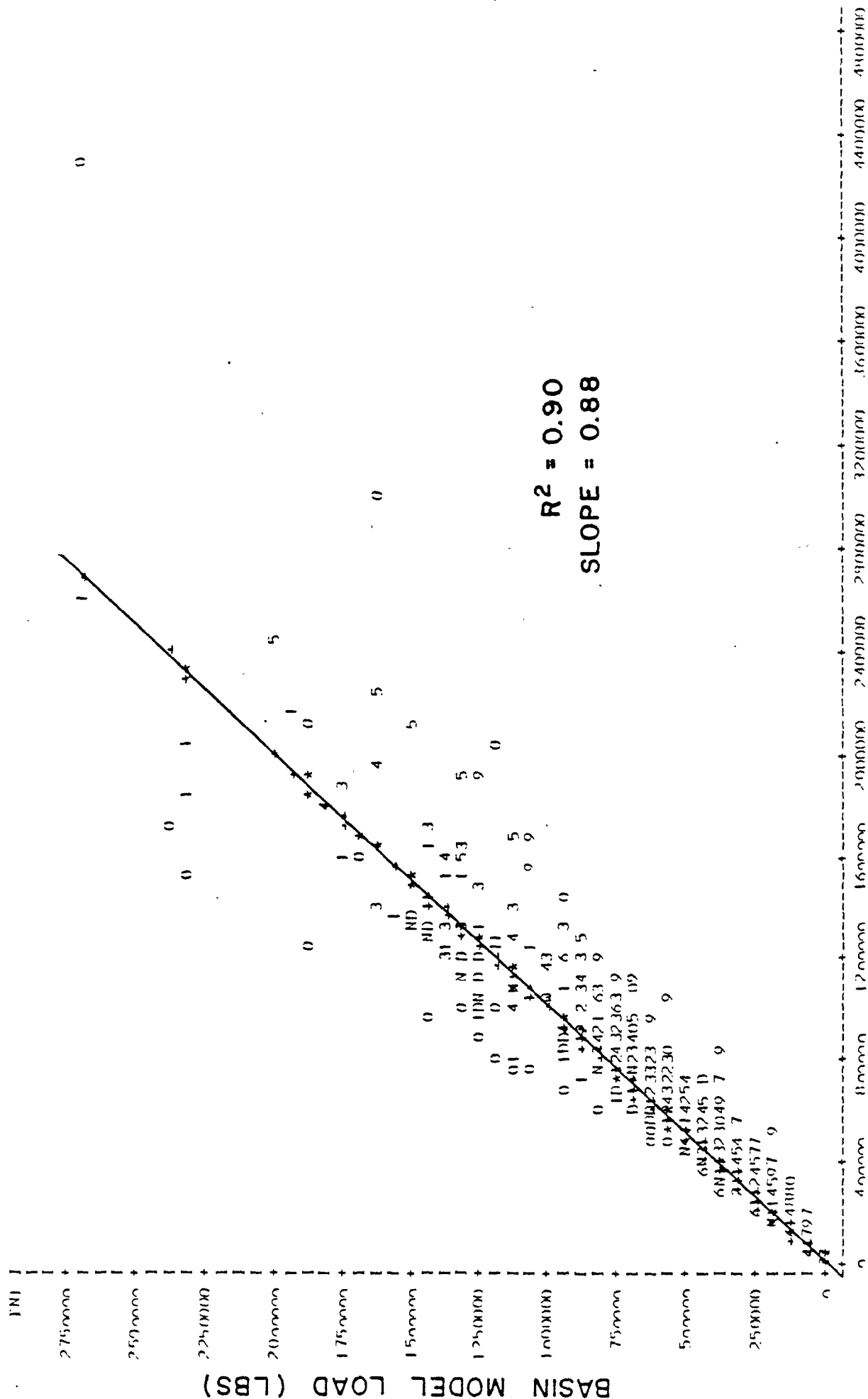


Figure 43. Comparison of Simulated Monthly Loads and Loads Based upon USGS Flow-Loading Relationships:
SUSQUEHANNA RIVER FALL LINE (1/1/74 - 12/31/78): MONTHLY TOTAL P

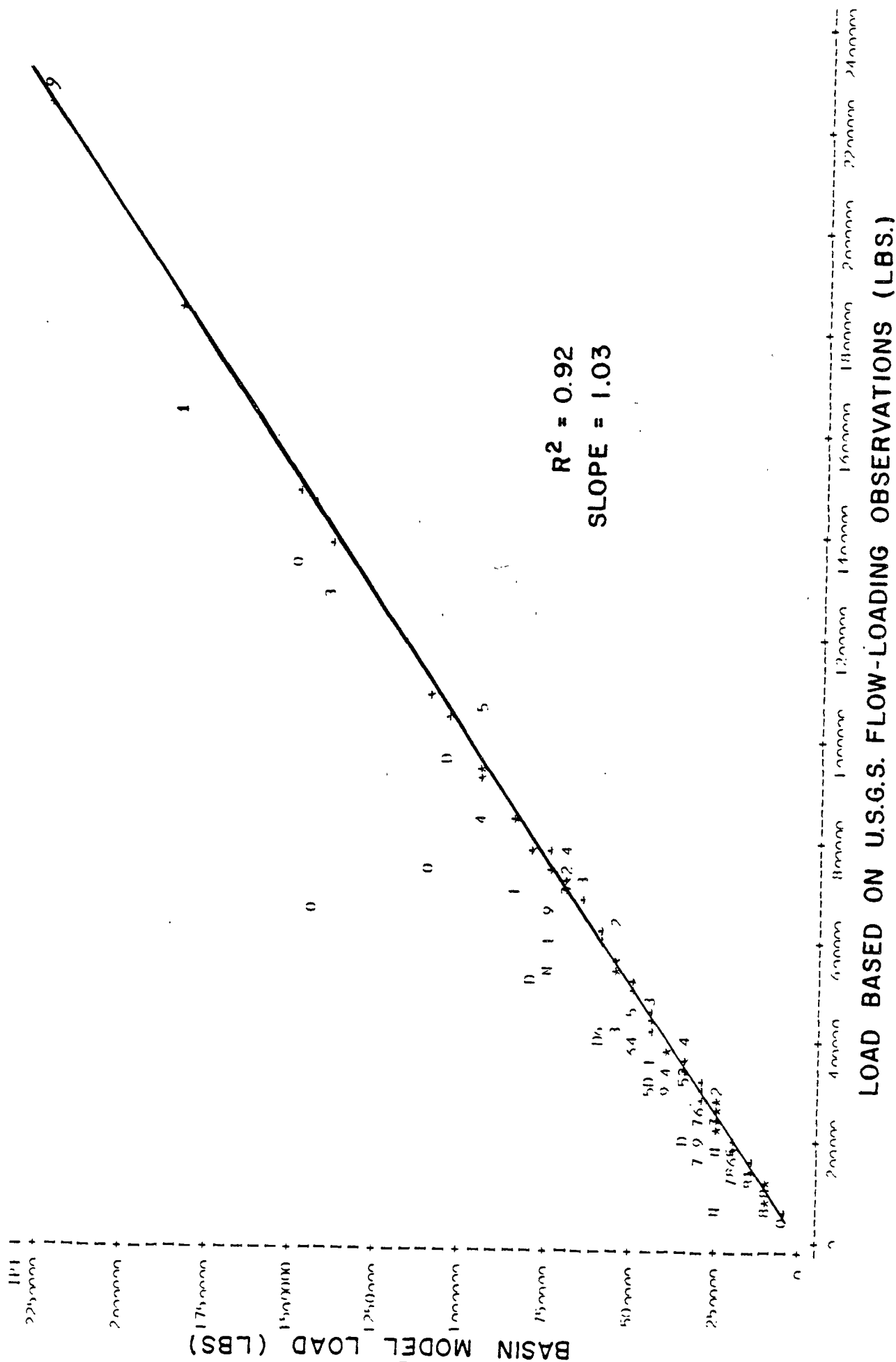


Figure 44. Comparison of Simulated Monthly Loads and Loads Based upon USGS Flow-Loading Relationships:
SUSQUEHANNA RIVER FALL LINE (1/1/74 - 12/31/78): MONTHLY INORGANIC P

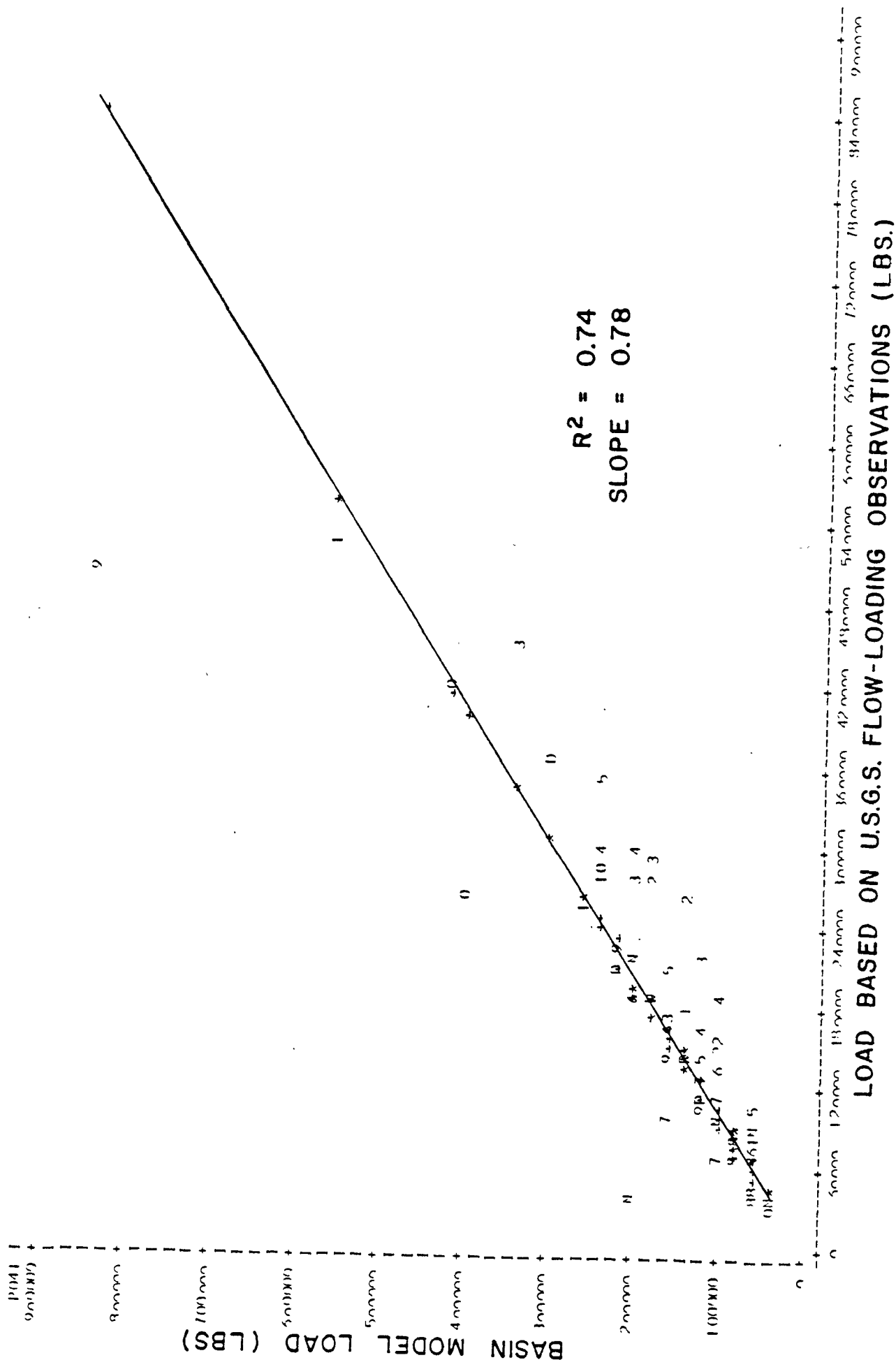


Figure 45. Comparison of Simulated Monthly Loads and Loads Based upon USGS Flow-Loading Relationships:

SUSQUEHANNA RIVER FALL LINE (1/1/74 - 12/31/78):MONTHLY TOTAL N

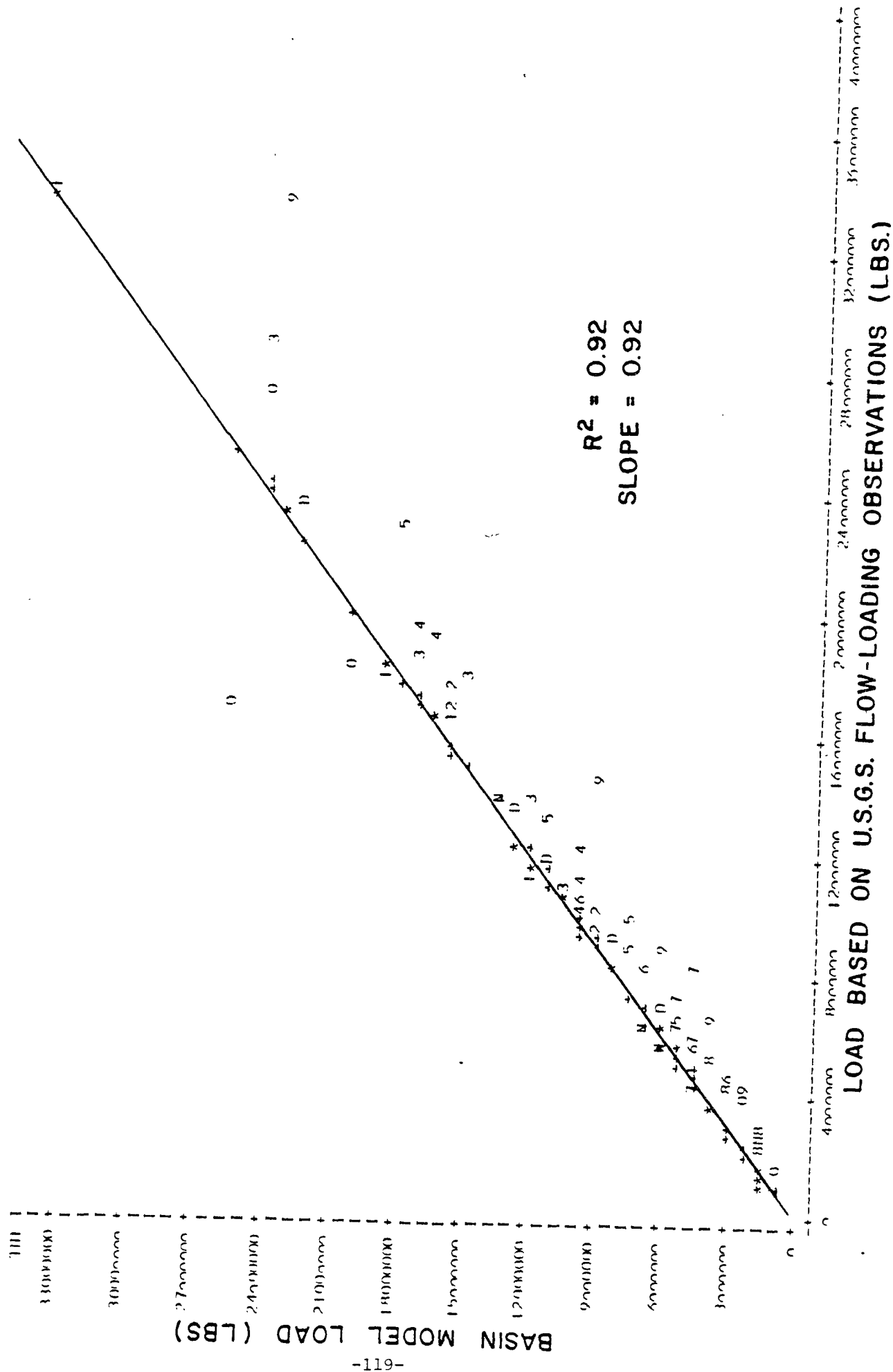


Figure 46. Comparison of Simulated Monthly Loads and Loads Based upon USGS Flow-Loading Relationships:

SUSQUEHANNA RIVER FALL LINE (1/1/74 - 12/31/78): MONTHLY NITRITE + NITRATE - N

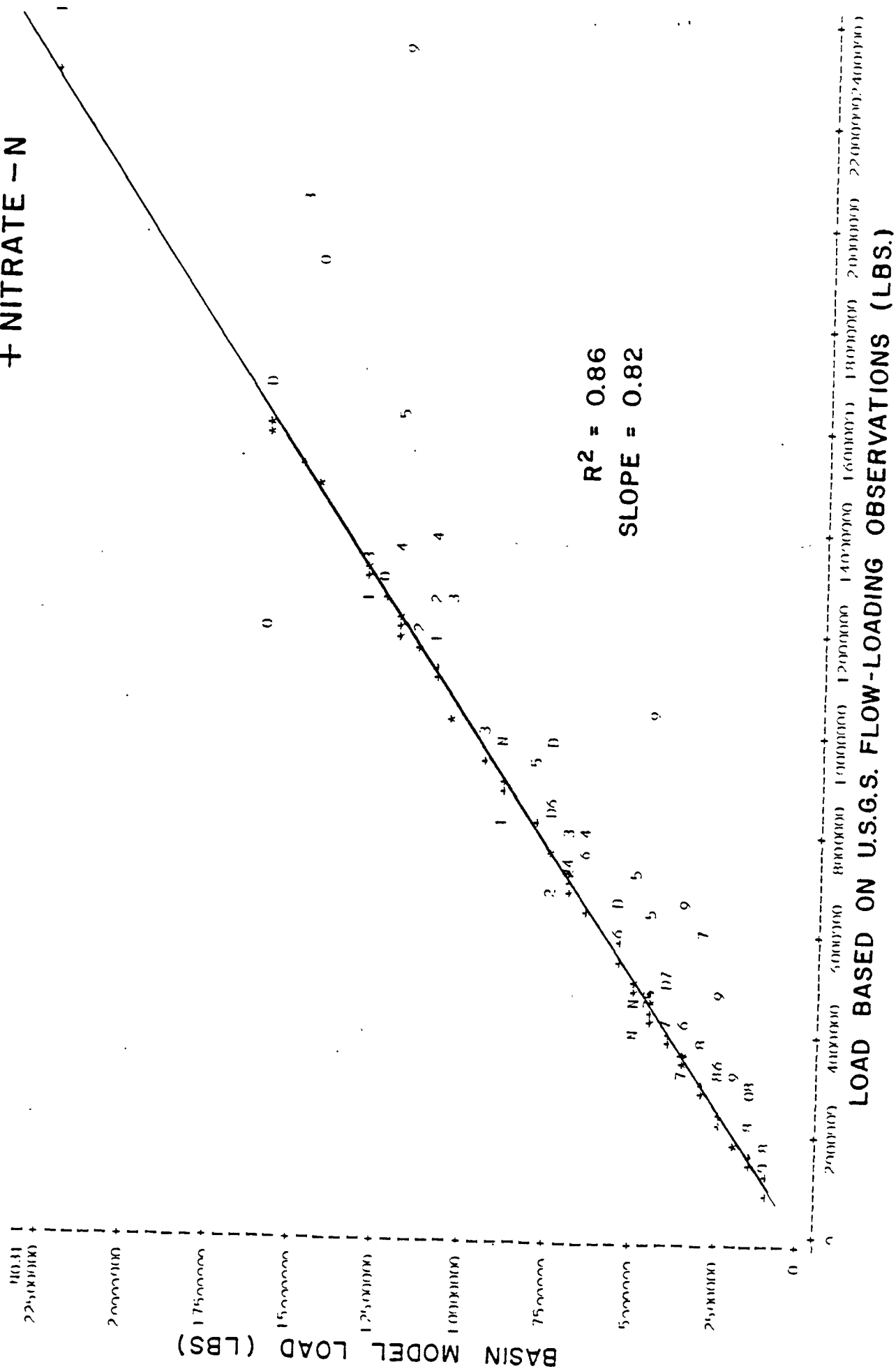


Figure 47. Comparison of Simulated Daily Loads and Loads Based upon USGS Flow-Loading Relationships:
SUSQUEHANNA RIVER FALL LINE (1/1/74 - 12/31/78): DAILY TOTAL P

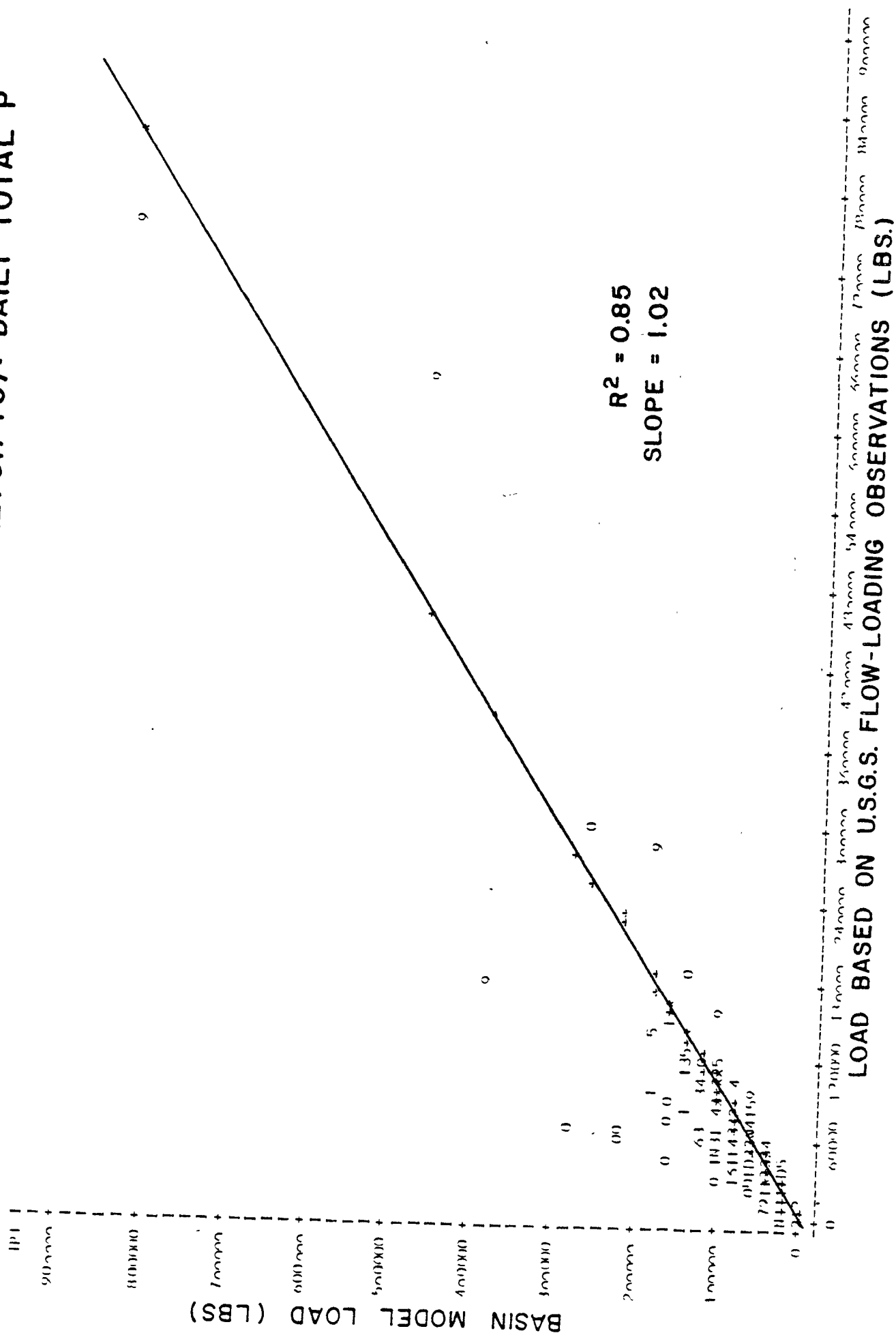


Figure 48. Comparison of Simulated Daily Loads and Loads Based upon USGS Flow-Loading Relationships:
SUSQUEHANNA RIVER FALL LINE (1/1/74 - 12/31/78): DAILY TOTAL N

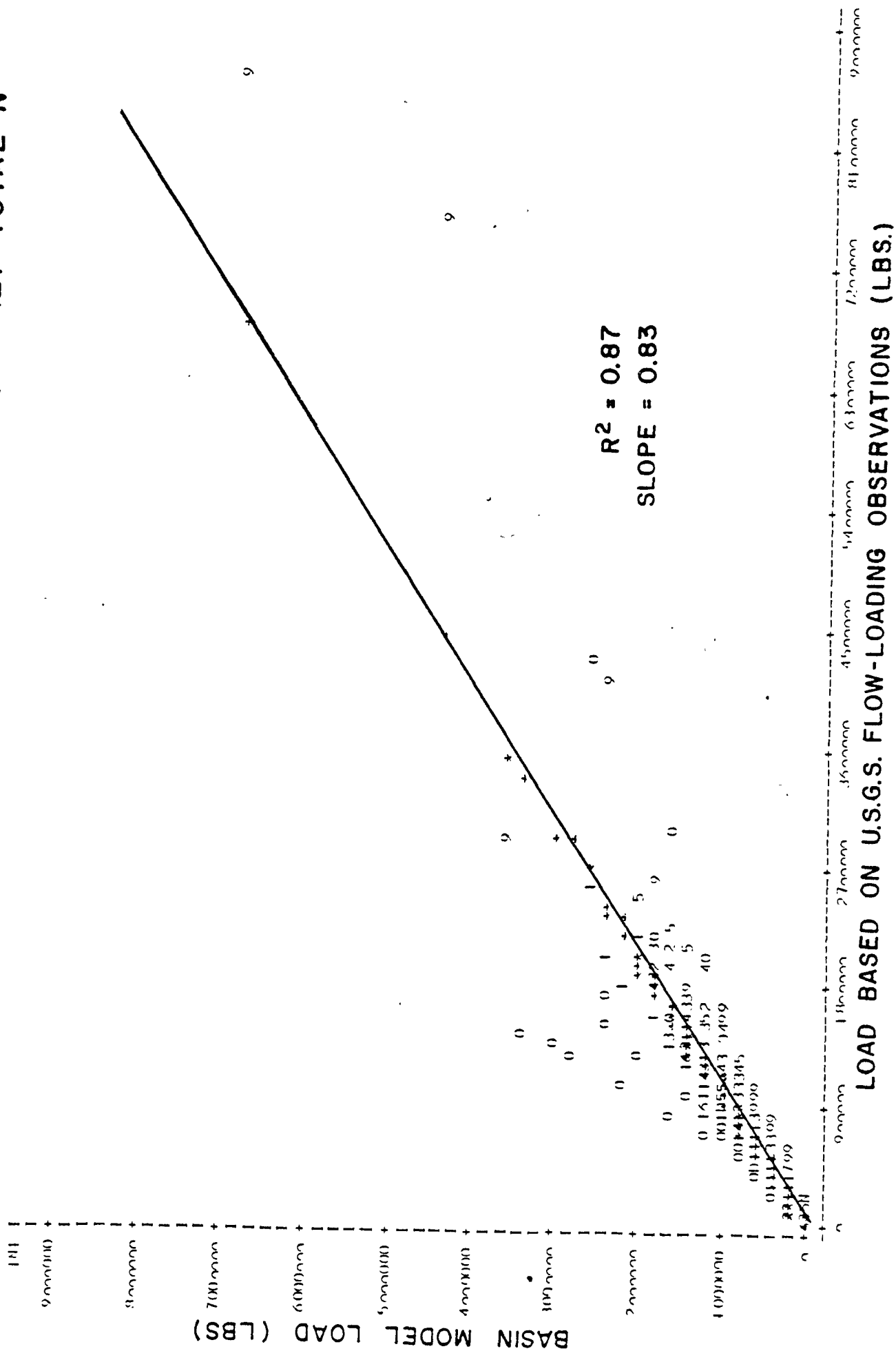


Figure 49. Comparison of Simulated Monthly Loads and Loads Based upon USGS Flow-Loading Relationships:
POTOMAC RIVER FALL LINE (1/1/74 - 12/31/75): MONTHLY TOTAL P

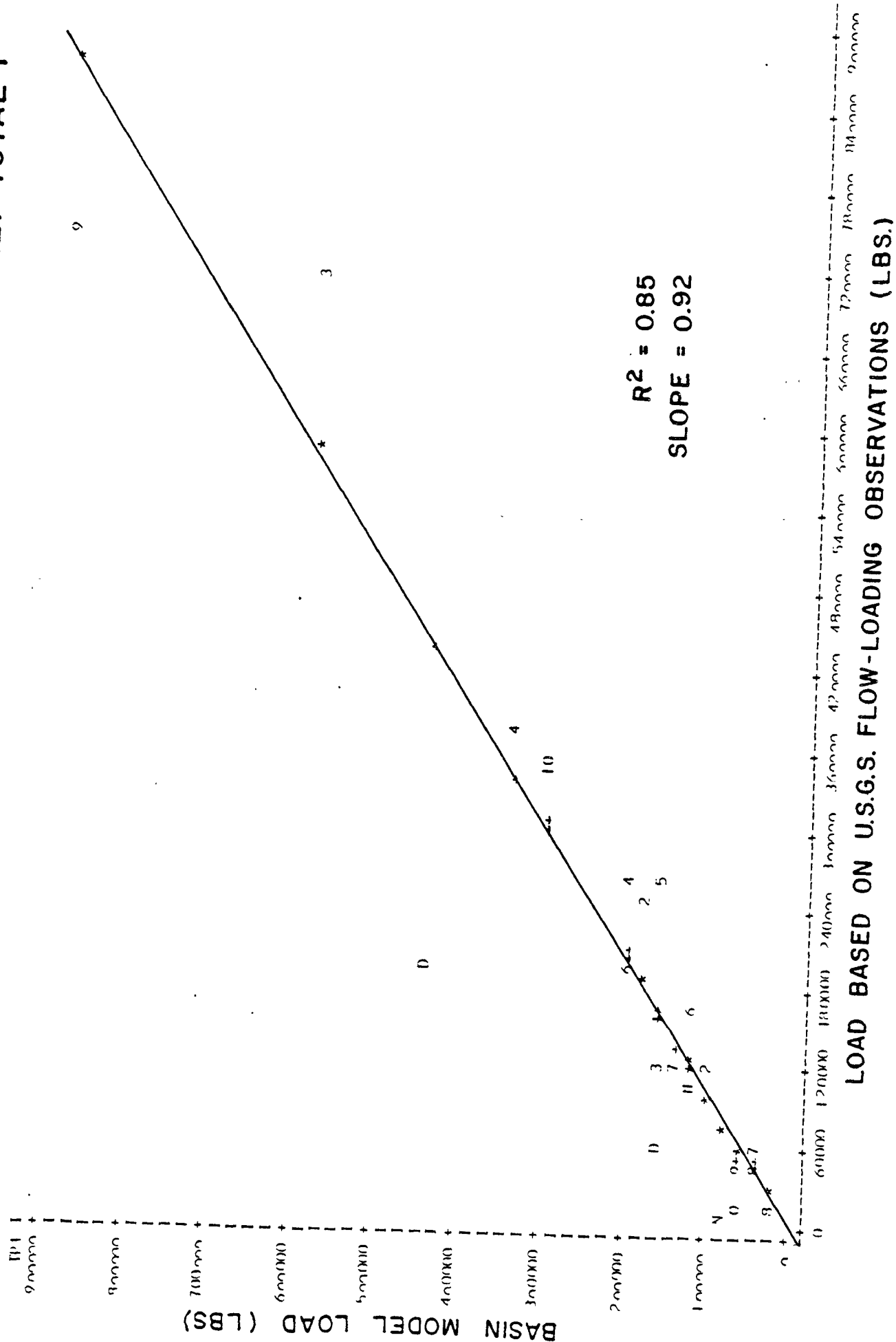


Figure 50. Comparison of Simulated Monthly Loads and Loads Based upon USGS Flow-Loading Relationships:

POTOMAC RIVER FALL LINE (1/1/74 - 12/31/75) : MONTHLY INORGANIC P

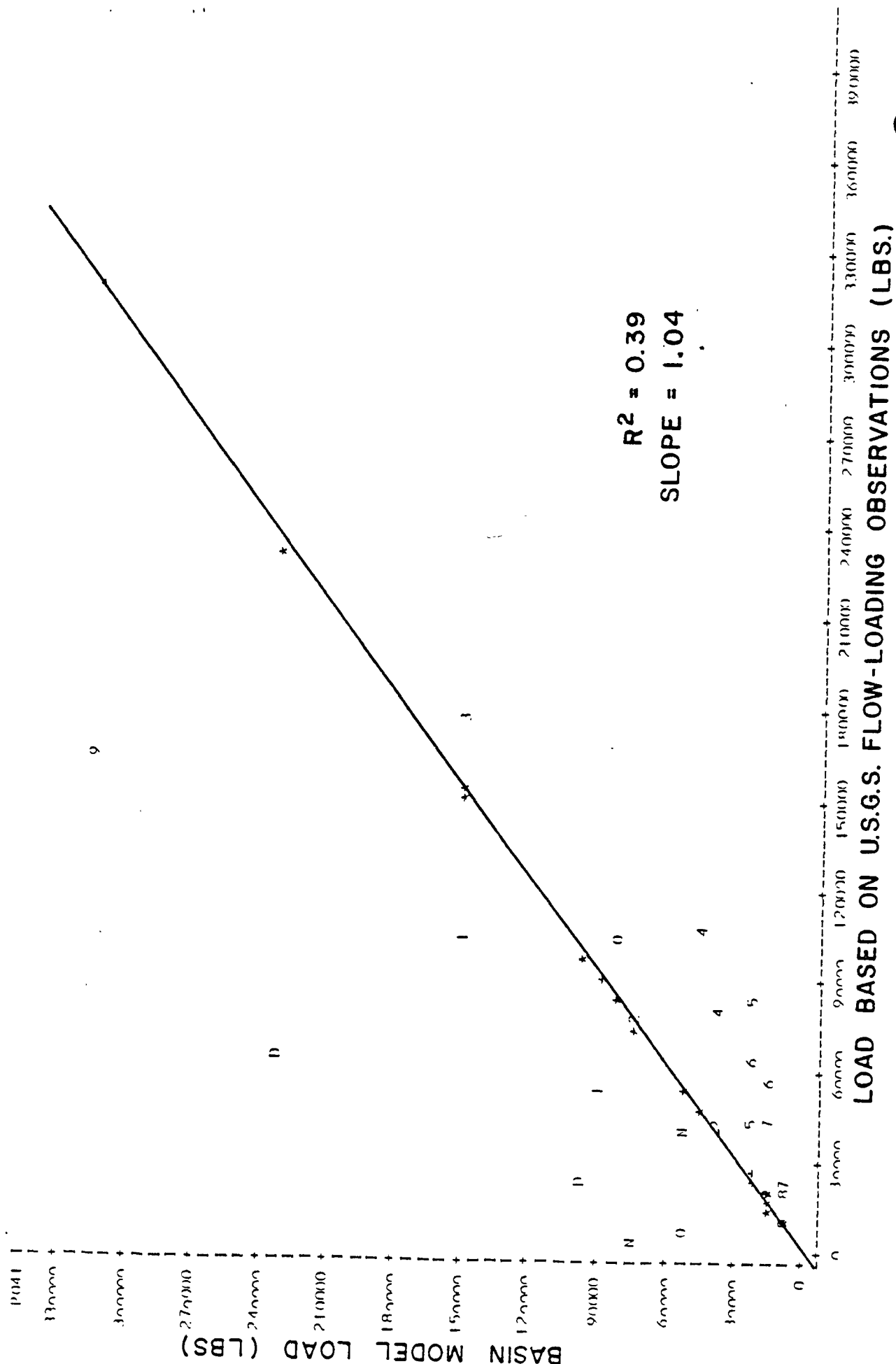


Figure 51. Comparison of Simulated Monthly Loads and Loads Based upon USGS Flow-Loading Relationships:
POTOMAC RIVER FALL LINE (1/1/74 - 12/31/75): MONTHLY TOTAL N

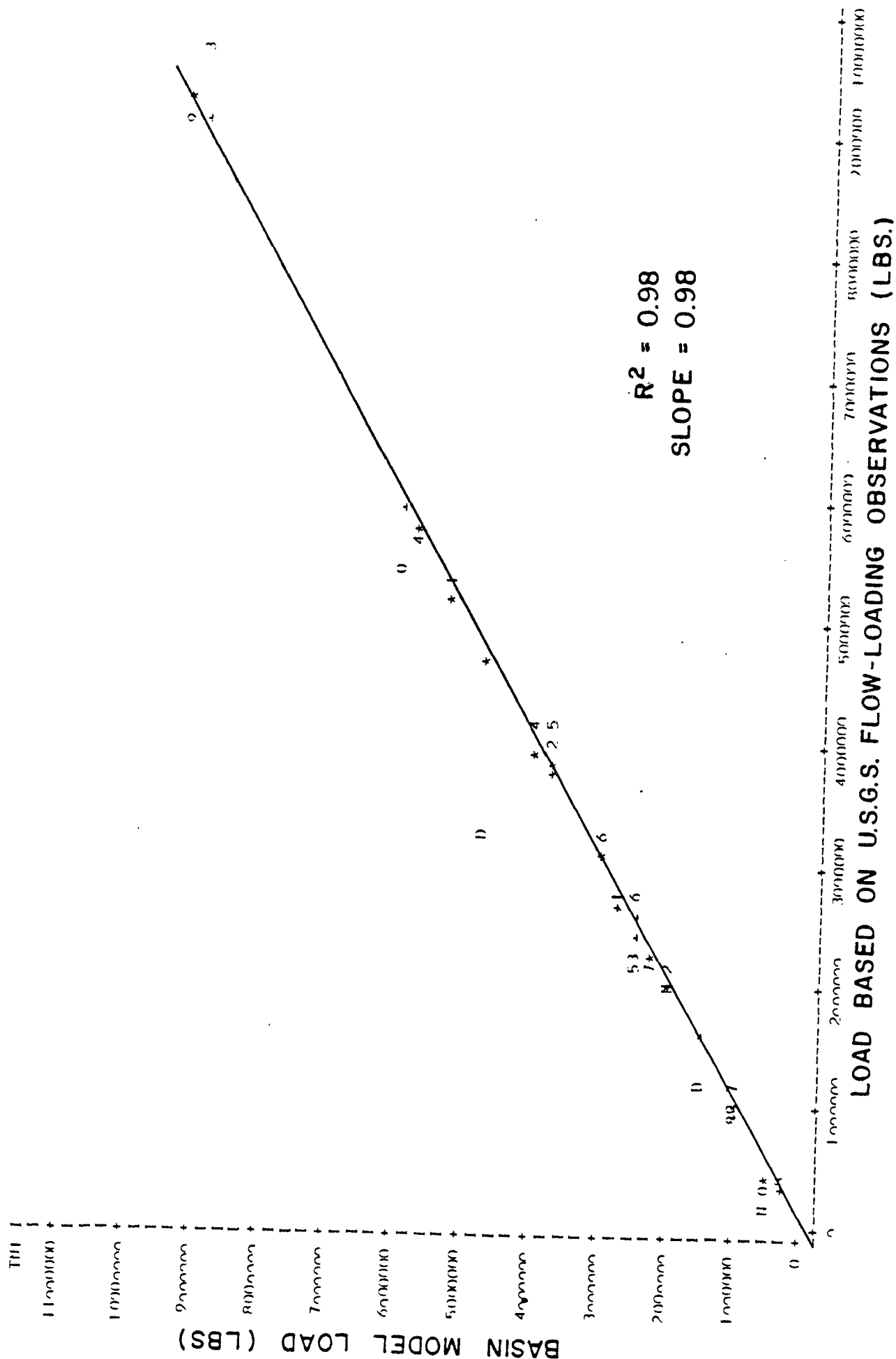


Figure 52. Comparison of Simulated Monthly Loads and Loads Based upon USGS Flow-Loading Relationships:
**POTOMAC RIVER FALL LINE (1/1/74 - 12/31/75) MONTHLY NITRITE
 + NITRATE - N**

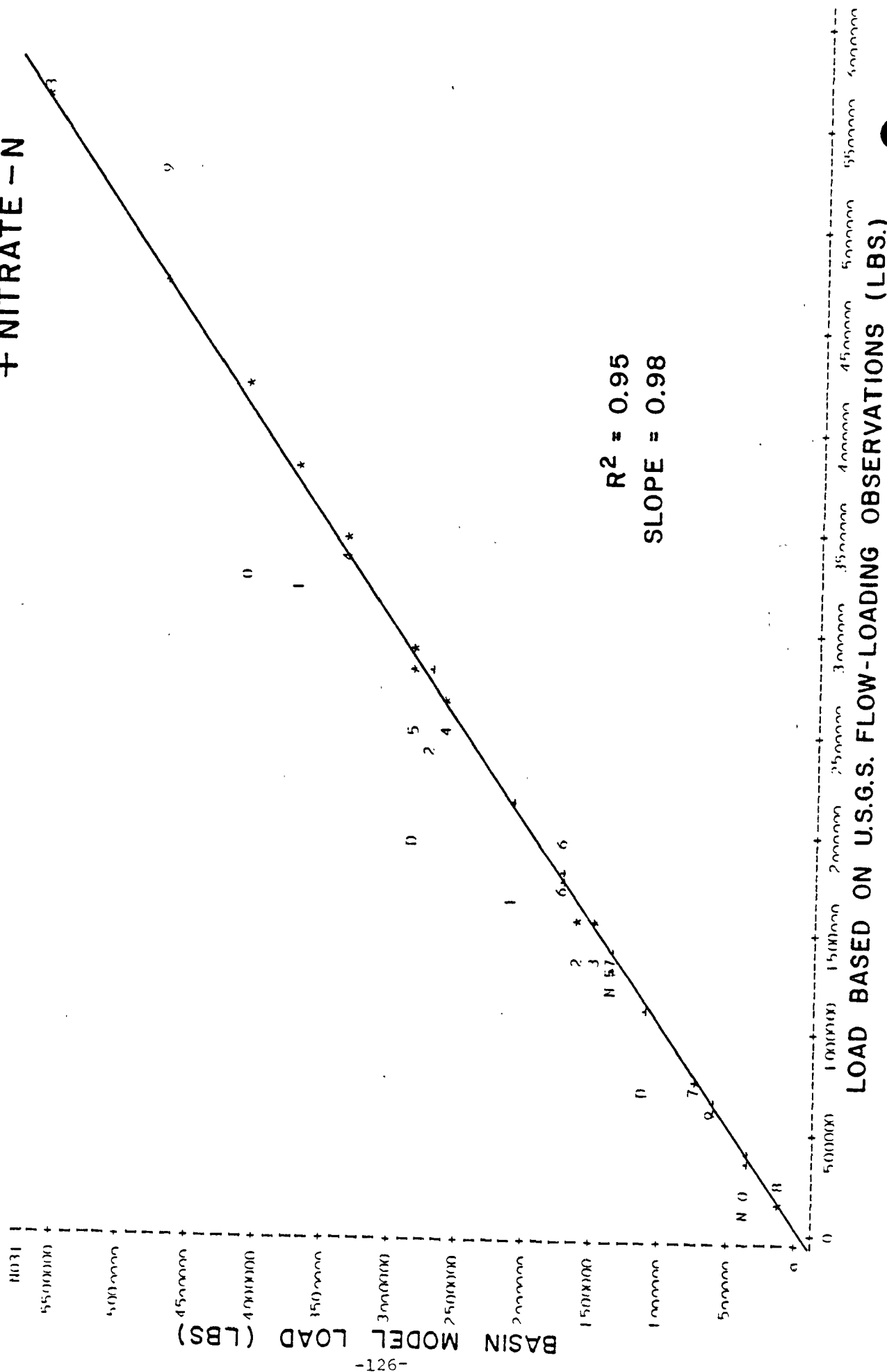


Figure 53. Comparison of Simulated Daily Loads and Loads Based upon USGS Flow-Loading Relationships:
POTOMAC RIVER FALL LINE (1/1/74 - 12/31/75): DAILY TOTAL P

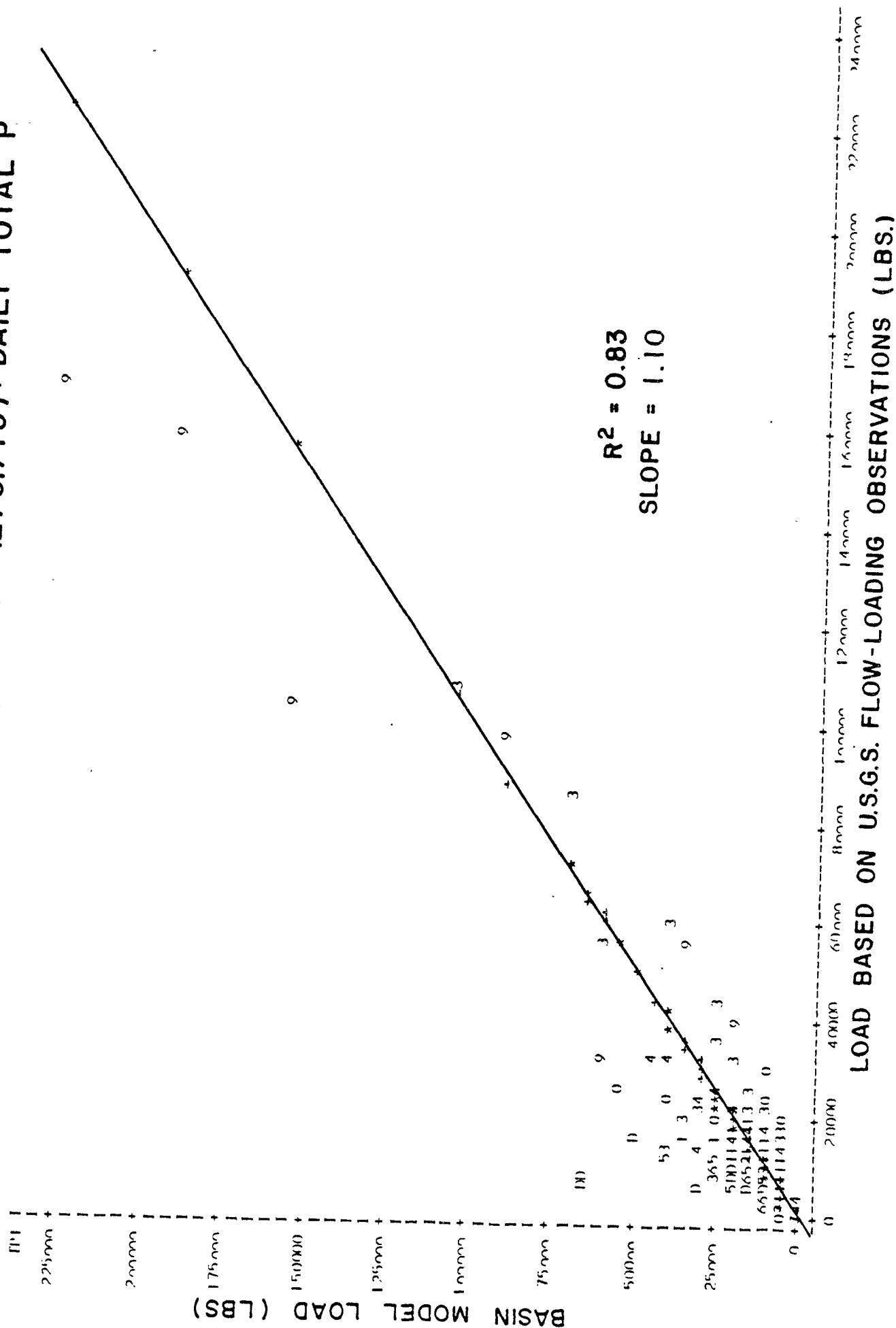


Figure 54. Comparison of Simulated Daily Loads and Loads Based upon USGS Flow-Loading Relationships:
POTOMAC RIVER FALL LINE (1/1/74 - 12/31/75): DAILY TOTAL N

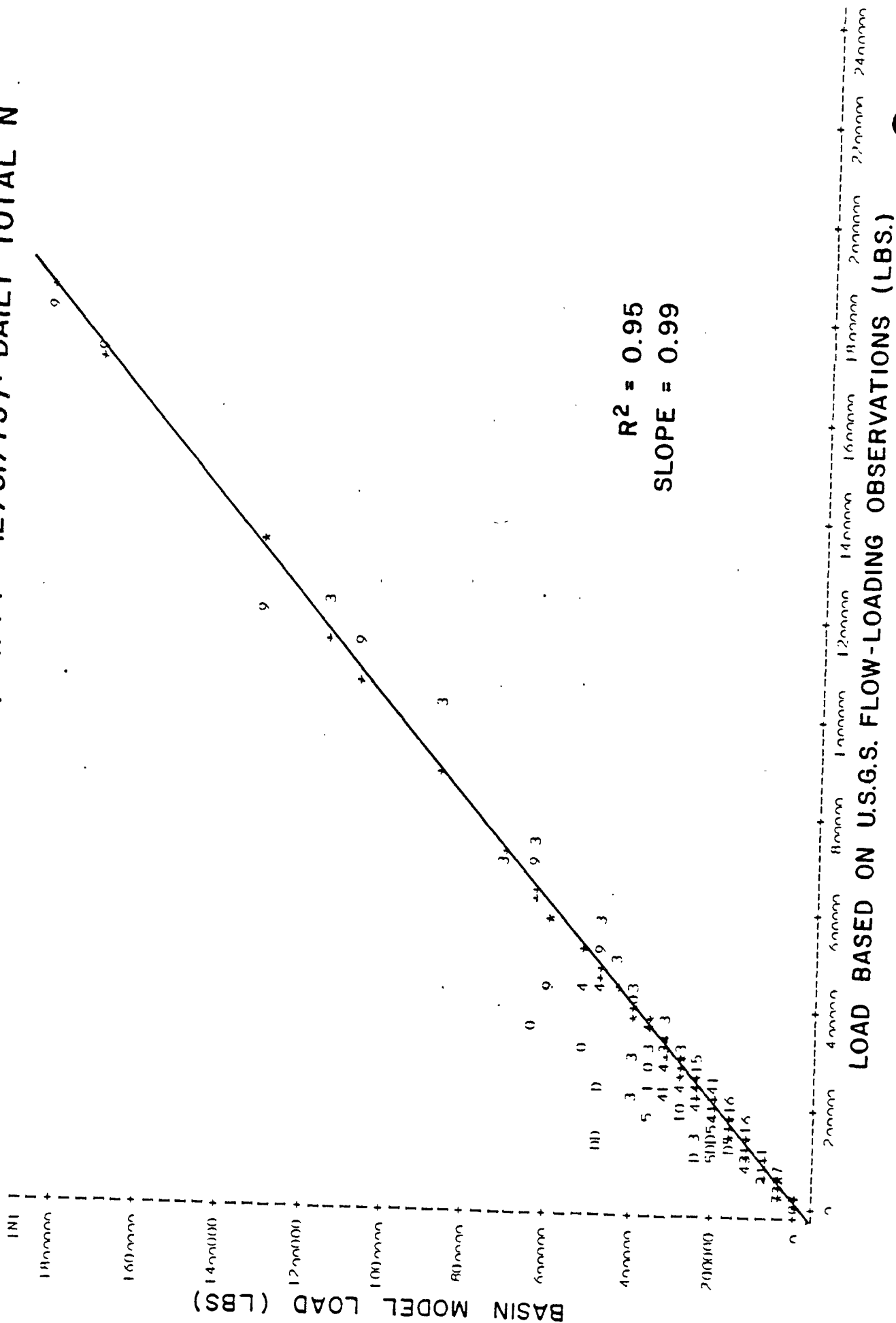


Figure 55. Comparison of Simulated Monthly Loads and Loads Based upon USGS Flow-Loading Relationships:
POTOMAC RIVER FALL LINE (1/1/76 - 12/31/78): MONTHLY TOTAL P

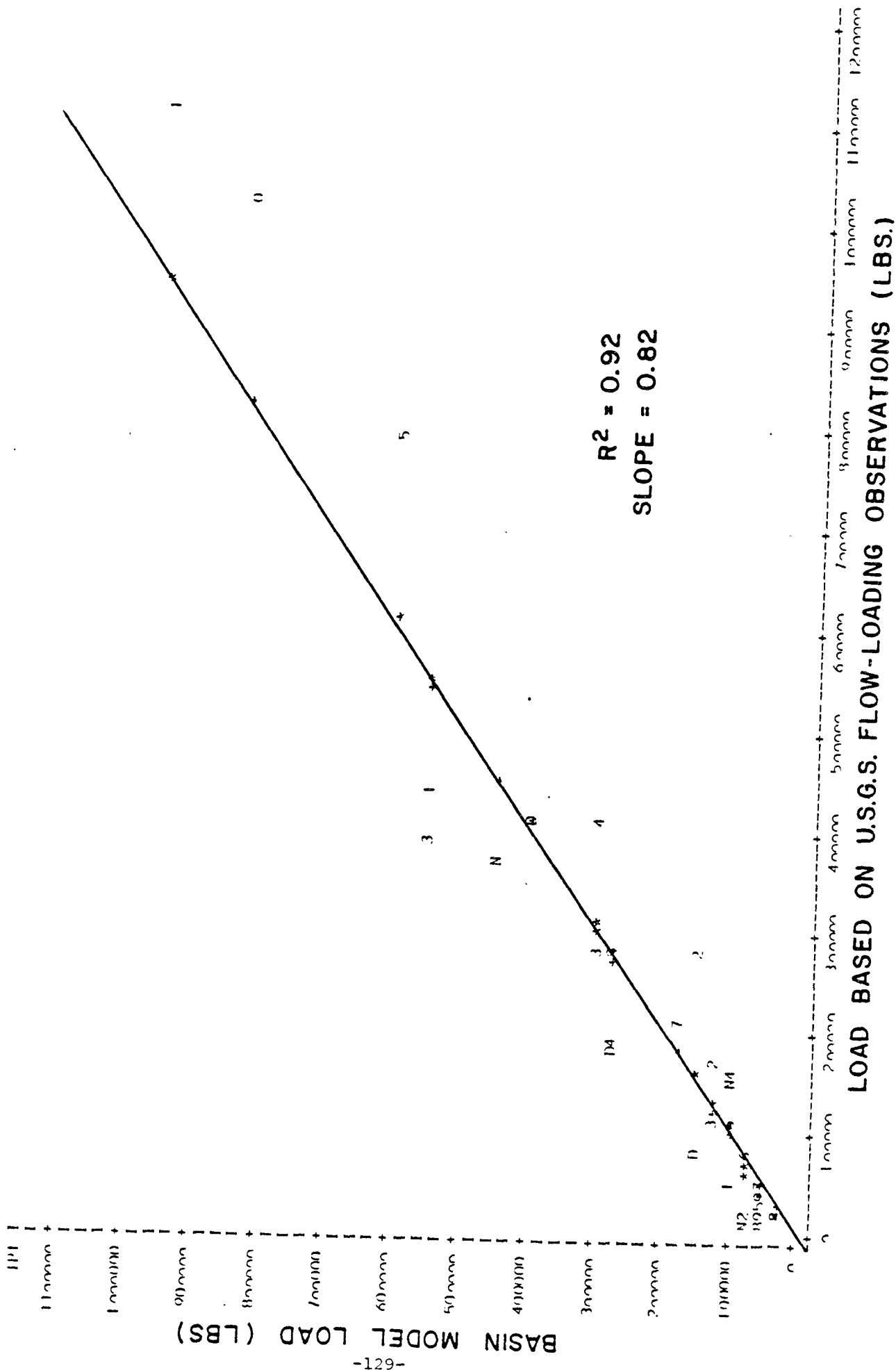


Figure 56. Comparison of Simulated Monthly Loads and Loads Based upon USGS Flow-Loading Relationships:
POTOMAC RIVER FALL LINE (1/1/76 - 12/31/78): MONTHLY INORGANIC P

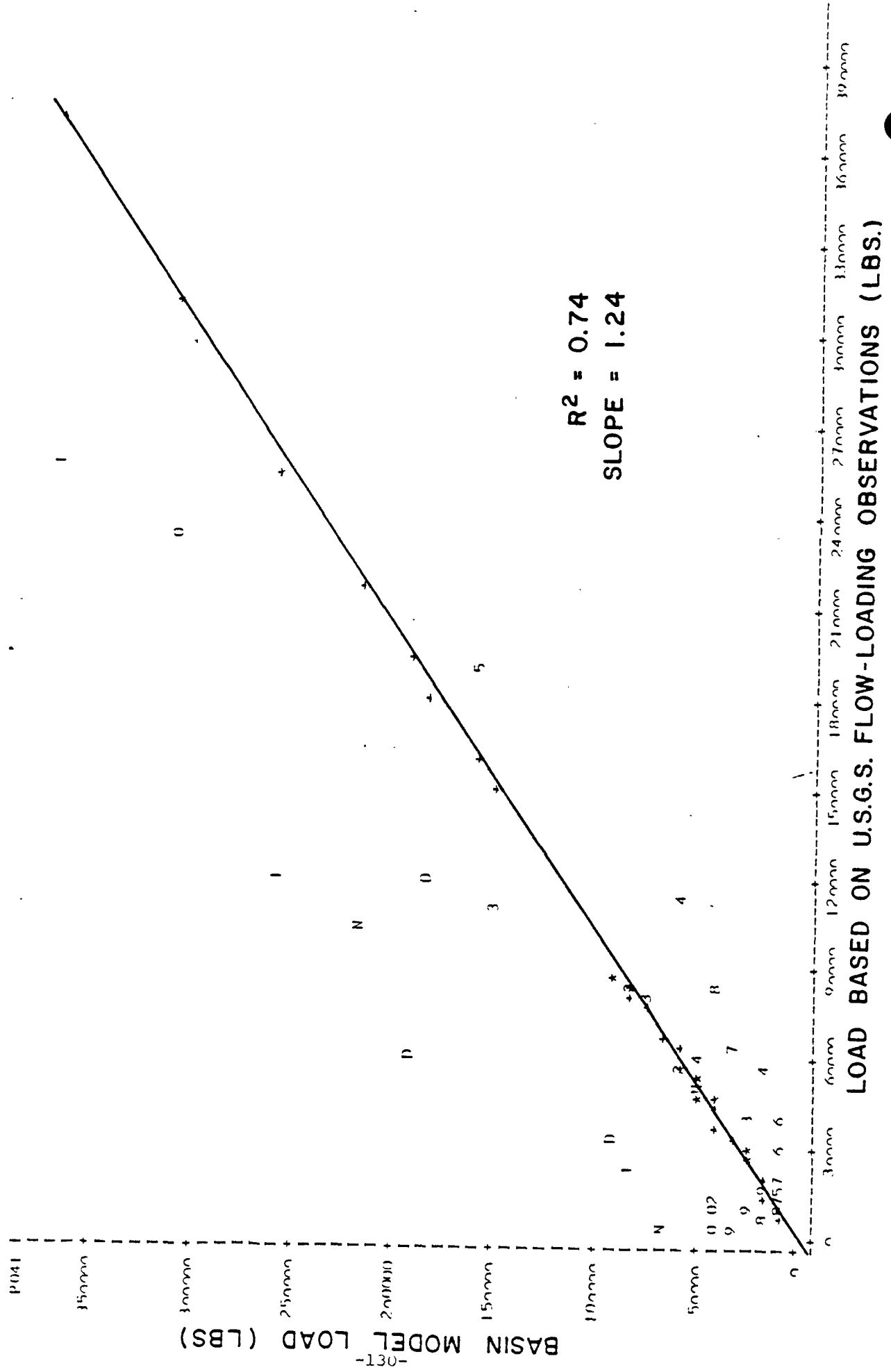


Figure 57. Comparison of Simulated Monthly Loads and Loads Based upon USGS Flow-Loading Relationships:
POTOMAC RIVER FALL LINE (1/1/76 - 12/31/78): MONTHLY TOTAL N

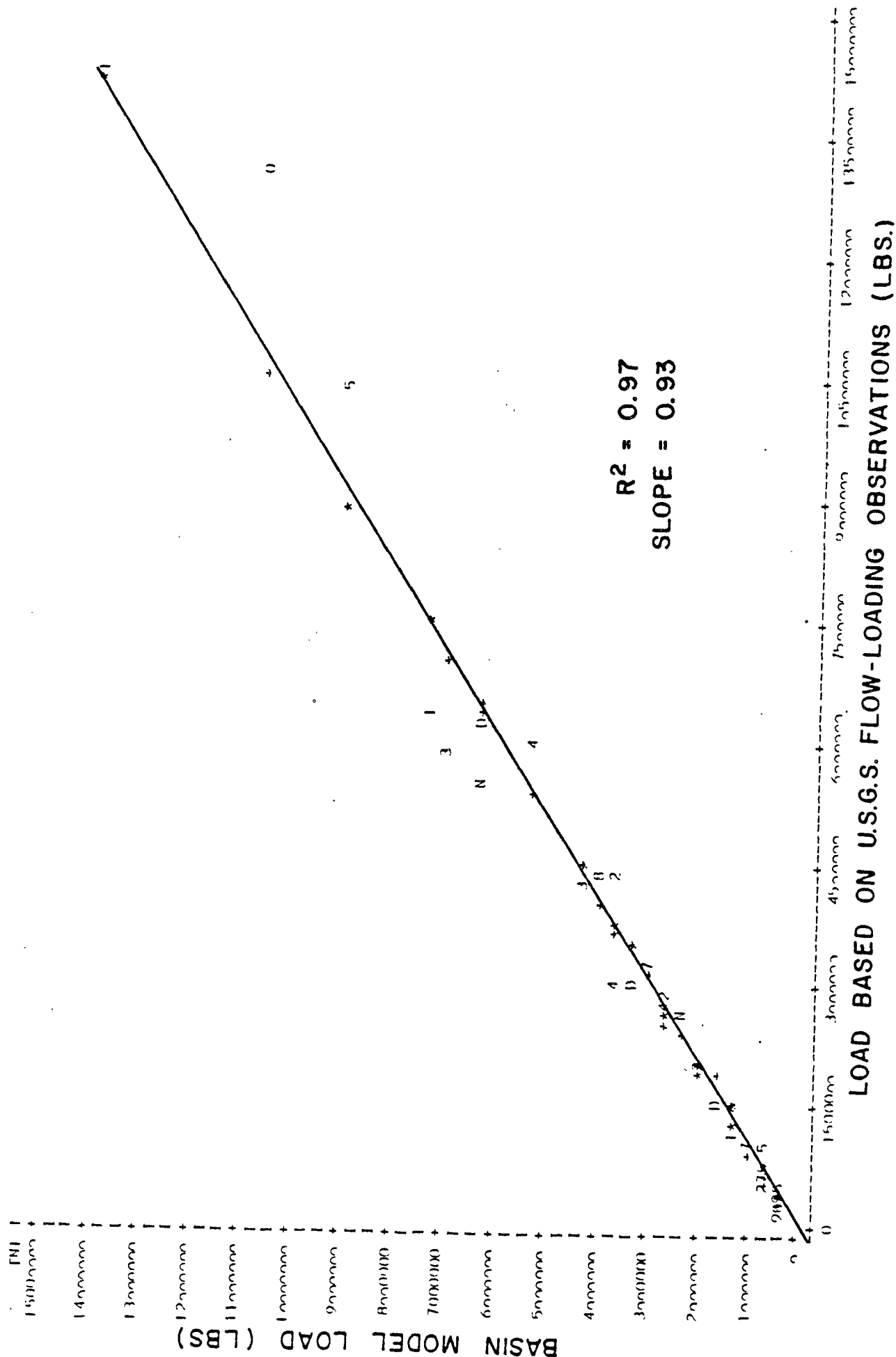


Figure 58. Comparison of Simulated Monthly Loads and Loads Based upon USGS Flow-Loading Relationships:
**POTOMAC RIVER FALL LINE (1/1/76 - 12/31/78): MONTHLY NITRITE
 + NITRATE - N**

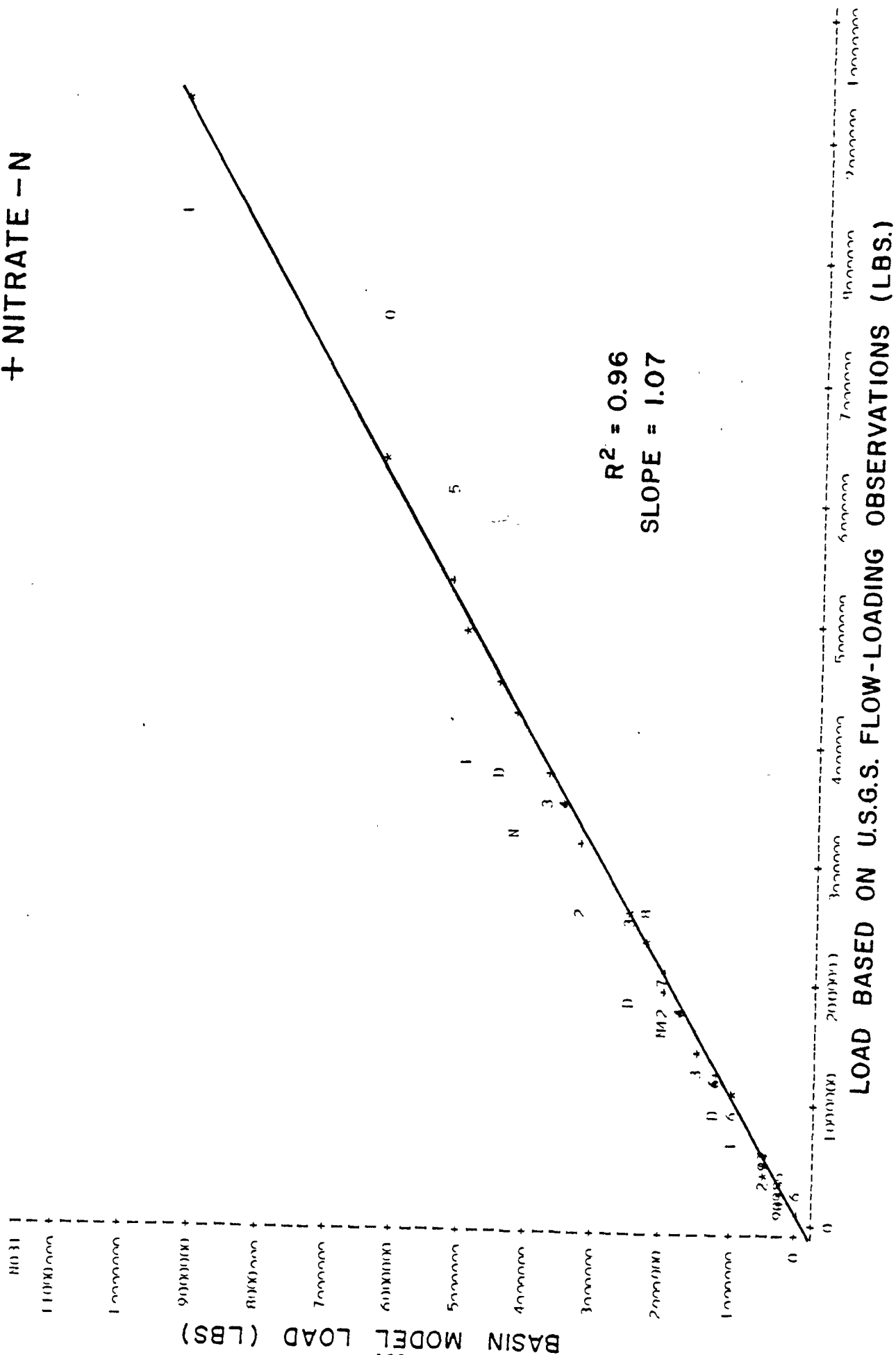


Figure 59. Comparison of Simulated Daily Loads and Loads Based upon USGS Flow-Loading Relationships:
POTOMAC RIVER FALL LINE (1/1/76 - 12/31/78): DAILY TOTAL P

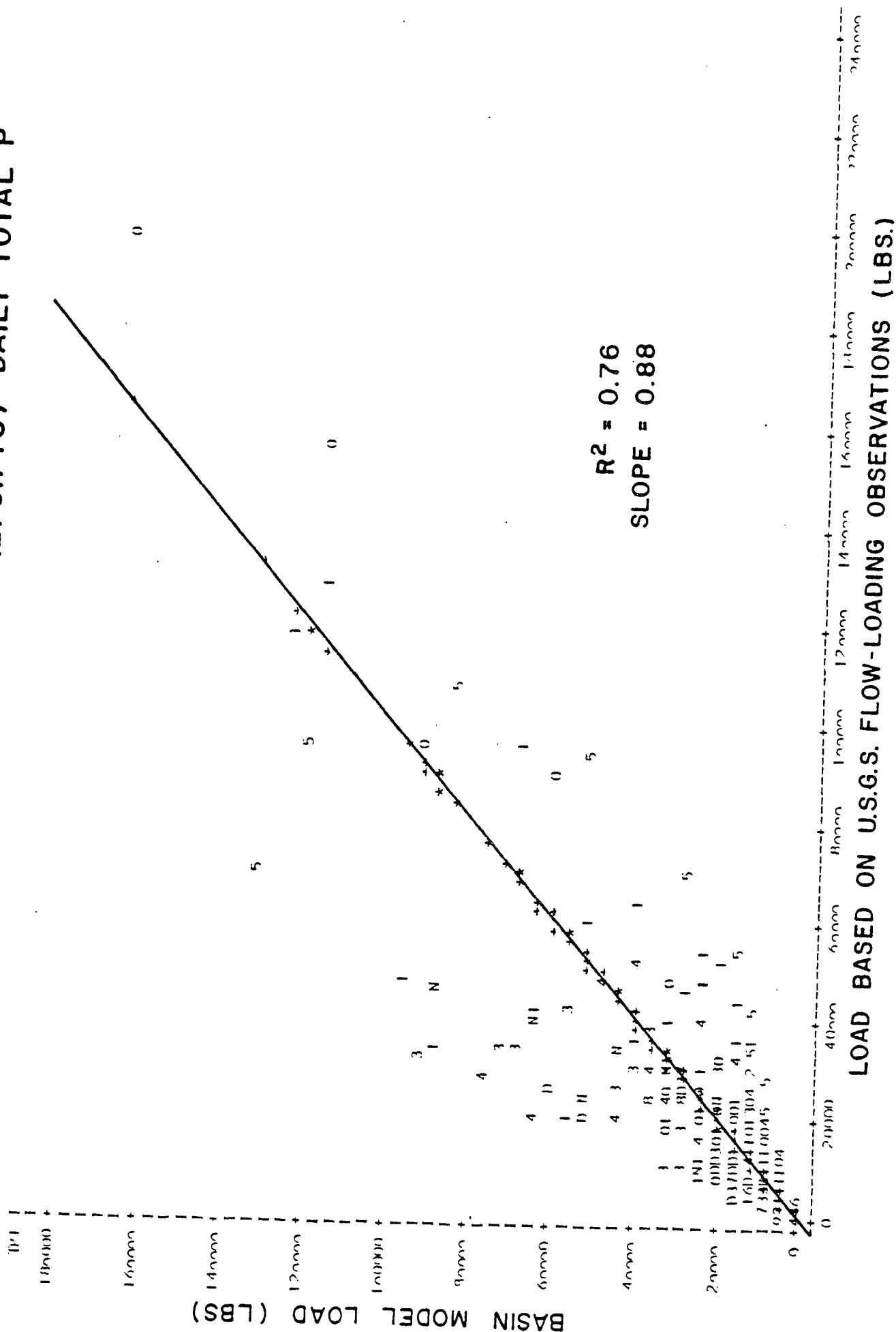


Figure 60. Comparison of Simulated Daily Loads and Loads Based upon USGS Flow-Loading Relationships: POTOMAC RIVER FALL LINE (1/1/76 - 12/31/78); DAILY TOTAL N

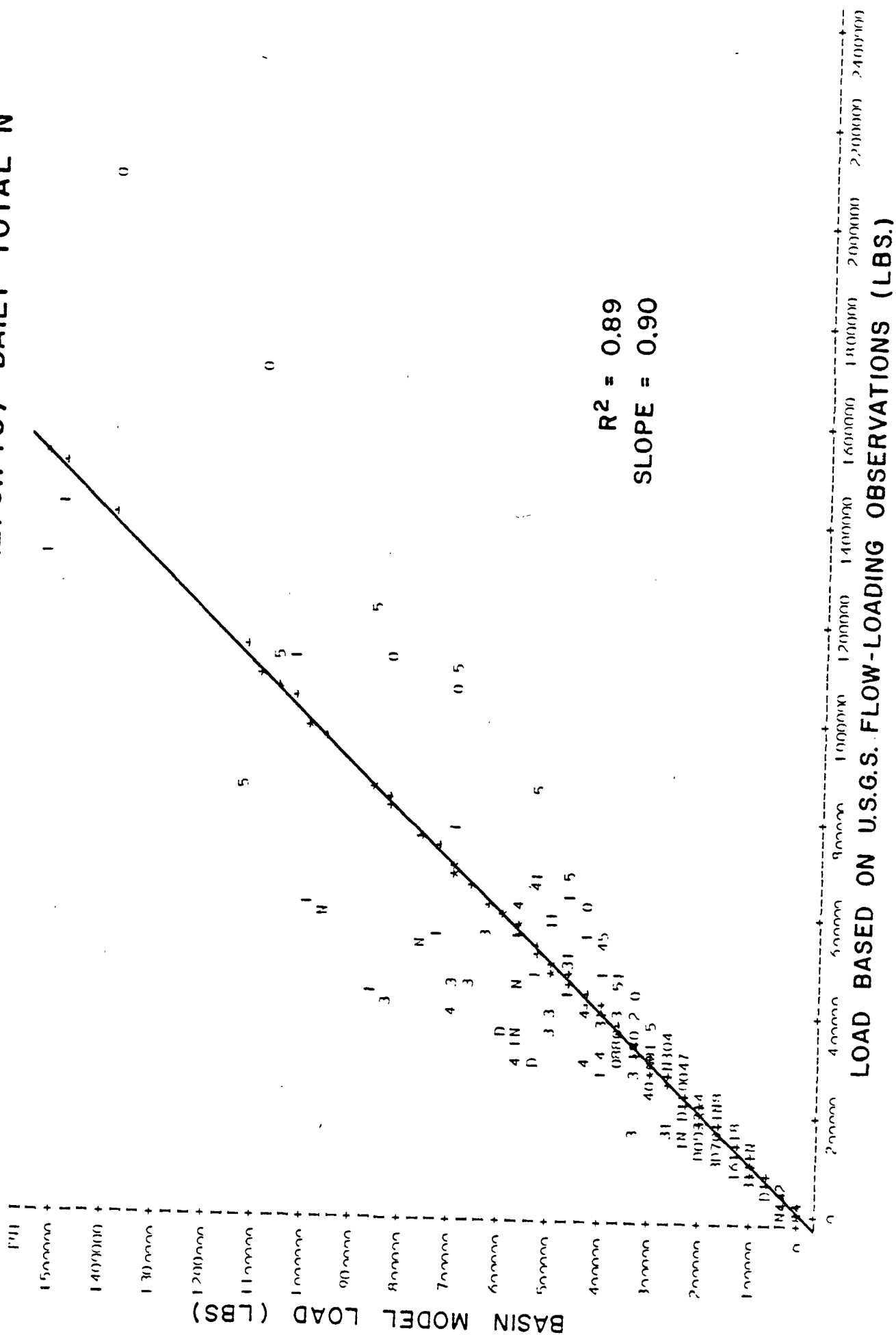


Figure 61. Comparison of Simulated Monthly Loads and Loads Based upon USGS Flow-Loading Relationships:
POTOMAC RIVER FALL LINE (1/1/74 - 12/31/78): MONTHLY TOTAL P

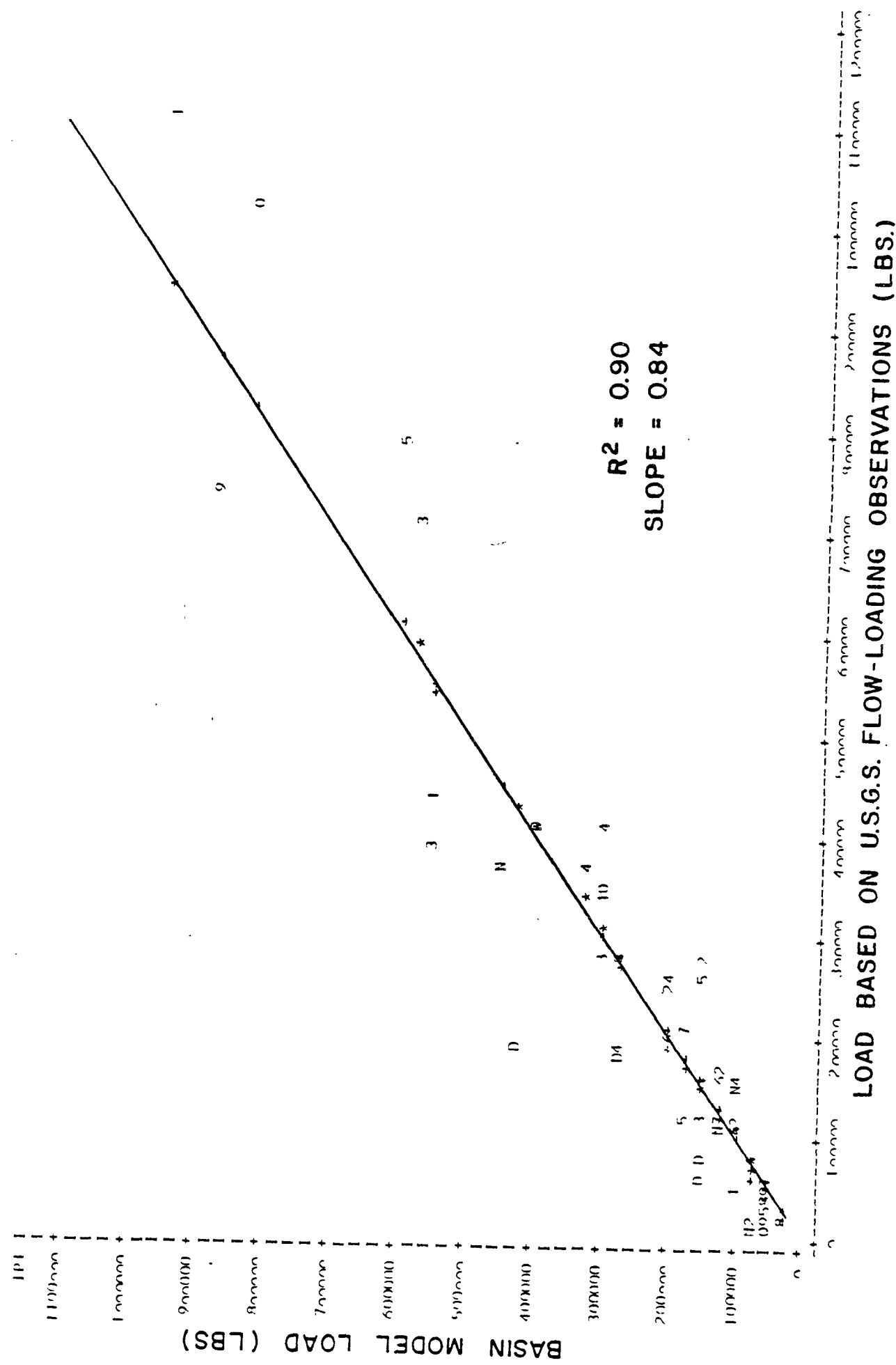


Figure 62. Comparison of Simulated Monthly Loads and Loads Based upon USGS Flow-Loading Relationships:
POTOMAC RIVER FALL LINE (1/1/74 - 12/31/78): MONTHLY INORGANIC P

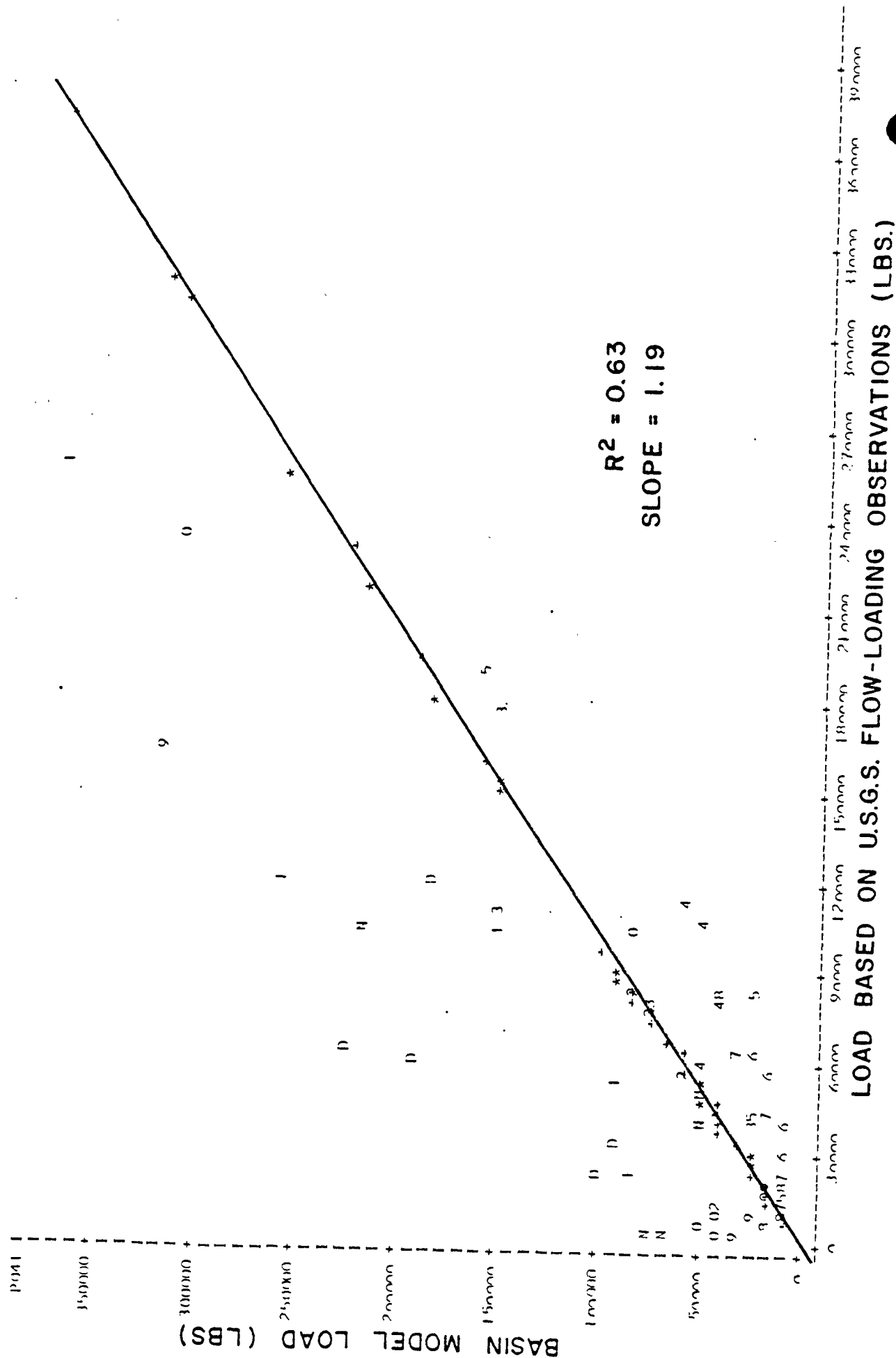


Figure 63. Comparison of Simulated Monthly Loads and Loads Based upon USGS Flow-Loading Relationships:
POTOMAC RIVER FALL LINE (1/1/74 - 12/31/78): MONTHLY TOTAL N

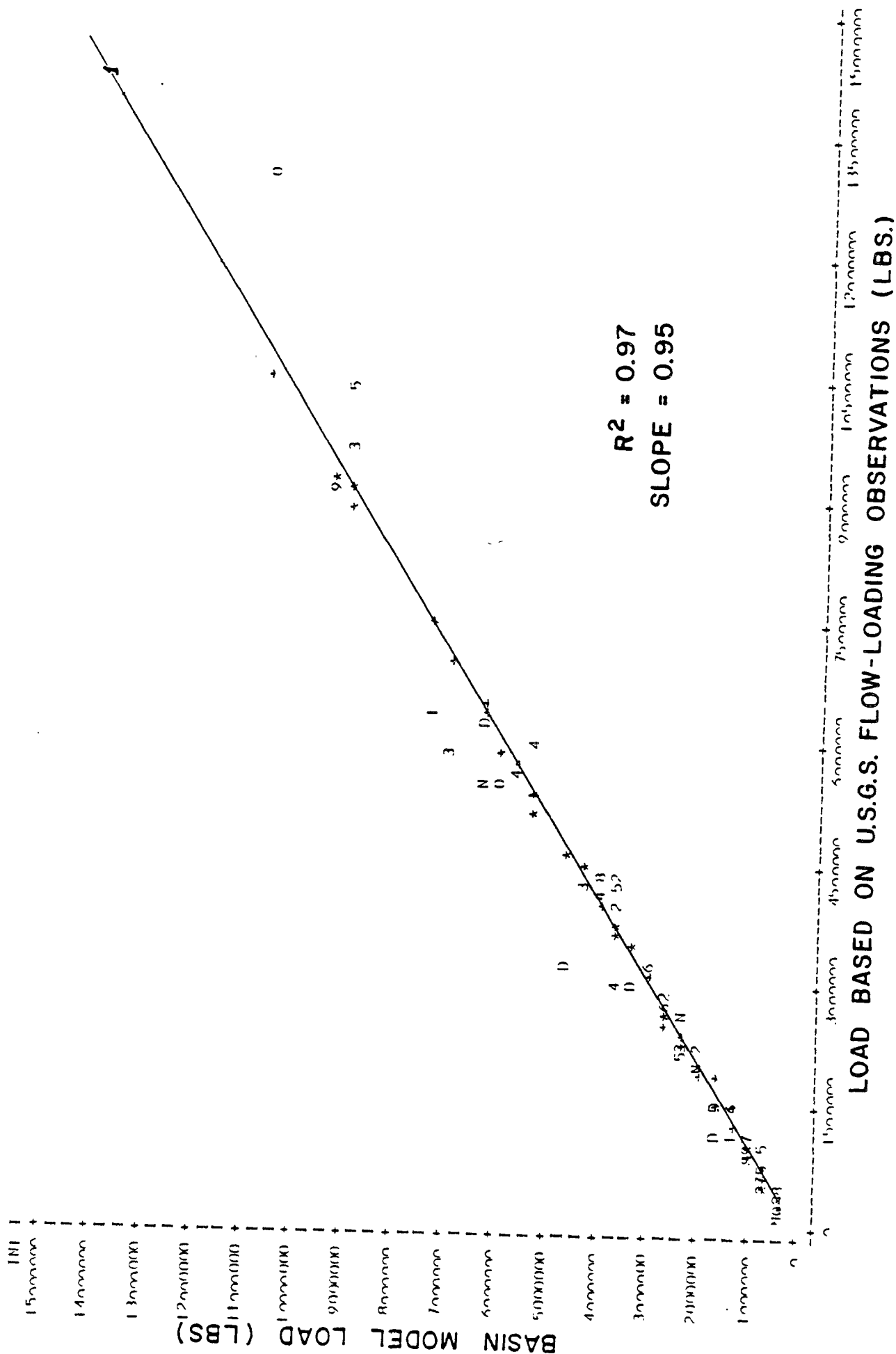


Figure 64. Comparison of Simulated Monthly Loads and Loads Based upon USGS Flow-Loading Relationships:
**POTOMAC RIVER FALL LINE (1/1/74 - 12/31/78): MONTHLY NITRITE
 + NITRATE - N**

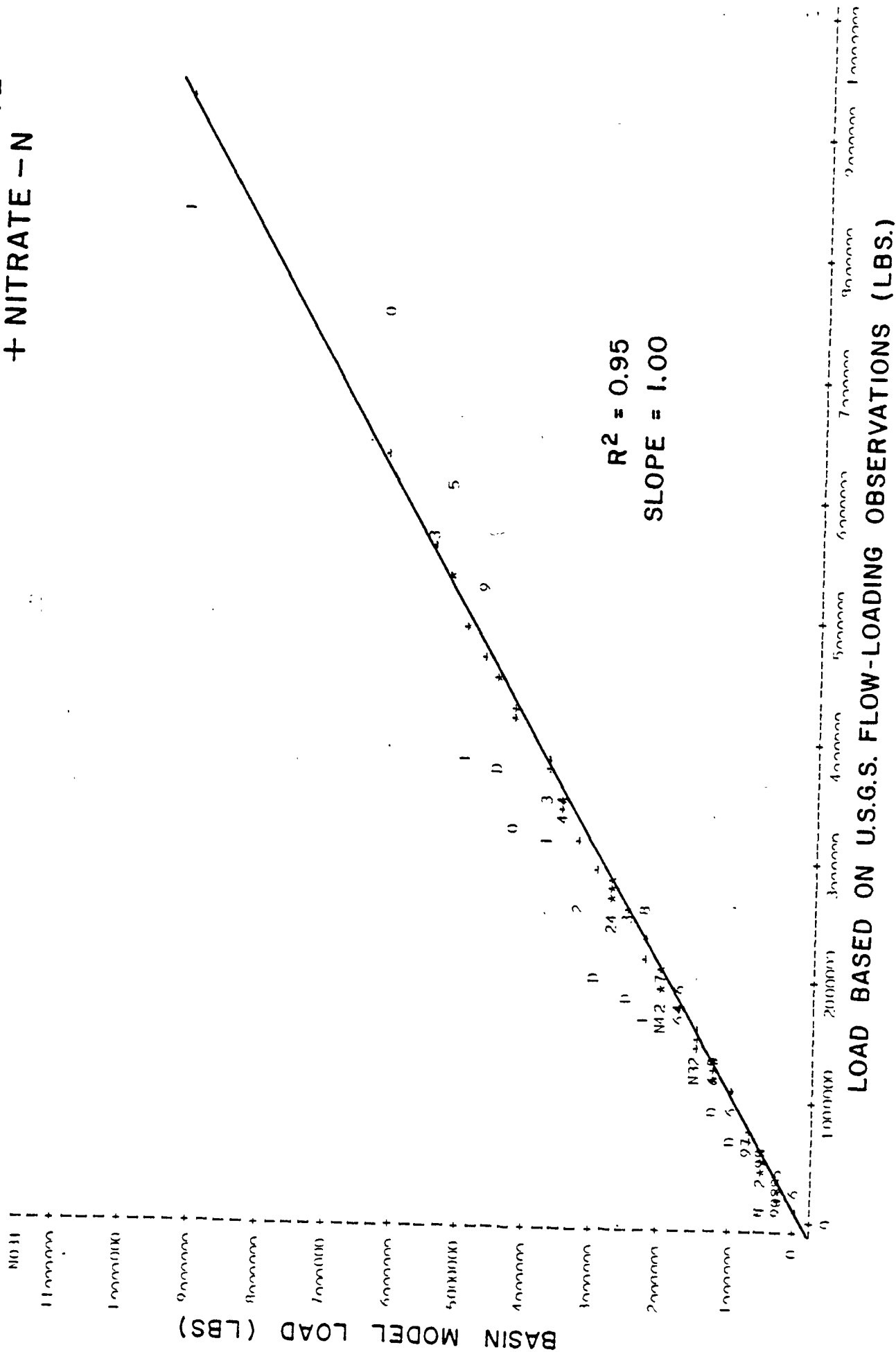


Figure 65. Comparison of Simulated Daily Loads and Loads Based upon USGS Flow-Loading Relationships:
POTOMAC RIVER FALL LINE (1/1/74 - 12/31/78): DAILY TOTAL P

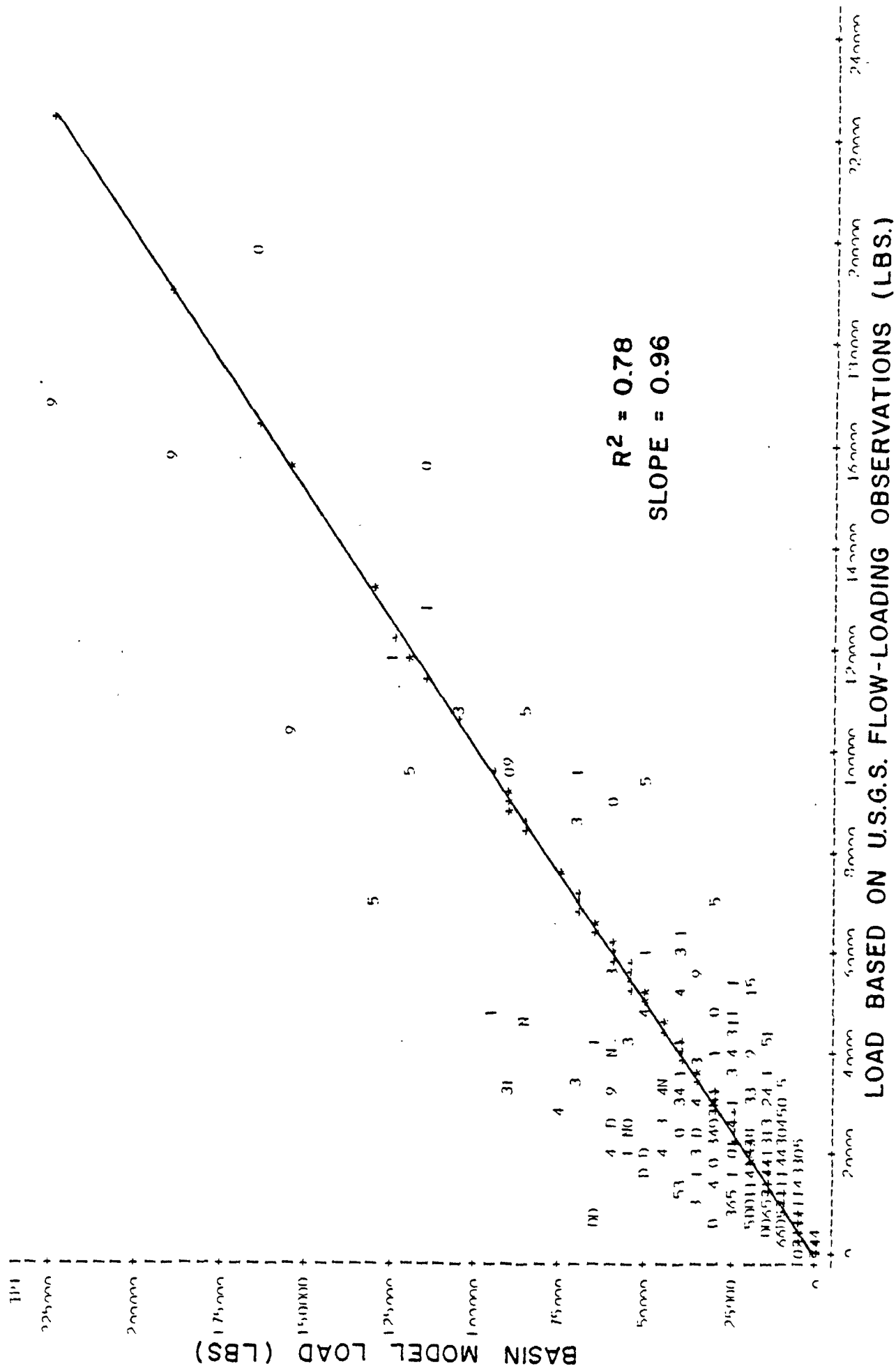


Figure 66. Comparison of Simulated Daily Loads and Loads Based upon USGS Flow-Loading Relationships:
POTOMAC RIVER FALL LINE (1/1/74 - 12/31/78): DAILY TOTAL N

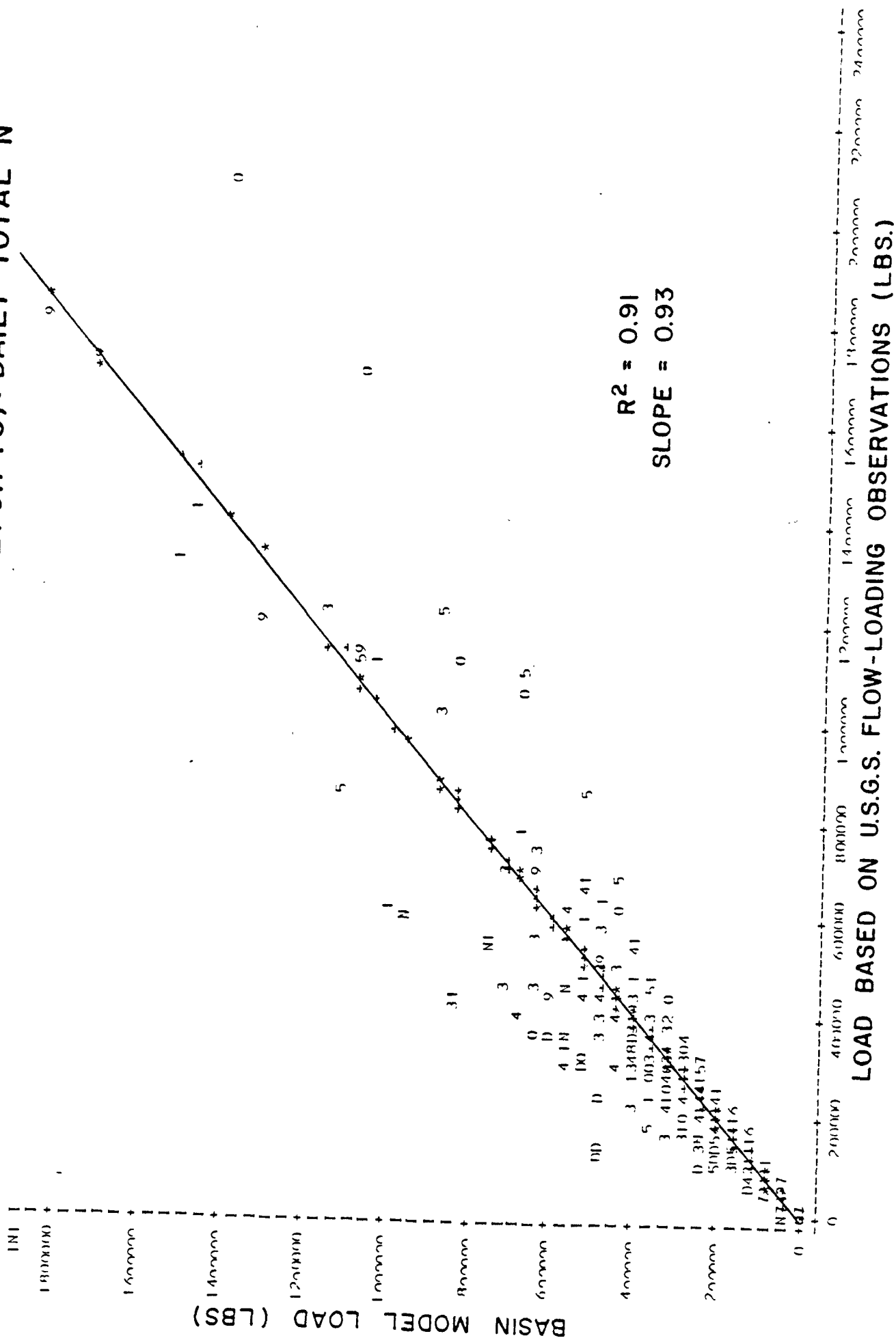


Figure 67. Comparison of Simulated Monthly Loads and Loads Based upon USGS Flow-Loading Relationships:
JAMES RIVER FALL LINE (1/1/74 - 12/31/75): MONTHLY TOTAL P

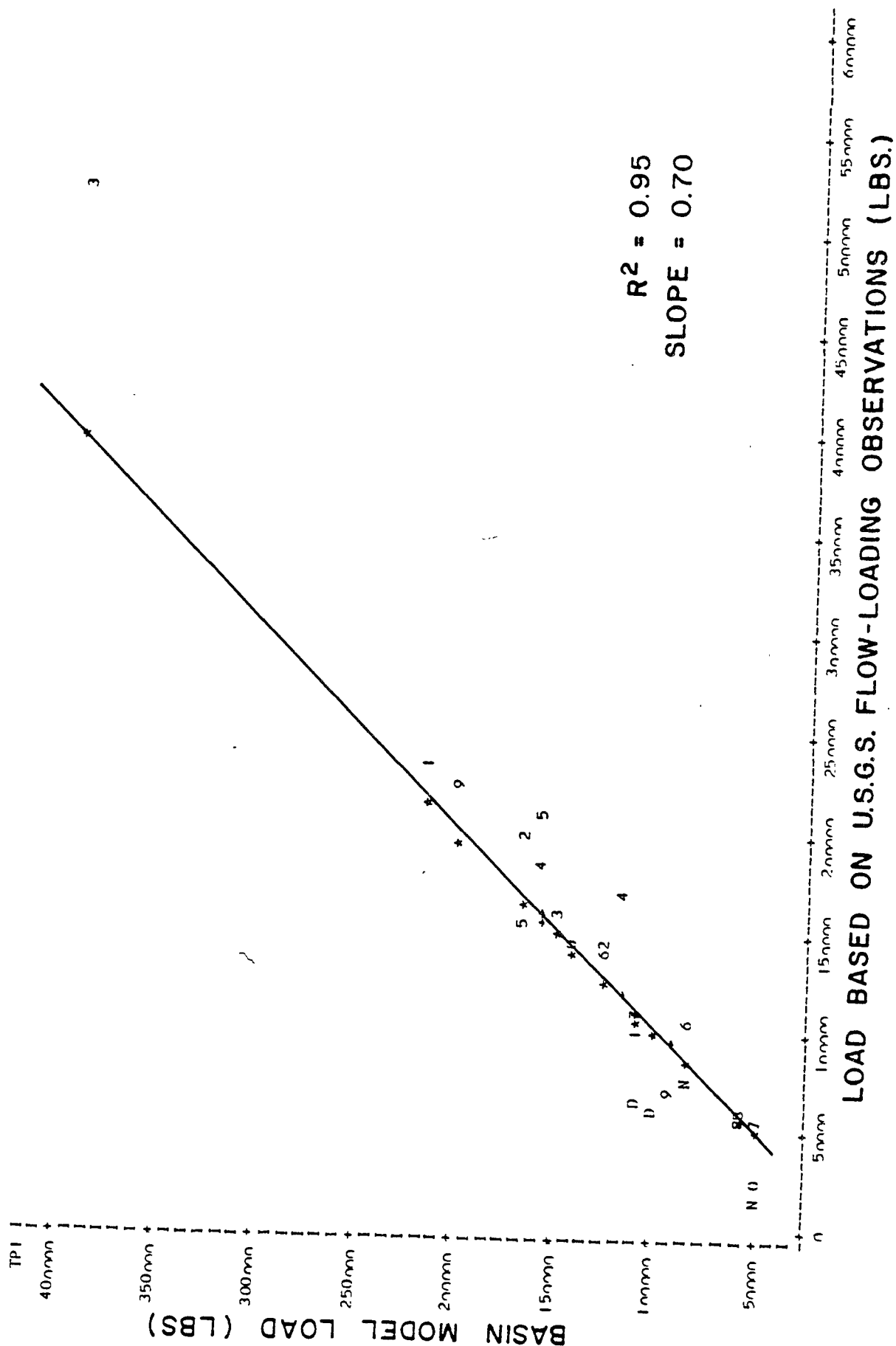


Figure 68. Comparison of Simulated Monthly Loads and Loads Based upon USGS Flow-Loading Relationships:
JAMES RIVER FALL LINE (1/1/74 - 12/31/75):MONTHLY INORGANIC P

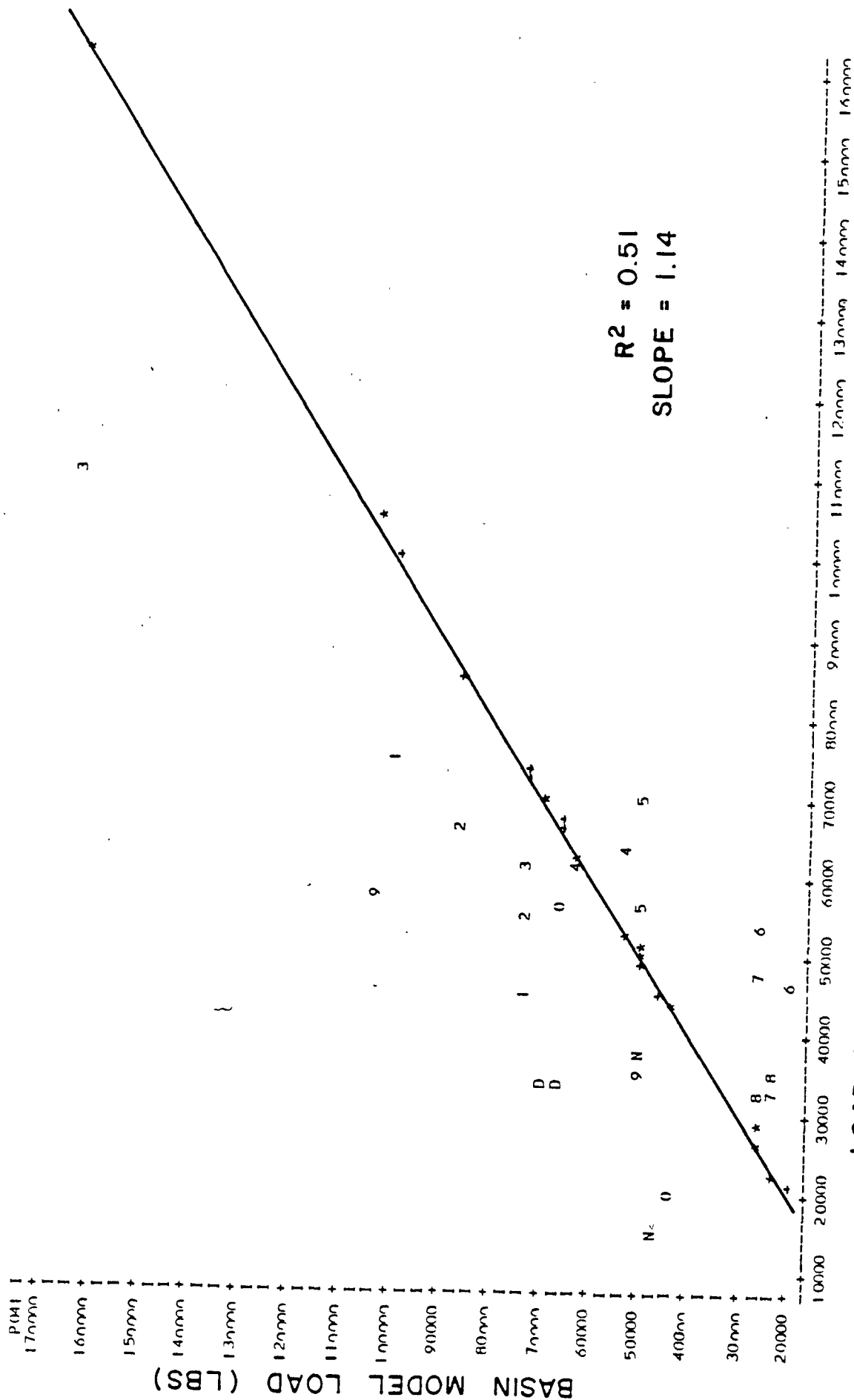


Figure 69. Comparison of Simulated Monthly Loads and Loads Based upon USGS Flow-Loading Relationships:
JAMES RIVER FALL LINE (1/1/74 - 12/31/75): MONTHLY TOTAL N

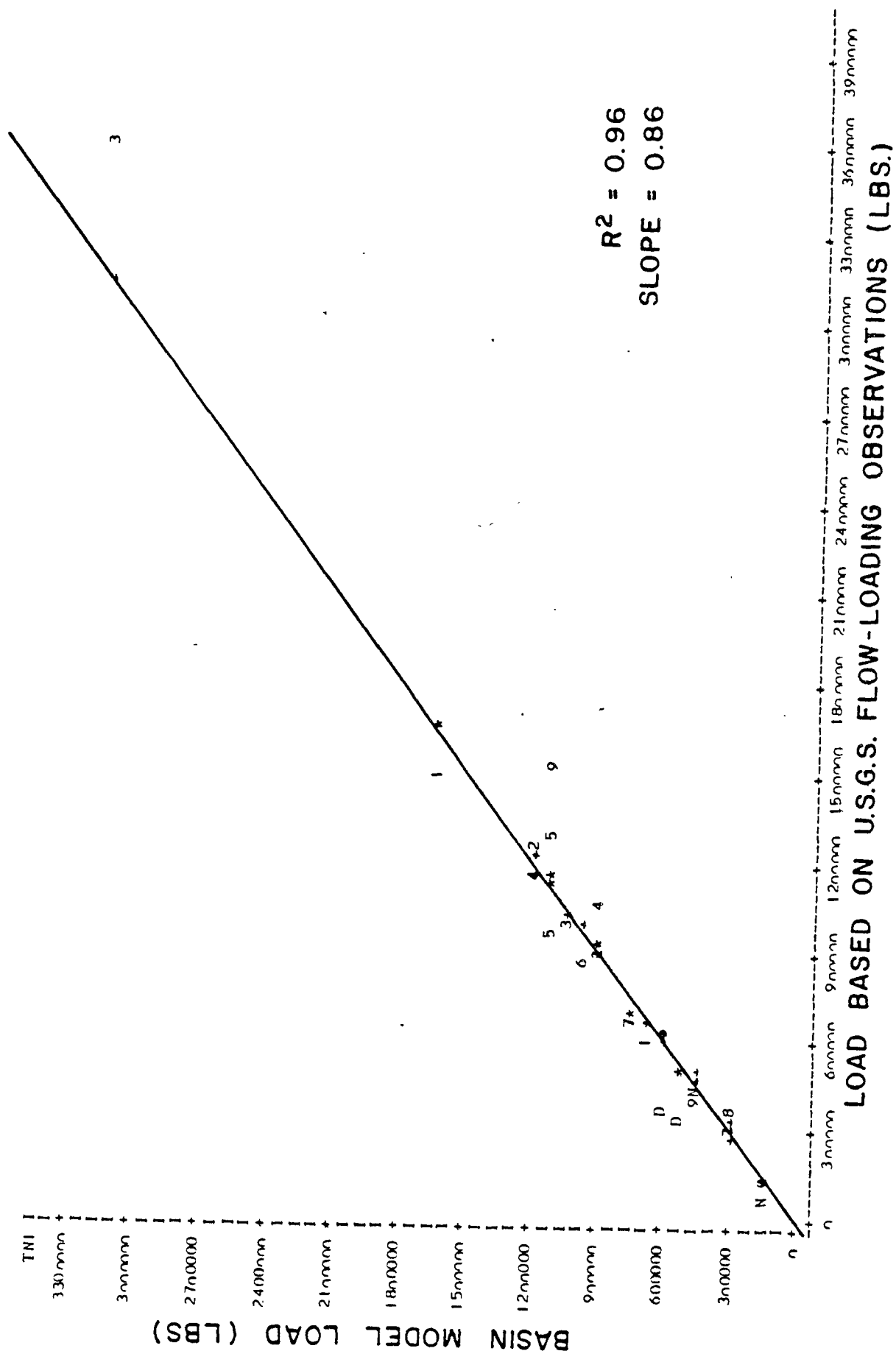


Figure 70. Comparison of Simulated Monthly Loads and Loads Based upon USGS Flow-Loading Relationships:
**JAMES RIVER FALL LINE (1/1/74 - 12/31/75) : MONTHLY NITRITE
 + NITRATE -N**

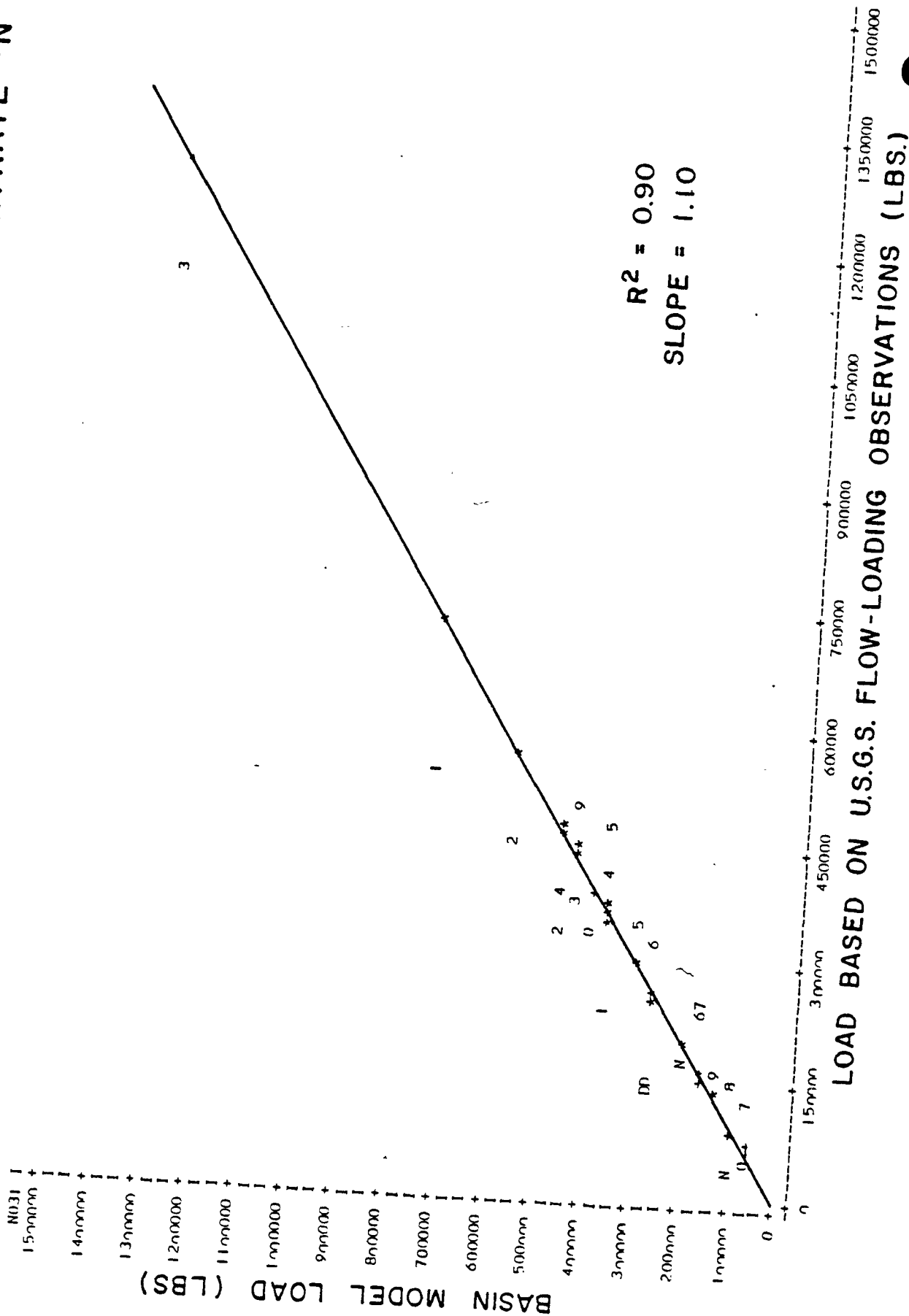


Figure 71. Comparison of Simulated Daily Loads and Loads Based upon USGS Flow-Loading Relationships:
JAMES RIVER FALL LINE (1/1/74 - 12/31/75): DAILY TOTAL P

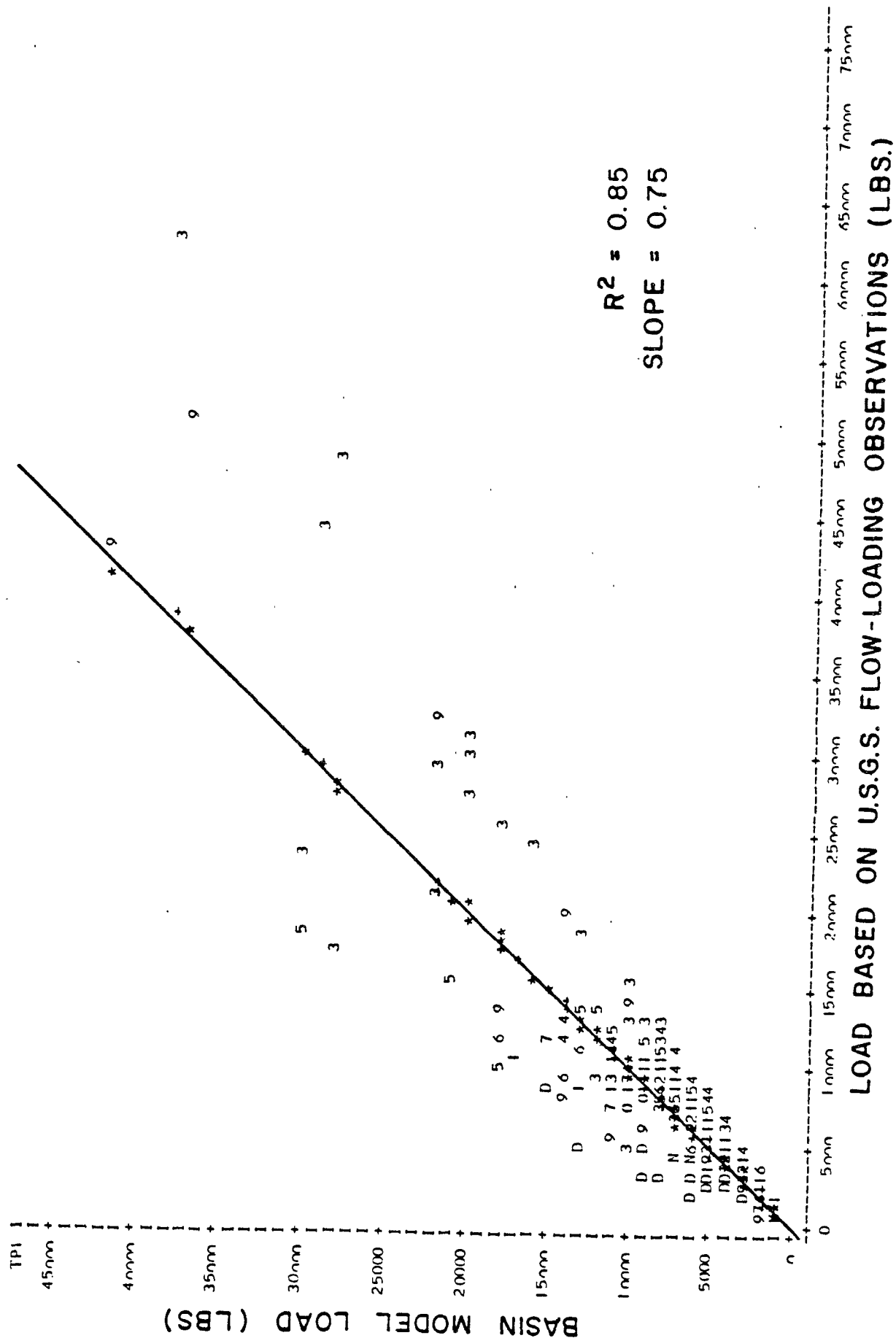


Figure 72. Comparison of Simulated Daily Loads and Loads Based upon USGS Flow-Loading Relationships:
JAMES RIVER FALL LINE (1/1/74 - 12/31/75): DAILY TOTAL N

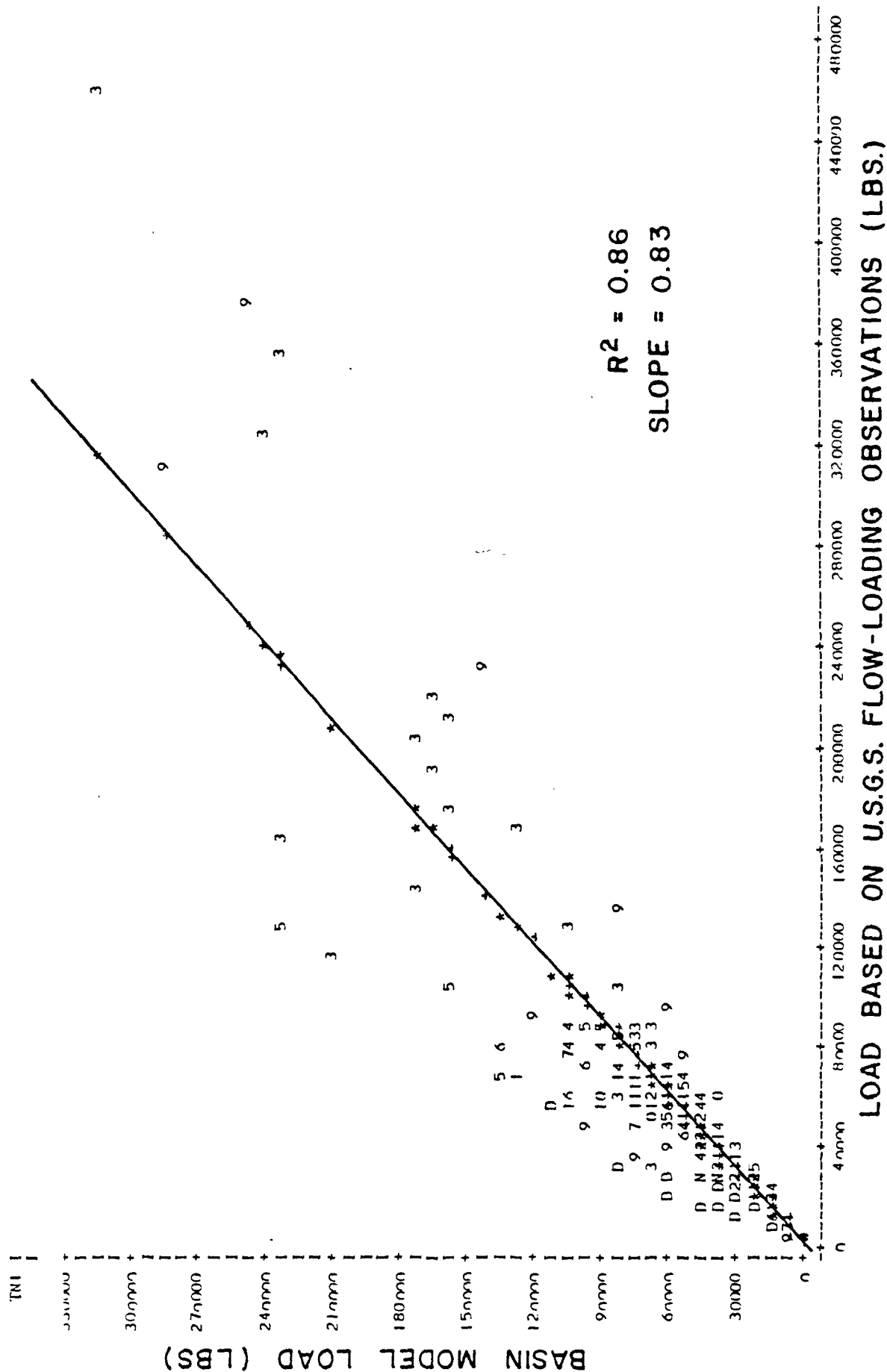


Figure 73. Comparison of Simulated Monthly Loads and Loads Based upon USGS Flow-Loading Relationships:
JAMES RIVER FALL LINE (1/1/76 - 12/31/78): MONTHLY TOTAL P

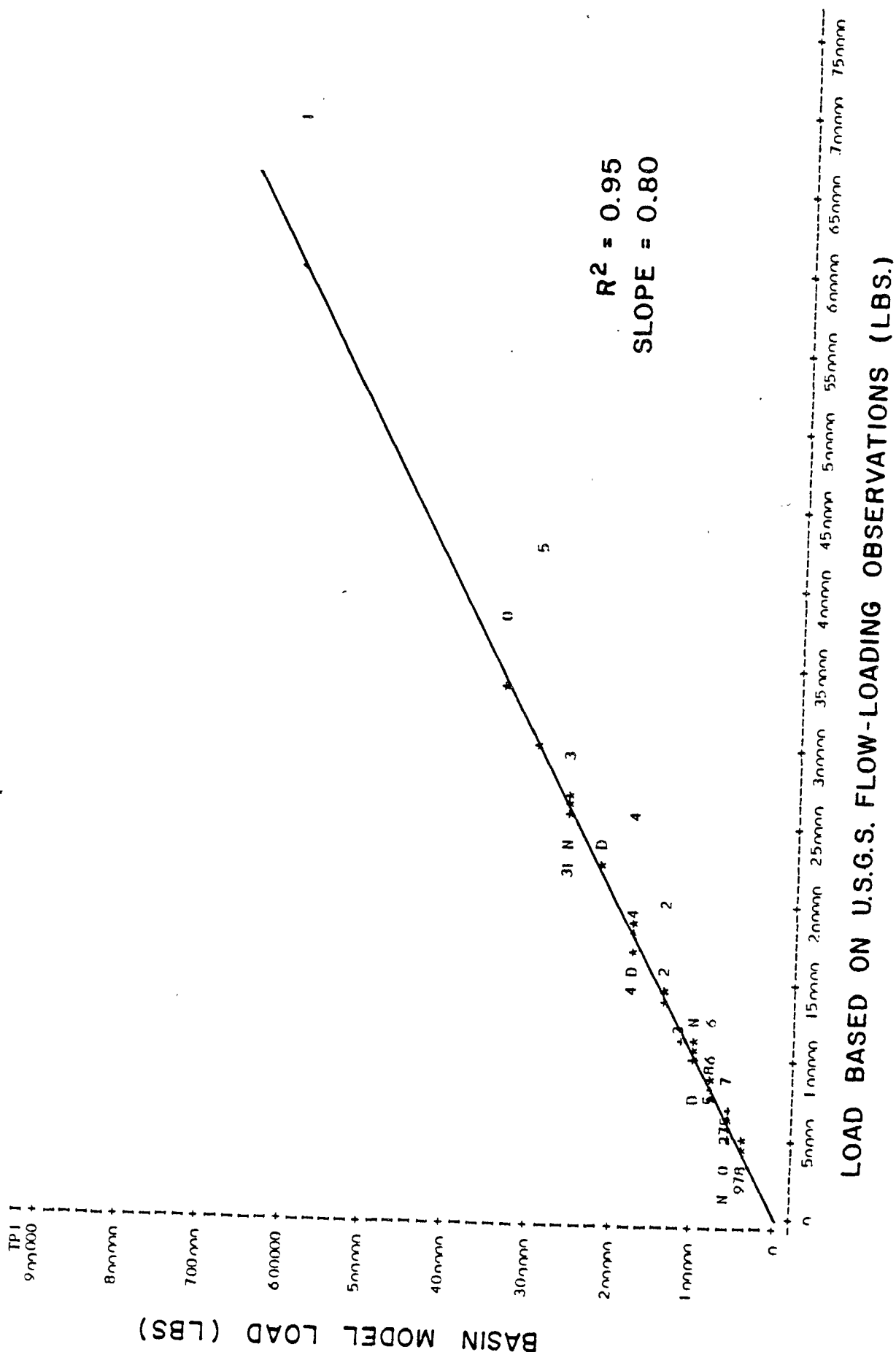
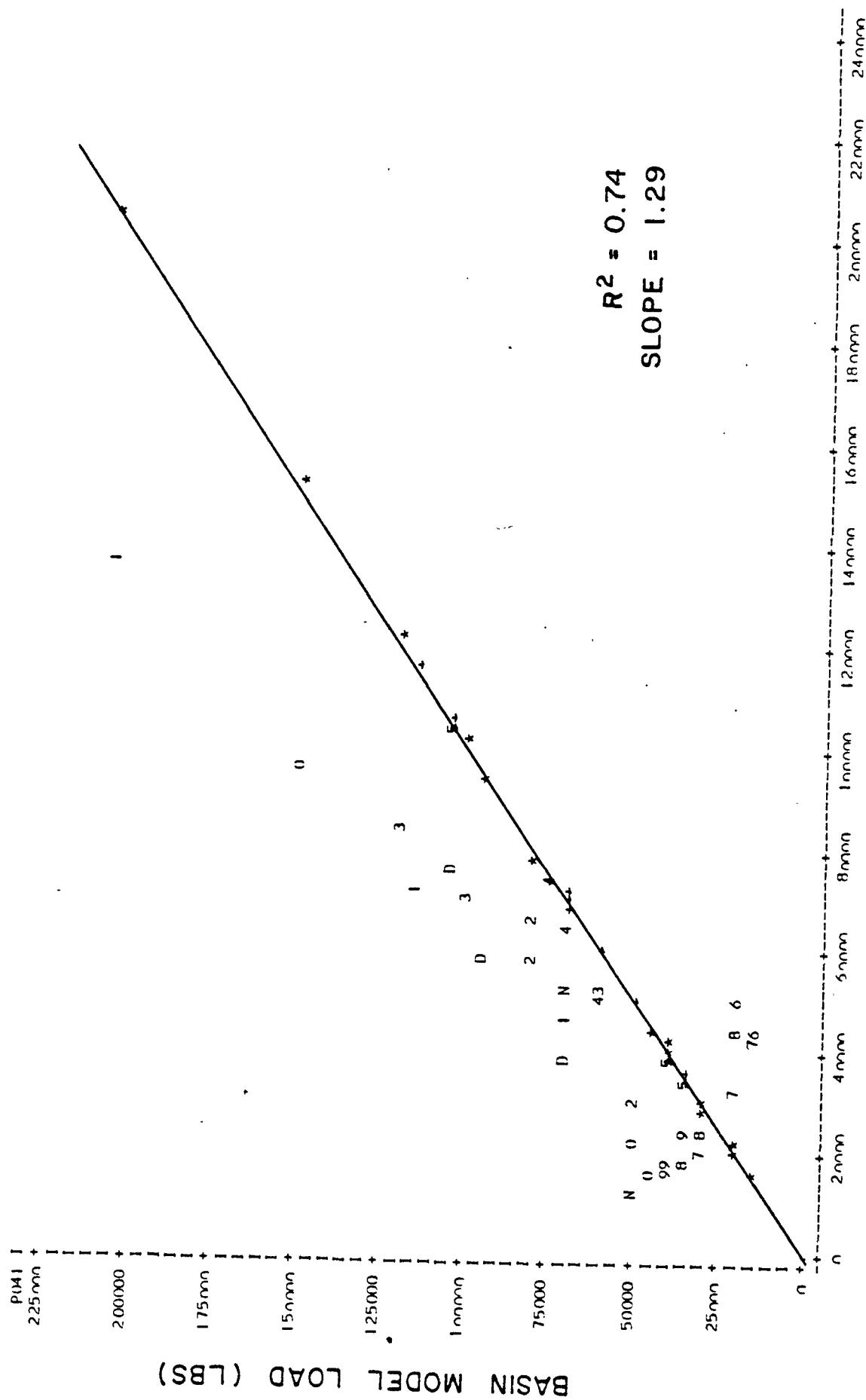


Figure 74. Comparison of Simulated Monthly Loads and Loads Based upon USGS Flow-Loading Relationships:
JAMES RIVER FALL LINE (1/1/76 - 12/31/78): MONTHLY INORGANIC P



LOAD BASED ON U.S.G.S. FLOW-LOADING OBSERVATIONS (LBS.)

Figure 75. Comparison of Simulated Monthly Loads and Loads Based upon USGS Flow-Loading Relationships:
JAMES RIVER FALL LINE (1/1/76 - 12/31/78): MONTHLY TOTAL N

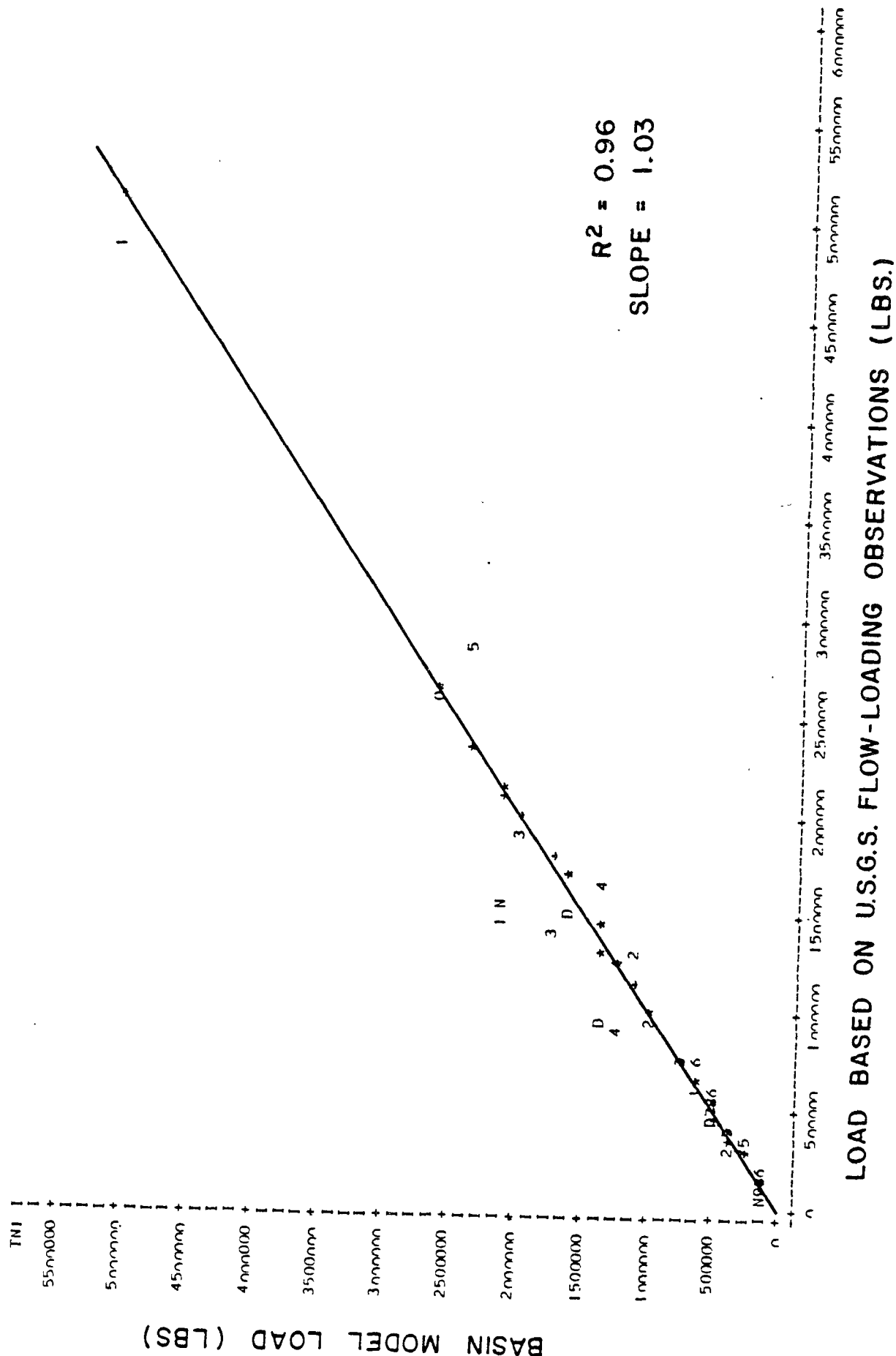


Figure 76. Comparison of Simulated Monthly Loads and Loads Based upon USGS Flow-Loading Relationships:
**JAMES RIVER FALL LINE (1/1/76 - 12/31/78): MONTHLY NITRITE
 + NITRATE - N**

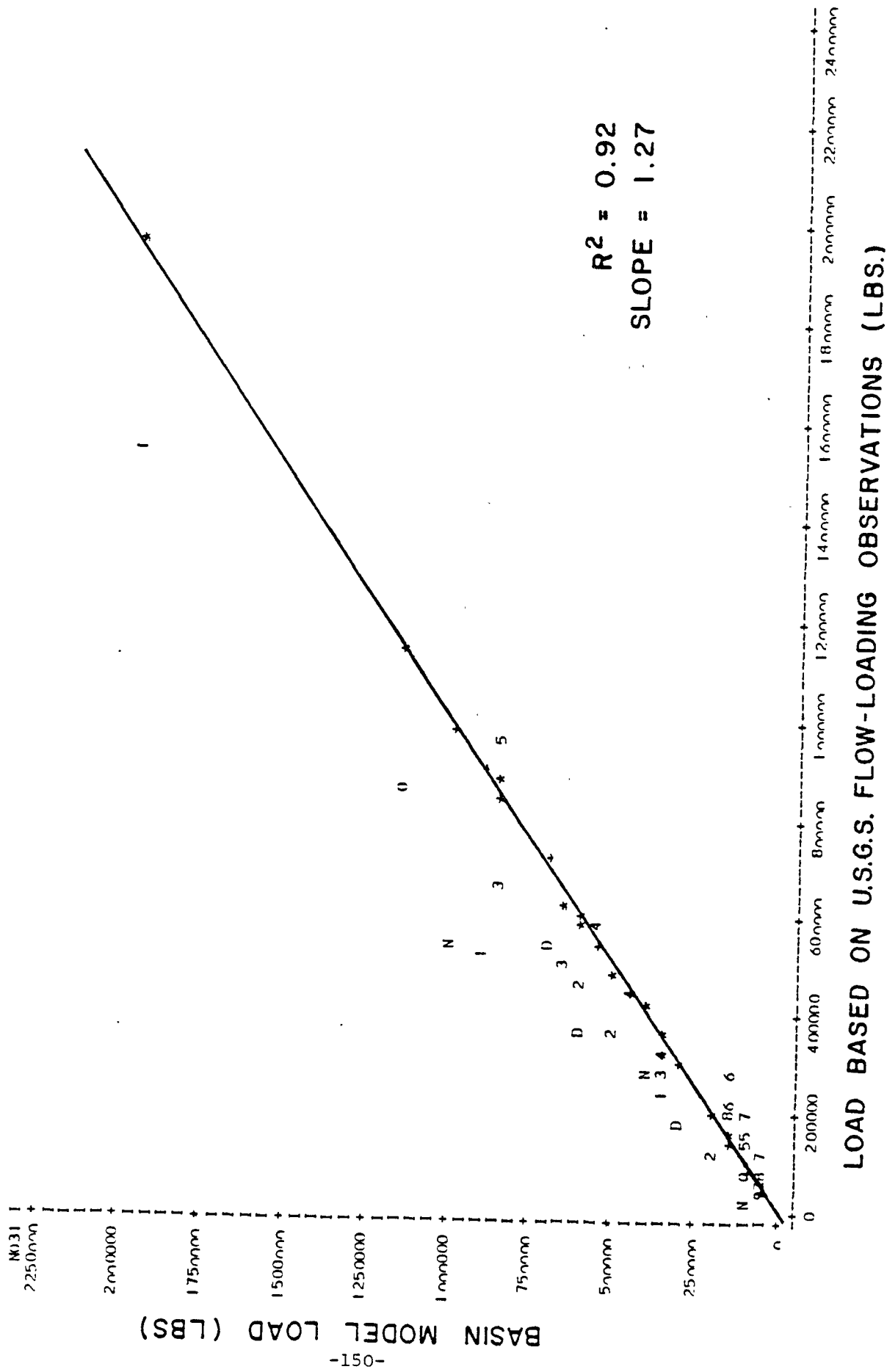


Figure 77. Comparison of Simulated Daily Loads and Loads Based upon USGS Flow-Loading Relationships:
JAMES RIVER FALL LINE (1/1/76 - 12/31/78): DAILY TOTAL P

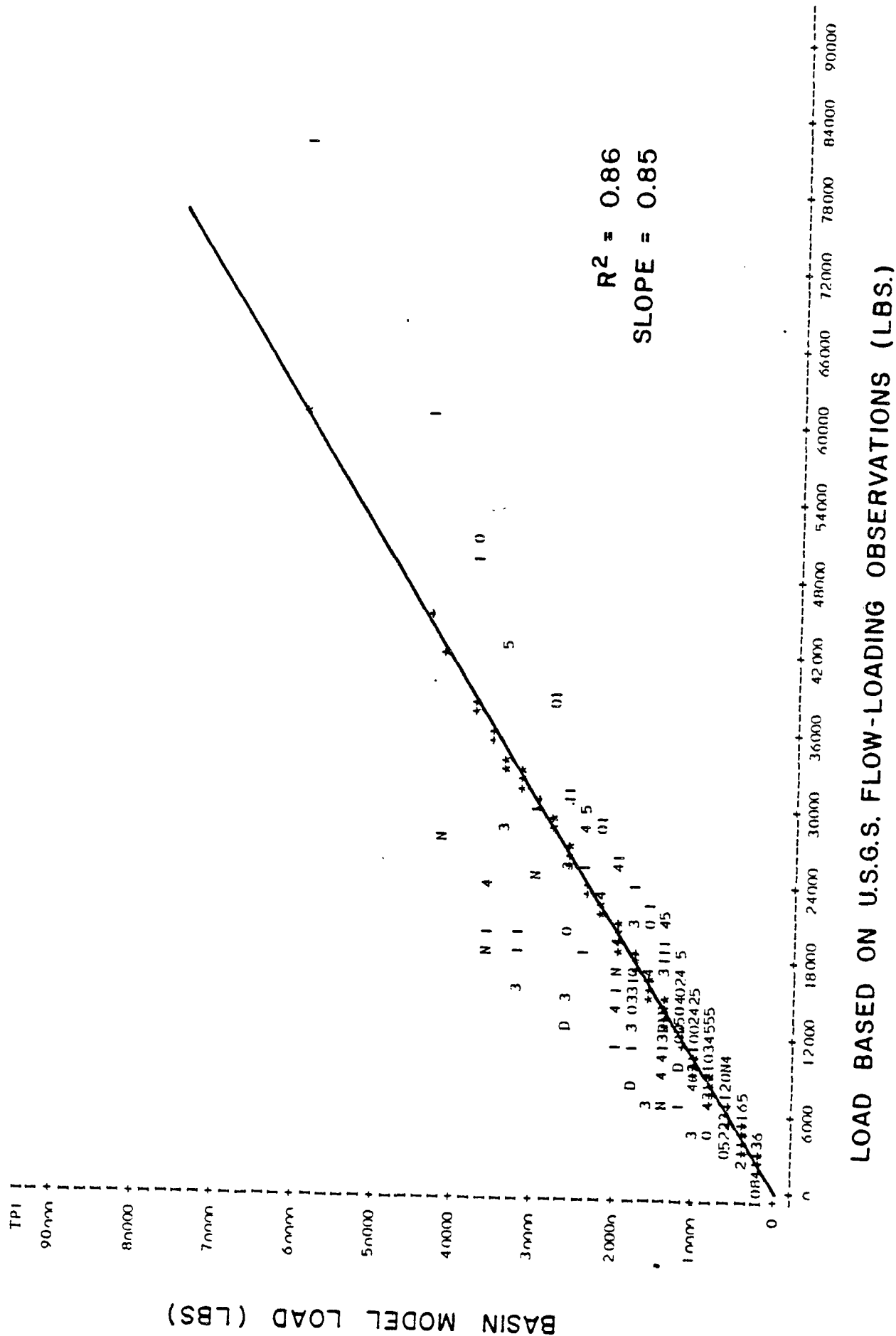


Figure 78. Comparison of Simulated Daily Loads and Loads Based upon USGS Flow-Loading Relationships:
JAMES RIVER FALL LINE (1/1/76 - 12/31/78): DAILY TOTAL N

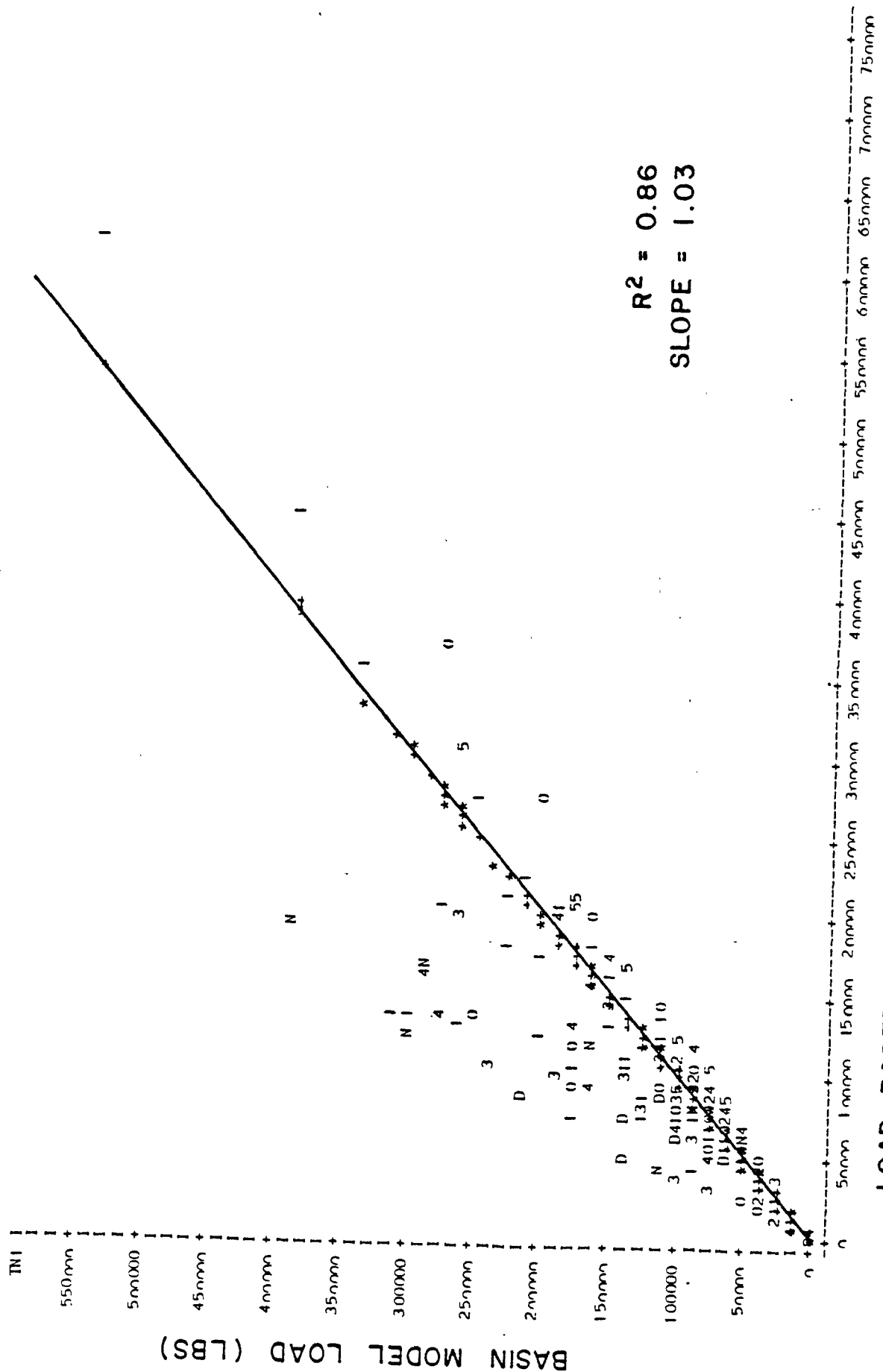


Figure 79. Comparison of Simulated Monthly Loads and Loads Based upon USGS Flow-Loading Relationships:
JAMES RIVER FALL LINE (1/1/74 - 12/31/78): MONTHLY TOTAL P

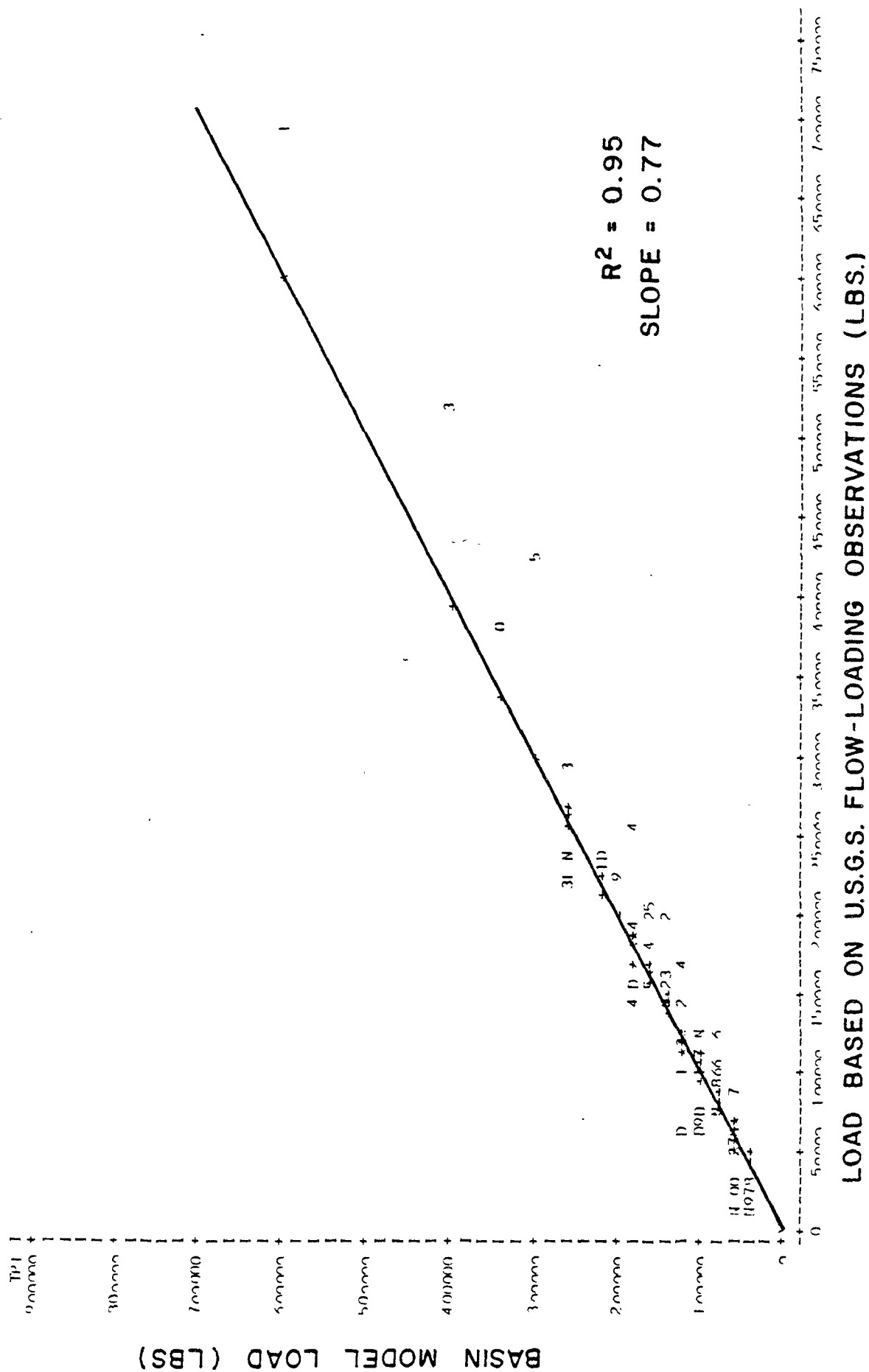


Figure 80. Comparison of Simulated Monthly Loads and Loads Based upon USGS Flow-Loading Relationships:
JAMES RIVER FALL LINE (1/1/74 - 12/31/78):MONTHLY INORGANIC P

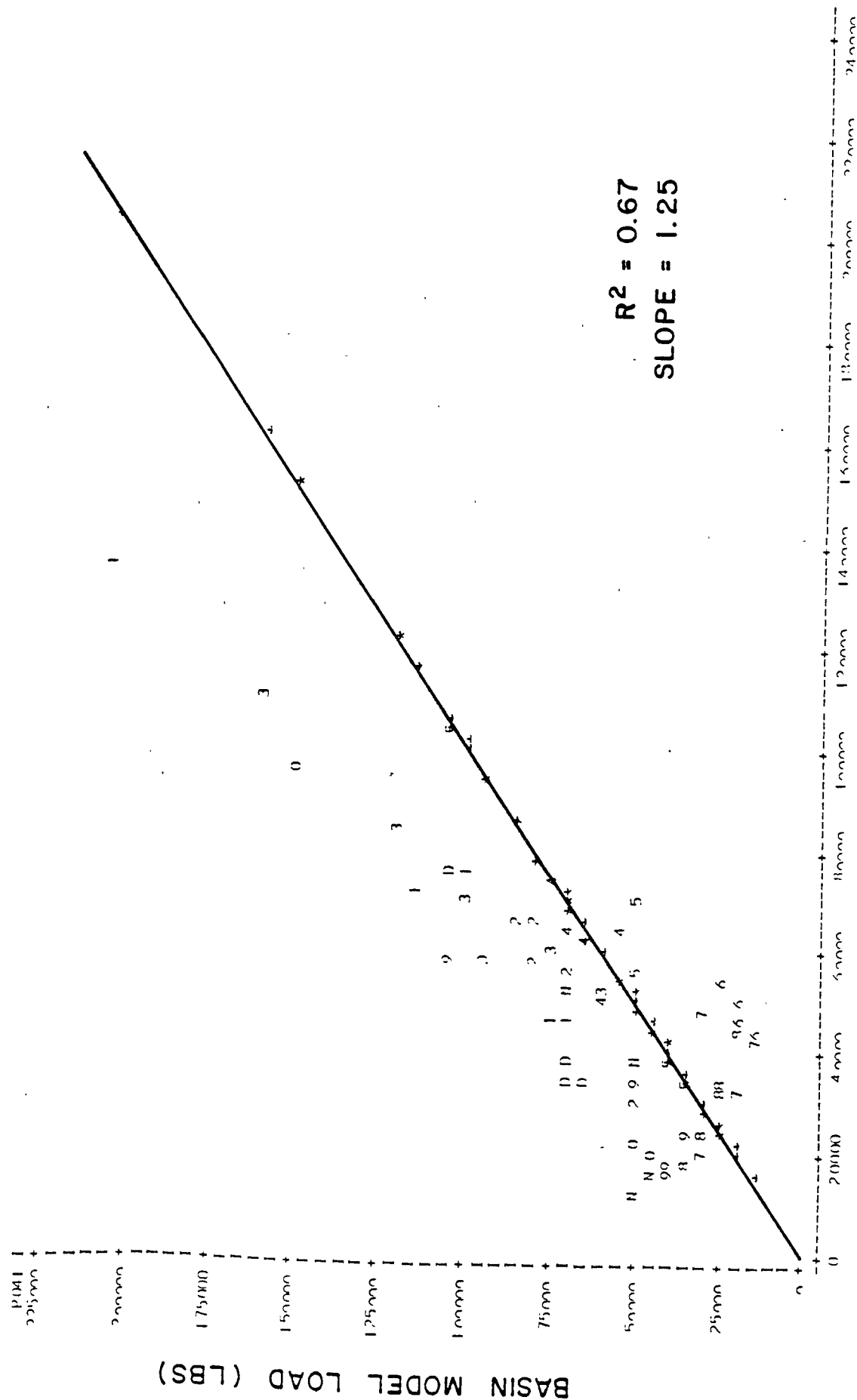


Figure 81. Comparison of Simulated Monthly Loads and Loads Based upon USGS Flow-Loading Relationships:
JAMES RIVER FALL LINE (1/1/74 - 12/31/78): MONTHLY TOTAL N

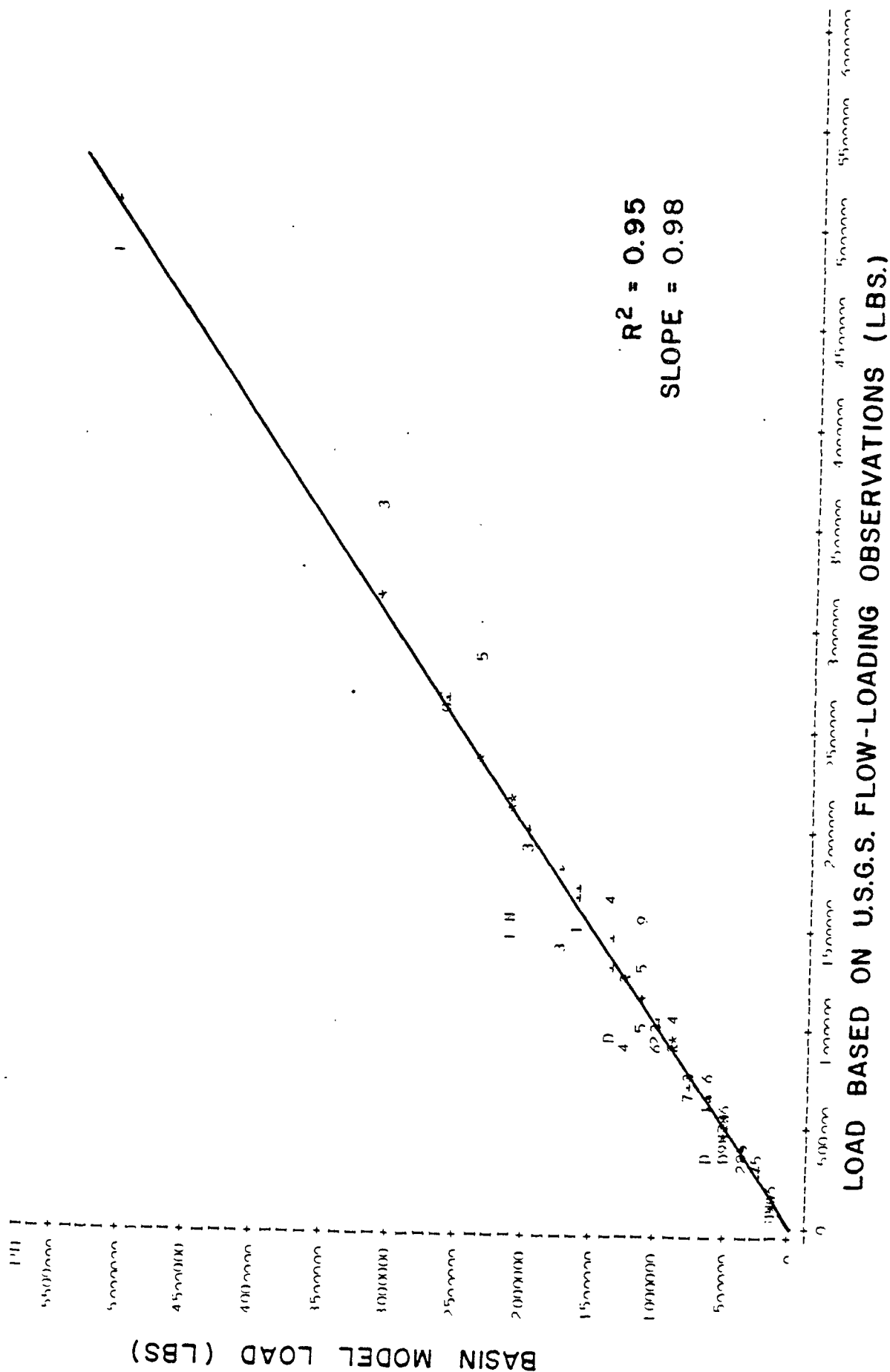


Figure 82. Comparison of Simulated Monthly Loads and Loads Based upon USGS Flow-Loading Relationships:
**JAMES RIVER FALL LINE (1/1/74 - 12/31/78): MONTHLY NITRITE
 + NITRATE - N**

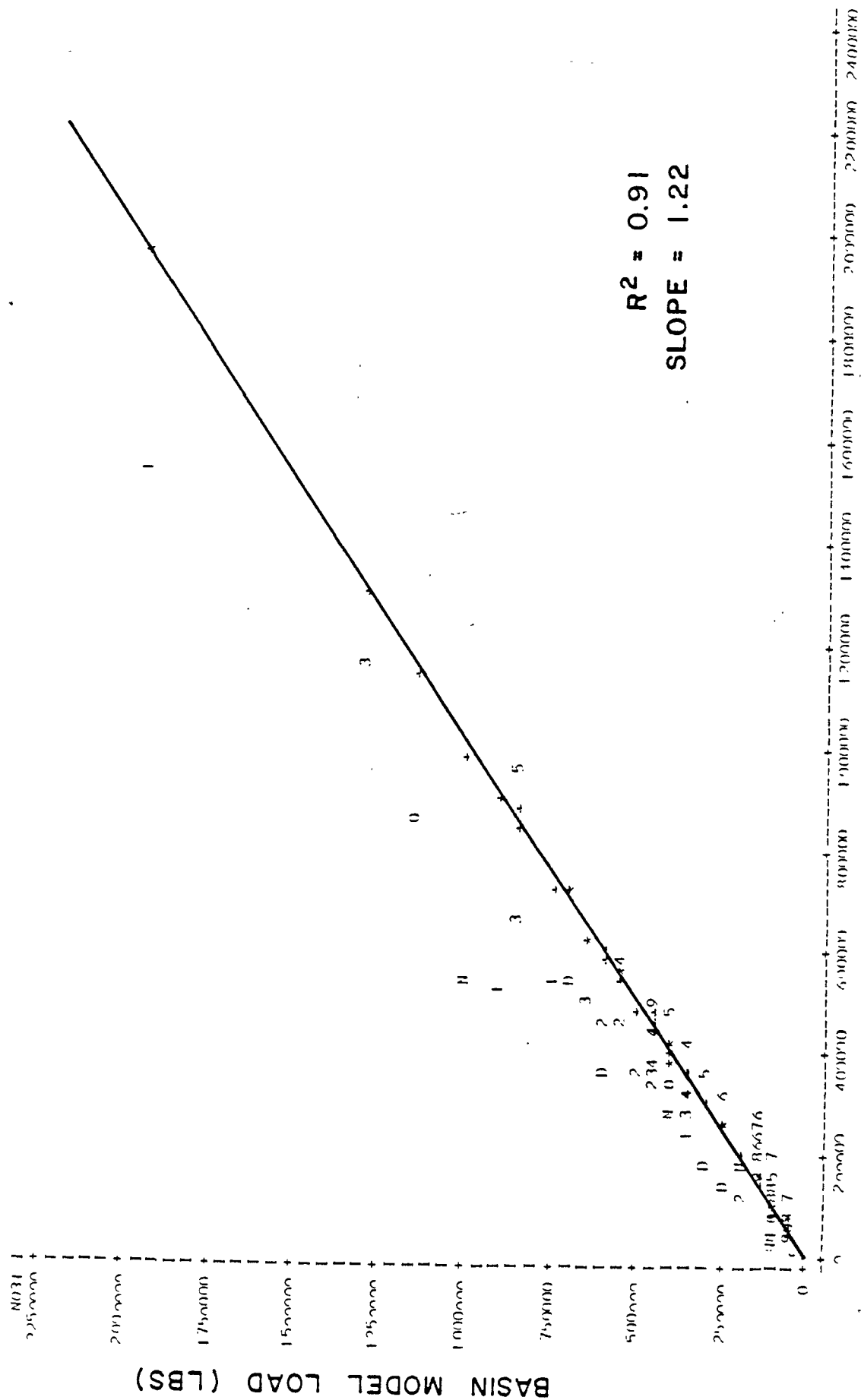


Figure 83. Comparison of Simulated Daily Loads and Loads Based upon USGS Flow-Loading Relationships:
JAMES RIVER FALL LINE (1/1/74 - 12/31/78): DAILY TOTAL P

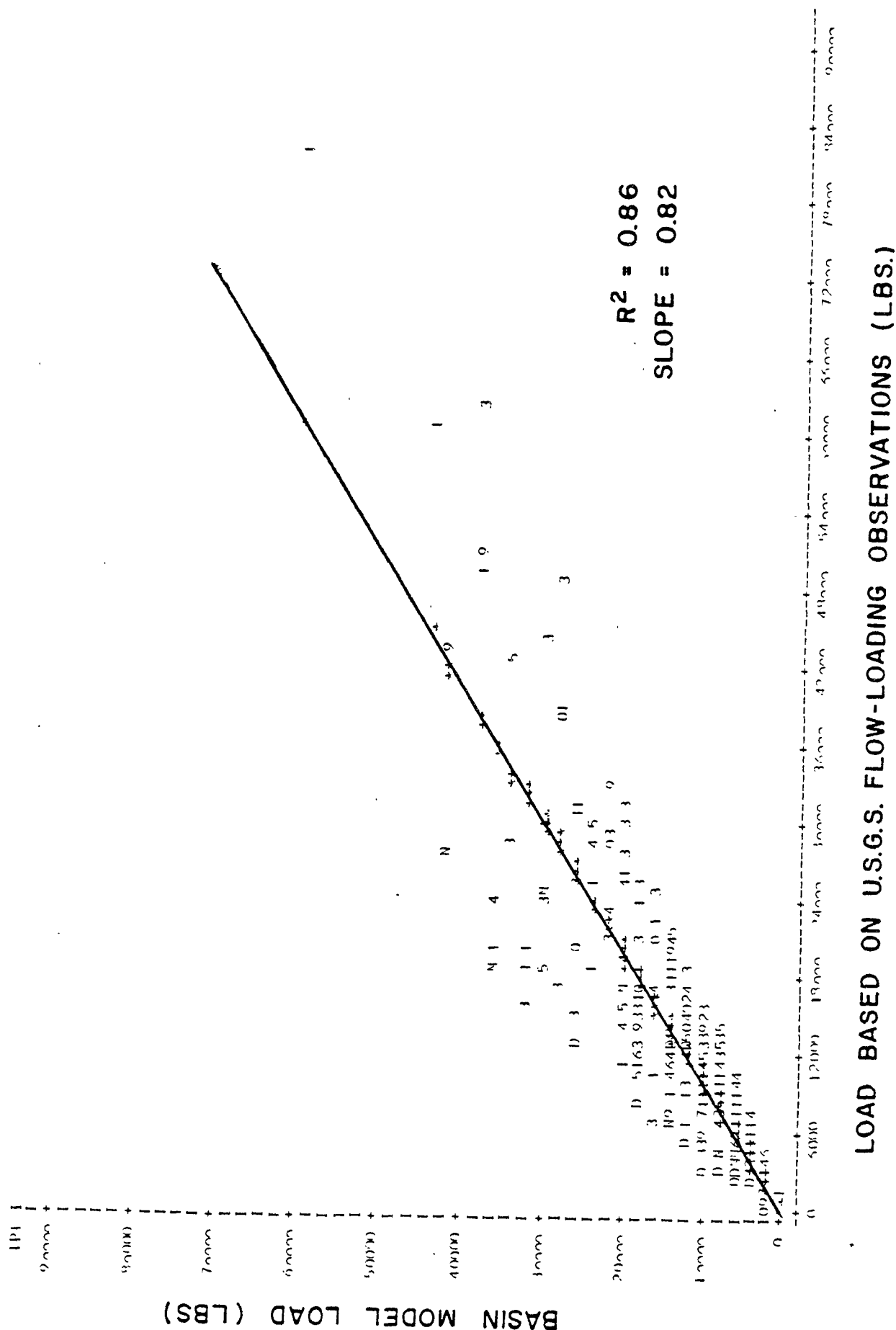
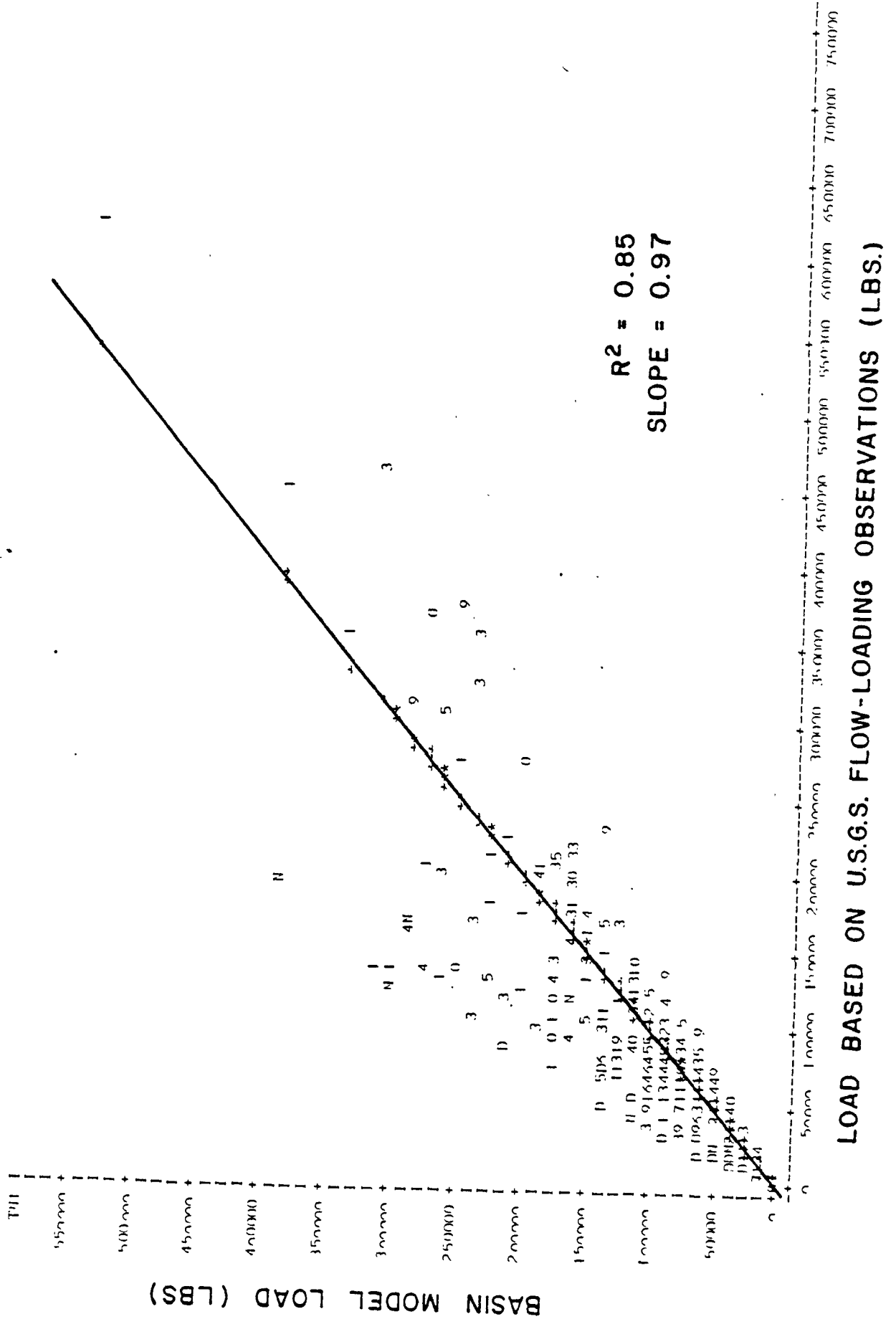


Figure 84. Comparison of Simulated Daily Loads and Loads Based upon USGS Flow-Loading Relationships:
JAMES RIVER FALL LINE (1/1/74 - 12/31/78): DAILY TOTAL N



- o As expected, monthly comparisons typically exhibit better goodness-of-fit than daily comparisons, due to the greater variability in daily loadings. However, given the typical response times of the Bay and the tributary estuaries to pollutant loading inputs, it is felt that monthly loads are more appropriate for goodness-of-fit assessments.
- o In general, goodness-of-fit for the verification period is as good as the agreement between simulated and USGS-based loads. Since the calibration period was characterized by higher streamflows than the verification period, this indicates that the Basin Model provides a reasonably good representation of a range of streamflow conditions.
- o In general, goodness-of-fit is somewhat better for total P and total N than for inorganic P and nitrate-N, respectively, although the results for the P and N fractions are typically quite acceptable.
- o The acceptable goodness-of-fit results for the three basins indicates that the Basin Model typically provides as good a representation of fall line loadings as the USGS flow-loading relationships. The major difference between the two techniques is that only the Basin Model can be used to determine the sources of loads delivered to the fall line and to project reductions in fall line loads for upstream water quality controls.

Comparisons of annual fall line loads of nitrogen and phosphorus for 1974-1978 are shown in Tables 18, 19, and 20 for the Susquehanna River Basin, Potomac River Basin, and James River Basin, respectively. In general, the agreement between the simulated annual load and the U.S.G.S.-based annual load is quite good, with most errors in the range $\pm 20\%$ and many in the range $\pm 10\%$. The agreement for annual loads of total N and total P is typically quite good. The organic and inorganic fractions of total N tend to be simulated somewhat better than the fractions of total P, probably because the majority of the N loads tends to be contributed by subsurface flow which is easier to model than surface runoff loads which accounted for the majority of the P loads. It should be noted that some of the error in Tables 18 through 20 can probably be attributed to the fact that the USGS flow-loading relationships does not explicitly account for seasonal differences (e.g., differences in cropland loadings that reflect changes in ground cover) in nonpoint pollution loadings whereas the Basin Model does. While the USGS-based loads do account for some seasonal differences, such as those associated with relatively high flows in the spring and relatively low flows in the winter, the potential for higher surface runoff loadings in early summer than in late summer (i.e., due to different ground cover conditions) as a result of identical daily streamflows can only be represented by the Basin Model. The fact that the majority of the simulated P loadings are contributed by surface runoff may account in part for the greater differences between simulated and USGS-based distributions of total P between organic and inorganic forms, since the

Table 18

COMPARISON OF ANNUAL FALL LINE LOADS SIMULATED BY RIVER BASIN MODEL
AND BASED ON U.S.G.S. "DAILY FLOW-LOADING" OBSERVATIONS:
SUSQUEHANNA RIVER FALL LINE

YEAR	TOTAL NITROGEN (lbs as N)			ORGANIC NITROGEN (lbs as N)			AMMONIA NITROGEN (lbs as N)			TOTAL KJELDAHL N (lbs as N)		
	Basin Model	Flow-Loading	Ratio	Basin Model	Flow-Loading	Ratio	Basin Model	Flow-Loading	Ratio	Basin Model	Flow-Loading	Ratio
1974	94,121,259	113,606,690	0.83	22,084,985	24,402,879	0.91	5,760,694	6,835,881	0.84	27,845,679	31,630,420	0.88
1975	147,074,457	159,159,566	0.92	38,135,240	34,871,757	1.09	8,981,293	9,921,128	0.91	47,116,533	44,689,499	1.05
1976	118,662,358	135,240,444	0.88	27,804,973	29,218,972	0.95	7,349,236	8,221,250	0.89	35,154,208	37,747,994	0.93
1977	130,451,612	154,096,761	0.85	35,554,954	33,559,781	1.06	8,637,463	9,497,548	0.91	44,192,417	43,161,407	1.02
1978	115,984,831	134,670,045	0.86	27,898,635	29,262,806	0.95	6,627,881	8,269,829	0.80	34,526,516	37,681,249	0.92

YEAR	NITRITE + NITRATE-N (lbs as N)			TOTAL PHOSPHORUS (lbs as P)			ORGANIC PHOSPHORUS (lbs as P)			INORGANIC PHOSPHORUS (lbs as P)		
	Basin Model	Flow-Loading	Ratio	Basin Model	Flow-Loading	Ratio	Basin Model	Flow-Loading	Ratio	Basin Model	Flow-Loading	Ratio
1974	66,275,580	80,902,645	0.82	4,827,740	3,974,877	1.21	3,150,290	2,202,442	1.43	1,677,450	1,775,617	0.94
1975	99,957,924	112,874,102	0.89	8,106,644	6,728,791	1.20	5,442,860	4,262,673	1.28	2,663,784	2,467,225	1.08
1976	83,508,150	96,189,485	0.87	5,713,576	4,978,429	1.15	3,962,037	2,871,413	1.38	1,751,539	2,108,530	0.83
1977	86,259,195	109,409,102	0.79	7,067,412	5,991,788	1.18	5,067,056	3,600,262	1.41	2,000,356	2,394,100	0.84
1978	81,458,315	95,668,093	0.85	5,858,896	5,201,060	1.13	3,969,822	3,108,750	1.28	1,889,074	2,094,596	0.90

Table 19

COMPARISON OF ANNUAL FALL LINE LOADS SIMULATED BY RIVER BASIN MODEL
AND BASED ON U.S.G.S. "DAILY FLOW-LOADING" OBSERVATIONS:
POTOMAC RIVER FALL LINE

YEAR	TOTAL NITROGEN (lbs as N)			ORGANIC NITROGEN (lbs as N)			AMMONIA NITROGEN (lbs as N)			TOTAL KJELDAHL N (lbs as N)		
	Basin Model	Flow-Loading	Ratio	Basin Model	Flow-Loading	Ratio	Basin Model	Flow-Loading	Ratio	Basin Model	Flow-Loading	Ratio
1974	27,978,875	26,584,281	1.05	8,257,521	7,890,768	1.05	1,079,861	850,749	1.27	9,337,382	8,741,517	1.07
1975	48,180,875	48,782,705	0.99	15,053,274	14,901,903	1.01	1,974,512	1,649,878	1.20	17,027,786	16,551,781	1.03
1976	34,559,837	35,870,130	0.96	10,736,710	10,918,408	0.98	1,628,684	1,205,668	1.35	12,365,394	12,124,077	1.02
1977	29,568,845	28,096,917	1.05	9,072,023	8,478,484	1.07	1,461,049	928,344	1.57	10,533,073	9,406,829	1.12
1978	47,345,849	49,279,147	0.96	13,754,115	15,178,744	0.91	2,195,121	1,692,954	1.30	15,949,236	16,871,698	0.95

YEAR	NITRITE + NITRATE-N (lbs as N)			TOTAL PHOSPHORUS (lbs as P)			ORGANIC PHOSPHORUS (lbs as P)			INORGANIC PHOSPHORUS (lbs as P)		
	Basin Model	Flow-Loading	Ratio	Basin Model	Flow-Loading	Ratio	Basin Model	Flow-Loading	Ratio	Basin Model	Flow-Loading	Ratio
1974	18,641,493	16,023,927	1.16	1,882,400	1,576,827	1.19	1,179,618	1,048,776	1.12	702,782	528,051	1.33
1975	31,153,089	28,976,097	1.08	3,135,061	3,273,115	0.96	2,150,237	2,340,262	0.92	984,824	932,853	1.06
1976	22,194,443	21,351,062	1.04	2,434,770	2,381,173	1.02	1,533,909	1,691,193	0.91	900,861	689,980	1.31
1977	19,035,772	16,795,797	1.13	2,155,051	1,790,845	1.20	1,295,956	1,244,488	1.04	859,095	546,357	1.57
1978	31,396,613	29,144,494	1.08	3,073,830	3,417,689	0.90	1,964,966	2,485,965	0.80	1,108,864	931,723	1.19

Table 20

COMPARISON OF ANNUAL FALL LINE LOADS SIMULATED BY RIVER BASIN MODEL
AND BASED ON U.S.G.S. "DAILY FLOW-LOADING" OBSERVATIONS;
JAMES RIVER FALL LINE

YEAR	TOTAL NITROGEN (lbs as N)			ORGANIC NITROGEN (lbs as N)			AMMONIA NITROGEN (lbs as N)			TOTAL KJELDAHL N (lbs as N)		
	Basin Model	Flow-Loading	Ratio	Basin Model	Flow-Loading	Ratio	Basin Model	Flow-Loading	Ratio	Basin Model	Flow-Loading	Ratio
1974	8,311,858	7,733,664	1.07	4,718,453	4,025,938	1.17	430,659	409,973	1.05	5,149,113	4,435,911	1.16
1975	12,298,803	12,977,341	0.95	6,783,325	7,179,091	0.94	666,156	647,250	1.03	7,449,481	7,826,340	0.95
1976	11,402,663	10,116,399	1.13	6,083,089	5,443,349	1.12	670,927	518,972	1.30	6,754,016	5,962,321	1.33
1977	8,995,339	8,064,974	1.12	4,688,309	4,312,118	1.09	537,222	416,847	1.29	5,225,532	4,728,966	1.11
1978	14,296,551	14,580,355	0.98	7,834,105	8,259,692	0.95	848,940	708,798	1.20	8,683,045	8,968,491	0.97

YEAR	NITRITE + NITRATE-N (lbs as N)			TOTAL PHOSPHORUS (lbs as P)			ORGANIC PHOSPHORUS (lbs as P)			INORGANIC PHOSPHORUS (lbs as P)		
	Basin Model	Flow-Loading	Ratio	Basin Model	Flow-Loading	Ratio	Basin Model	Flow-Loading	Ratio	Basin Model	Flow-Loading	Ratio
1974	3,162,746	2,888,704	1.09	1,301,651	1,261,898	1.03	674,028	736,054	0.92	627,622	526,139	1.19
1975	4,849,322	4,578,135	1.06	1,767,786	2,018,825	0.88	968,983	1,344,213	0.72	798,802	674,612	1.18
1976	4,648,647	3,664,268	1.27	1,644,165	1,608,805	1.02	869,007	1,012,378	0.86	775,159	569,517	1.30
1977	3,769,807	2,941,652	1.28	1,405,955	1,289,917	1.09	669,755	786,316	0.85	736,200	503,958	1.46
1978	5,613,506	5,021,820	1.12	1,947,723	2,223,458	0.88	1,119,179	1,550,603	0.72	828,544	674,979	1.23

seasonal differences in instream P transformations (i.e., conversion from inorganic to organic forms due to chlorophyll-a uptake) during wet-weather flow periods are handled by the Basin Model, but not by the USGS flow-loading relationship.

Tables 18 through 20 are also of interest because they indicate the predominant form of N and P loads delivered to the outlets of the three river basins. In the Susquehanna and Potomac basins, the majority of the annual N loads delivered to the fall line are in the form of nitrate-N, whereas organic-N loads predominate in the James basin. By comparison, the majority of the annual P loads delivered to the fall line are in the form of organic P for all three river basins, with the highest inorganic P fractions (%) found at the Susquehanna River fall line. This examination of organic and inorganic nutrient fractions further illustrates the different sources of N and P loadings delivered to the fall lines. As indicated in Table 8, the organic fractions of N and P typically exhibit much higher NPS loading factors than the inorganic fractions. Consequently, the majority of N and P loadings delivered to streams by stormwater runoff is in the organic form. While instream transformations during transport to the fall line can result in higher inorganic N and P fractions than were delivered to streams by stormwater runoff, the organic fraction should still constitute a higher percentage of the stormwater loadings of N and P that reach the fall line. The fact that the majority of the annual P loads are in the organic form whereas the majority of the annual N loads are in the inorganic form suggests that stormwater runoff is probably not the most significant contributor of N loadings.

Tables 21 through 24 summarize calibrated baseflow and interflow concentrations of nitrate-N, ammonia-N, inorganic P, and BOD, respectively. As may be seen, subsurface flow concentrations of nitrate-N are relatively high and typically highest (i.e., on the order of 2.0 mg/L) in the Susquehanna River Basin, which has a higher percentage of agricultural land than most other major river basins. By comparison, inorganic P concentrations in interflow/baseflow are relatively low (i.e., 0.01 - 0.02 mg/L) in all river basins. Thus, Tables 21 through 24 are further indication of the greater significance of subsurface flow contributions of nitrogen. Model production runs that are not described in detail herein confirm the nonpoint pollution loading trends evident in Tables 21-24 and previous tables: subsurface flow is the principal source of nitrogen loads (i.e., primarily nitrate-N) delivered to the fall line, while surface runoff is the principal source of phosphorus loads.

Results Based upon Upstream and Fall Line Gages. Simulated and recorded daily loads were compared at seven USGS gaging stations for the period 1974-1978: 4 stations in the Susquehanna River Basin; 2 stations in the Potomac River Basin; and 1 station in the James River Basin. These daily loading comparisons fulfilled two major objectives: (1) Since the USGS flow-loading relationships used for fall line loading comparisons were based upon monitoring data collected from 1979 through 1981, goodness-of-fit assessments based upon actual monitoring data for 1979-1981 provide an

Table 21

BASEFLOW/INTERFLOW CONCENTRATIONS: NITRATE-N

SUB-BASIN	FLOW# TYPE	MEAN MONTHLY CONCENTRATIONS (mg/L)											
		JAN	FEB	MAR	APRIL	MAY	JUNE	JULY	AUG	SEPT	OCT	NOV	DEC
10, 20, 30, 40	I	2.10	2.10	2.20	2.20	2.30	2.60	2.60	2.80	2.60	2.40	2.20	2.20
	B	2.10	2.10	2.20	2.20	2.30	2.60	2.60	2.80	2.60	2.40	2.20	2.20
50, 60, 70	I	1.20	1.20	1.20	1.20	1.30	1.50	1.50	1.50	1.50	1.30	1.20	1.20
	B	1.20	1.20	1.20	1.20	1.30	1.50	1.50	1.50	1.50	1.30	1.20	1.20
80, 110, 120, 140	I	2.20	2.20	2.30	2.30	2.40	2.70	2.70	3.10	2.70	2.60	2.30	2.30
	B	2.20	2.20	2.30	2.30	2.40	2.70	2.70	3.10	2.70	2.60	2.30	2.30
90, 100	I	1.80	1.80	1.90	1.90	2.0	2.0	2.0	2.40	2.20	2.10	1.90	1.90
	B	1.80	1.80	1.90	1.90	2.0	2.0	2.0	2.40	2.20	2.10	1.90	1.90
160, 170, 175	I	1.20	1.20	1.350	1.350	1.40	1.450	1.50	1.60	1.50	1.30	1.20	1.20
	B	1.20	1.20	1.350	1.350	1.40	1.450	1.50	1.60	1.50	1.30	1.20	1.20
180, 190, 200, 220	I	1.20	1.20	1.350	1.350	1.40	1.450	1.50	1.60	1.50	1.30	1.20	1.20
	B	1.20	1.20	1.350	1.350	1.40	1.450	1.50	1.60	1.50	1.30	1.20	1.20
235, 240, 250, 260, 270, 280, 290, 300 310, 320	I	0.201	0.201	0.201	0.201	0.201	0.402	0.402	0.402	0.201	0.201	0.201	0.201
	B	0.300	0.300	0.300	0.300	0.300	0.600	0.600	0.600	0.300	0.300	0.300	0.300
ALL COASTAL AREAS	I	1.00	1.00	1.00	1.00	1.00	1.00	1.00	1.00	1.00	1.00	1.00	1.00
	B	1.00	1.00	1.00	1.00	1.00	1.00	1.00	1.00	1.00	1.00	1.00	1.00
230, 330, 340	I	0.90	0.90	0.90	0.90	0.90	0.90	0.90	0.90	0.90	0.90	0.90	0.90
	B	0.90	0.90	0.90	0.90	0.90	0.90	0.90	0.90	0.90	0.90	0.90	0.90

* I = INTERFLOW
B = BASEFLOW

Table 22

BASEFLOW/INTERFLOW CONCENTRATIONS: AMMONIA-N

SUB-BASIN	FLOW* TYPE	MEAN MONTHLY CONCENTRATIONS (mg/L)											
		JAN	FEB	MAR	APRIL	MAY	JUNE	JULY	AUG	SEPT	OCT	NOV	DEC
10, 20, 30, 40	I	0.05	0.05	0.05	0.05	0.05	0.08	0.08	0.08	0.05	0.033	0.033	0.05
	B	0.05	0.05	0.05	0.05	0.05	0.08	0.08	0.08	0.05	0.033	0.033	0.05
50, 60, 70	I	0.05	0.05	0.05	0.05	0.05	0.08	0.08	0.08	0.05	0.033	0.033	0.05
	B	0.05	0.05	0.05	0.05	0.05	0.08	0.08	0.08	0.05	0.033	0.033	0.05
80, 110, 120, 140	I	0.05	0.05	0.05	0.05	0.05	0.08	0.08	0.08	0.05	0.033	0.033	0.05
	B	0.05	0.05	0.05	0.05	0.05	0.08	0.08	0.08	0.05	0.033	0.033	0.05
90, 100	I	0.05	0.05	0.05	0.05	0.05	0.08	0.08	0.08	0.05	0.033	0.033	0.05
	B	0.05	0.05	0.05	0.05	0.05	0.08	0.08	0.08	0.05	0.033	0.033	0.05
160, 170, 175	I	0.05	0.05	0.05	0.05	0.05	0.05	0.05	0.05	0.05	0.05	0.05	0.05
	B	0.05	0.05	0.05	0.05	0.05	0.05	0.05	0.05	0.05	0.05	0.05	0.05
180, 190, 200, 220	I	0.05	0.05	0.05	0.05	0.05	0.05	0.05	0.05	0.05	0.05	0.05	0.05
	B	0.05	0.05	0.05	0.05	0.05	0.05	0.05	0.05	0.05	0.05	0.05	0.05
235, 240, 250, 260, 270, 280, 290, 300 310, 320	I	0.05	0.05	0.05	0.05	0.05	0.05	0.05	0.05	0.05	0.05	0.05	0.05
	B	0.05	0.05	0.05	0.05	0.05	0.05	0.05	0.05	0.05	0.05	0.05	0.05
ALL COASTAL AREAS	I	0.05	0.05	0.05	0.05	0.05	0.05	0.05	0.05	0.05	0.05	0.05	0.05
	B	0.05	0.05	0.05	0.05	0.05	0.05	0.05	0.05	0.05	0.05	0.05	0.05
230, 330, 340	I	0.05	0.05	0.05	0.05	0.05	0.05	0.05	0.05	0.05	0.05	0.05	0.05
	B	0.05	0.05	0.05	0.05	0.05	0.05	0.05	0.05	0.05	0.05	0.05	0.05

* I = INTERFLOW
B = BASEFLOW

Table 23

BASEFLOW/INTERFLOW CONCENTRATIONS: INORGANIC PHOSPHORUS

SUB-BASIN	FLOW* TYPE	MONTHLY CONCENTRATIONS (mg/l NH -N)											
		JAN	FEB	MAR	APRIL	MAY	JUNE	JULY	AUG	SEPT	OCT	NOV	DEC
10, 20, 30, 40	I	0.01	0.01	0.01	0.02	0.02	0.02	0.02	0.02	0.02	0.02	0.01	0.01
	B	0.01	0.01	0.01	0.02	0.02	0.02	0.02	0.02	0.02	0.02	0.01	0.01
50, 60, 70	I	0.01	0.01	0.01	0.015	0.015	0.015	0.015	0.015	0.015	0.015	0.01	0.01
	B	0.01	0.01	0.01	0.015	0.015	0.015	0.015	0.015	0.015	0.015	0.01	0.01
80, 110, 120, 140	I	0.01	0.01	0.01	0.02	0.02	0.02	0.02	0.02	0.02	0.02	0.01	0.01
	B	0.01	0.01	0.01	0.02	0.02	0.02	0.02	0.02	0.02	0.02	0.01	0.01
90, 100	I	0.01	0.01	0.01	0.02	0.02	0.02	0.02	0.02	0.02	0.02	0.01	0.01
	B	0.01	0.01	0.01	0.02	0.02	0.02	0.02	0.02	0.02	0.02	0.01	0.01
160, 170, 175	I	0.01	0.01	0.01	0.01	0.01	0.01	0.01	0.01	0.01	0.01	0.01	0.01
	B	0.01	0.01	0.01	0.01	0.01	0.01	0.01	0.01	0.01	0.01	0.01	0.01
180, 190, 200, 220	I	0.01	0.01	0.01	0.01	0.01	0.01	0.01	0.01	0.01	0.01	0.01	0.01
	B	0.01	0.01	0.01	0.01	0.01	0.01	0.01	0.01	0.01	0.01	0.01	0.01
235, 240, 250, 260, 270, 280, 290, 300 310, 320	I	0.02	0.02	0.02	0.02	0.02	0.05	0.05	0.05	0.05	0.02	0.02	0.02
	B	0.01	0.01	0.01	0.01	0.01	0.025	0.025	0.025	0.025	0.01	0.01	0.01
ALL COASTAL AREAS	I	0.015	0.015	0.015	0.015	0.015	0.015	0.015	0.015	0.015	0.015	0.015	0.015
	B	0.015	0.015	0.015	0.015	0.015	0.015	0.015	0.015	0.015	0.015	0.015	0.015
230, 330, 340	I	0.02	0.02	0.02	0.02	0.02	0.02	0.02	0.02	0.02	0.02	0.02	0.02
	B	0.02	0.02	0.02	0.02	0.02	0.02	0.02	0.02	0.02	0.02	0.02	0.02

* I = INTERFLOW
B = BASEFLOW

Table 24

BASEFLOW/INTERFLOW CONCENTRATIONS: BOD

SUB-BASIN	FLOW* TYPE	MEAN MONTHLY CONCENTRATIONS (mg/L)											
		JAN	FEB	MAR	APRIL	MAY	JUNE	JULY	AUG	SEPT	OCT	NOV	DEC
10, 20, 30, 40	I	2.50	2.50	2.50	2.50	2.50	2.50	2.50	2.50	2.50	2.50	2.50	2.50
	B	2.50	2.50	2.50	2.50	2.50	2.50	2.50	2.50	2.50	2.50	2.50	2.50
50, 60, 70	I	1.50	1.50	1.50	1.50	1.50	1.50	1.50	1.50	1.50	1.50	1.50	1.50
	B	1.50	1.50	1.50	1.50	1.50	1.50	1.50	1.50	1.50	1.50	1.50	1.50
80, 110, 120, 140	I	2.50	2.50	2.50	2.50	2.50	2.50	2.50	2.50	2.50	2.50	2.50	2.50
	B	2.50	2.50	2.50	2.50	2.50	2.50	2.50	2.50	2.50	2.50	2.50	2.50
90, 100	I	2.50	2.50	2.50	2.50	2.50	2.50	2.50	2.50	2.50	2.50	2.50	2.50
	B	2.50	2.50	2.50	2.50	2.50	2.50	2.50	2.50	2.50	2.50	2.50	2.50
160, 170, 175	I	2.50	2.50	2.50	2.50	2.50	2.50	2.50	2.50	2.50	2.50	2.50	2.50
	B	2.50	2.50	2.50	2.50	2.50	2.50	2.50	2.50	2.50	2.50	2.50	2.50
180, 190, 200, 220	I	2.50	2.50	2.50	2.50	2.50	2.50	2.50	2.50	2.50	2.50	2.50	2.50
	B	2.50	2.50	2.50	2.50	2.50	2.50	2.50	2.50	2.50	2.50	2.50	2.50
235, 240, 250, 260, 270, 280, 290, 300 310, 320	I	12.0	12.0	9.0	9.0	9.0	6.0	6.0	6.0	6.0	9.0	12.0	12.0
	B	8.0	8.0	6.0	6.0	6.0	4.0	4.0	4.0	4.0	6.0	8.0	8.0
ALL COASTAL AREAS	I	2.50	2.50	2.50	2.50	2.50	2.50	2.50	2.50	2.50	2.50	2.50	2.50
	B	2.50	2.50	2.50	2.50	2.50	2.50	2.50	2.50	2.50	2.50	2.50	2.50
230, 330, 340	I	2.50	2.50	2.50	2.50	2.50	2.50	2.50	2.50	2.50	2.50	2.50	2.50
	B	2.50	2.50	2.50	2.50	2.50	2.50	2.50	2.50	2.50	2.50	2.50	2.50

* I = INTERFLOW
B = BASEFLOW

Table 25
GOODNESS-OF-FIT STATISTICS FOR DAILY LOAD SIMULATIONS (LBS/DAY):
SUSQUEHANNA RIVER AT HARRISBURG, PA (USGS Gage #01570500: 24,100 sq mi)

CONSTITUENT/PERIOD	DATASET LIMITS		N SIM	N OBS	DISTRIBUTION	K-S DISTRIBUTION TEST		WILCOXON RANK SUM TEST LEVEL OF SIGNIFICANCE
						LEVEL OF SIGNIFICANCE		
						TWO-SIDED	SIMULATED OBSERVED	
TOTAL P								
1974-75	March-October		490	39	N/A	0.39	N/A	0.36
1976-78	March-October		735	55	N/A	0.51	N/A	0.54
1974-78	March-October		1,225	94	N/A	0.33	N/A	0.28
TOTAL N								
1974-75	Entire Period		730	52	N/A	0.61	N/A	0.41
1976-78	Entire Period		1,096	55	N/A	0.91	N/A	0.99
1974-78	Entire Period		1,826	107	N/A	0.51	N/A	0.55
NITRITE + NITRATE-N								
1974-75	March-October		490	39	N/A	0.59	N/A	0.50
1976-78	March-October		735	54	N/A	0.59	N/A	0.93
1974-78	March-October		1,225	93	N/A	0.50	N/A	0.67
TKN								
1974-75	Entire Period		730	52	N/A	0.89	N/A	0.81
1976-78	Entire Period		1,096	56	N/A	0.37	N/A	0.41
1974-78	Entire Period		1,826	108	N/A	0.74	N/A	0.32
ORGANIC N								
1974-75	Entire Period		730	51	N/A	0.69	N/A	0.51
1976-78	Entire Period		1,096	52	N/A	0.35	N/A	0.38
1974-78	Entire Period		1,826	103	N/A	0.91	N/A	0.87
AMMONIA-N								
1974-75	March-October		490	38	N/A	0.37	N/A	0.15
1976-78	March-October		735	52	N/A	0.81	N/A	0.99
1974-78	March-October		1,225	90	N/A	0.21	N/A	0.33
FLOW								
1974-75	Entire Period		730	52	N/A	0.37	N/A	0.22
1976-78	Entire Period		1,096	67	N/A	0.30	N/A	0.99
1974-78	Entire Period		1,826	119	N/A	0.27	N/A	0.40
FLOW								
1974-75	March-October		490	39	N/A	0.55	N/A	0.40
1976-78	March-October		735	55	Lognormal	*	*	0.65
1974-78	March-October		1,225	94	Lognormal	*	*	0.84

*Level of significance is less than 0.05

Table 26
GOODNESS-OF-FIT STATISTICS FOR DAILY LOAD SIMULATIONS (LBS/DAY):
SUSQUEHANNA RIVER AT DANVILLE, PA (USGS Gage #01540500: 11,220 sq mi)

CONSTITUENT/PERIOD	DATASET LIMITS	N SIM	N OBS	K-S DISTRIBUTION TEST		WILCOXON RANK SUM TEST LEVEL OF SIGNIFICANCE
				DISTRIBUTION	LEVEL OF SIGNIFICANCE	
					TWO-SIDED SIMULATED OBSERVED	
TOTAL P						
1974-75	March-October (W.Q. Sample Days)	34	34	N/A	N/A	0.10
1976-78	March-October (W.Q. Sample Days)	50	50	Lognormal	0.05	0.34
1974-78	March-October (W.Q. Sample Days)	84	84	Lognormal	*	0.08
TOTAL N						
1974-75	Entire Period (W.Q. Sample Days)	47	47	N/A	N/A	0.87
1976-78	Entire Period	1,096	57	N/A	N/A	0.61
1974-78	Entire Period	1,826	104	N/A	N/A	0.85
NITRITE + NITRATE-N						
1974-75	Entire Period	730	47	N/A	N/A	0.47
1976-78	Entire Period	1,096	60	N/A	N/A	0.86
1974-78	Entire Period	1,826	107	N/A	N/A	0.51
TKN						
1974-75	Entire Period (W.Q. Sample Days)	22	22	N/A	N/A	0.77
1976-78	Entire Period (W.Q. Sample Days)	147	147	N/A	N/A	0.55
1974-78	Entire Period (W.Q. Sample Days)	169	169	N/A	N/A	0.88
AMMONIA-N						
1974-75	March-October (W.Q. Sample Days)	32	32	N/A	N/A	0.22
1976-78	Entire Period (W.Q. Sample Days)	57	57	N/A	N/A	0.69
1974-78	March-October (W.Q. Sample Days)	79	79	N/A	N/A	0.37
FLOW						
1974-75	Entire Period (W.Q. Sample Days)	47	47	N/A	N/A	0.82
1976-78	Entire Period (W.Q. Sample Days)	60	60	N/A	N/A	0.75
1974-78	Entire Period (W.Q. Sample Days)	107	107	N/A	N/A	0.76
FLOW						
1974-75	Entire Period	73	47	N/A	N/A	0.88
1976-78	Entire Period	1,096	60	N/A	N/A	0.49
1974-78	Entire Period	1,826	107	N/A	N/A	0.56
FLOW						
1974-75	March-October (W.Q. Sample Days)	34	34	N/A	N/A	0.96
1976-78	March-October (W.Q. Sample Days)	50	50	N/A	N/A	0.99
1974-78	March-October (W.Q. Sample Days)	84	84	Lognormal	N/A	0.87

*Level of significance is less than 0.05

Table 27

GOODNESS-OF-FIT STATISTICS FOR DAILY LOAD SIMULATIONS (LBS/DAY):
WEST BRANCH SUSQUEHANNA RIVER AT LEWISBURG, PA (USGS Gage #01553500: 6,847 sq mi)

CONSTITUENT/PERIOD	DATASET LIMITS	N		N OBS	DISTRIBUTION	K-S DISTRIBUTION TEST		WILCOXON RANK SUM TEST	
		SIM	OBS			LEVEL OF SIGNIFICANCE		OBSERVED	LEVEL OF SIGNIFICANCE
						TWO-SIDED	SIMULATED		
TOTAL P									
1974-75	Entire Period (W.Q. Sample Days)	15	15	15	N/A	>0.10	N/A	N/A	0.26
1976-78	Entire Period (W.Q. Sample Days)	30	30	30	N/A	0.42	N/A	N/A	0.19
1974-78	Entire Period (W.Q. Sample Days)	45	45	45	N/A	0.26	N/A	N/A	0.10
TOTAL N									
1974-75	Entire Period (W.Q. Sample Days)	15	15	15	N/A	>0.10	N/A	N/A	0.99
1976-78	Entire Period (W.Q. Sample Days)	27	27	27	N/A	0.63	N/A	N/A	0.99
1974-78	Entire Period (W.Q. Sample Days)	42	42	42	N/A	0.51	N/A	N/A	0.91
NITRITE + NITRATE-N									
1974-75	Entire Period	730	15	15	N/A	0.41	N/A	N/A	0.61
1976-78	Entire Period	1,096	30	30	N/A	0.89	N/A	N/A	0.67
1974-78	Entire Period	1,826	45	45	N/A	0.89	N/A	N/A	0.95
TKN									
1974-75	Entire Period (W.Q. Sample Days)	15	15	15	N/A	>0.10	N/A	N/A	0.43
1976-78	Entire Period (W.Q. Sample Days)	27	27	27	N/A	0.51	N/A	N/A	0.84
1974-78	Entire Period (W.Q. Sample Days)	42	42	42	N/A	0.71	N/A	N/A	0.82
AMMONIA-N									
1974-75	Entire Period (W.Q. Sample Days)	12	12	12	N/A	>0.11	N/A	N/A	0.94
1976-78	March-October	735	12	12	N/A	0.56	N/A	N/A	0.54
1974-78	Entire Period	1,826	28	28	N/A	0.90	N/A	N/A	0.72
FLOW									
1974-75	Entire Period (W.Q. Sample Days)	15	15	15	N/A	>0.18	N/A	N/A	0.21
1976-78	Entire Period (W.Q. Sample Days)	30	30	30	N/A	>0.20	N/A	N/A	0.45
1974-78	Entire Period (W.Q. Sample Days)	45	45	45	N/A	0.22	N/A	N/A	0.19
FLOW									
1974-75	Entire Period	730	15	15	N/A	0.51	N/A	N/A	0.39
1976-78	Entire Period	1,096	30	30	N/A	0.27	N/A	N/A	0.19
1974-78	Entire Period	1,826	45	45	N/A	0.28	N/A	N/A	0.12

*Level of significance is less than 0.05

Table 28

GOODNESS-OF-FIT STATISTICS FOR DAILY LOAD SIMULATIONS (LBS/DAY):
JUNIATA RIVER AT NEWPORT, PA (USGS Gage #01567000: 3,354 sq mi)

CONSTITUENT/PERIOD	DATASET LIMITS	N		OBS	DISTRIBUTION	K-S DISTRIBUTION TEST		WILCOXON RANK SUM TEST
		SIM	N			LEVEL OF SIGNIFICANCE		
						TWO-SIDED	SIMULATED	
TOTAL P								
1974-75	Entire Period (Flows greater than 1,500 cfs)	526	13		N/A	0.34	N/A	0.40
1976-78	Entire Period (Flows greater than 2,000 cfs)	732	19		N/A	0.73	N/A	0.57
1974-78	Entire Period (Flows greater than 2,000 cfs)	1,184	29		N/A	0.19	N/A	0.20
TOTAL N								
1974-75	Entire Period	730	11		N/A	0.58	N/A	0.64
1976-78	Entire Period (Flows greater than 2,000 cfs)	732	15		N/A	0.78	N/A	0.60
1974-78	Entire Period (Flows greater than 2,000 cfs)	1,184	22		N/A	0.59	N/A	0.88
NITRITE + NITRATE-N								
1974-75	Entire Period	730	14		N/A	0.50	N/A	0.74
1976-78	Entire Period (Flows greater than 2,000 cfs)	732	19		N/A	0.58	N/A	0.94
1974-78	Entire Period (Flows greater than 2,000 cfs)	1,184	29		N/A	0.58	N/A	0.99
TKN								
1974-75	Entire Period (Flows greater than 1,500 cfs)	526	10		N/A	0.39	N/A	0.14
1976-78	Entire Period (Flows greater than 2,500 cfs)	634	15		N/A	0.44	N/A	0.36
1974-78	Entire Period (Flows greater than 2,500 cfs)	1,013	21		N/A	0.11	N/A	0.08
AMMONIA-N								
1974-75	Entire Period	730	14		N/A	0.68	N/A	0.55
1976-78	Entire Period	1,096	22		N/A	0.48	N/A	0.33
1974-78	Entire Period	1,826	36		N/A	0.78	N/A	0.69
FLOW								
1974-75	Entire Period	730	14		N/A	0.15	N/A	0.13
1976-78	Entire Period	1,096	22		Lognormal	*	*	*
1974-78	Entire Period	1,826	36		Lognormal	*	>0.20	*
FLOW								
1974-75	Entire Period (Flows greater than 1,500 cfs)	526	13		N/A	0.48	N/A	0.82
1976-78	Entire Period (Flows greater than 2,000 cfs)	732	19		N/A	0.21	N/A	0.33
1976-78	Entire Period (Flows greater than 2,500 cfs)	634	18		N/A	0.61	N/A	0.68
1974-78	Entire Period (Flows greater than 2,000 cfs)	1,184	29		N/A	0.14	N/A	0.15
1974-78	Entire Period (Flows greater than 2,500 cfs)	1,013	27		N/A	0.59	N/A	0.40

*Level of significance is less than 0.05

Table 29

GOODNESS-OF-FIT STATISTICS FOR DAILY LOAD SIMULATIONS (LBS/DAY):
POTOMAC RIVER AT POINT OF ROCKS, MD (USGS Gage #01638500: 9,651 sq mi)

CONSTITUENT/PERIOD	DATASET LIMITS	N SIM	N OBS	K-S DISTRIBUTION TEST		WILCOXON RANK SUM TEST	
				DISTRIBUTION	LEVEL OF SIGNIFICANCE	LEVEL OF SIGNIFICANCE	
TOTAL P							
1974-75	Entire Period (W.Q. Sample Days)	16	16	N/A	N/A	N/A	0.13
1976-78	March-October (W.Q. Sample Days)	19	19	N/A	N/A	N/A	0.99
1974-78	Entire Period (W.Q. Sample Days)	42	42	N/A	N/A	N/A	0.99
NITRITE + NITRATE-N							
1974-75	Entire Period	730	16	N/A	N/A	N/A	0.59
1976-78	Entire Period (W.Q. Sample Days)	26	26	N/A	0.20	0.10	0.16
1974-78	Entire Period (W.Q. Sample Days)	42	42	N/A	0.23	0.20	0.27
FLOW							
1974-75	Entire Period	730	16	N/A	0.63	N/A	0.81
1974-75	Entire Period (W.Q. Sample Days)	16	16	N/A	>0.21	N/A	0.99
1976-78	March-October (W.Q. Sample Days)	19	19	N/A	>0.20	N/A	0.79
1974-78	Entire Period (W.Q. Sample Days)	42	42	N/A	>0.79	N/A	0.74

*Level of significance is less than 0.05

Table 30

GOODNESS-OF-FIT STATISTICS FOR DAILY LOAD SIMULATIONS (LBS/DAY):
POTOMAC RIVER AT CHAIN BRIDGE (USGS Gage #01646580: 11,570 sq mi)

CONSTITUENT/PERIOD	DATASET LIMITS	N		DISTRIBUTION	K-S-DISTRIBUTION TEST		WILCOXON RANK SUM TEST	
		SIM	OBS		LEVEL OF SIGNIFICANCE		LEVEL OF SIGNIFICANCE	
					TWO-SIDED	SIMULATED	OBSERVED	
TOTAL P								
1974-75	Entire Period	730	22	N/A	0.95	N/A	N/A	0.62
1976-78	March-October	735	117	N/A	0.06	N/A	N/A	0.83
1974-78	March-October	1,225	133	N/A	0.42	N/A	N/A	0.87
TOTAL N								
1974-75	Entire Period (W.Q. Sample Days)	22	22	N/A	>0.20	N/A	N/A	0.84
1976-78	Entire Period (W.Q. Sample Days)	38	38	N/A	0.90	N/A	N/A	0.61
1974-78	Entire Period (W.Q. Sample Days)	60	60	N/A	0.98	N/A	N/A	0.80
NITRITE + NITRATE-N								
1974-75	Entire Period (W.Q. Sample Days)	22	22	N/A	>0.20	N/A	N/A	0.45
1976-78	Entire Period (W.Q. Sample Days)	43	43	Lognormal	*	0.10	0.05	0.32
1974-78	Entire Period (W.Q. Sample Days)	65	65	N/A	0.06	N/A	N/A	0.30
TKN								
1974-75	Entire Period (W.Q. Sample Days)	22	22	Lognormal	0.10	N/A	N/A	0.27
1976-78	Entire Period (W.Q. Sample Days)	147	147	Lognormal	0.07	N/A	N/A	0.16
1974-78	Entire Period (W.Q. Sample Days)	169	169	Lognormal	*	0.05	*	0.09
FLOW								
1974-75	Entire Period	730	22	N/A	0.99	N/A	N/A	0.97
1976-78	March-October	117	117	Lognormal	*	0.10	0.20	0.94
1974-78	March-October	1,225	13	N/A	0.21	N/A	N/A	0.05
FLOW								
1974-75	Entire Period (W.Q. Sample Day: Total P)	22	22	N/A	>0.20	N/A	N/A	0.73
1976-78	Entire Period (W.Q. Sample Day: Total P)	152	152	N/A	0.90	N/A	N/A	0.62
1974-78	Entire Period (W.Q. Sample Day: Total P)	174	174	N/A	0.93	N/A	N/A	0.73
FLOW								
1974-75	Entire Period (W.Q. Sample Day: Nitrate-N)	22	22	N/A	>0.20	N/A	N/A	0.73
1976-78	Entire Period (W.Q. Sample Day: Nitrate-N)	43	43	N/A	>0.99	N/A	N/A	0.88
1974-78	Entire Period (W.Q. Sample Day: Nitrate-N)	65	65	N/A	>0.99	N/A	N/A	0.75

*Level of significance is less than 0.05

Table 31

GOODNESS-OF-FIT STATISTICS FOR DAILY LOAD SIMULATIONS (LBS/DAY):
JAMES RIVER AT CARTERSVILLE, VA (USGS Gage #02035000: 6,257 sq mi)

CONSTITUENT/PERIOD	DATASET LIMITS	N		N OBS	DISTRIBUTION	K-S DISTRIBUTION TEST			WILCOXON RANK SUM TEST
		SIM	OBS			LEVEL OF SIGNIFICANCE			
						TWO-SIDED	SIMULATED	OBSERVED	
TOTAL P									
1974-75	March-October (W.Q. Sample Days)	30	30	30	Lognormal	N/A	*	0.2	0.11
1976-78	March-October (W.Q. Sample Days)	46	46	46	Lognormal	N/A	*	*	*
1974-78	March-October (W.Q. Sample Days)	76	76	76	Lognormal	N/A	*	0.05	*
TOTAL N									
1974-75	Entire Period (W.Q. Sample Days)	43	43	43	N/A	0.79	N/A	N/A	0.22
1976-78	Entire Period (W.Q. Sample Days)	67	67	67	N/A	0.95	N/A	N/A	0.63
1974-78	Entire Period (W.Q. Sample Days)	110	110	110	N/A	0.93	N/A	N/A	0.76
NITRITE + NITRATE-N									
1974-75	Entire Period (W.Q. Sample Days)	43	43	43	N/A	0.07	N/A	N/A	0.07
1976-78	Entire Period (W.Q. Sample Days)	67	67	67	N/A	0.58	N/A	N/A	0.79
1974-78	Entire Period (W.Q. Sample Days)	110	110	110	N/A	0.16	N/A	N/A	0.18
TKN									
1974-75	March-October	30	30	30	N/A	0.88	N/A	N/A	0.81
1976-78	March-October	46	46	46	N/A	0.66	N/A	N/A	0.47
1974-78	March-October	76	76	76	N/A	0.47	N/A	N/A	0.49
FLOW									
1974-75	Entire Period (W.Q. Sample Days)	43	43	43	N/A	0.43	N/A	N/A	0.24
1976-78	Entire Period (W.Q. Sample Days)	67	67	67	N/A	0.95	N/A	N/A	0.68
1974-78	Entire Period (W.Q. Sample Days)	110	110	110	N/A	0.93	N/A	N/A	0.68
FLOW									
1974-75	March-October (W.Q. Sample Days)	30	30	30	N/A	>0.20	N/A	N/A	0.66
1976-78	March-October (W.Q. Sample Days)	46	46	46	N/A	0.99	N/A	N/A	0.78
1974-78	March-October (W.Q. Sample Days)	76	76	76	N/A	0.99	N/A	N/A	0.92
FLOW									
1974-75	March-October	490	32	32	N/A	0.24	N/A	N/A	0.31
1976-78	March-October	735	46	46	N/A	0.93	N/A	N/A	0.95
1974-78	March-October	1,225	78	78	N/A	0.11	N/A	N/A	0.46

*Level of significance is less than 0.05

opportunity to test the reliability of the fall line loading comparisons in Figures 31 through 84 and Tables 18 through 20; and (2) For the Susquehanna and Potomac river basins, the USGS gaging data for 1974-1978 permits assessments of goodness-of-fit at upstream locations in the river basin.

Recorded daily loads were based upon the product of the mean daily flow and instantaneous concentration (i.e., grab sample) reported for each USGS gage. Simulated daily loads were based upon the sum of hourly loads calculated from the product of simulated hourly streamflows and hourly concentrations. Therefore, in addition to error associated with gaging measurements, some of the difference between simulated and recorded daily loads can be attributed to the use of an instantaneous concentration for the recorded dataset and to errors in streamflow simulations.

Comparisons of simulated and recorded daily loads were based upon the following simulated datasets:

- #1: Entire Period (January through October of each year)
- #2: March-October
- #3: Entire Period (Water Quality Sampling Days Only)
- #4: March-October (Water Quality Sampling Days Only)

Comparisons based upon simulated datasets #1 and #2 are felt to be the most rigorous, since they involve comparing simulated loadings on each day of the period (e.g., 1974-1975; 1976-1978; 1974-1978) with recorded loadings on sampling days. In other words, due to the relatively low water quality sampling frequency during 1974-1978, evaluations based on simulated datasets #1 and #2 involved comparing a relatively small number of recorded values with a relatively large number of simulated values. The assumption made for goodness-of-fit assessments based on datasets #1 and #2 is the same one used to support most monitoring programs--statistics associated with recorded data collected on a weekly or biweekly basis is assumed to be representative of long-term statistics. Goodness-of-fit comparisons based upon simulated datasets #3 and #4 involved matching recorded data with simulated values on each sampling day. In general, goodness-of-fit statistics based upon simulated datasets #3 and #4 were higher than statistics based upon simulated datasets #1 and #2. Likewise, because they represented a little more than two seasons rather than four, goodness-of-fit statistics based upon the March-October period (datasets #2 and #4) were typically higher than statistics based upon the entire period (datasets #1 and #3). In the goodness-of-fit tables that follow, results for only one simulated dataset are reported. The selection of the simulated dataset which is reported in the goodness-of-fit tables is based upon the hierarchy shown above, with the most rigorous evaluations based upon dataset #1 and the least rigorous (but still acceptable) evaluations based upon dataset #2. That is, dataset #1 is considered first, followed by #2, #3, and #4 in that order until a satisfactory goodness-of-fit statistic is obtained. Since the first simulated dataset producing satisfactory statistics is reported, different simulated datasets are sometimes reported for different constituents. It should be noted that, since the Basin Model is intended for simulations of

the period March through October, the comparisons based upon simulated datasets for the "Entire Period" (January-December) are probably excessively rigorous. Likewise, since the calibration and verification periods were treated separately, goodness-of-fit statistics for the 1974-1978 period are not as important as statistics for the other two periods.

Box-and-whisker plots were developed for the simulated and recorded datasets for graphical assessments of goodness-of-fit. Figures 85 through 91 present sample box-and-whisker plots for streamflow and P and N loads at the Susquehanna River gage at Harrisburg. As may be seen, separate plots are presented for the calibration (1974-1975) and verification (1976-1978) periods and for the two periods combined (1974-1978). The simulated datasets in these figures are based upon the Entire Period (dataset #1), while the recorded dataset is based upon the same period. Based upon an inspection of these figures, there appears to be good agreement between simulated and recorded datasets for all three periods for all constituents.

Nonparametric statistical tests were used to quantify goodness-of-fit for the daily loading comparisons at each gage. Tables 25 through 31 present the goodness-of-fit statistics for the seven gages. The entries in the "Dataset Limits" column indicates the simulated (i.e., #1, #2, #3, or #4) and recorded datasets used for goodness-of-fit assessments. In other words, if simulated dataset #2 was used to derive the statistics reported in the table, "March-October" appears in the Dataset Limits column and both simulated and recorded data were restricted to March through October of the indicated years. In cases where a satisfactory level of significance was obtained from the two-sided K-S test, the value is reported in the column labeled "Two-Sided." In cases where the two-sided K-S test produced a level of significance less than 0.05, one-sided K-S tests were performed on both the simulated and recorded datasets to determine whether they both exhibited a lognormal distribution, with the resulting level of significance values reported in the "Simulated" and "Observed" columns. The one-sided K-S statistic is reported in cases where graphical comparisons of simulated and recorded distributions indicated similar distributions, but outliers in the datasets resulted in a relatively low level of significance for the two-sided K-S test. In cases where both the simulated and recorded datasets are shown to be characterized by lognormal distributions, the Wilcoxon Rank Sum test may be used to evaluate whether there is a significant difference between the two datasets assuming that their variances are approximately similar.

Based on a 0.05 probability cutoff for the 95% confidence interval, the level of significance statistics in Tables 25 through 31 indicate that there is typically no significant difference between simulated and recorded daily values for all three periods. Only total P at the James River gage exhibits an unacceptable agreement between simulated and recorded daily values. Potential sources of error in the simulation of total P concentrations on sampling days at the James River at Cartersville gage are presented below. In summary, the acceptable level of significance values in Tables 25-31 are further evidence of the reliability of the earlier comparisons based upon

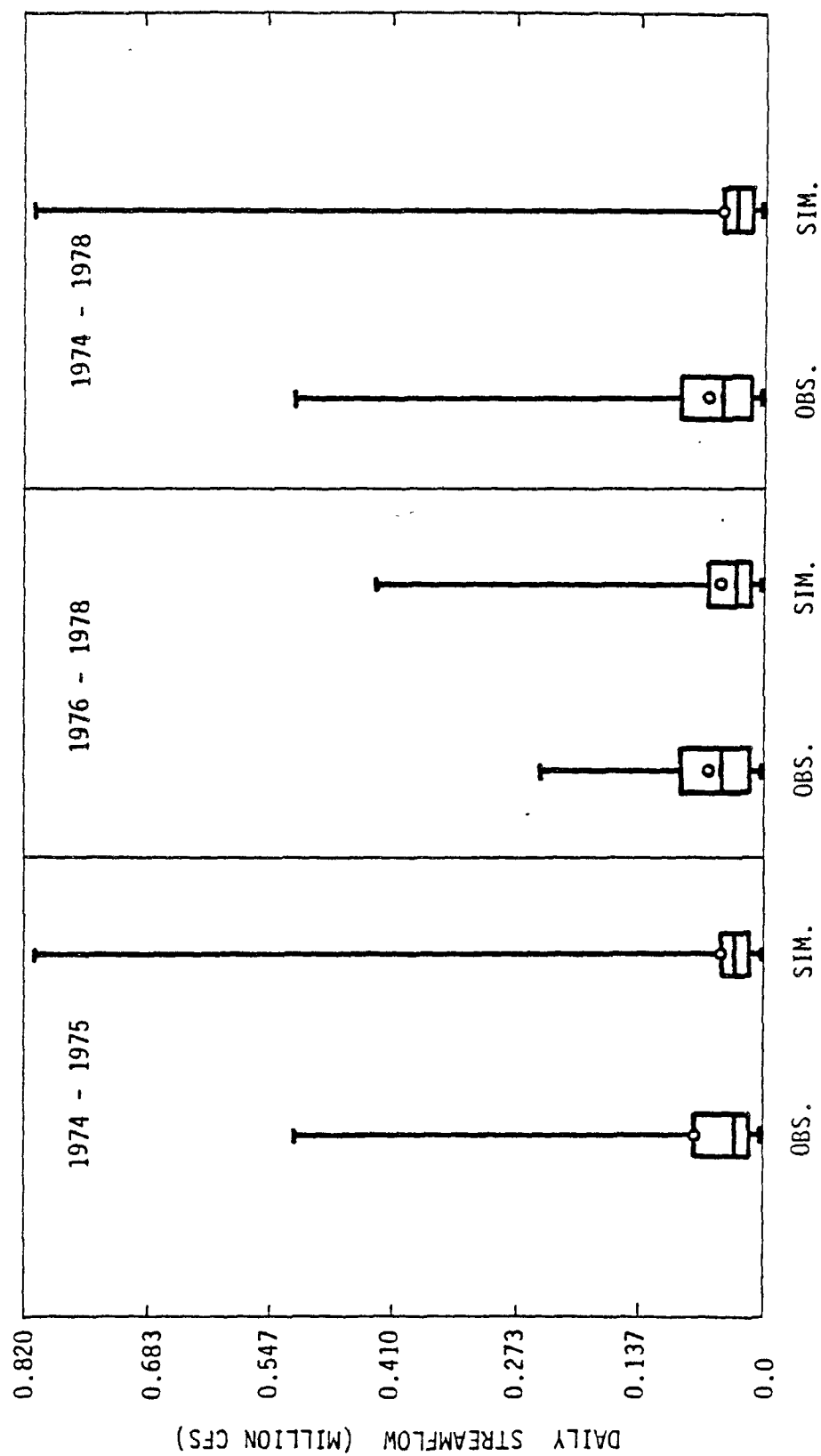


Figure 85. Comparisons of Simulated (SIM) and Observed (OBS) Box and Whisker Plots for Susquehanna River at Harrisburg, PA Gage: Daily Streamflow

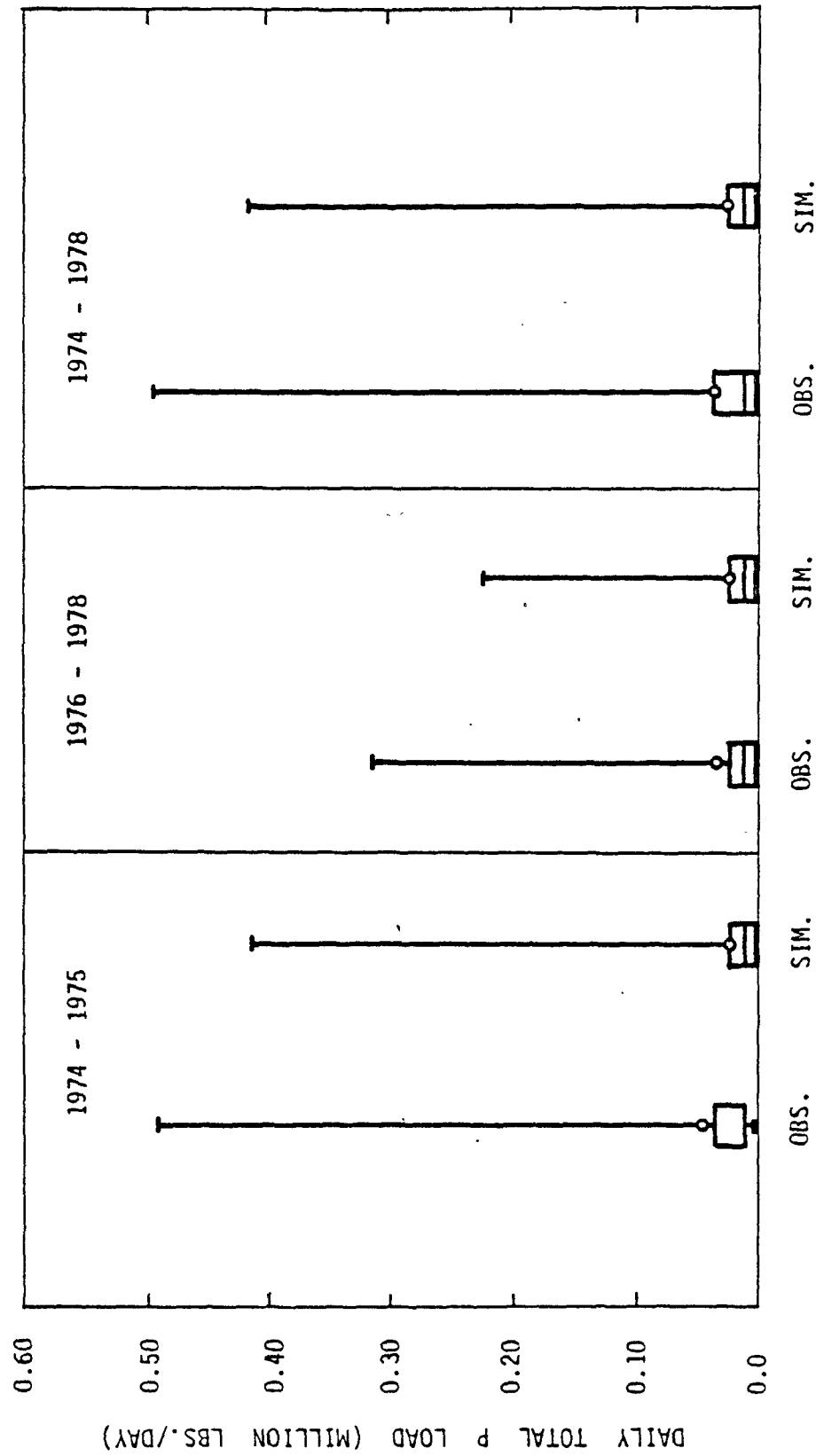


Figure 86. Comparisons of Simulated (SIM) and Observed (OBS) Box and Whisker Plots for Susquehanna River at Harrisburg, PA Gage: Daily Total P Load

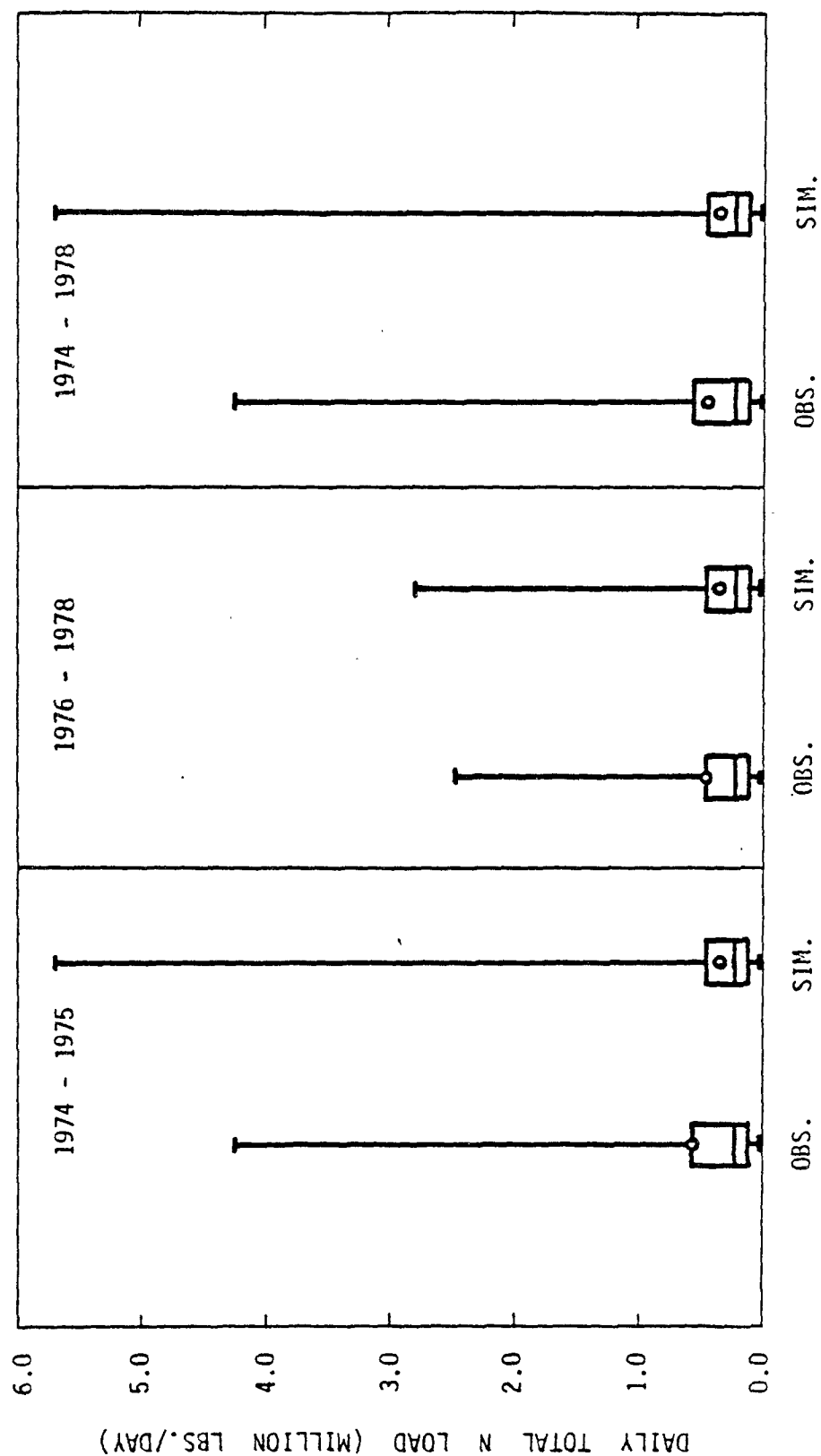


Figure 87. Comparisons of Simulated (SIM) and Observed (OBS) Box and Whisker Plots for Susquehanna River at Harrisburg, PA Gage: Daily Total N Load

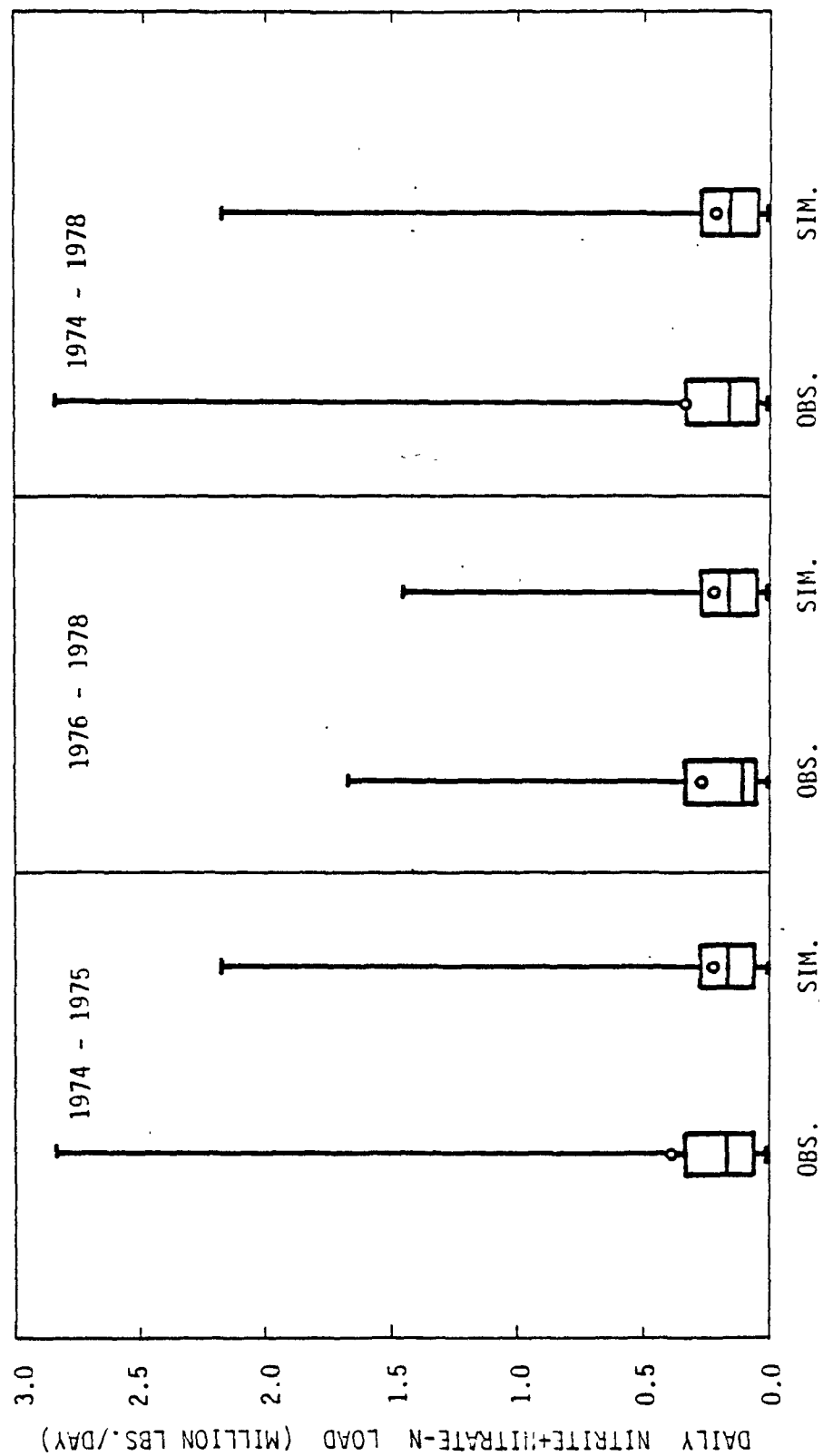


Figure 88. Comparisons of Simulated (SIM) and Observed (OBS) Box and Whisker Plots for Susquehanna River at Harrisburg, PA Gage: Daily Nitrite + Nitrate-N Load

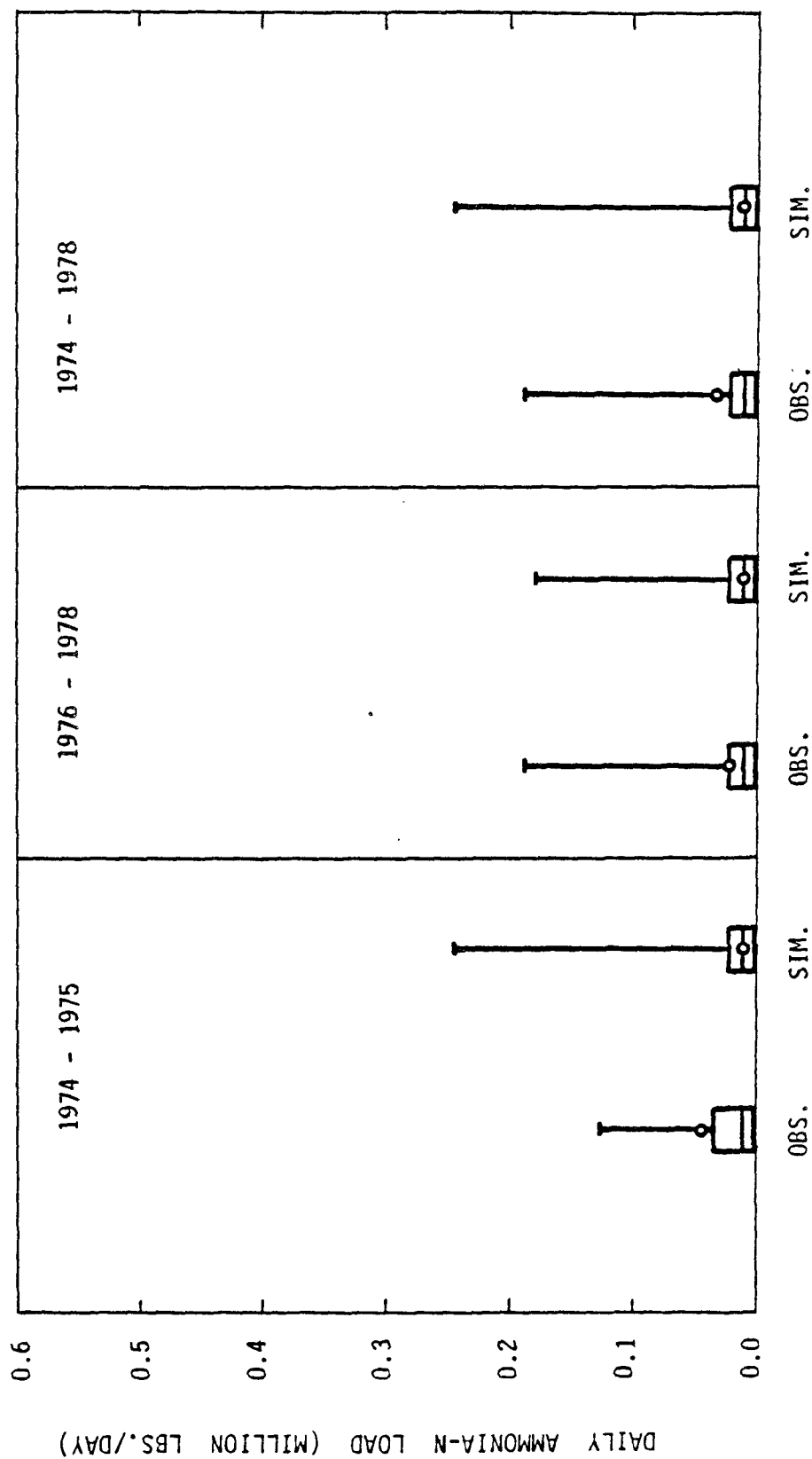


Figure 89. Comparisons of Simulated (SIM) and Observed (OBS) Box and Whisker Plots for Susquehanna River at Harrisburg, PA Gage: Daily Ammonia-N Load

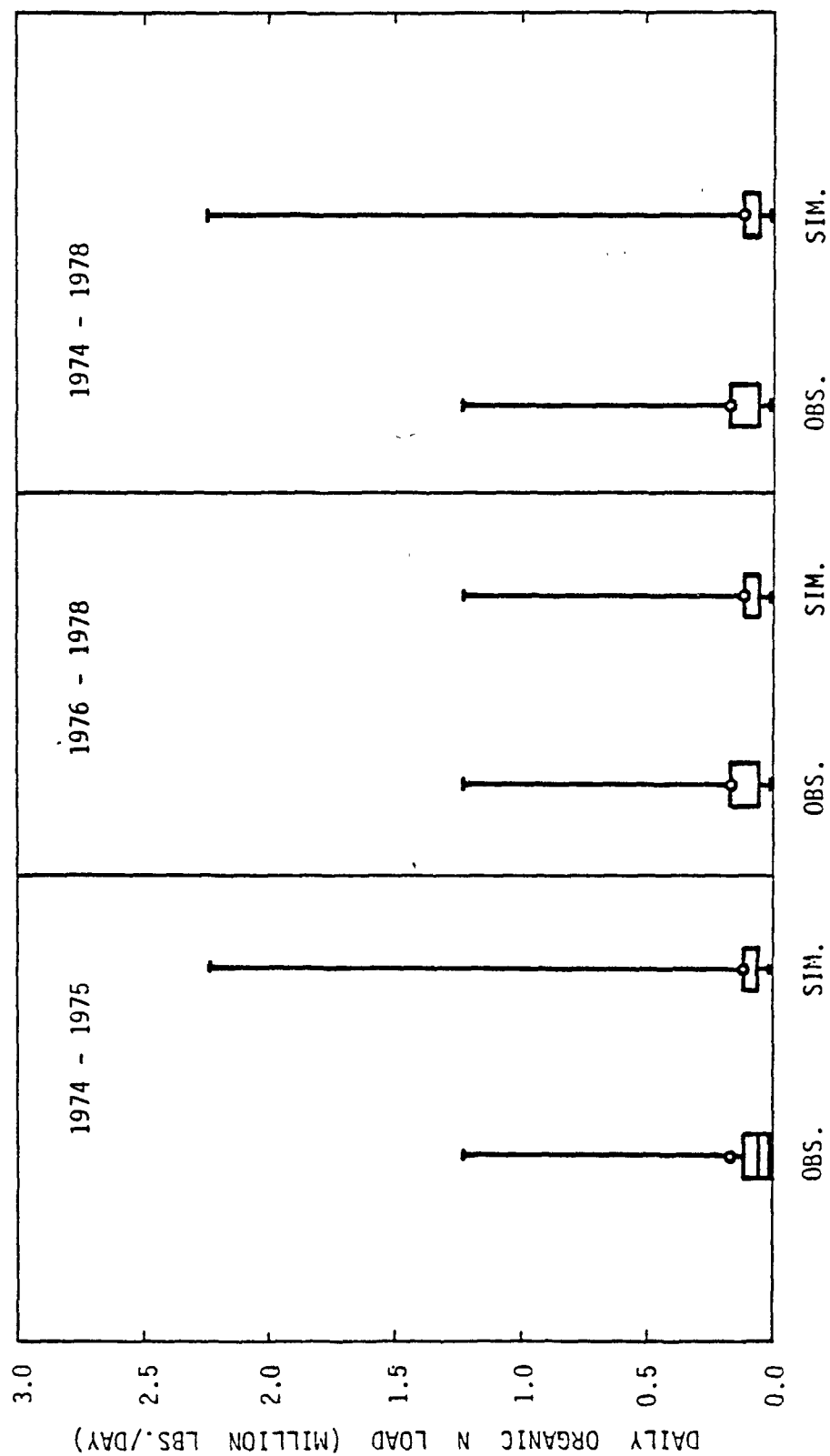


Figure 90. Comparisons of Simulated (SIM) and Observed (OBS) Box and Whisker Plots for Susquehanna River at Harrisburg, PA Gage: Daily Organic-N Load

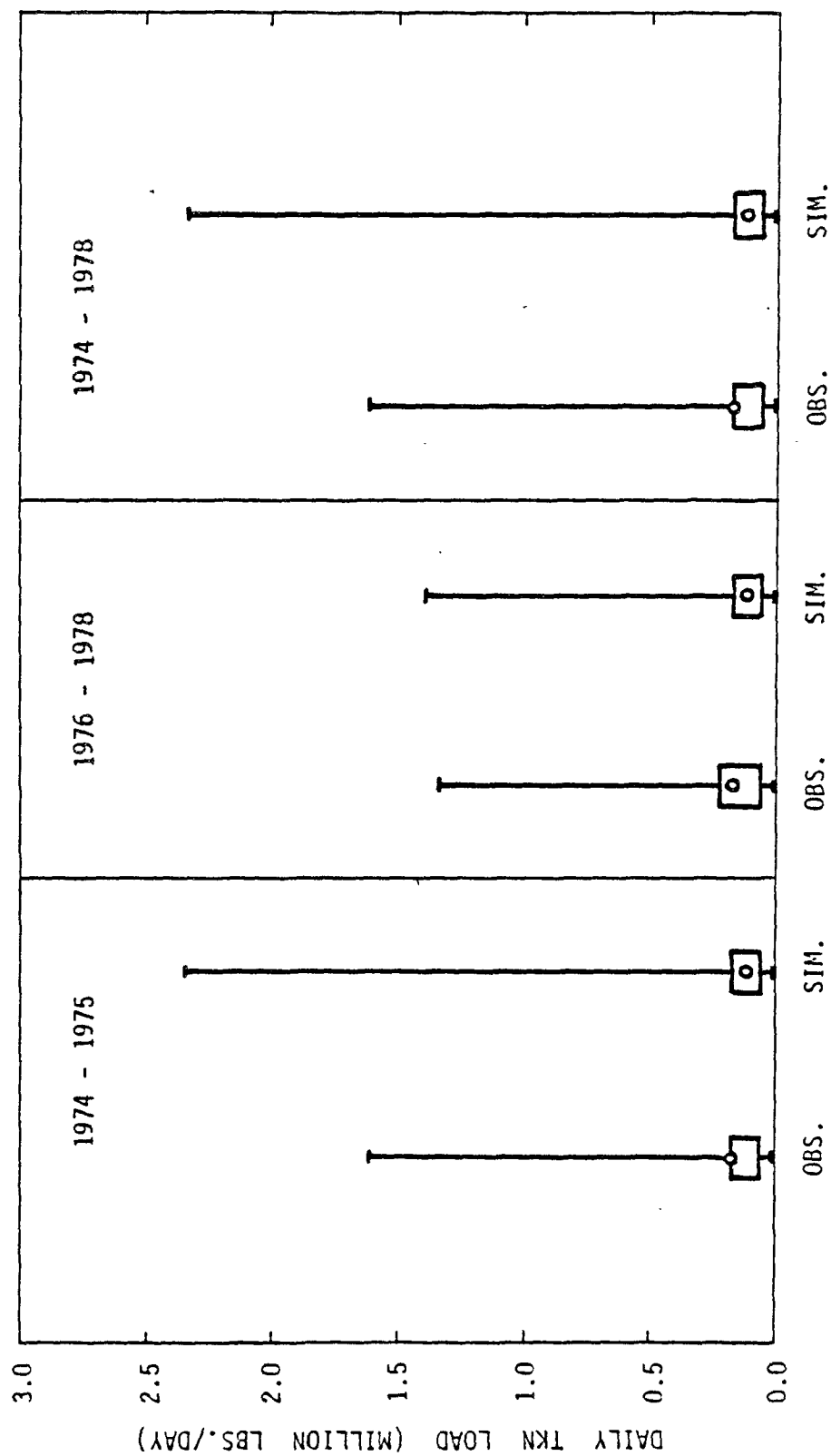


Figure 91. Comparisons of Simulated (SIM) and Observed (OBS) Box and Whisker Plots for Susquehanna River at Harrisburg, PA Gage: Daily TKN Load

fall line loading relationships and of the Basin Model's ability to represent important pollutant loading/transport processes in the major river basins.

It is felt that the poor fit of simulated and recorded total P concentrations for the James River at Cartersville gage can be attributed in large part to errors in the wastewater treatment plant discharge data (i.e., municipal and industrial) used for the 1974-1978 simulations. During the calibration study of the James River Basin, the wastewater discharge files were changed three times by EPA/CBP staff in response to inquiries by NVPDC staff based upon poor agreement between simulated and recorded concentration data. Sensitivity study runs with the calibrated James River parameter set revealed that the deletion of all nonpoint pollution loadings (i.e., surface runoff plus baseflow/interflow) resulted in only 10%-20% reductions in the simulated mean concentration of total P and inorganic P for the calibration and verification periods. This indicates that the assumed wastewater discharges are the most significant contributors to simulated concentrations for the majority of the calibration/verification period, and therefore that errors in the discharge records can have a very significant impact on comparisons of simulated and recorded concentrations. As indicated below, a comparison of recorded concentrations for 1974-78 (calibration/verification period) and 1979-80 (USGS fall line monitoring study) indicates that the latter period exhibited higher mean total P and inorganic P concentrations even though the mean streamflows were on the order of 30%-90% higher than those encountered during the earlier period.

PERIOD	RECORDED TOTAL P		RECORDED INORGANIC P	
	N	MEAN	N	MEAN
March-Oct., 1974-78	69	0.086 mg/L	19	0.022 mg/L
1979-80	47	0.12 mg/L	39	0.05 mg/L

The much higher inorganic P concentration for 1979-80 is particularly suggestive of different wastewater discharge contributions, since the majority of nonpoint pollution loadings of phosphorus are in the organic form. The simulated mean total P concentration for 1974-1978 is in good agreement with the recorded mean for 1979-80, while the simulated inorganic P value exhibits much better agreement with the 1979-80 mean than with the 1974-78 mean. Given the significant differences between recorded mean concentrations for 1974-78 and 1979-80 and the relative insignificance of nonpoint pollution loadings on simulated means, more extensive checks of the wastewater discharge records assumed for 1974-78 are required before any conclusions can be reached regarding goodness-of-fit of total P concentrations for the calibration/verification period. In the absence of further checks of the wastewater discharge files, it can be stated that goodness-of-fit assessments based upon the USGS fall line loading relationships indicate that total P loads from the James River Basin are satisfactorily simulated on an annual, monthly, and daily basis.

Since the main stem reservoirs near the mouth of the Susquehanna River were found to have a significant impact on the delivery of point source loadings to Chesapeake Bay, agreement between simulated and recorded data was checked for Conowingo Reservoir which is the largest of the three major reservoirs and the one with the most extensive database. Table 32 summarizes simulated and recorded means and medians for Conowingo Reservoir for the period 1974 through 1978. The simulated means are based upon each day of the five-year period, as indicated by the relatively high N's reported in the table. As may be seen, simulated and recorded values are typically within approximately $\pm 20\%$ for phosphorus, nitrogen, and chlorophyll-a. The satisfactory agreement between simulated and recorded chlorophyll-a is particularly encouraging, in light of subsequent model production runs that indicate that chlorophyll-a levels in the lower Susquehanna Reservoirs are one of the controlling factors for upstream point sources. For example, production runs that examined the impacts of a reduction in wastewater discharges of phosphorus indicated that the resulting reduction in chlorophyll-a within the lower Susquehanna Reservoirs would pass higher loadings of dissolved nitrogen through the reservoirs into the upper Chesapeake Bay. While this response seemed nonintuitive at first, further study revealed that the higher nitrogen loadings could be attributed to the reduction in chlorophyll-a concentrations which reduced nitrogen uptake conversion to suspended organic forms which could be removed within the reservoirs. Similar trends have been noted in the upper Potomac Estuary where reductions in wastewater discharges of phosphorus have reduced chlorophyll-a levels, thereby resulting in the delivery of higher dissolved nitrogen levels to downstream reaches. The relatively good agreement between simulated and recorded chlorophyll-a concentrations for the calibration period, particularly the fact that the model typically undersimulates rather than oversimulates chlorophyll-a in Conowingo Reservoir, indicates that the Basin Model should provide a relatively accurate characterization of secondary impacts of management strategies that affect algal growth in the lower Susquehanna Reservoir system. Nonetheless, since chlorophyll-a levels in these reservoirs appear to have a significant impact on nutrient delivery to upper Chesapeake Bay, field studies of existing eutrophication levels (e.g., follow-up studies related to 43) and relationships to long-term pollutant trap efficiency might be considered for future funding.

EPA/CBP did not supply any recorded chlorophyll-a data for comparison with simulated data for the Potomac River and James River fall lines. However, a general assessment of chlorophyll-a simulations for the Potomac River fall line can be based on the boundary conditions used for previous modeling studies of the upper Potomac Estuary by the Metropolitan Washington Council of Governments (44). Based upon analyses of recorded data and Potomac Estuary Model calibration studies for periods of relatively low streamflow, a mean chlorophyll-a concentration of 25 ug/L is used as the boundary condition for the Potomac River fall line. By comparison, the simulated mean concentration of chlorophyll-a at the Potomac River fall line for the calibration/verification period (1974-78) is approximately 16 ug/L. By raising the chlorophyll-a/algal phosphorus ratio by a relatively small

Table 32

COMPARISON OF SIMULATED AND OBSERVED CONCENTRATIONS
FOR CONOWINGO RESERVOIR:
1/1/74 - 12/31/78

<u>Parameter</u>	<u>Sim Mean</u>	<u>Sim S.D.</u>	<u>Sim N</u>	<u>OBS Mean</u>	<u>OBS S.D.</u>	<u>OBS N</u>	<u>Sim Mean OBS Mean</u>
TP	0.058	0.030	43,824	0.075	0.066	67	0.77
TN	1.250	0.361	43,824	--	--	--	--
BOD ₂₀	3.341	2.733	43,824	--	--	--	--
DO	11.156	2.577	43,824	9.4	3.3	68	1.18
NH ₃	0.063	0.043	43,824	--	--	--	--
NO ₃	0.939	0.268	43,824	0.775	0.469	67	1.21
ORG. N	0.247	0.165	43,824	--	--	--	--
ORG. P	0.035	0.023	43,824	--	--	--	--
PO ₄	0.023	0.016	43,824	0.026	0.039	46	0.88
Chla	11.841	4.6	43,824	14.82	12.64	70	0.80

<u>Parameter</u>	<u>Sim Median</u>	<u>Sim MAX</u>	<u>Sim Min</u>	<u>OBS Median</u>	<u>OBS MAX</u>	<u>OBS Min</u>	<u>Sim Median OBS Median</u>
TP	0.045	0.342	0.029	0.059	0.400	0	0.76
TN	1.25	4.203	0.522	--	--	--	--
BOD	2.50	29.786	0.354	--	--	--	--
DO	11.00	15.888	4.225	9.6	15.2	1.0	1.14
NH ₃	0.060	0.386	0.005	--	--	--	--
NO ₃	0.95	2.067	0.286	0.70	2.482	0	1.36
ORG. N	0.20	1.774	0.032	--	--	--	--
ORG. P	0.03	0.253	0.005	--	--	--	--
PO ₄	0.020	0.183	0.010	0.010	0.230	0	2.00
Chla	10.00	46.906	2.198	10.80	52.87	0.80	0.93

percentage, the simulated mean chlorophyll-a levels for the Potomac River fall line could be increased to more closely agree with the uptake of nitrogen and phosphorus in the Potomac River. Since the simulated mean chlorophyll-a concentraton is in the same ballpark and less than the upper Potomac Estuary boundary condition, it appears that the Basin Model should provide a reasonably good representation of management strategies which will affect chlorophyll-a levels in the prototype.

CHAPTER VI

FRAMEWORK FOR MANAGEMENT STUDIES

Introduction

Following the calibration/verification of the Basin Model, it was used for production runs to assess the impact of alternate management strategies on pollutant loadings delivered to the bay system. This chapter covers the periods selected for the management studies, the interpretation of model output, and a discussion of typical production runs for which the model can be used.

A detailed summary of actual production run results is beyond the scope of this report. Several management study runs were performed to generate loading data for input to the stand-alone models of the Bay's estuarine system. Time series output files for these management studies have previously been transmitted to the Virginia Institute of Marine Science (VIMS) for input to the receiving water models of the Bay system. In addition, tabulations of simulated fall line data on seasonal loadings and concentration-frequency relationships have been transmitted to EPA/CBP for analyses and inclusion in upcoming EPA/CBP reports. However, since the budget for this modeling study did not cover a detailed report on production run results (i.e., scope of study was restricted to transmittal of time series output to VIMS), only the framework for model production runs is presented herein.

Periods Selected for Management Studies

The selection of the periods for which the Bay model package would be operated was an important decision that was based on the type of management strategies to be studied. To provide an indication of long-term impacts of point and nonpoint sources, the model package should be set up to represent a particular point/nonpoint management strategy and then operated for the period of record for available rainfall data. The frequency of water quality criteria violations simulated by the Main Bay model would represent the long-term impacts of each management option. In the case of low flow, high flow, and long-term assessments, model operations should concentrate on receiving water quality impacts during the spring, summer, and fall which are the seasons when water temperatures are high enough to result in the most critical water quality problems within the Bay's estuarine system. Summarized below is the methodology for identifying the periods used for management strategy studies.

Analyses of Long-Term Point/Nonpoint Source Impacts. It is technically possible to execute the Bay model package with many years of rainfall and streamflow records in order to assess long-term water quality impacts of a particular management strategy. However, since the costs of long-term simulations with state-of-the-art models can be very high, it is becoming

common practice to identify a short period (e.g., a full year; several seasons) which can serve as a less expensive surrogate for the multi-year period of interest (1,45,46). This shorter "typical" period should be characterized by streamflow and water quality statistics that are reasonably close to the period of record for the meteorologic data which would be used for a long-term simulation. Production runs of the model package with meteorologic records for the typical period are then assumed to produce streamflow and water quality statistics which approximate the statistics that would result from a model production run covering the entire period. In terms of streamflow statistics, this typical period can also be referred to as a period of "average wetness" since its flow-duration curve will most closely approximate the long-term curve; however, the term typical period is felt to more accurately describe the applications for continuous simulation model production runs. Since the use of a "typical" period permits simulations of long-term water quality impacts at a reasonable cost, this approach was selected for management studies with the Basin Model.

Since the spring, summer, and fall seasons are most critical from a eutrophication management standpoint, it was decided that the assessments of long-term water quality impacts should focus on the seven-month period extending from April 1st through October 31st. Because the available meteorologic record for Basin Model studies covered the period 1966-1978, the selection of the typical period was based on analyses of the daily streamflow statistics associated with April through October of each year in this thirteen-year period. The year with April-October streamflow statistics which come closest to the statistics for the full thirteen-year period can be designated as a typical year for assessments of long-term impacts with the Bay model package.

In order to ensure that the selected typical period was characterized by similar frequencies of occurrence for a range of daily flow levels, simulated daily flow-duration curves served as the basis for comparison of individual years with the full thirteen-year period. The fall-line monitoring study by the U.S. Geological Survey (11) had previously demonstrated a positive relationship between daily streamflow and pollutant loadings at the mouths of the Susquehanna, Potomac, and James rivers. The USGS study produced regression equations relating streamflow and pollutant loadings which can be used to produce loading-frequency relationships from a daily flow-duration curve. Therefore, a year characterized by a daily flow-duration curve that approximates the streamgage's long-term flow-duration curve is also characterized by loading-frequency relationships which approximate long-term loading statistics.

Simulated flow-duration curves for individual years were plotted with the simulated flow-duration curve for 1966-1978 and the assessment of similarity in distribution was based upon visual inspection. Comparisons were based upon simulated flow-duration curves for streamgages located at the mouths of the Susquehanna River (25,990 sq mi), Potomac River (11,560 sq mi), and James River (6,257 sq mi) and a composite flow-duration curve based upon the sum of simulated daily streamflows for these three river basins

(43,807 sq mi). Based on a preliminary screening, the following three years were given detailed consideration for designation as the typical year: 1971, 1974, and 1976. As may be seen in Figures 92 through 95, each gage's flow-duration curve for the period 1966-1978 is most closely approximated by the curves for 1974 and 1976. Since 1974 exhibits closer agreement with the long-term plots for the Susquehanna, Potomac, and "summation" gages, it was selected for use as a typical year. In other words, Basin Model executions with meteorologic conditions for the period April-October 1974 (preceded by executions for a sufficient antecedent period) should produce streamflow and loading statistics for Bay Model input which closely approximate April-October streamflow and loading statistics that would result from executing the Basin Model for a full 13-year period (1966-1978).

Analyses of "Worst Case" Point Source Impacts. As suggested above, model operations for an extended low streamflow period can be expected to provide the greatest insights into the Baywide impacts of wastewater treatment strategies for the Chesapeake Bay Basin. Selection of a "dry year" with a spring, summer, and fall characterized by an extended low flow period was based upon comparisons of April-October flow-duration curves for each year in the period 1966-1978. Based upon a preliminary screening, the following 3 years were selected for detailed analysis: 1966, 1968, and 1977. In the case of the Susquehanna, Potomac, and "summation" gages, extreme low flows occur more often in 1966 than in 1968 and 1977. In the case of the James, 1977 appears to be characterized by the most frequent occurrences of extreme low flows. In terms of total streamflow volumes during the April-October period, inspection of the areas beneath the flow-duration curves indicates that 1966 exhibits the lowest total inflows to the Bay for the Susquehanna and "summation" gages, while 1977 exhibits the lowest total inflows for the Potomac and James gages. Because it is characterized by the highest frequency of extreme low flows in the two largest river basins and the lowest overall volumes for the sum of Susquehanna, Potomac, and James basin streamflows, April-October 1966 was designated for dry year production runs of the Basin Model.

Analyses of "Worst Case" Nonpoint Source Impacts. Model operations for a "wet year" characterized by relatively high streamflows provide the greatest insights into "worst case" impacts of nonpoint sources of pollution. Based upon a preliminary screening of April-October flow-duration curves for each year in the period 1966-1978, the following three years were selected for detailed analyses: 1972, 1973, and 1975. The simulated flow-duration curves for the Susquehanna River Basin are shown in Figure 96. A review of simulated flow-duration curves for the Susquehanna, Potomac, and James basins and the summation dataset indicates that 1972 is the wettest year for all four gages, with 1975 the second wettest. It should be noted that the period April-October 1972 includes Hurricane Agnes, a storm event with a very low probability of occurrence. Since a period which includes an event as rare as Hurricane Agnes may not be an appropriate "design condition" for basinwide assessments of nonpoint pollution controls, the second wettest year, 1975, was selected for wet year production runs.

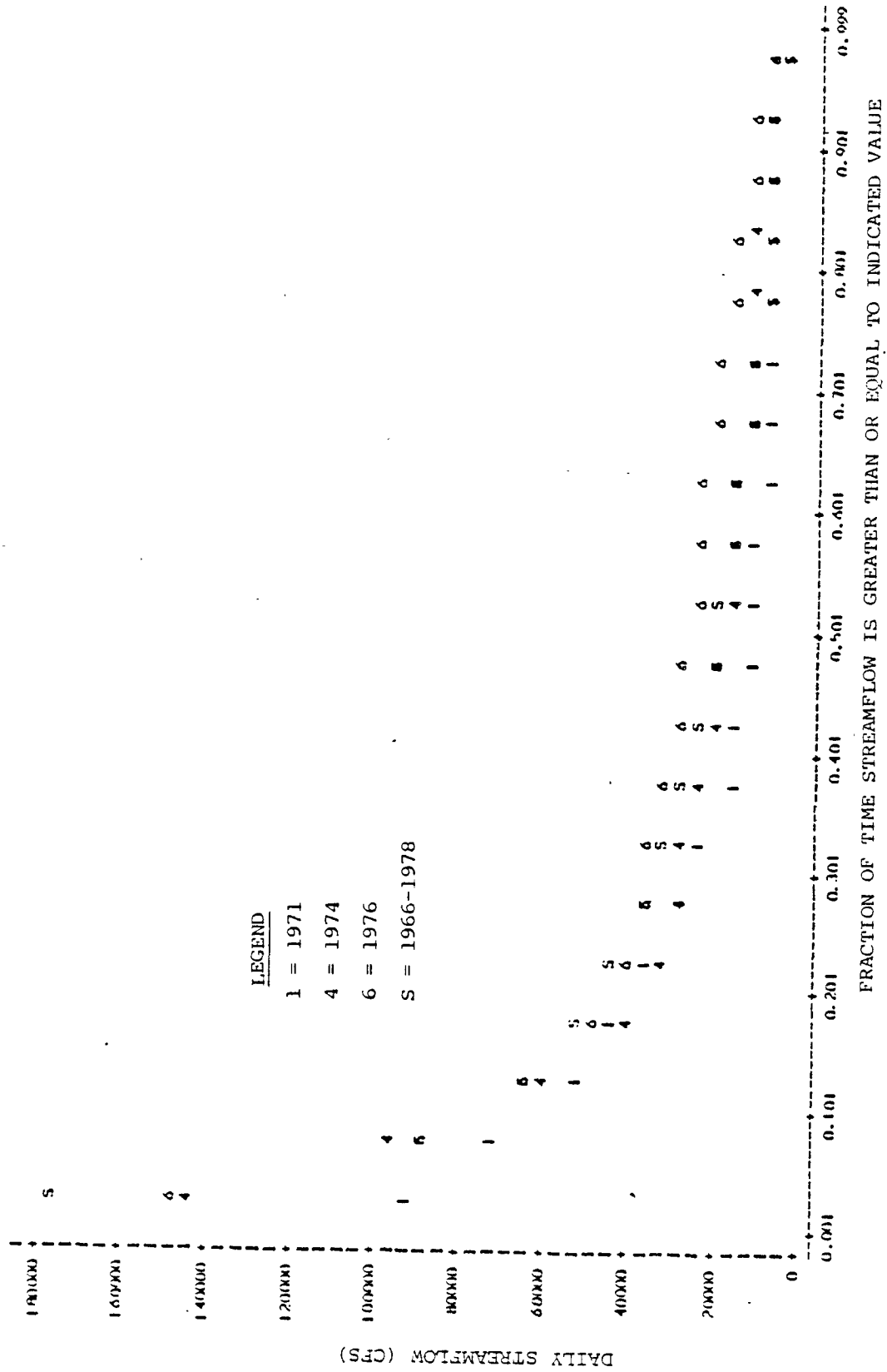


Figure 92. "Flow-Duration" Curves for Recorded Daily Streamflows for Susquehanna River at Marietta, PA (April 1st through October 31st for Indicated Period): Typical Year Analysis

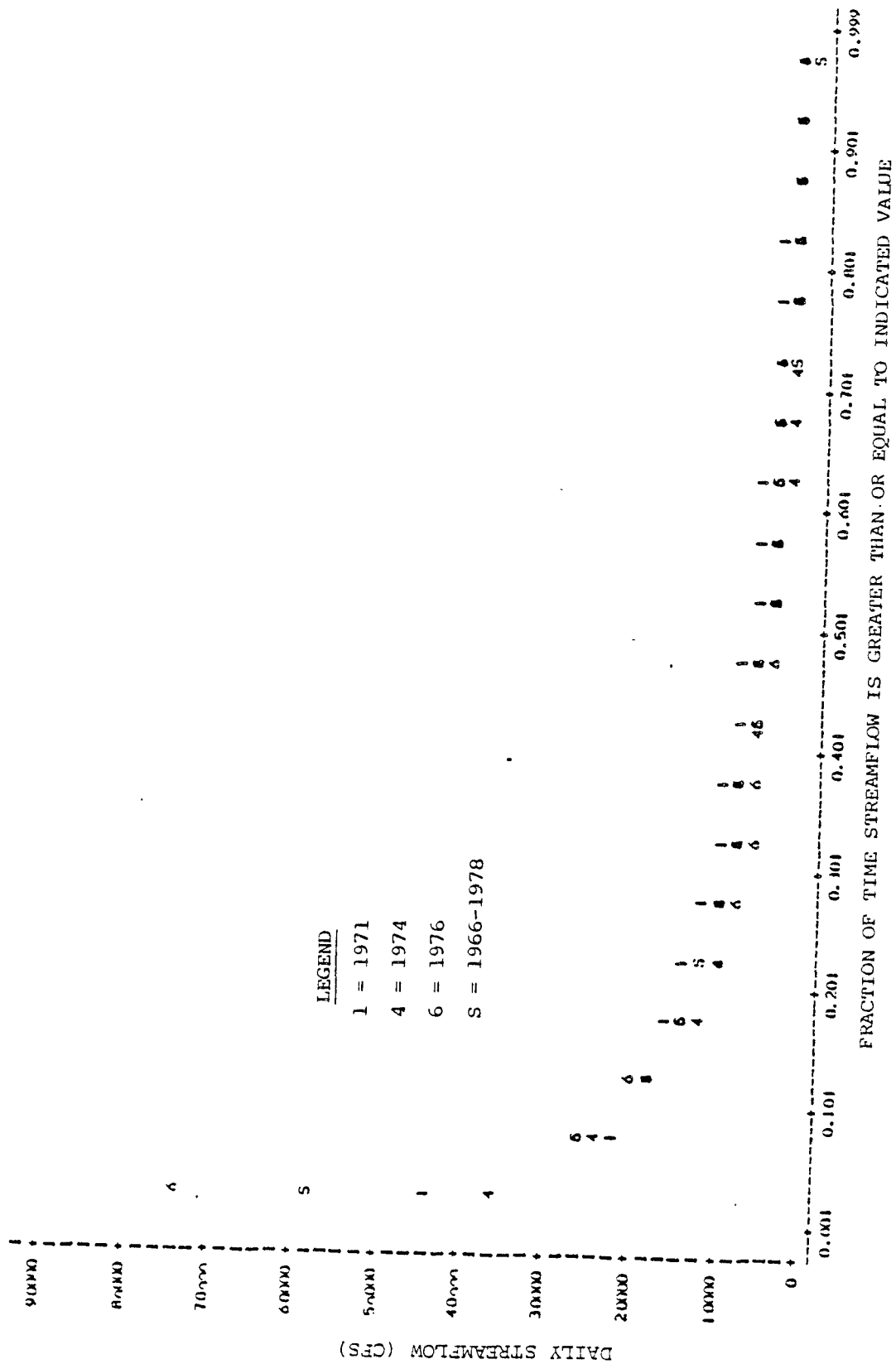


Figure 93. "Flow-Duration" Curves for Recorded Daily Streamflows for Potomac River near Washington, D.C. (April 1st through October 31st of Indicated Period): Typical Year Analysis

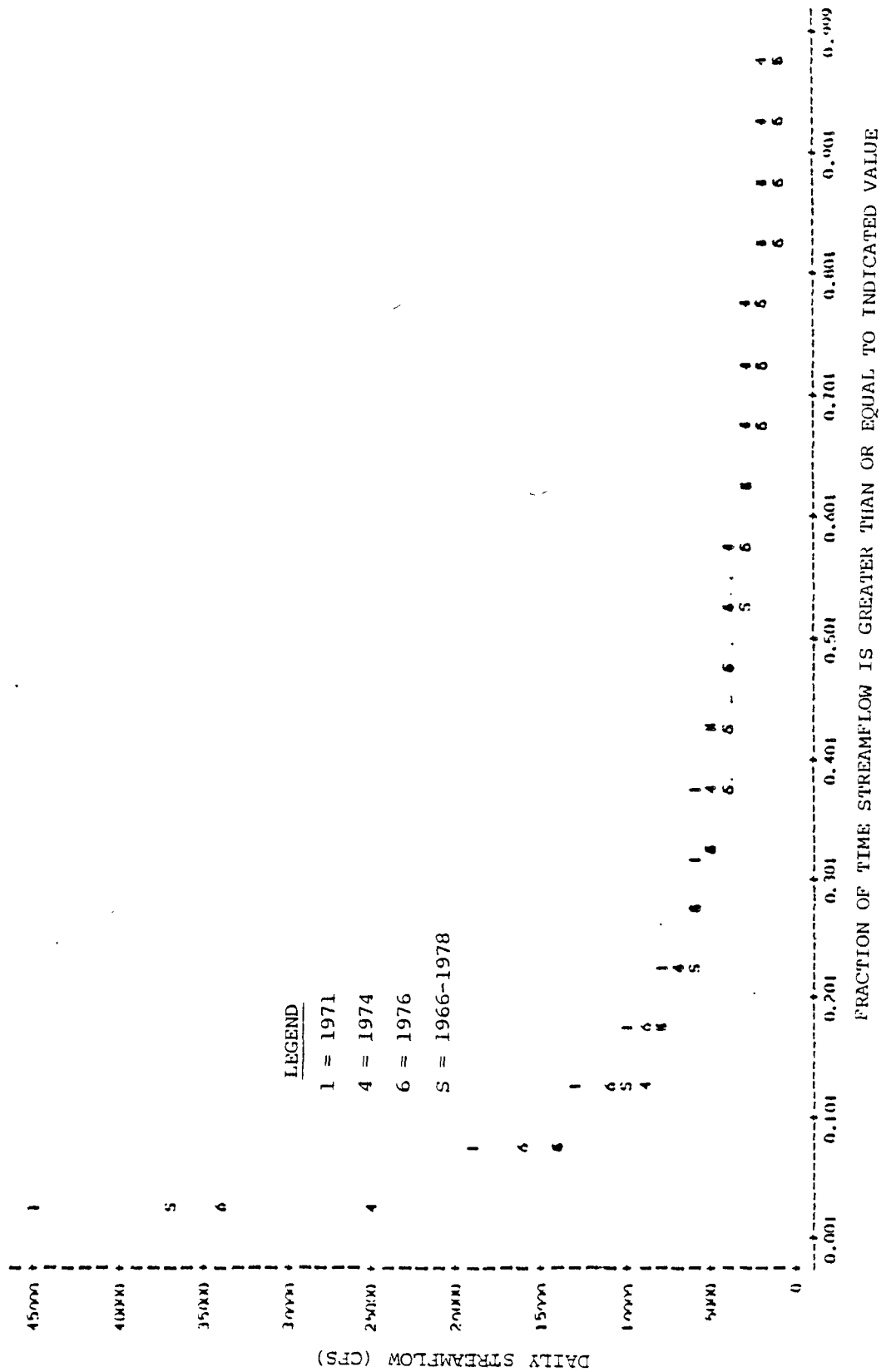


Figure 94. "Flow-Duration" Curves for Recorded Daily Streamflows for James River at Cartersville, VA (April 1st through October 31st of Indicated Period): Typical Year Analysis

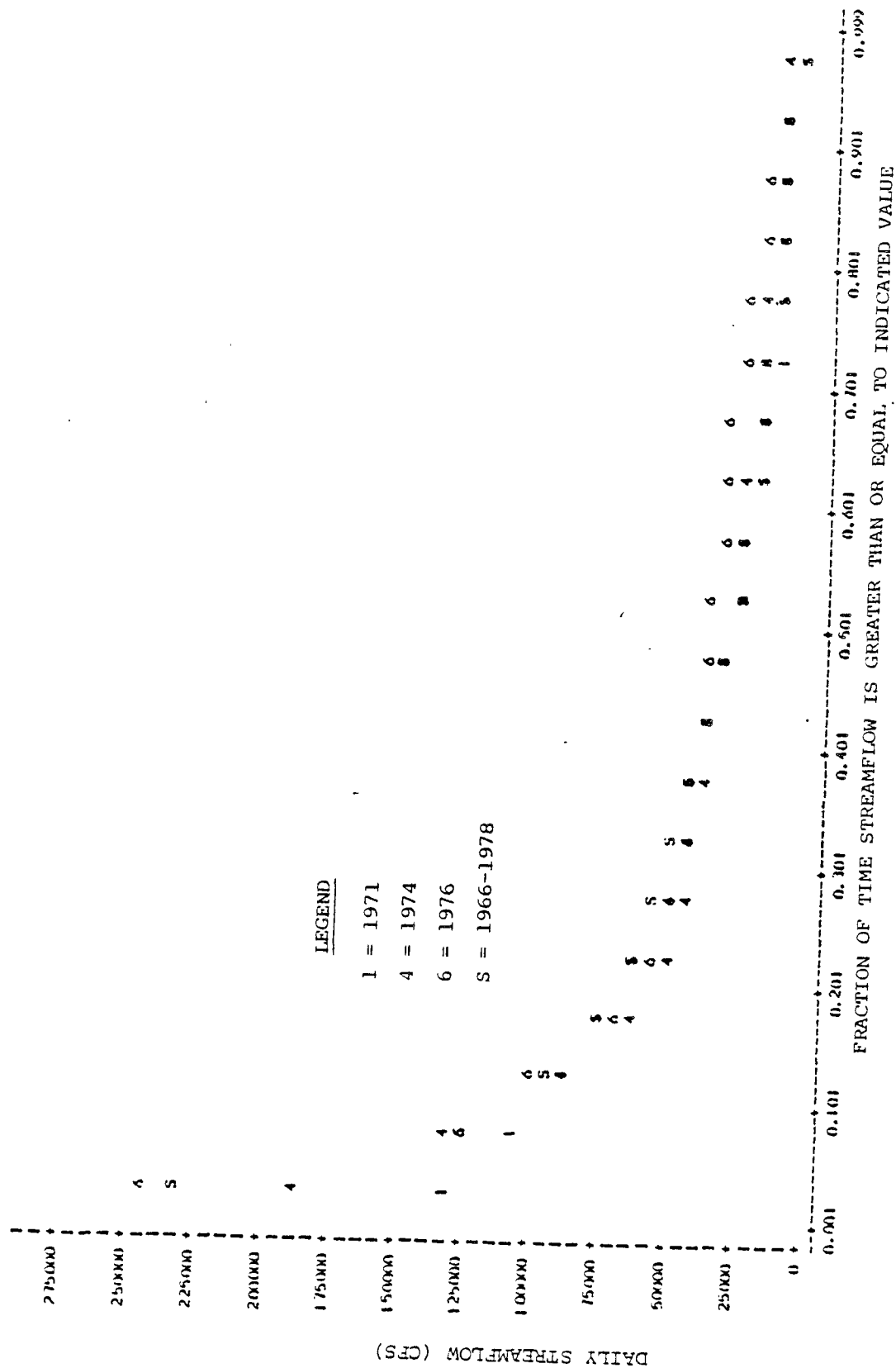


Figure 95. "Flow-Duration" Curves for Summation of Recorded Daily Streamflows for Susquehanna River at Marietta, PA, Potomac River near Washington, D.C., and James River at Cartersville, VA. (April 1st through October 31st of Indicated Period): Typical Year Analysis

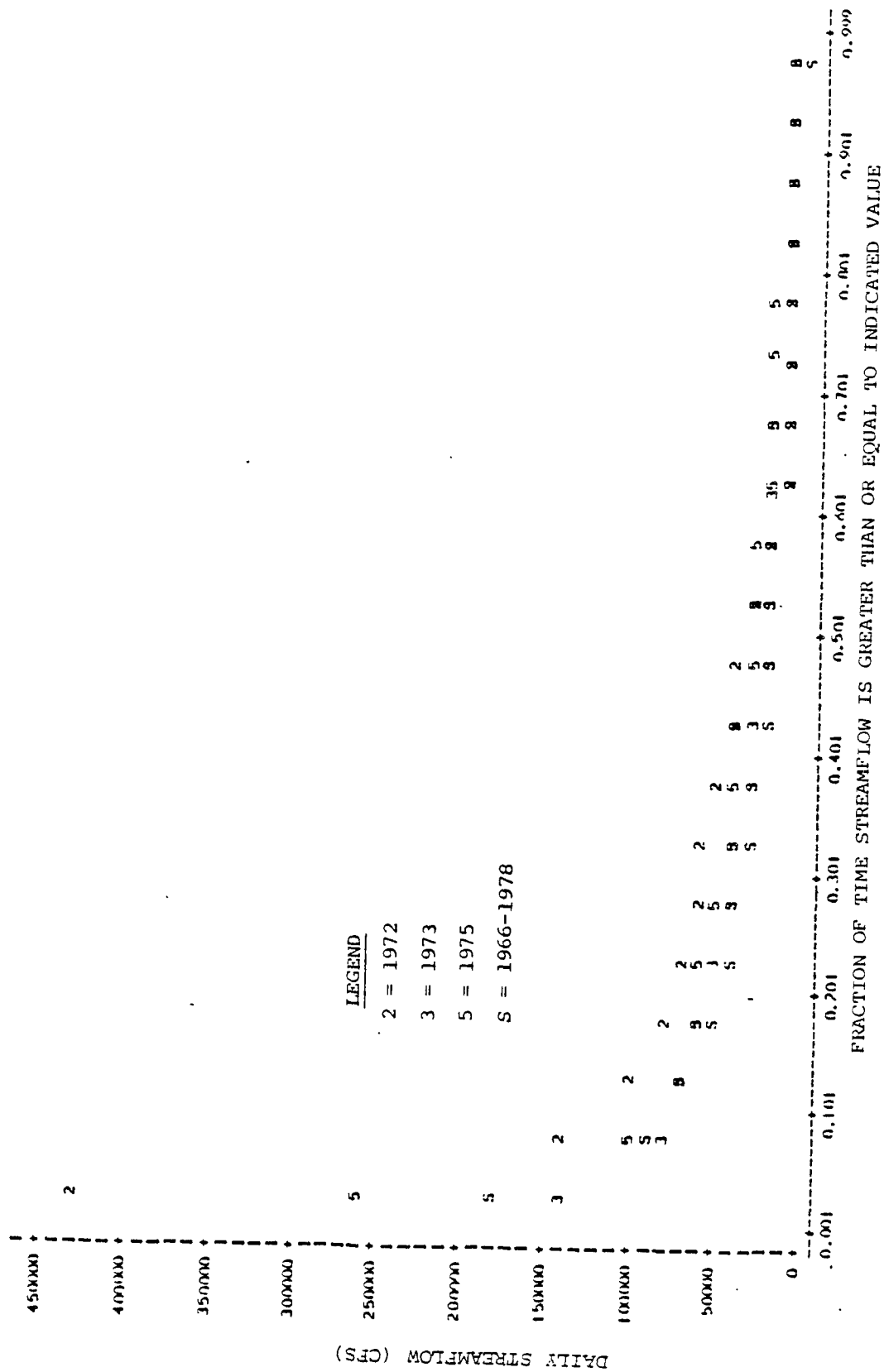


Figure 96. "Flow-Duration" Curves for Recorded Daily Streamflows for Susquehanna River at Marietta, PA (April 1st through October 31st of Indicated Period): Wet Year Analysis

Further Evaluations of Selected Periods. The aforementioned designations of a typical year, dry year, and wet year were based upon the period 1966-1978 since this is the period covered by the NWS hourly rainfall records acquired for the EPA Chesapeake Bay Program. The decision to restrict the rainfall records to the period 1966-1978 was one based primarily on costs in an effort to keep the budget for the acquisition and analysis of NWS rainfall tapes from becoming prohibitive. Since NWS hourly rainfall records for the Chesapeake Bay Basin recording gages are currently available for 17 additional years (i.e., 1949-1965), it was necessary to screen observed April-October flow-duration curves for each year in the period 1949-1978 to demonstrate that the selected years were the most appropriate for model production runs.

For the typical year comparisons, the flow-duration curves for the period 1966-1978 were found to adequately approximate the curves for the full 30-year period (1949-1978) covered by NWS hourly rainfall records, indicating that selections of a typical year based on comparisons with the shorter period were certainly appropriate. Further, 1974 exhibited as good an agreement with the 1949-1978 period as did the only two years (1950 and 1961) in the earlier period which merited consideration as a typical year.

For the dry year comparisons, three earlier years (1954, 1957, and 1963) merited consideration as a design dry year. However, although the total April-October streamflow volumes for at least one (1963) of these earlier years are less than April-October 1966 volumes, the similar and even higher frequencies of extreme low flows during 1966 reinforces its selection for the dry year production runs.

For the wet year comparisons, it was determined that none of the earlier years produced April-October flow-duration curves which approached 1972 and only one year (1960) approached 1975. Inspection of the flow-duration plots indicated that 1975 is typically very similar to 1960 in terms of the frequency of high flows and superior to 1960 in terms of the frequency of low-to-moderate flows. Thus, the comparison of flow-duration curves for the period 1949-1978 supports the selection of 1975 for the wet year production runs.

Interpretation of Model Output

For each production run, the Basin Model can be operated in its entirety and loading output for the April-October period (plus a one-month antecedent period) will be input to the Bay system models to project receiving water quality impacts. In addition, loadings delivered to the Bay system can be tabulated on a seasonal, monthly, and daily basis for general assessments of management strategies.

By subjecting the output time series to frequency analyses, concentration-frequency relationships at the fall line can be derived for each management strategy simulation. Concentration-frequency relationships for typical year production runs may be assumed to represent the average

impacts over a thirty-year period. In other words, the number of days (or hours) with water quality criteria violations projected for the typical year simulation may be assumed to represent the average number of violations per year if the management strategy were applied over a thirty-year period characterized by a good mix of wet years, dry years, and average years. Likewise, concentration-frequency relationships for dry year and wet year production runs define the duration of water quality criteria violations for two periods which can be expected to occur relatively infrequently over a thirty-year period. Since the selected wet year and dry year represent extreme conditions, one would expect the frequency of any water quality criteria violations during these two simulation periods to be greater than under typical year simulations which are assumed to represent average algal growing season conditions in the receiving waters.

By relating the simulated concentration-frequency relationships to beneficial use criteria, water quality damages may be inferred from full line concentration simulations. Reductions in water quality damages achieved by a particular management strategy can then be expressed in terms of reductions in the frequency of undesirable concentrations. However, it should be cautioned that since the models are idealized representations of the prototype river systems, water quality output is best viewed in a relative sense to provide insights into differences among management strategies.

Framework for Model Production Runs

The first set of production runs to be carried out with the Basin Model package were daily loading projections for the existing land use pattern and the land use pattern projected for the Year 2000. As previously indicated the existing land use pattern is based upon LANDSAT data interpretations. The 2000 land use projection was derived by increasing the existing urban land use in each sub-basin by the ratio of the 2000 population projection to the 1980 population and reducing forest land to represent the consumption of undeveloped land by urban development. Wastewater discharges and water supply diversions for the Year 2000 were generally derived by multiplying the 1980 values by the ratio of population values. The assumption that only forest land will be consumed by urban development occurring between 1980 and 2000 is a conservative one designed to ensure a worst case projection of Year 2000 water quality impacts. This assumption preserves the agricultural land use distribution at 1980 levels while increasing urban development to reflect population increases, thereby resulting in what is probably a conservatively high estimate of nonpoint pollution loadings in the Year 2000. The comparison of existing and future land use impacts on the Bay's estuarine system should provide considerable insight into the impacts of urban development on Baywide water quality. These two model runs will also establish the baseline receiving water quality conditions (i.e., concentration-frequency and loading-frequency relationships) for evaluations of alternate management strategies.

Included among the management strategy evaluations which were the subject of model production runs are the following:

- A. General Comparisons of Point Source and Nonpoint Source Loadings:
The contributions of point and nonpoint sources to fall line loadings were determined by operating the Basin Model without any point source loadings (i.e., with only the flow, temperature, and dissolved oxygen associated with each wastewater discharge). The difference between simulated fall line loadings "with" and "without" point source inputs represents the fraction of the fall line load that can be attributed to point sources. Since these production runs were intended to evaluate both point and nonpoint sources, they were based on all three hydrologic conditions (i.e., typical year, dry year, and wet year).
- B. General Comparisons of Water Quality Benefits Promised by Cropland Best Management Practices (BMP's): Initial production runs focussed on the relative loading contributions of cropland areas. The Basin Model was operated without surface runoff loadings from forest, pasture, and urban land uses, and no change in subsurface flow loadings. The difference between fall line loadings for this run and previous runs represented the contribution of non-cropland land uses. In general, the non-cropland contributions were not more than about one-third of the total fall line load of N and P for average and wet years, indicating the significance of cropland contributions. The principal cropland BMP which was studied involved converting high tillage cropland areas to low tillage cropland. The potential benefits of this cropland BMP were determined by comparing Basin Model projections "with" and "without" the low tillage BMP.
- C. Assessments of Locational Differences in Nonpoint Pollution Loading Delivery to the Bay's Estuarine System: As previously indicated, it would be incorrect to assume that all nonpoint pollution loadings released into the Basin's receiving waters are transported to the Bay's estuaries. The Basin Model was used to develop "pollutant delivery ratios" for different sections of the three major river basins. By removing the nonpoint pollution loadings produced by sub-basin clusters one cluster at a time (i.e., including only flow, temperature, and dissolved oxygen time series for clusters deleted from the simulations), the Basin Model was used to estimate the fraction of sub-basin nonpoint pollution loadings which is delivered to the Chesapeake Bay's estuarine system. The difference between simulated annual loadings at the mouth of each river basin for "with" and "without" sub-basin cluster conditions may be assumed to be the total annual nonpoint pollution loadings delivered to the Bay's estuarine system by each sub-basin cluster. Pollutant delivery ratio estimates for different sections of the Chesapeake Bay Basin can be used by management agencies to identify those areas where nonpoint

pollution controls promise the greatest benefit. For example, maps showing pollutant delivery ratio contours could be developed for use in comparing the Chesapeake Bay impacts of nonpoint pollution loads from the various physiographic provinces in the Basin and to determine whether nonpoint pollution controls should be concentrated in downstream sections (e.g., Coastal Plain and Piedmont provinces) of the Basin or extended into upland sections (e.g., Appalachian Ridge & Valley and Appalachian Plateau provinces) as well. Since these production runs are restricted to nonpoint source impacts, they were based on typical year and wet year meteorologic conditions only.

- D. Assessments of Locational Differences in Point Source Pollution Delivery to the Bay's Estuarine System: Using the same approach outlined under C, loadings from point source clusters were removed from the Basin Model one cluster at a time to develop estimates of each cluster's contribution to the total fall line load. Estimates of locational differences in the delivery of point source loadings to the fall line were developed for different sections of the three major river basins. Point source contributions were also defined for each state traversed by the river basin. These production runs were based upon all three hydrologic conditions (i.e., typical year, dry year, and wet year).
- E. Assessments of Point Source Management Strategies: The impacts of higher wastewater treatment levels on fall line loadings were assessed with the Basin Model. The majority of the wastewater management strategies involved more stringent effluent levels for phosphorus. At least one management strategy involved more stringent treatment levels for both nitrogen and phosphorus. These production runs were typically restricted to dry year and average year conditions.

REFERENCES

1. Hydrocomp, Inc., "The Occoquan Basin Computer Model: Calibration, Verification, and User's Manual," prepared for Northern Virginia Planning District Commission, Falls Church, VA, May 1978.
2. Johanson, R.C., Imhoff, J.C., and Davis, H.H., "Users Manual for Hydrological Simulation Program - FORTRAN (HSPF)," EPA-600/9-80-015, U.S. Environmental Protection Agency, Environmental Research Laboratory, Athens, GA, April 1980.
3. Linsley, R.K. and Crawford, N.H., "Continuous Simulation Models in Urban Hydrology," Geophysical Research Letters, Vol. 1, No. 1, May 1974, pp. 59-62.
4. Linsley, R.K. and Crawford, N.H., "Computation of a Synthetic Streamflow Record on a Digital Computer," Journal of International Association of Scientific Hydrology, No. 51, 1960, pp. 526-538.
5. Donigian, A.S. and Crawford, N.H., "Modeling Nonpoint Pollution from the Land Surface," EPA-600/3-76-083, U.S. Environmental Protection Agency, Environmental Research Laboratory, Athens, GA, July 1976.
6. Hartigan, J.P., Quasebarth, T.F., and Southerland, E., "Use of Continuous Simulation Model Calibration Techniques to Develop Nonpoint Pollution Loading Factors," Proceedings of Stormwater and Water Quality Management Modeling Users Group Meeting: March 25-26, 1982, EPA-600/9-82-015, U.S. Environmental Protection Agency, Environmental Research Laboratory, Athens, GA, 1982, pp. 101-127.
7. Northern Virginia Planning District Commission and Virginia Polytechnic Institute and State University, "Occoquan/Four Mile Run Nonpoint Source Correlation Study," Final Report prepared for Metropolitan Washington Council of Governments, Washington, D.C., July 1978.
8. Northern Virginia Planning District Commission, "Guidebook for Screening Urban Nonpoint Pollution Management Strategies," prepared for Metropolitan Washington Council of Governments, Washington, D.C., November 1979.
9. Hartigan, J.P., et al., "Calibration of Urban Nonpoint Pollution Loading Models," Proceedings of ASCE Hydraulics Division Specialty Conference on Verification of Mathematical and Physical Models in Hydraulic Engineering, American Society of Civil Engineers, New York, NY, August 1978, pp. 363-372.
10. Grizzard, T.J., Hartigan, J.P., and Randall, C.W., "The Development of Water Quality Management Plans Using Data from Automatic Stormwater Monitoring Networks," Proceedings of IAWPR International Workshop on Water Quality Monitoring, held at Munich, Germany, June 22-25, 1981.

11. U.S. Geological Survey, "Water Quality of the Three Major Tributaries to the Chesapeake Bay, January 1979 - April 1981: Estimated Loads and Examinations of Selected Water Quality Constituents," prepared for USEPA Chesapeake Bay Program, November 1981.
12. Hartigan, J.P., et al., "Areawide and Local Frameworks for Urban Nonpoint Pollution Management in Northern Virginia," Stormwater Management Alternatives, Tourbier, J.T. and Westmacott, R., eds., University of Delaware, DE, April 1980, pp. 211-245.
13. Biggers, D.J., Hartigan, J.P., and Bonuccelli, H.A., "Urban Best Management Practices (BMP's): Transition from Single-Purpose to Multipurpose Stormwater Management," Proceedings of Seventh International Symposium on Urban Storm Runoff, Report No. UKYBU121, College of Engineering, University of Kentucky, Lexington, Kentucky, July 1980, pp. 249-274.
14. Northern Virginia Planning District Commission, "Follow-up Assessments of Alternate AWT Operating Rules with Occoquan Basin Computer Model," prepared for Camp, Dresser, McKee, Inc., consultants to Virginia State Water Control Board, Richmond, VA, February 1980.
15. Northern Virginia Planning District Commission, "Recommended Operating Procedure for Nitrogen Treatment Facilities at UOSA AWT Plant," prepared for Upper Occoquan Sewage Authority, Fairfax County Water Authority, and Occoquan Watershed Monitoring Laboratory, May 1981.
16. Northern Virginia Planning District Commission, "Modeling Study of Nonpoint Pollution Loadings from Potomac Embayment Watersheds," Final Report prepared for Virginia State Water Control Board, Richmond, VA, March 1981.
17. CH₂M-Hill, "Stormwater Management: A Comprehensive Study of the Muddy Branch and Seneca Creek Watersheds," prepared for Montgomery County (MD) Planning Board, Silver Spring, MD, April 1975.
18. Montgomery County Planning Board, "Conservation and Management Report on the Rock Creek Watershed, Montgomery County," Silver Spring, MD, 1978.
19. Metropolitan Washington Council of Governments, "The Seneca Creek Watershed Model: Documentation of the Hydrologic Calibration and Verification," Washington, D.C., April 1982.
20. Northern Virginia Planning District Commission, "Technical Plan for a Modeling Study of Nonpoint Pollution Loadings and Transport in the Chesapeake Bay Basin," Interim Report prepared for USEPA Chesapeake Bay Program, Annapolis, MD, February 1981.

21. Roffe, K.A., "Computerized Mapping for Assessment of Environmental Impacts," presented at Annual Conference of American Institute of Planners, held at Kansas City, MO, October 8-12, 1977.
22. Arbruster, J.T., "Flow Routing in the Susquehanna River Basin: Part I - Effects of Raystown Lake on the Low-Flow Frequency Characteristics of the Juniata and Lower Susquehanna Rivers, Pennsylvania," U.S. Geological Survey Water Resources Investigations 77-12, USGS, Harrisburg, PA, April 1977.
23. Wischmeier, W.H. and Smith, D.D., "Predicting Rainfall Erosion Losses from Cropland East of the Rocky Mountains," Agricultural Handbook No. 282, Soil Conservation Service, U.S. Department of Agriculture, Washington, D.C., May 1965.
24. Northern Virginia Planning District Commission, "Assessments of Water Quality Management Strategies with the Occoquan Basin Computer Model," prepared for Occoquan Technical Review Committee, January 1979.
25. Hydrocomp, Inc., "Hydrocomp Simulation Programming: Water Quality Simulation Operations Manual," Palo Alto, Cal., 1977.
26. Zison, S.W., et al., "Rates, Constants, and Kinetics Formulations in Surface Water Quality Modeling," EPA-600/3-78-105, Environmental Research Laboratory, U.S. Environmental Protection Agency, Athens, GA, December 1978.
27. Northern Virginia Planning District Commission, "Water Quality Modeling Study of Goose Creek, Broad Run, and Sugarland Run Watersheds," Falls Church, VA, June 1980.
28. Northern Virginia Planning District Commission, "Occoquan Basin Computer Model: Summary of Calibration Results," Falls Church, VA, January 1979.
29. Lumb, A.M. and James, L.D., "Runoff Files for Flood Hydrograph Simulation," Journal of the Hydraulics Division, ASCE, Vol. 102, No. HY10, October 1976, pp. 1515-1531.
30. Lumb, A.M., "UROS04: Urban Flood Simulation Model, Part 1: Documentation and Users Manual," School of Civil Engineering, Georgia Institute of Technology, Atlanta, GA, March 1975.
31. Ross, G.A., "The Stanford Watershed Model: The Correlation of Parameter Values Selected by a Computerized Procedure with Measureable Physical Characteristics of the Watershed," Research Report No. 35, Water Resources Institute, University of Kentucky, Lexington, Ky., 1970.
32. Hydrocomp, Inc., Hydrocomp Simulation Programming: Hydrology Simulation Operations Manual, Palo Alto, CA, January 1976.

33. Winter, T.C., "Uncertainties in Estimating the Water Balances of Lakes," Water Resources Bulletin, Vol. 17, No. 1, February 1981, pp. 82-115.
34. Cavacas, A., et al., "Hydrologic Modeling for Studies of Pollutant Loadings and Transport in Large River Basins," Proceedings of Stormwater and Water Quality Management Modeling Users Group Meeting: March 25-26, 1982, EPA-600/9-82-015, U.S. Environmental Protection Agency, Environmental Research Laboratory, Athens, GA, 1982, pp. 69-89.
35. American Public Health Association, Standard Methods for the Examination of Water and Wastewater, 14th Edition, APHA, Washington, D.C., 1976.
36. U.S. Environmental Protection Agency, "Methods for Chemical Analysis of Water and Wastes," EPA-625/6-74-003, National Environmental Research Center, Washington, D.C., 1974.
37. Hollander, M. and Wolfe, D.A., Nonparametric Statistical Methods, John Wiley and Sons, New York, NY, 1973.
38. Northern Virginia Planning District Commission, "Reverification of Occoquan Computer Model for Post-AWT Conditions," prepared for NVPDC Occoquan Basin Nonpoint Pollution Management Program, Annandale, VA, November 1982.
39. Smullen, J.T. and Taft, J.L., "Nutrient and Sediment Sources to the Water Column of the Chesapeake Bay," USEPA Chesapeake Bay Program Synthesis Paper, U.S. Environmental Protection Agency, Annapolis, MD, February 1982.
40. Northern Virginia Planning District Commission, "NURP Study Quarterly Report: October - December 1981," prepared for Metropolitan Washington Council of Governments, Washington, D.C., February 1982.
41. Wright, R.M. and McDonnell, A.J., "In-Stream Deoxygenation Rate Prediction," Journal of Environmental Engineering Division, ASCE, Vol. 105, No. EE2, April 1979, pp. 323-335.
42. Bansal, M.K., "Nitrification in Natural Streams," Journal of Water Pollution Control Federation, Vol. 48, No. 10, October 1976, pp. 2380-2393.
43. Roy F. Weston, Inc., "Susquehanna River Water Quality Study Pertaining to the Safe Harbor and Holtwood Hydroelectric Projects: Interim Report," prepared for Penna. Power and Light Co. and Safe Harbor Water Power Corporation, February 1982.
44. Personal communication from Stuart Freudberg, Metropolitan Washington Council of Governments, June 22, 1982.

45. Huber, W., "Discussion Remarks," Proceedings of Seminar on Design Storm Concept, Ecole Polytechnique de Montreal, Montreal, Quebec, 1979.
46. Southerland, E., "A Continuous Simulation Modeling Approach to Nonpoint Pollution Management," Dissertation presented to Virginia Polytechnic Institute and State University, Blacksburg, VA, in December 1981, in partial fulfillment of the requirements for the degree Doctor of Philosophy in Environmental Sciences and Engineering.



APPENDIX A

SUBBASIN MAPS
WITH
PRECIPITATION GAGE LOCATIONS

Figure A1

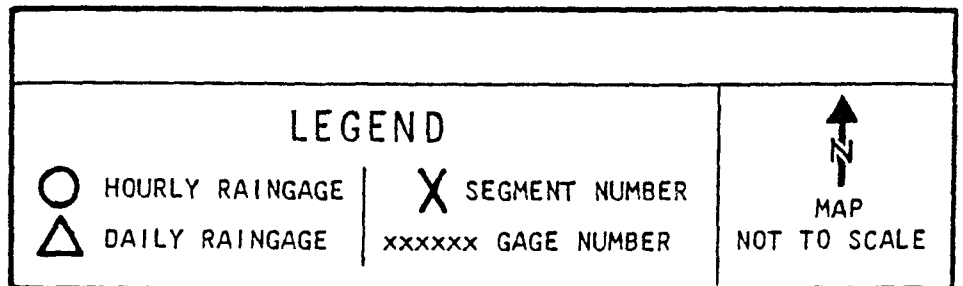
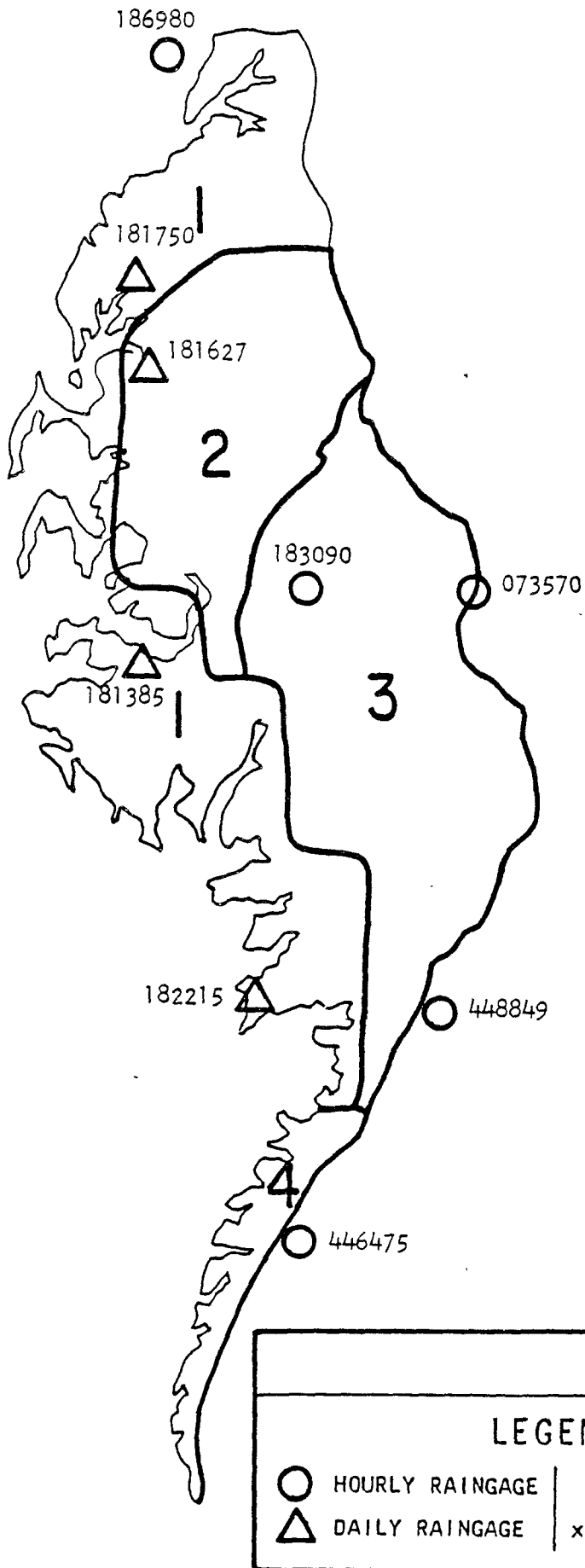
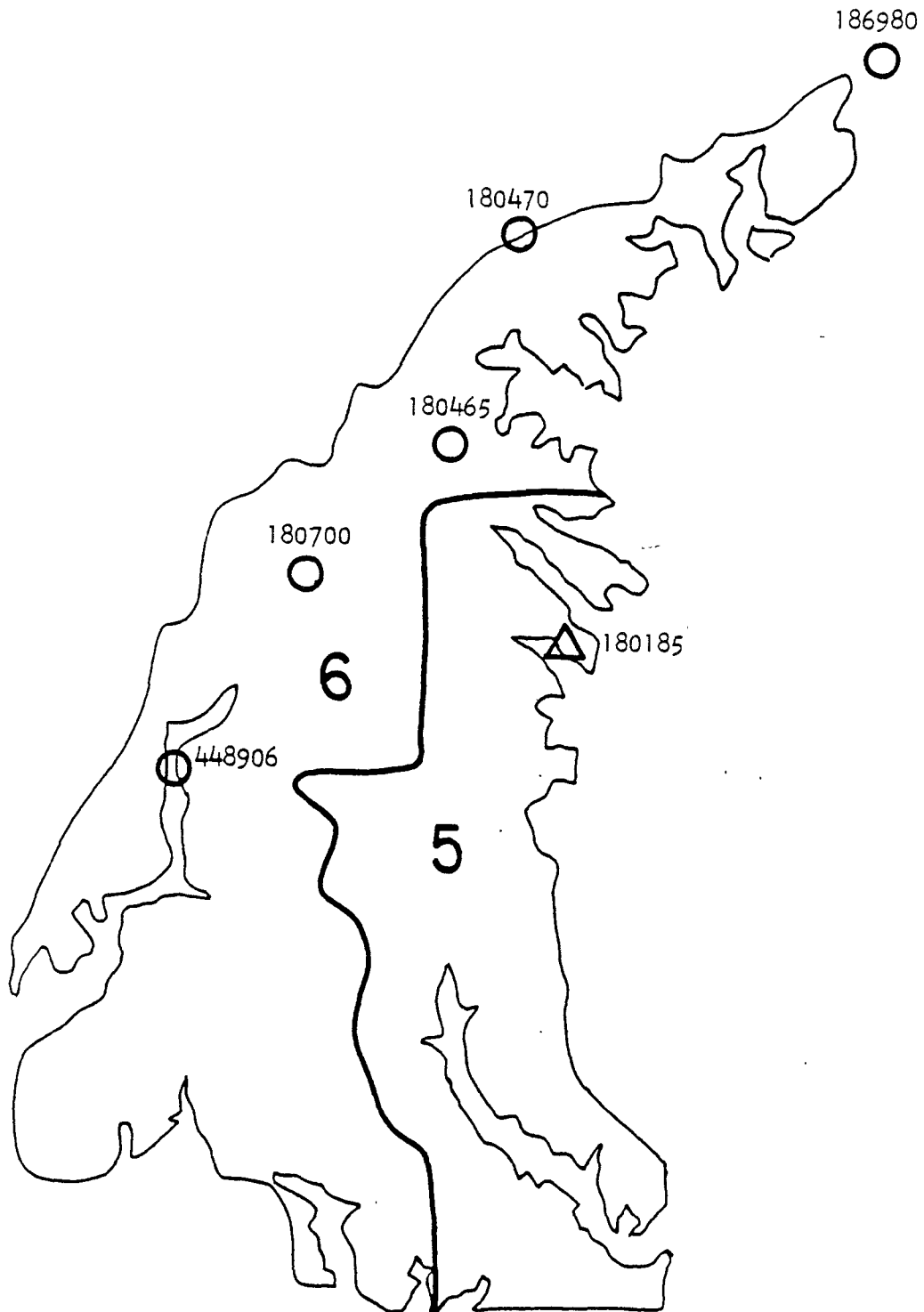


Figure A2




LEGEND		
○	HOURLY RAINGAGE	X SEGMENT NUMBER
△	DAILY RAINGAGE	xxxxxx GAGE NUMBER
		 MAP NOT TO SCALE

Figure A3

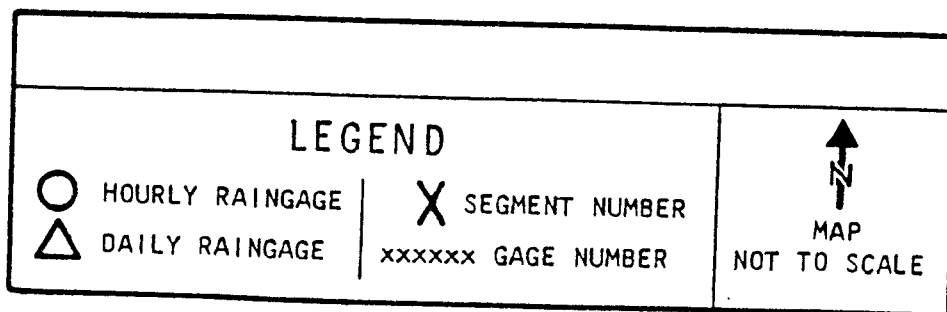
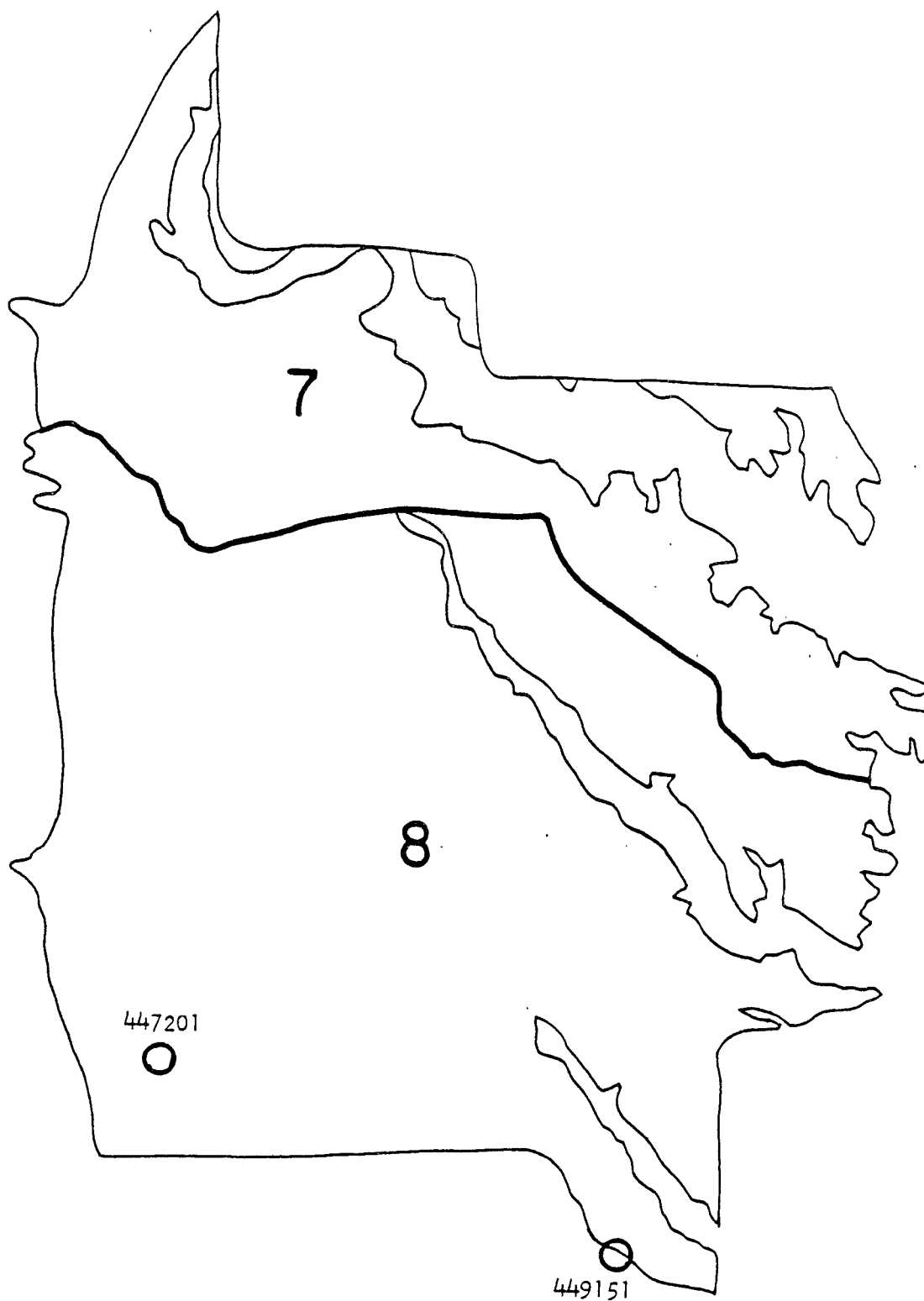


Figure A4

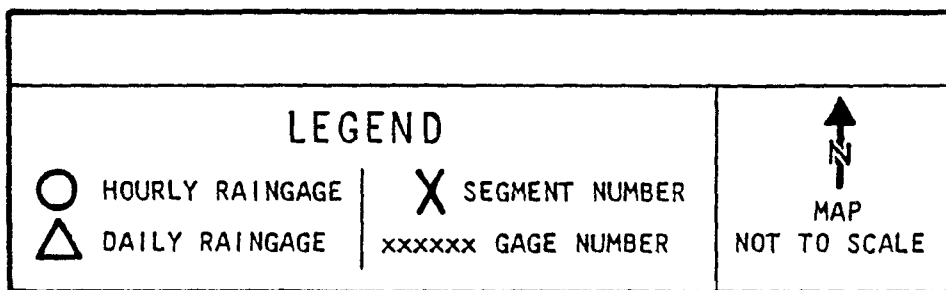
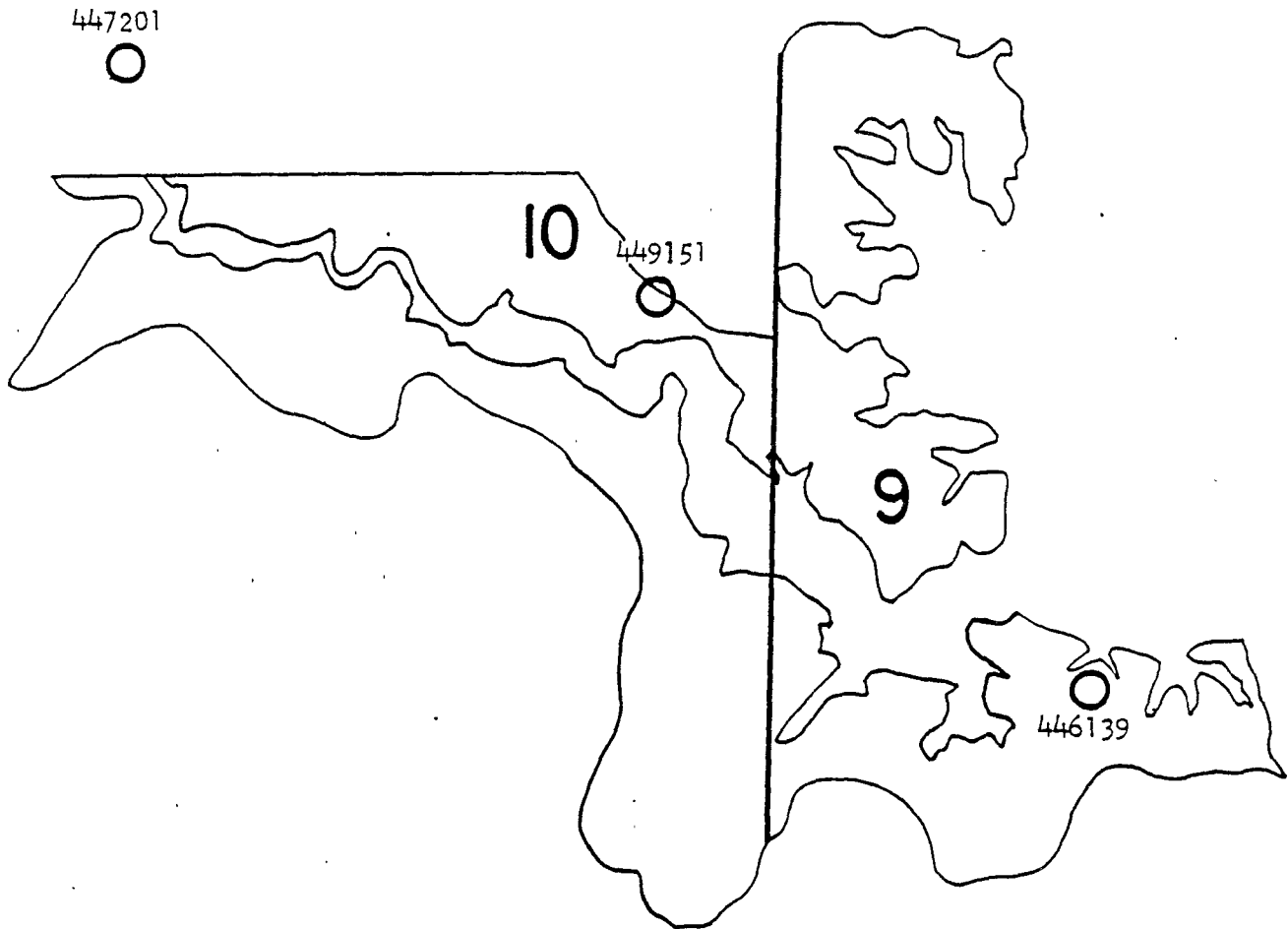


Figure A5

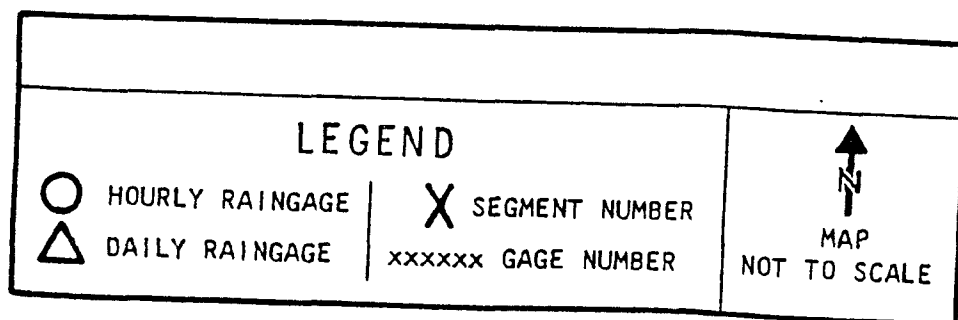
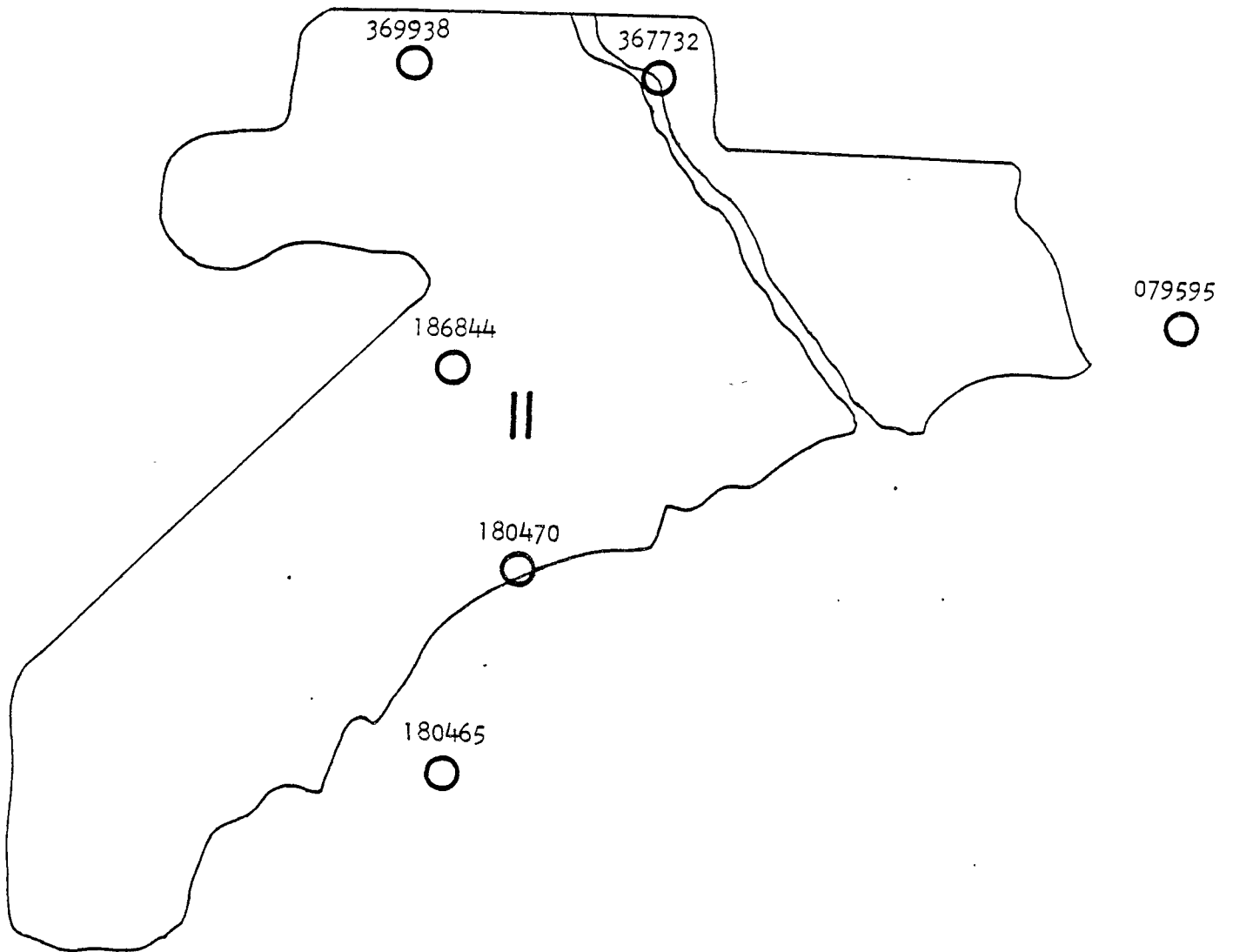


Figure A6

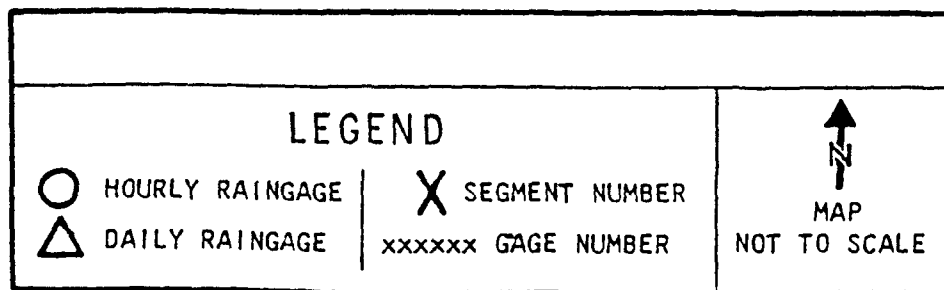
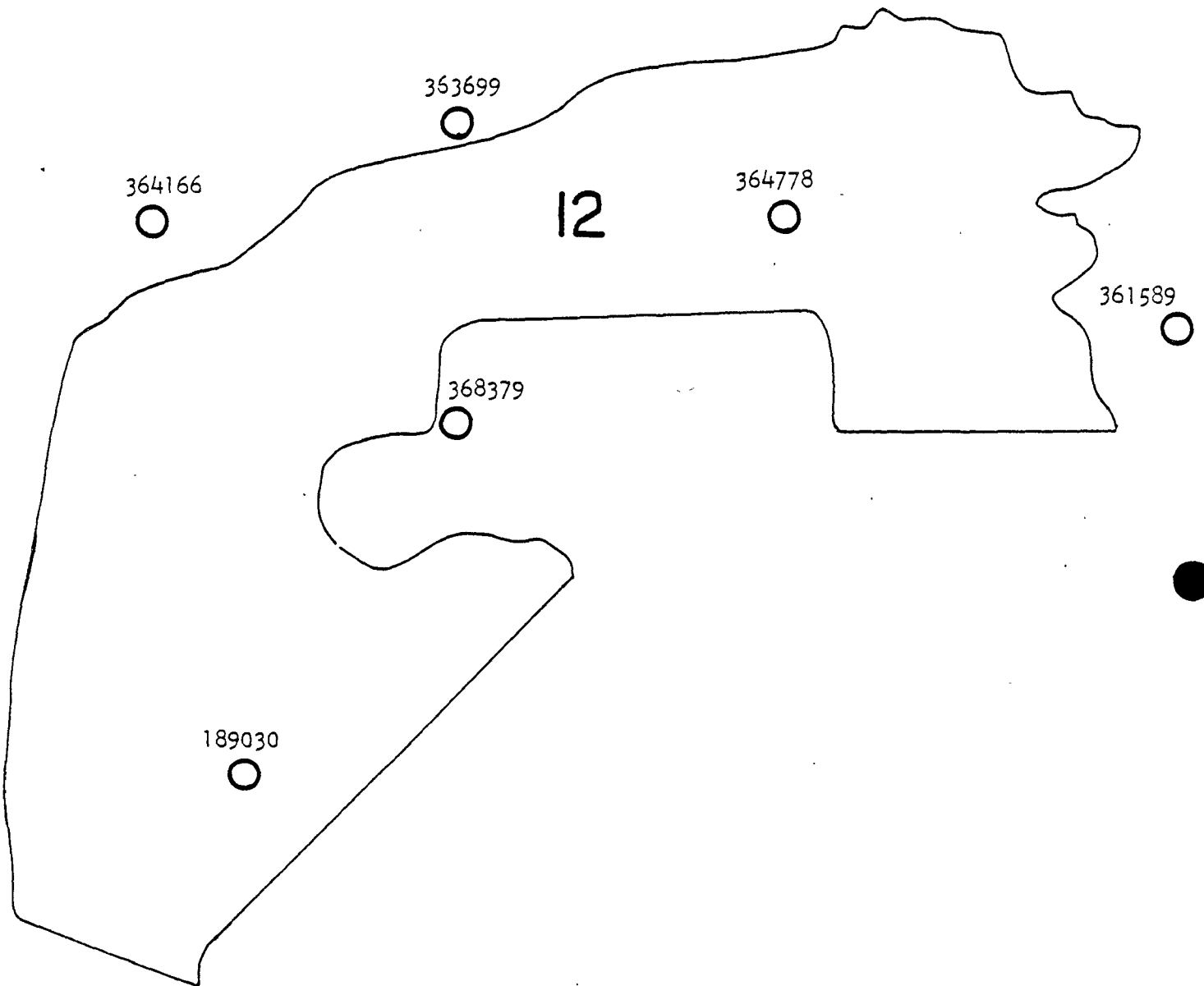
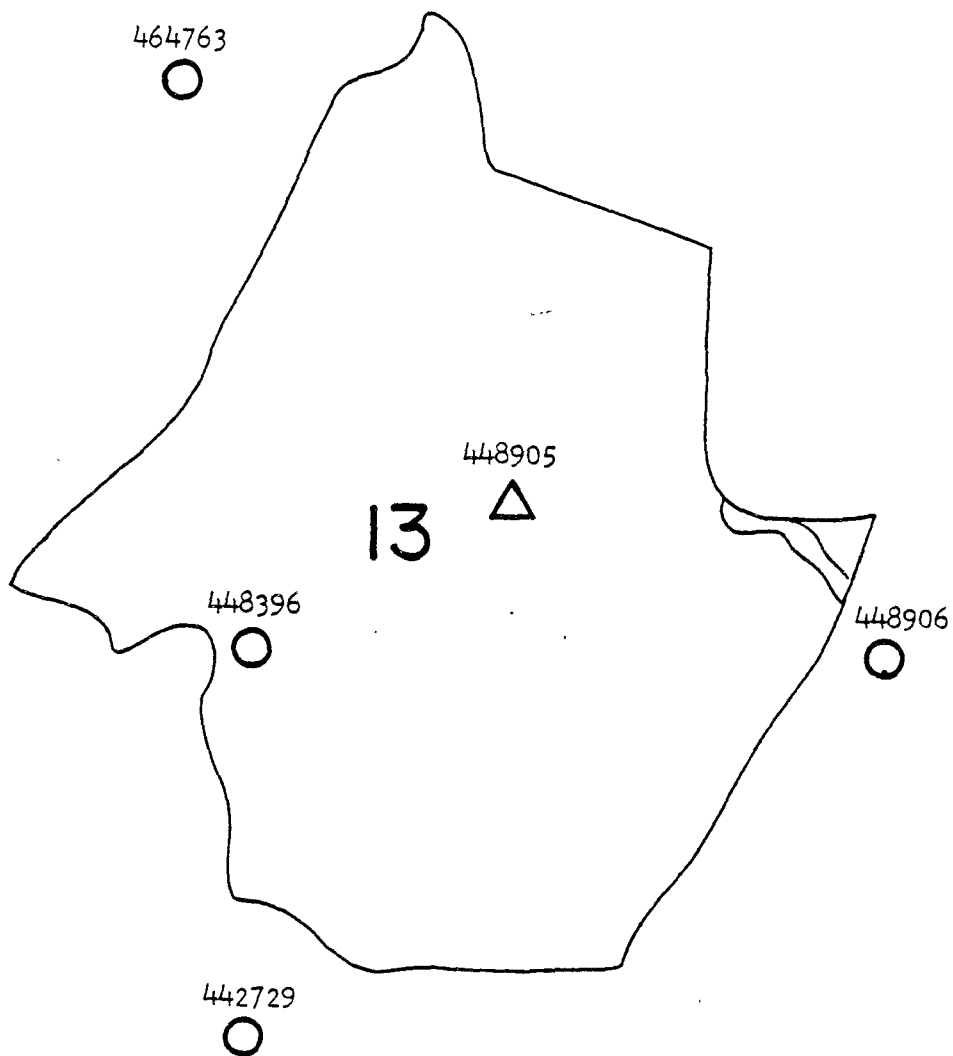


Figure A7




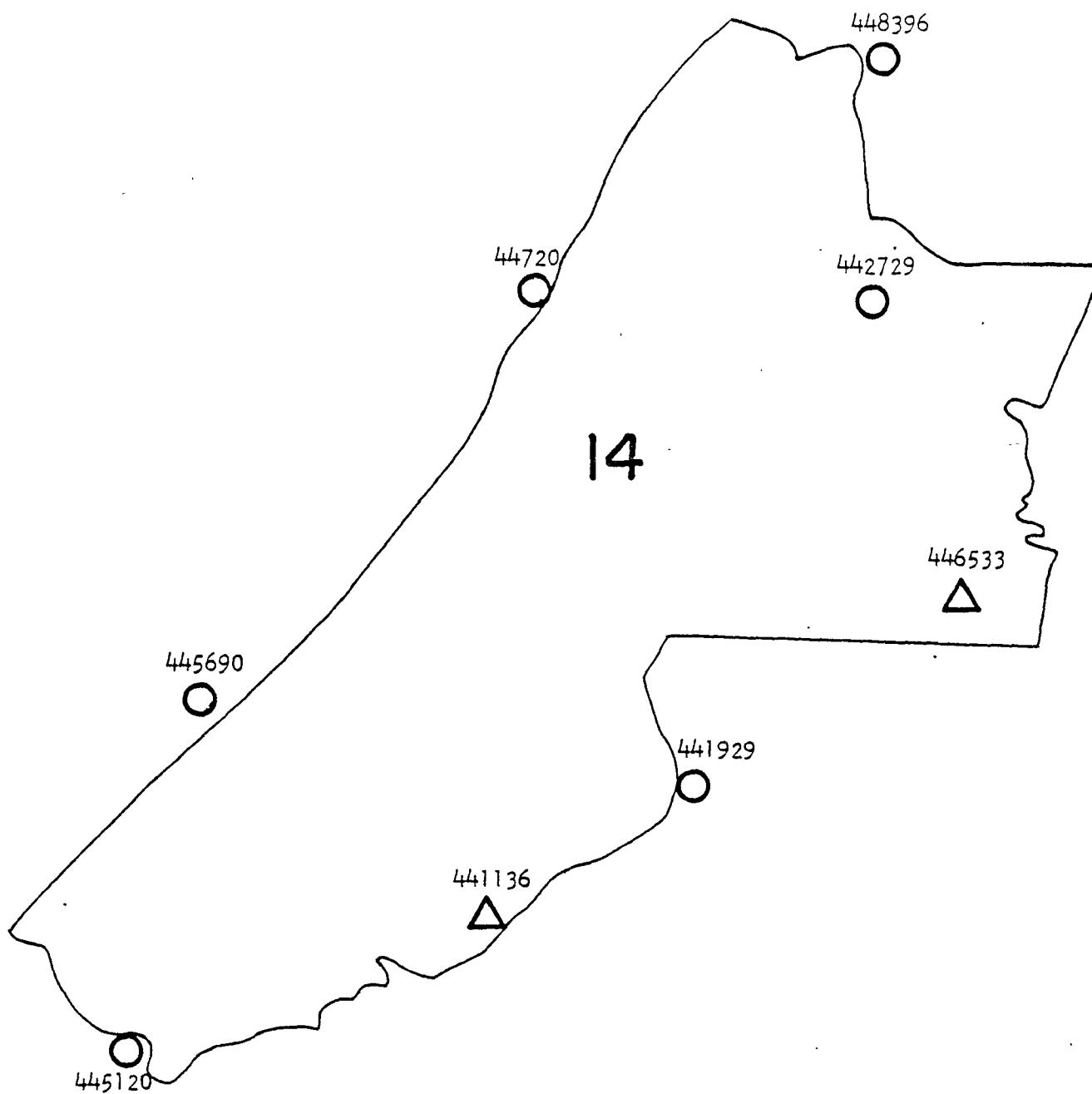
LEGEND		
○	HOURLY RAINGAGE	X SEGMENT NUMBER
△	DAILY RAINGAGE	xxxxxx GAGE NUMBER
		 MAP NOT TO SCALE

Figure A8




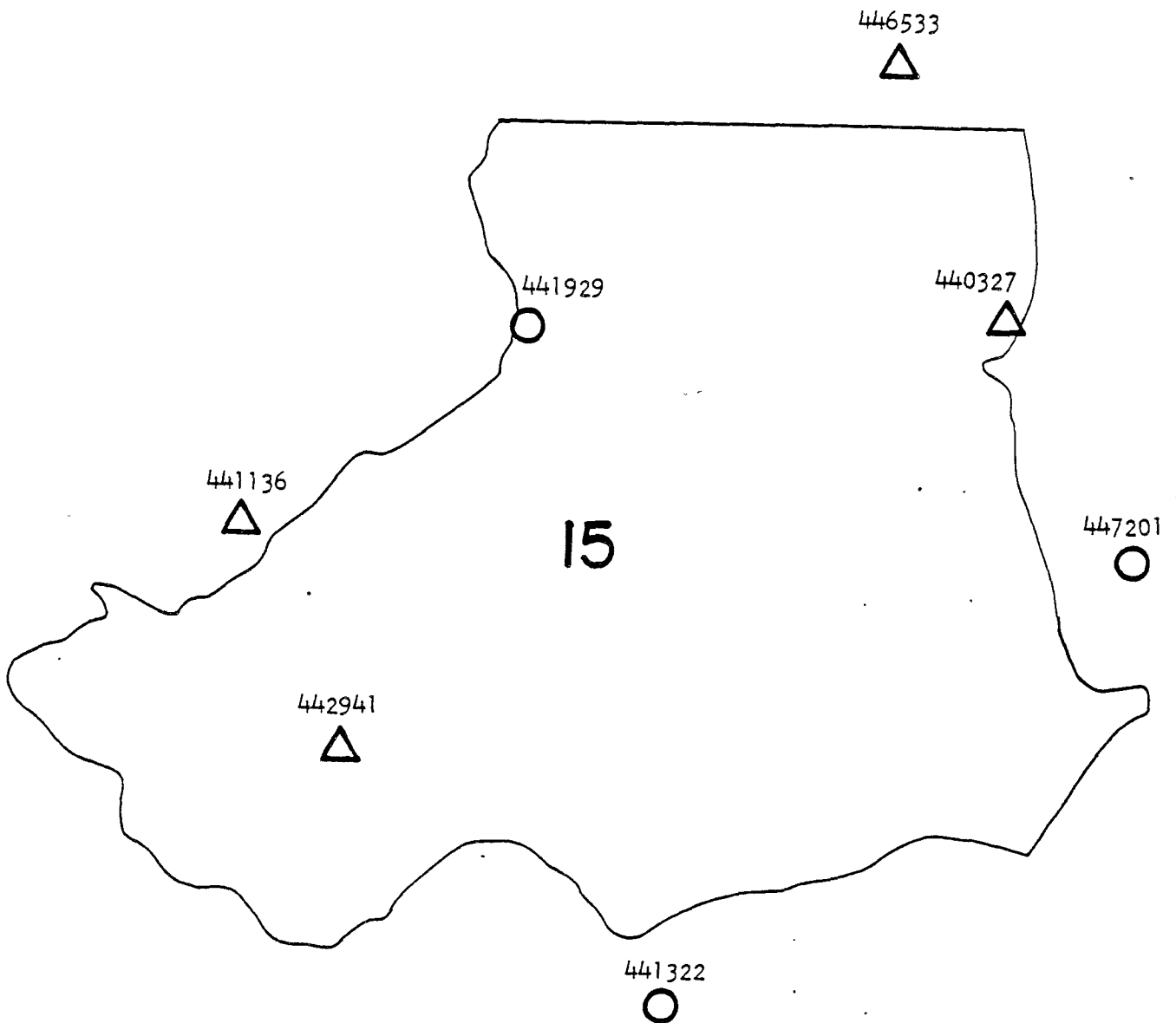
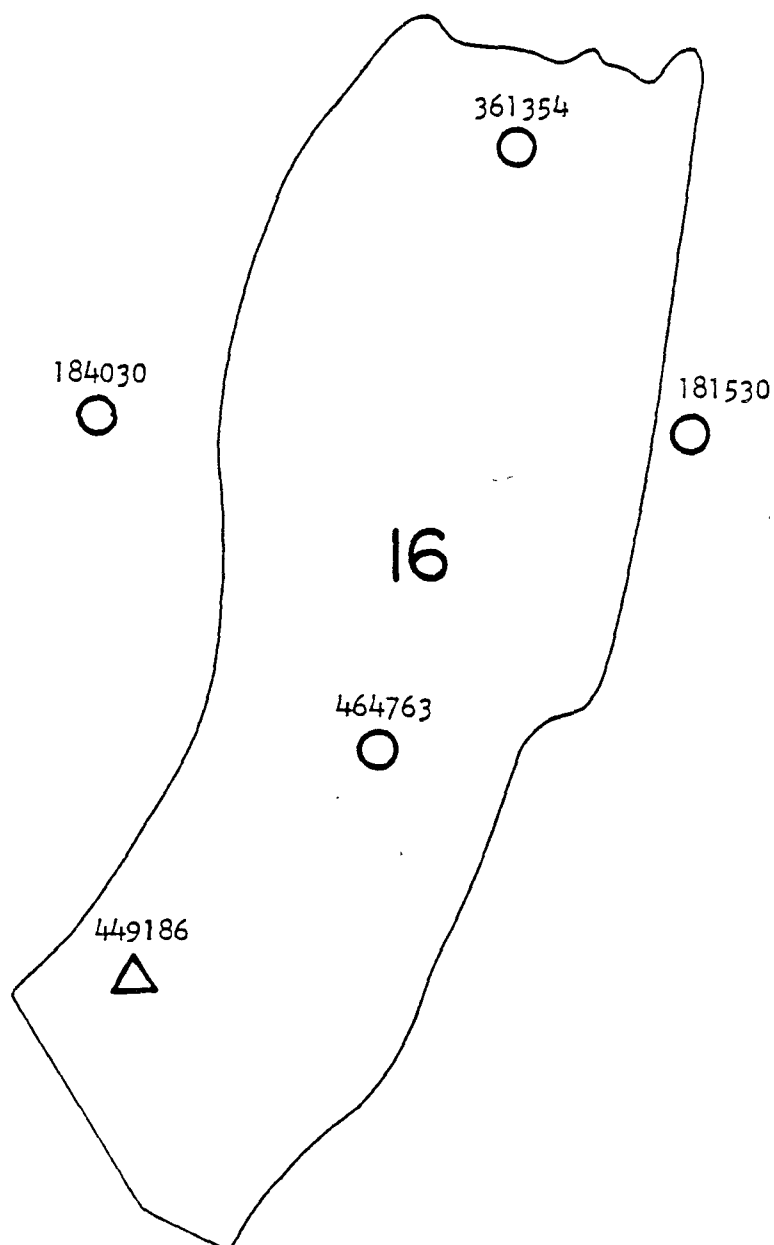
LEGEND		
○	HOURLY RAINGAGE	X SEGMENT NUMBER
△	DAILY RAINGAGE	xxxxxx GAGE NUMBER
		 MAP NOT TO SCALE

Figure 9



LEGEND		
○	HOURLY RAINGAGE	X SEGMENT NUMBER
△	DAILY RAINGAGE	xxxxxxx GAGE NUMBER
		MAP NOT TO SCALE

Figure 10




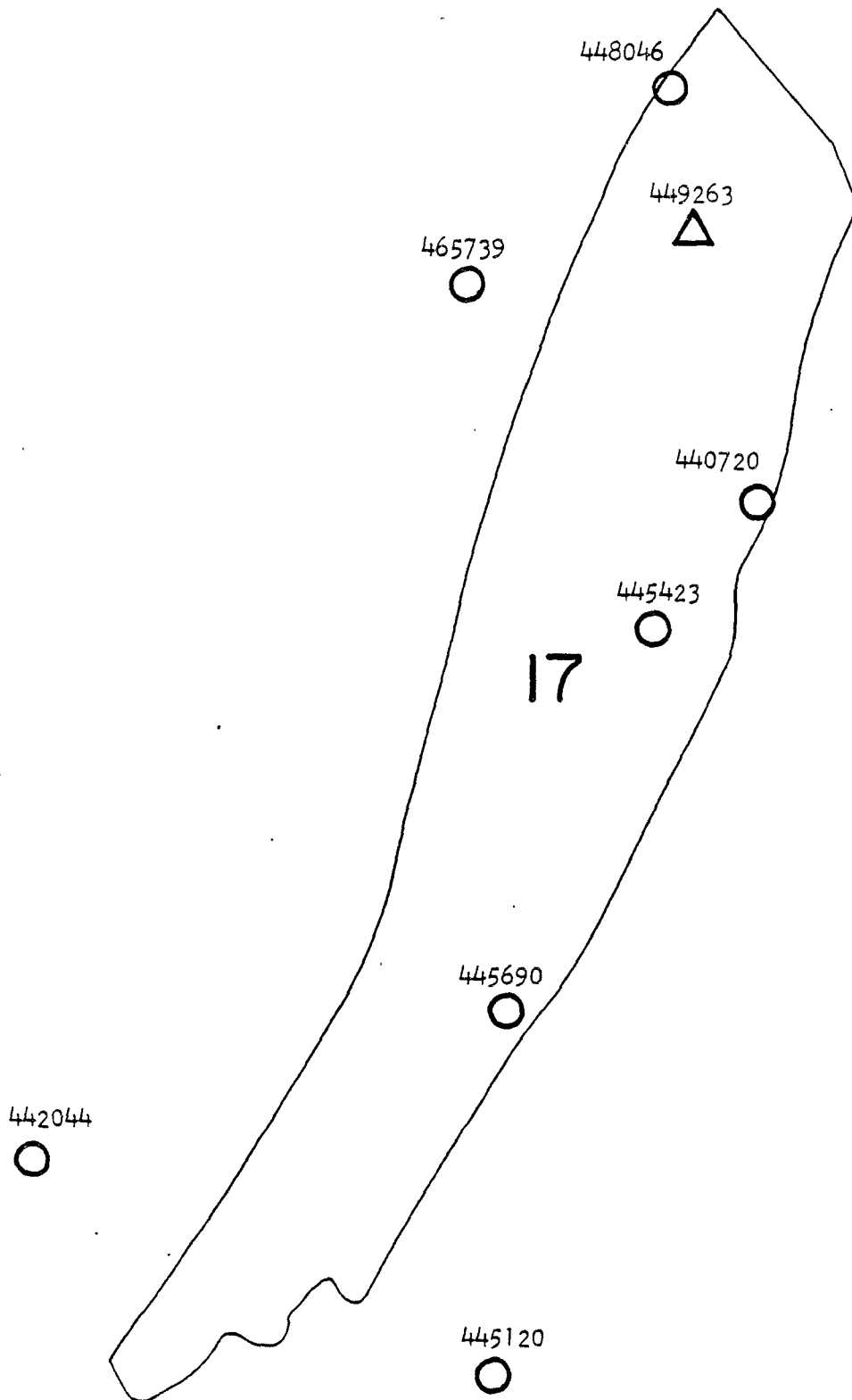
LEGEND		
○	HOURLY RAINGAGE	X SEGMENT NUMBER
△	DAILY RAINGAGE	xxxxxx GAGE NUMBER
		 MAP NOT TO SCALE

Figure 11




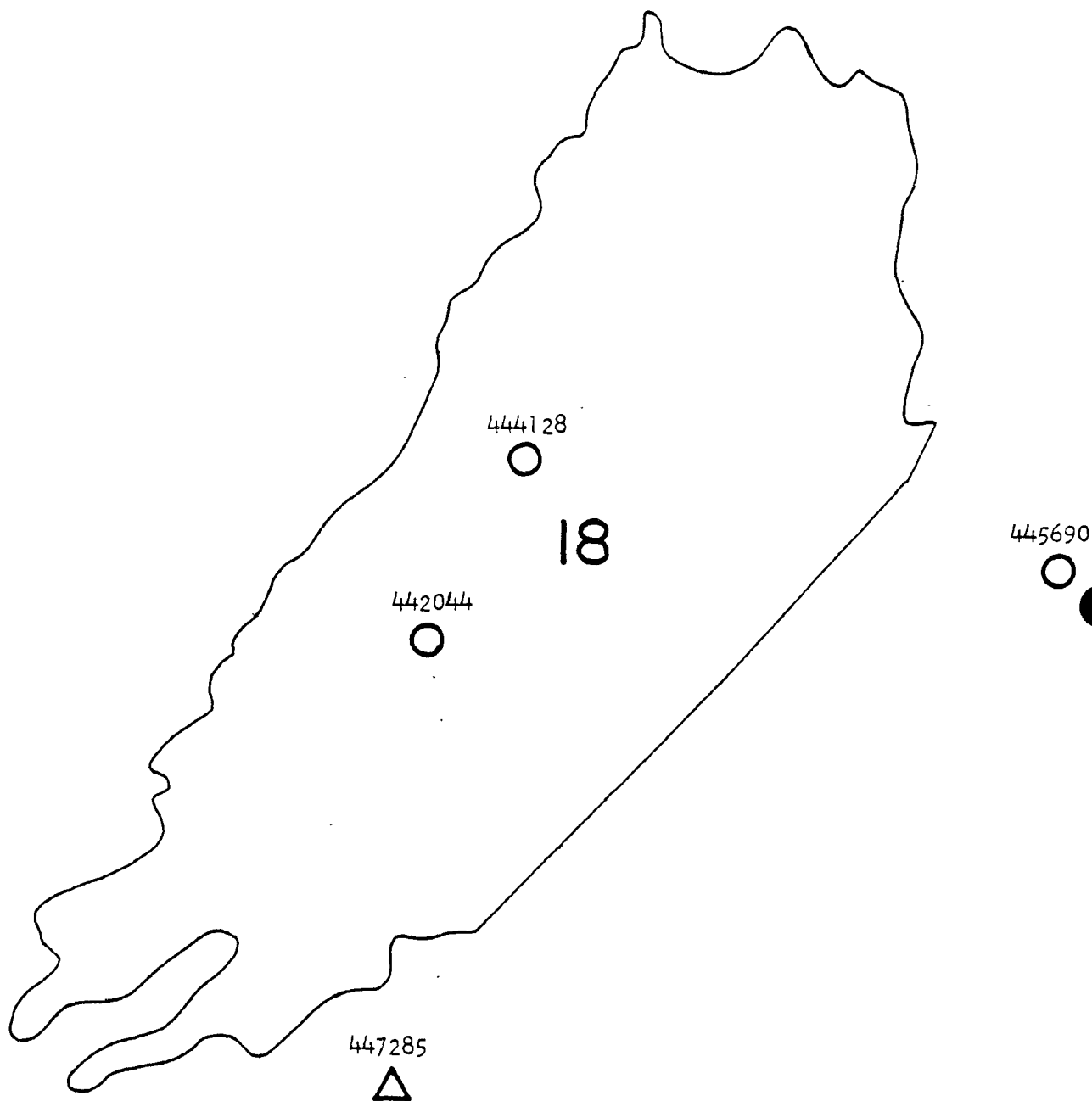
LEGEND		
○	HOURLY RAINGAGE	X SEGMENT NUMBER
△	DAILY RAINGAGE	xxxxxx GAGE NUMBER
		 MAP NOT TO SCALE

Figure 12




LEGEND		
○	HOURLY RAINGAGE	X SEGMENT NUMBER
△	DAILY RAINGAGE	xxxxxx GAGE NUMBER
		 MAP NOT TO SCALE

Figure 13

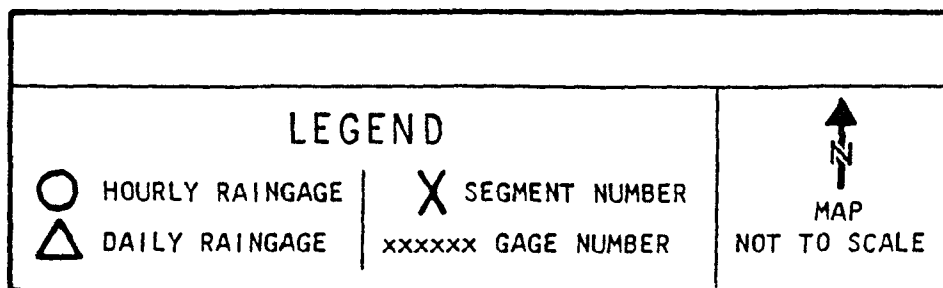
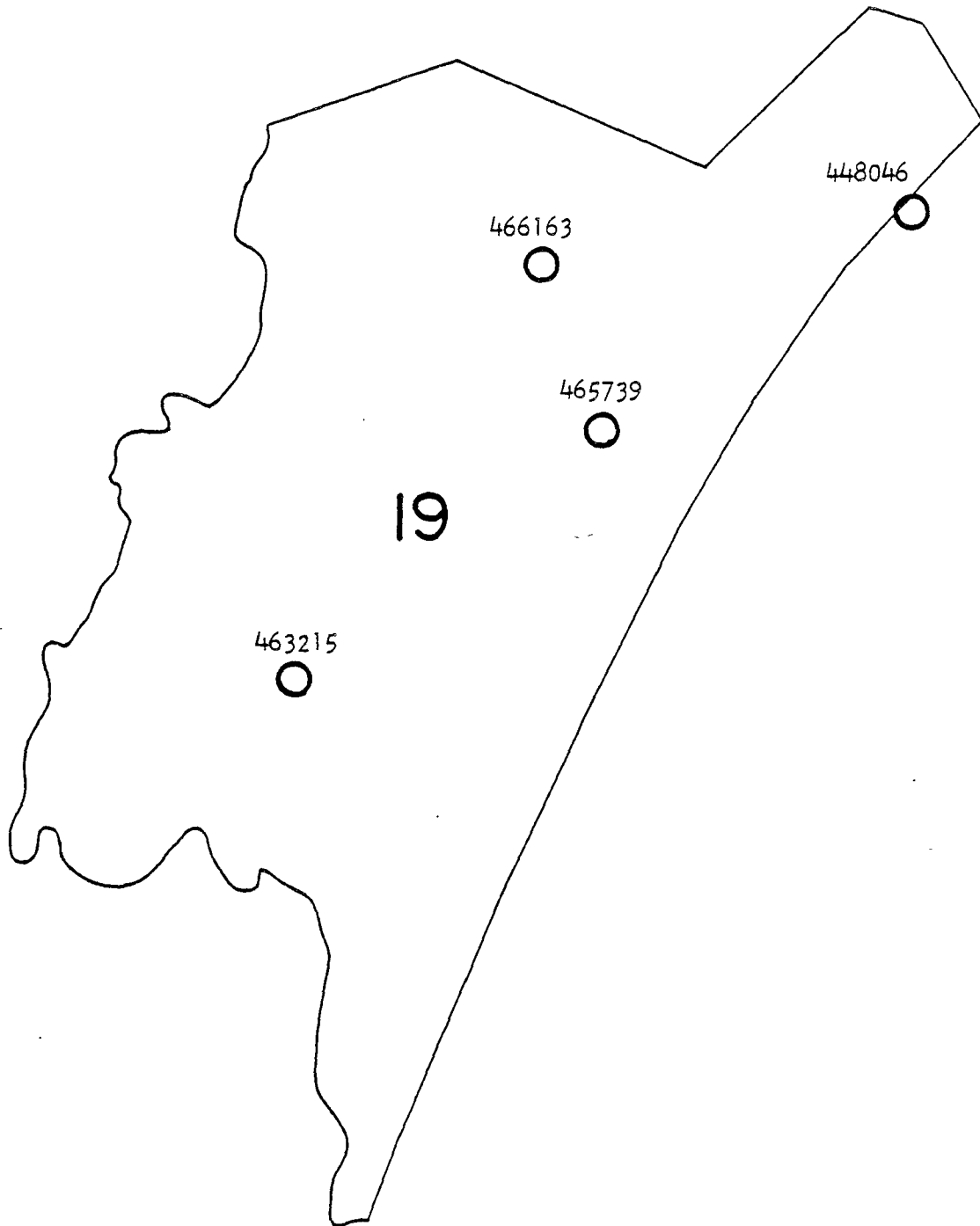


Figure 14

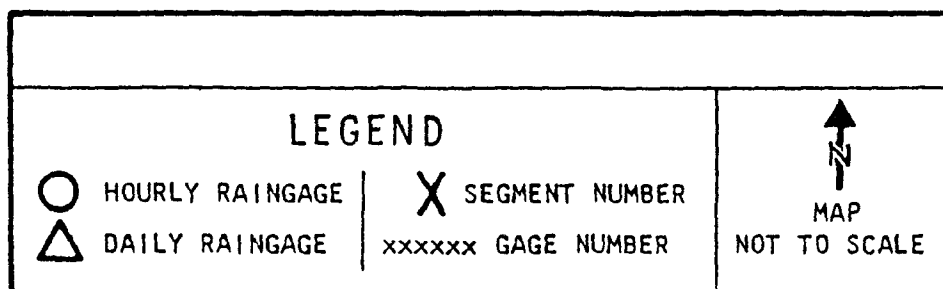
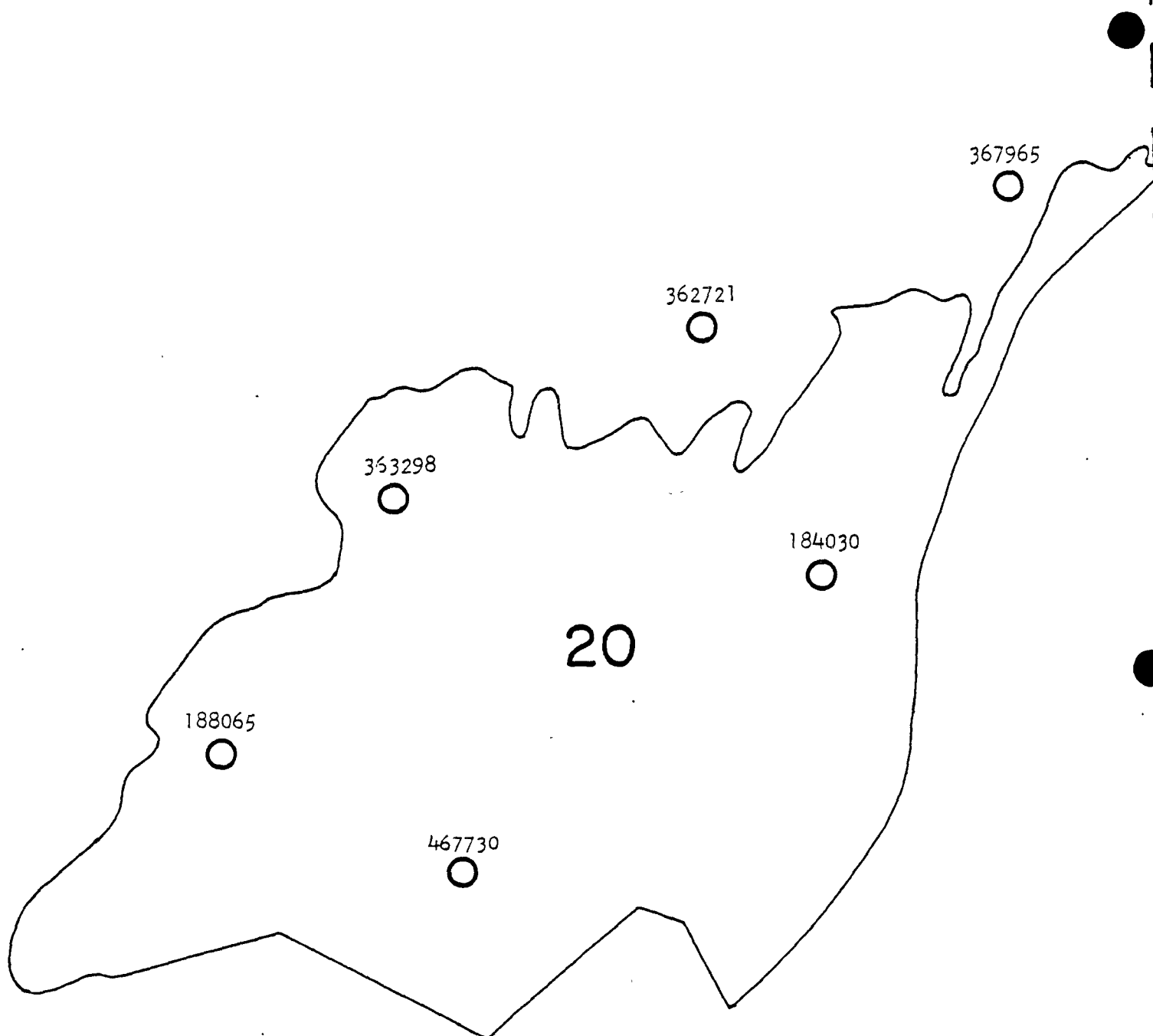


Figure 15

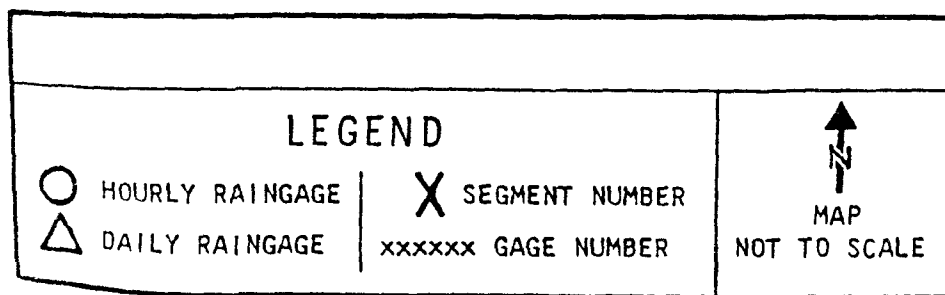
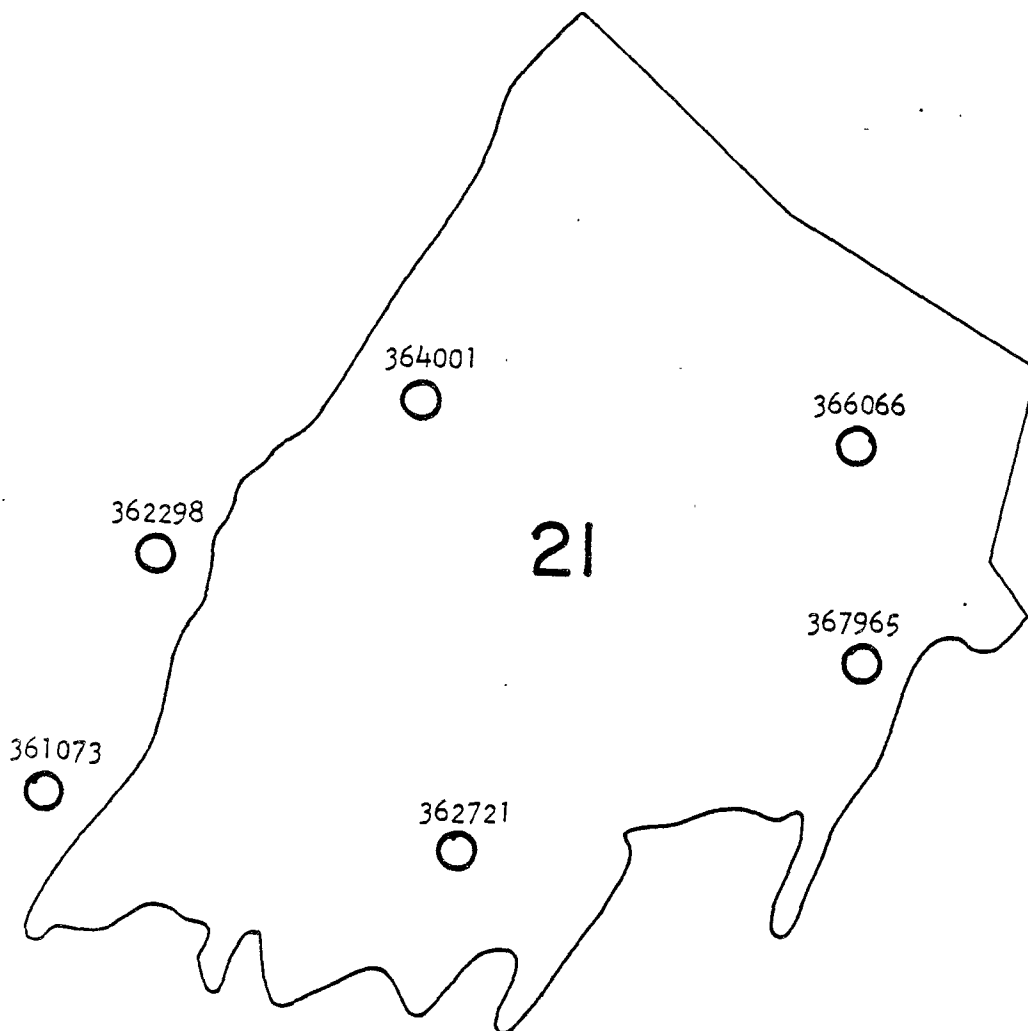
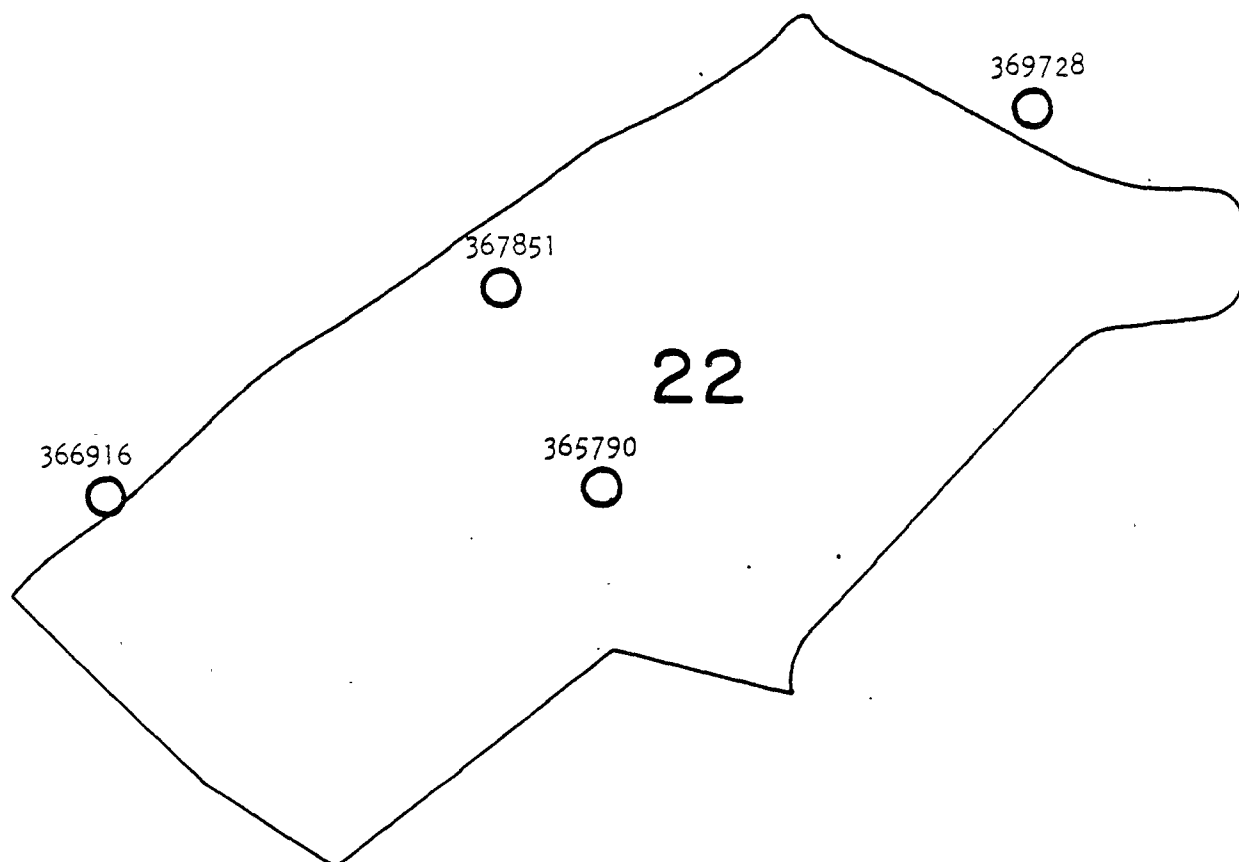


Figure 16




LEGEND		
○	HOURLY RAINGAGE	X SEGMENT NUMBER
△	DAILY RAINGAGE	xxxxxx GAGE NUMBER
		 MAP NOT TO SCALE

Figure 17

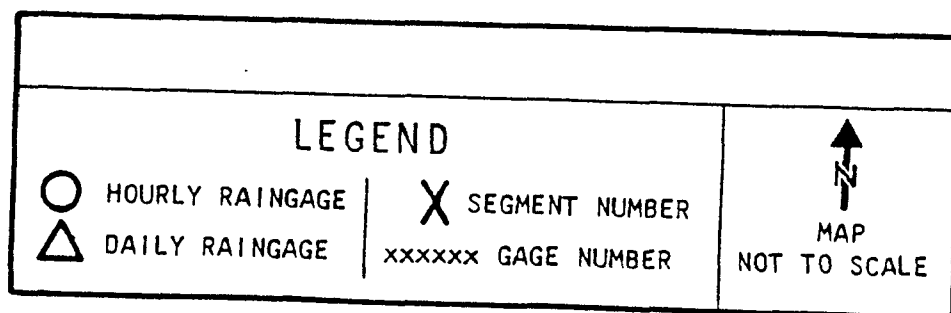
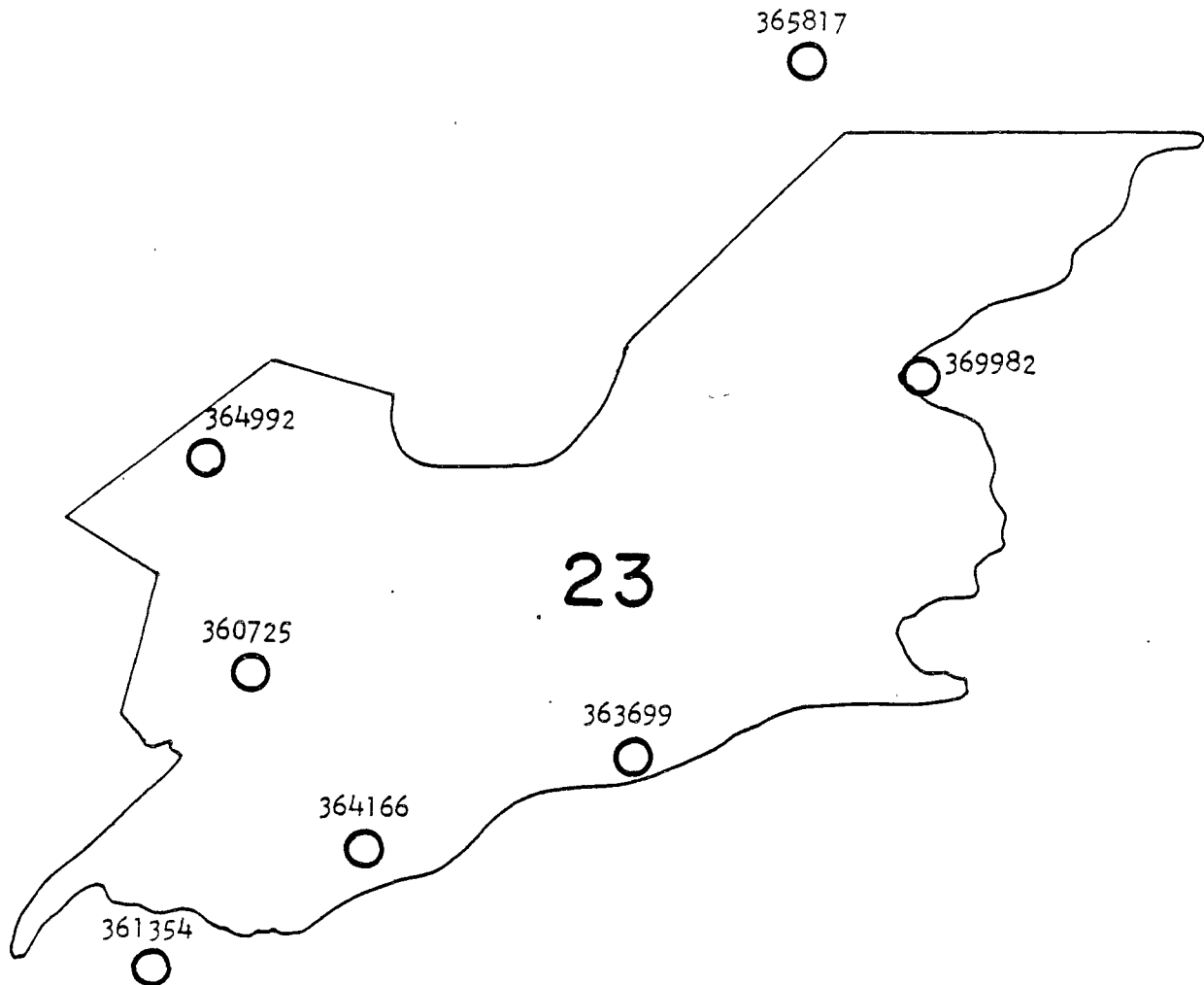


Figure 18

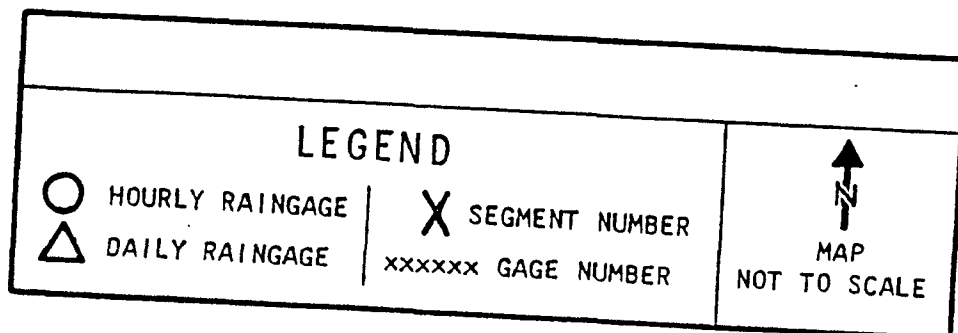
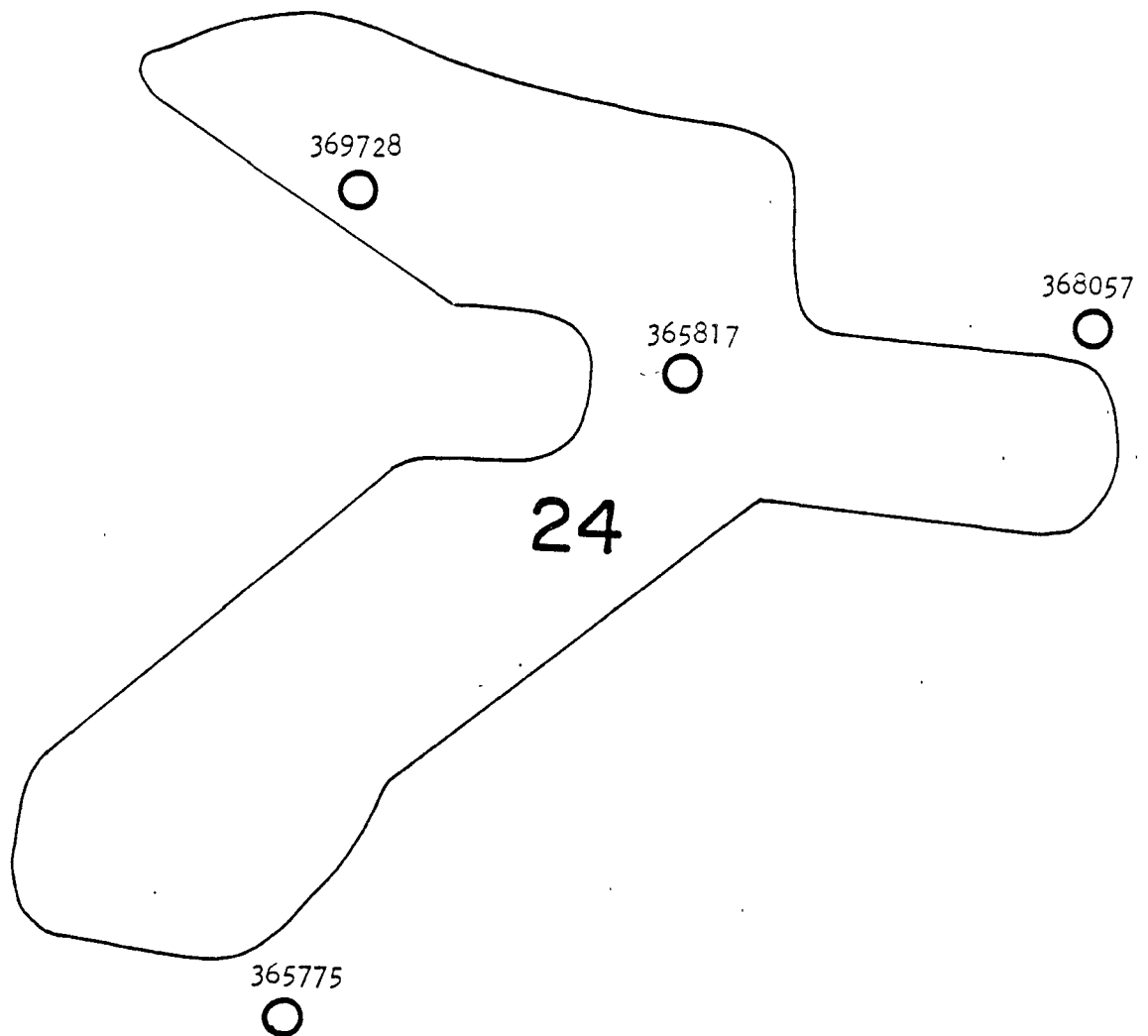
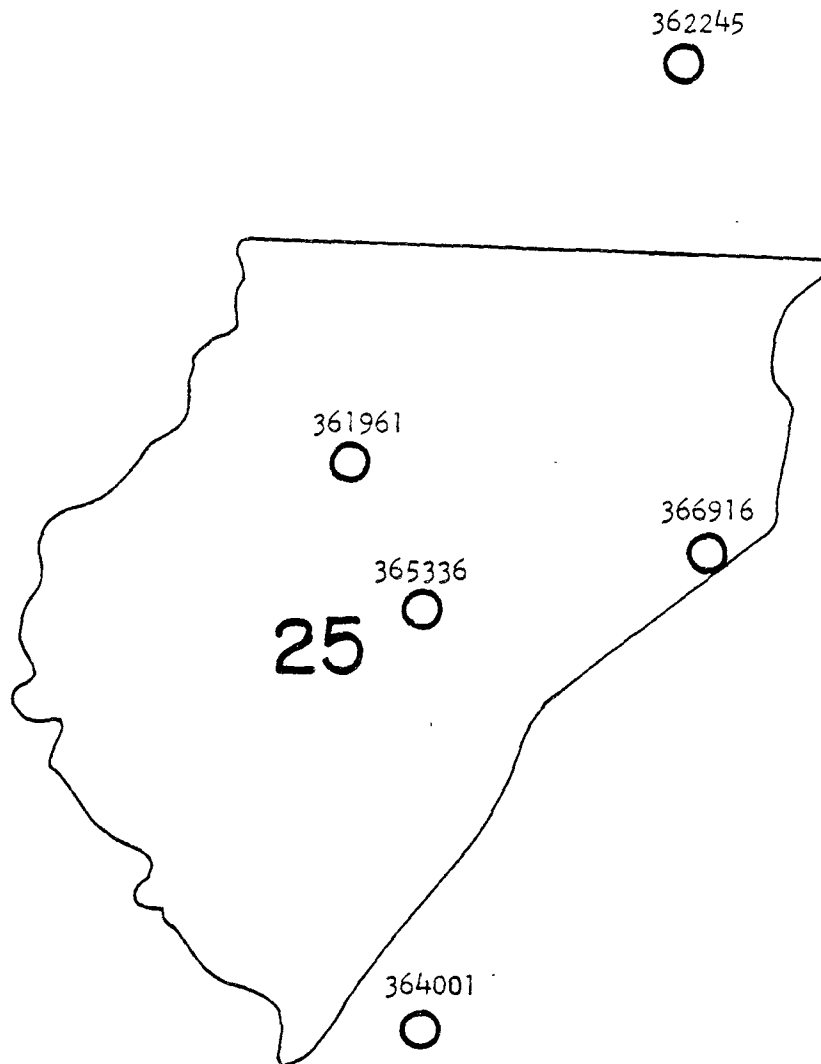
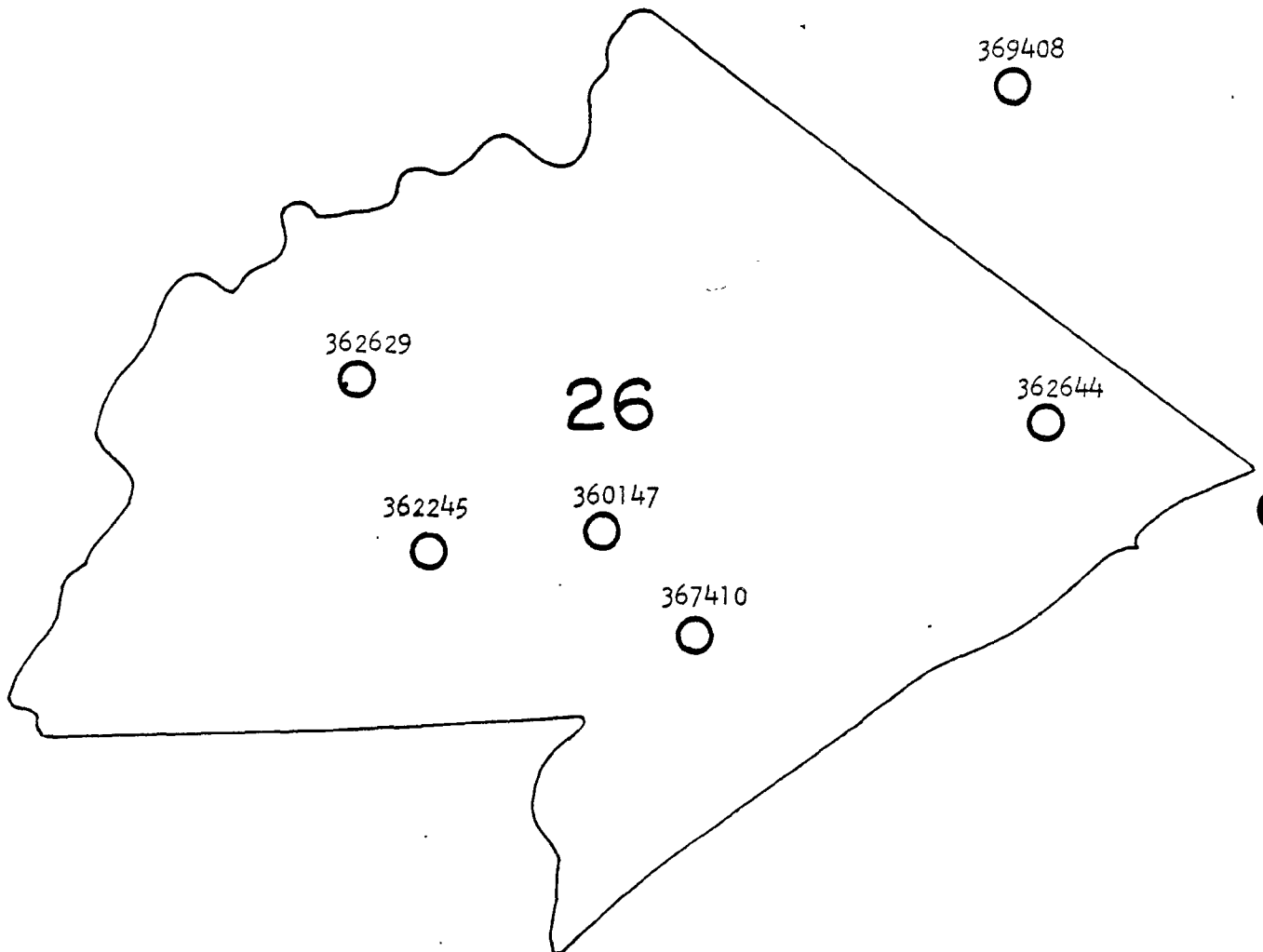


Figure 19



LEGEND		
○	HOURLY RAINGAGE	X SEGMENT NUMBER
△	DAILY RAINGAGE	xxxxxx GAGE NUMBER
		MAP NOT TO SCALE

Figure 20







LEGEND		
 HOURLY RAINGAGE	 SEGMENT NUMBER	 MAP NOT TO SCALE
 DAILY RAINGAGE	xxxxxx GAGE NUMBER	

Figure 21

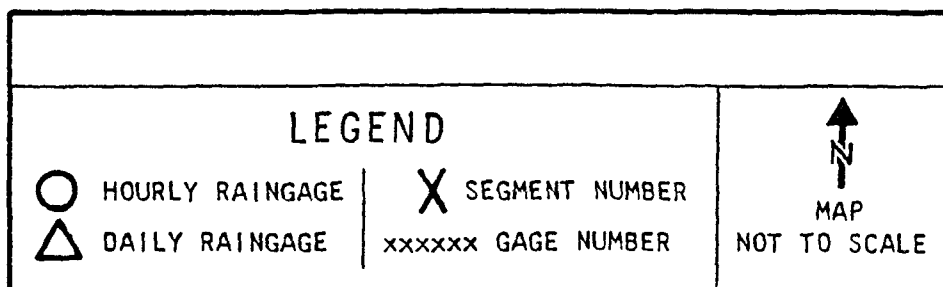
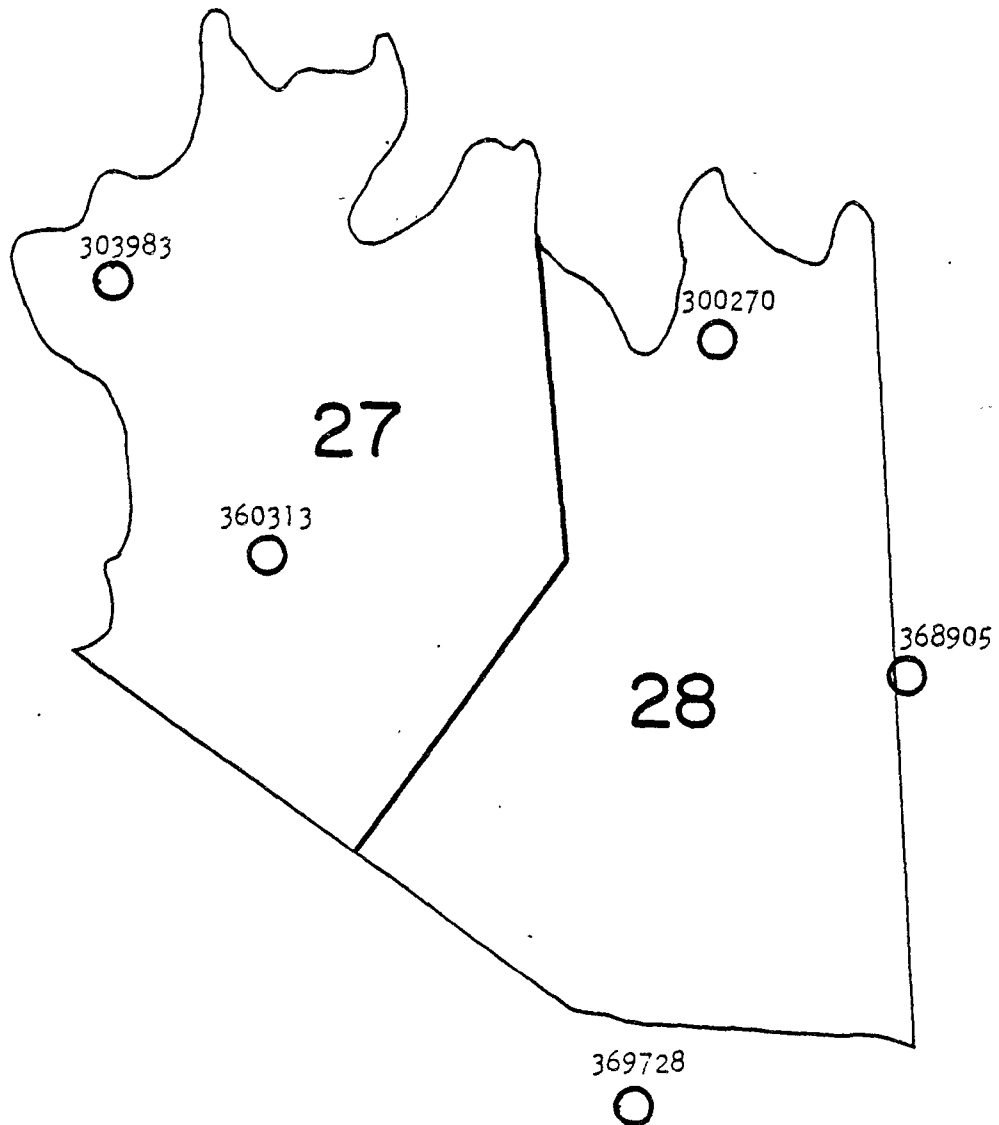
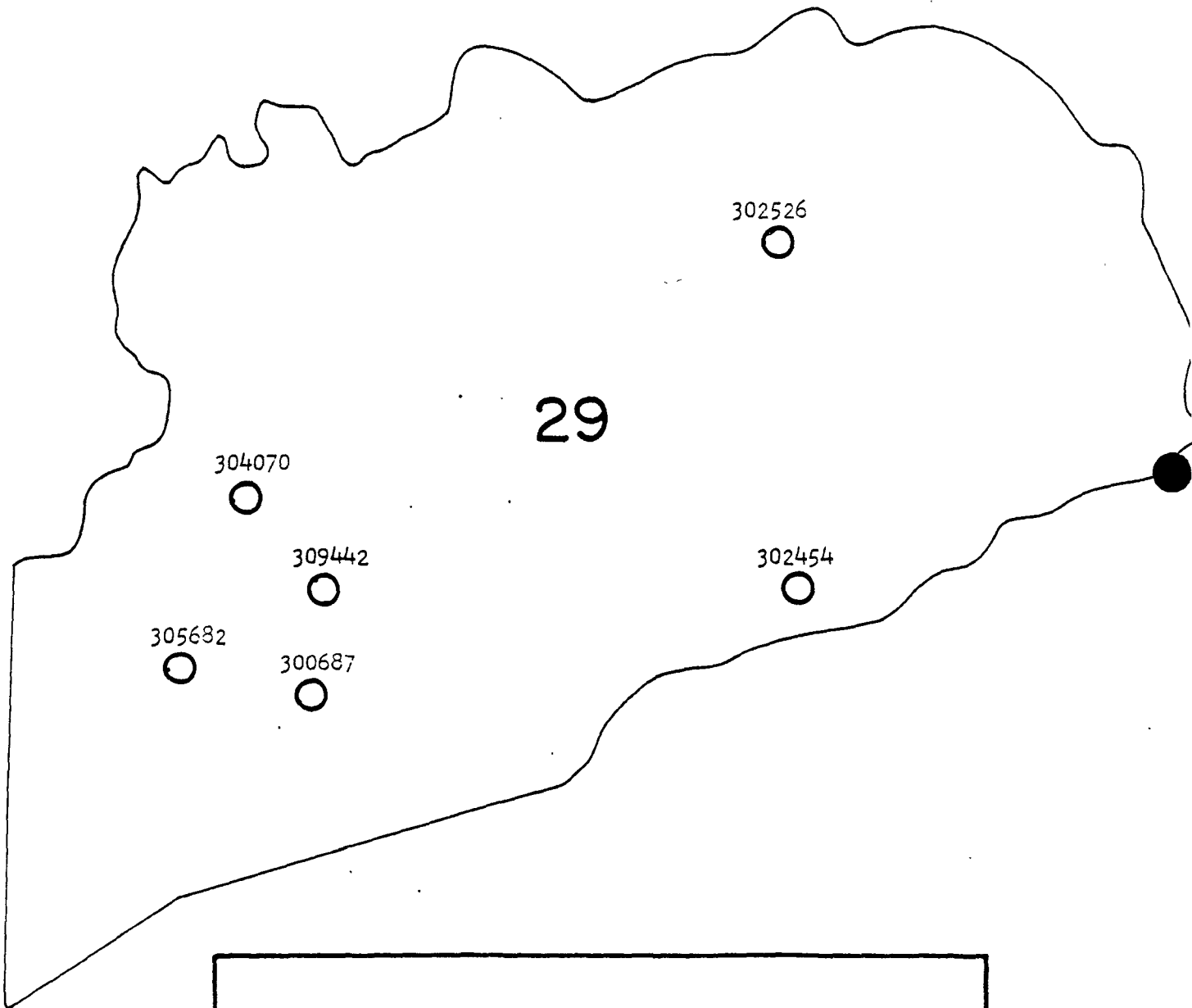


Figure 22







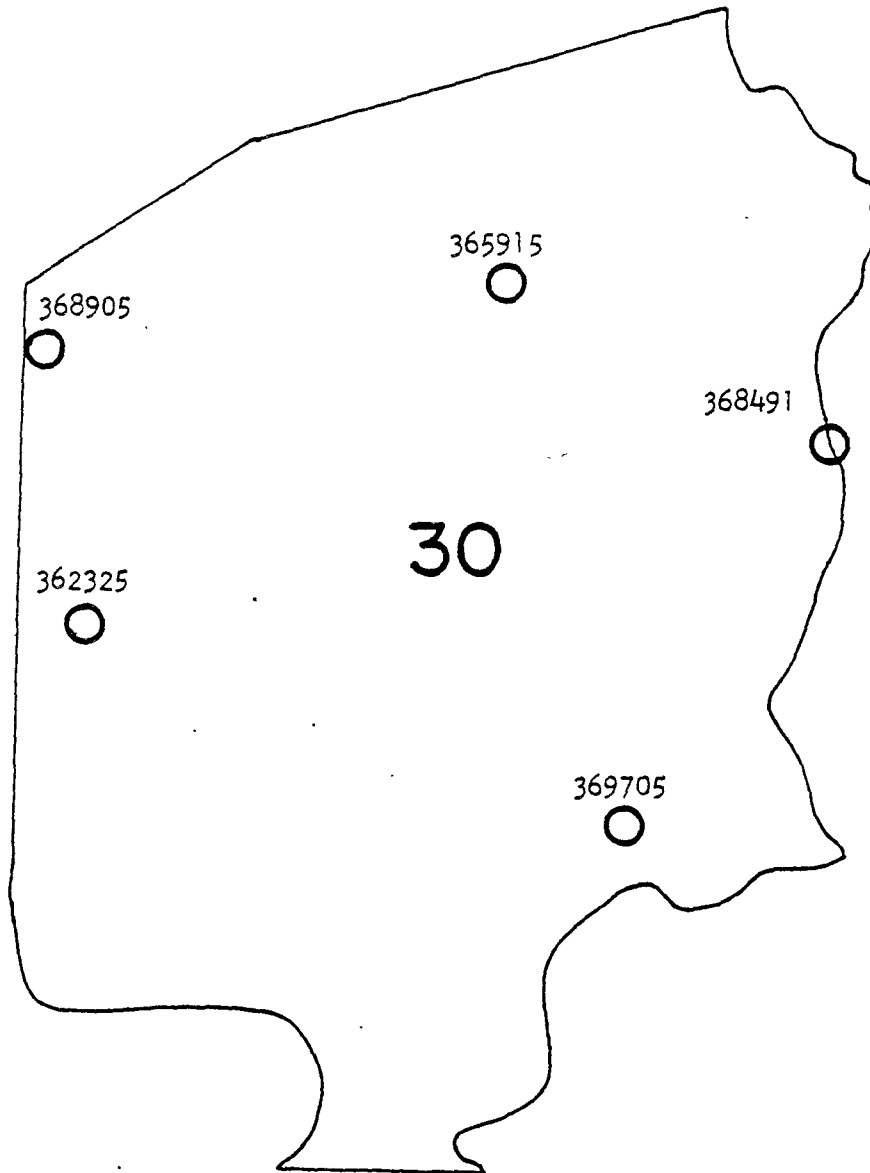
LEGEND		
	HOURLY RAINGAGE	 SEGMENT NUMBER
	DAILY RAINGAGE	xxxxxx GAGE NUMBER
		 MAP NOT TO SCALE

Figure 23



LEGEND		
○	HOURLY RAINGAGE	X SEGMENT NUMBER
△	DAILY RAINGAGE	xxxxxx GAGE NUMBER
		↑ N MAP NOT TO SCALE

APPENDIX B

LANDSAT LAND USE DATA ACQUISITION AND ANALYSIS

LANDSAT OVERVIEW

Landsat is a satellite data acquisition system dedicated to earth resource investigation. The three Landsat satellites are in circular, near polar orbits at an altitude of 570 miles (920 km). The orbit brings an individual satellite over the same point on the earth, at the same time of day, every 18 days. The satellites pass over the equator from north to south at approximately 9:30 a.m.

The primary sensor on Landsat is the Multispectral Scanner (MSS). The MSS collects data for each Landsat scene over an area 185 x 185 km (13,000 square miles). The data is collected in the following spectral bands:

Band 4	0.5 - 0.6 micrometers
Band 5	0.6 - 0.7 micrometers
Band 6	0.7 - 0.8 micrometers
Band 7	0.8 - 1.1 micrometers

which correspond to the colors blue-green, green-yellow, red, and near-infrared, respectively. The instantaneous field of view (INFOV) or resolution of the MSS is 79 meters x 56 meters. The data is collected in each of the four bands in west to east strips called scan lines in a Landsat scene. Each scan line is divided into picture elements (pixels) that are 56 meters in length. Hereafter, when referring to the location of individual pixels, a scan line will be called a line, and the elements in a scan line will be called samples. Therefore, each Landsat scene is comprised of over

7,500,000 pixels (3440 scan lines x 3300 PIXELS)
(LANDSAT SCENE SCAN LINE)

Each pixel has an area of 1.1 acres (79 meters x 56 meters); and there are 4 spectral reflectance values for each pixel.

Each land cover type (soil, vegetation, water, etc.) has a distinct spectral reflectance pattern called its spectral signature. Using the spectral signatures for each land cover, one can assign or "classify" each pixel to a land cover type from the pixel's spectral reflectance. For more information on Landsat, consult "Landsat Data Users Handbook," U.S. Geological Survey, 1200 South Eads Street, Arlington, VA or "Manual of Remote Sensing" by the American Society of Photogrammetry, 105 N. Virginia Avenue, Falls Church, VA.

OBJECTIVES

The objectives of this project were to:

- o Produce a Level I land cover classification from Landsat data of the Chesapeake Bay watershed.
- o Within the agricultural land cover, determine tillage practices.
- o Tabulate the land cover statistics by river subbasin.

GENERAL PROCEDURES

The land cover analysis was performed on the Eastern Regional Remote Sensing Application Center's (ERRSAC) Hewlett-Packard 3000 computer. The land cover dataset was developed using the Interactive Digital Image Manipulation System (IDIMS) and Geographic Entry System (GES) software packages.

An IDIMS file containing a whole Landsat scene was created for each of the twelve scenes covering the Chesapeake Bay drainage basin. For the eight Landsat scenes with dates prior to 1979, the known Landsat distortions were removed using IDIMS automated preprocessing programs (keskewing and rotating to true north). The three 1979 scenes were ordered in a geometrically correct format.

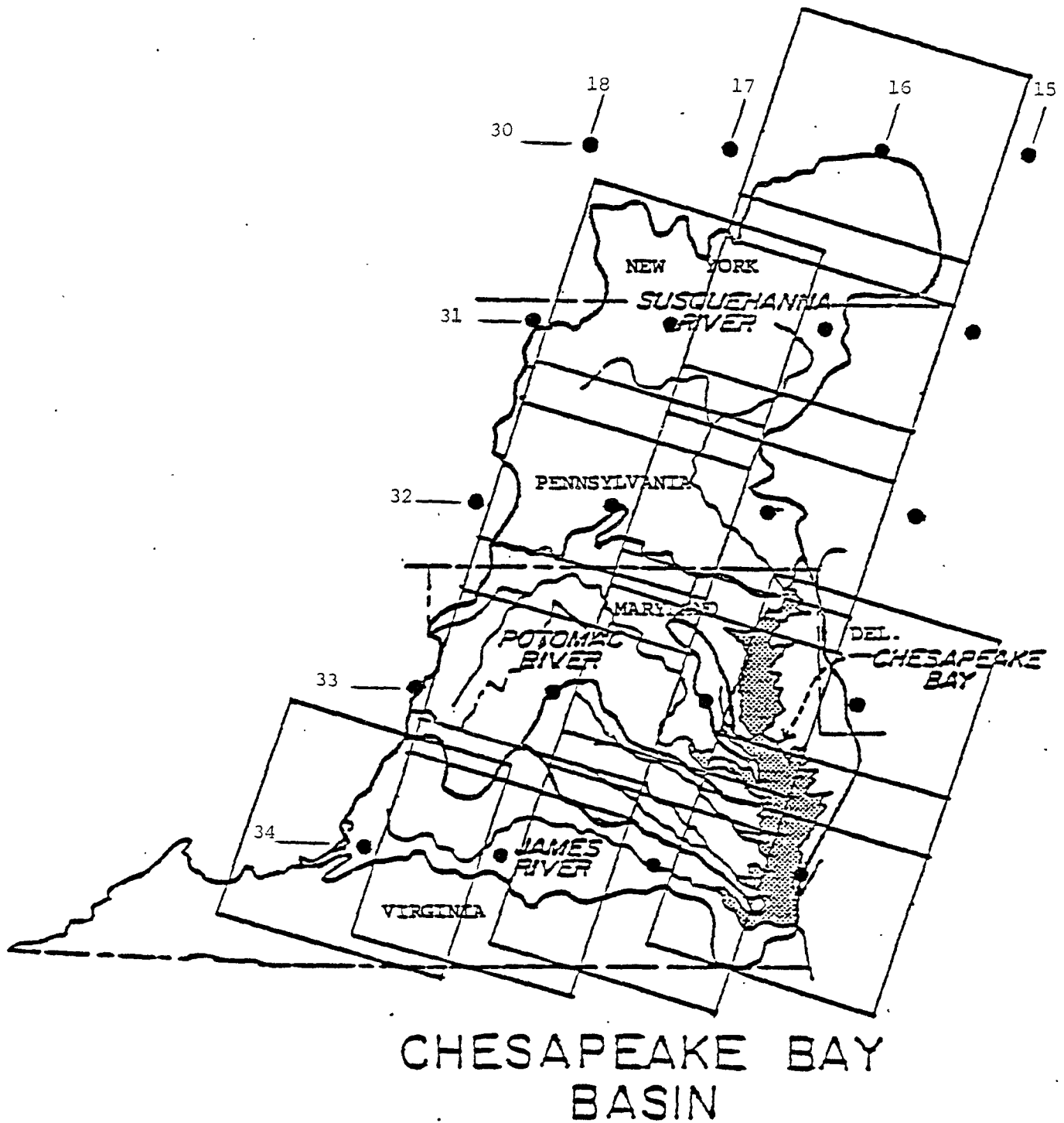
Each Landsat scene was divided into subscenes with similar physiographic and land cover characteristics. Land cover signatures were developed for each subscene from subsampled areas by an unsupervised classification program. The signatures from the unsupervised classification were used to produce a land cover map of the subscene. Figure B1 shows the subscene location and Table B1 the names of the images and Land Cover Spectral Signatures statfile for each of the Landsat scenes.

High altitude color infrared, high altitude black and white, and orthophotquads of ground truth sites were used to verify the land cover dataset. Thematic line printer maps (line printer maps with grouped spectral classes) were produced for each of the ground truth sites, and the verification work was done at the Northern Virginia Planning District Commission (NVPDC) office. If the land cover maps were not adequate, a supervised approach was used to augment the land cover signatures.

The digitized subbasin boundaries were registered and superimposed on the final land cover map. Pixel counts for each land cover type were tabulated by subbasin.

To establish the validity of the land cover statistics, the land cover statistics were compared with data from: NVPDC, Maryland State Planning, Susquehanna River Basin Commission, Soil Conservation Service Rockingham County, and Piedmont Planning District. In addition, eight sites of approximately four square miles each were randomly selected and their land cover statistics compared with land cover statistics interpreted from 1:222,000 scale color infrared photography.

Figure B1
LANDSAT SUBSCENE LOCATION



PATH-ROW	RAW-DATA SCENE NAME PIXEL SIZE IN METERS	SUB-SECTION DISTRIBUTION	TABLE B1 RAW DATA SUB-SCENE NAME	CLASSIFIED SUB-SCENE NAME	STAT-FILE
16 - 30	CORTLAND	<div> <div>LH</div> <div>RH</div> </div>	CORTLAND.LH	CORTLAND.LH.CLASFY	JMCORTLH
	57x79		CORTLAND.RH	CORTLAND.R.H.CLASFY	JMCORTRH
16 - 31	SCRANTON	<div> <div>UH</div> <div>LH</div> </div>	SCRANTON.UH	SCRANTON.UH.CLASFY	JMSCRAUH
	57x79		SCRANTON.LH	SCRANTON.L.H.CLASFY	JMSCRALH
17 - 31	WILLIAMSPORT	<div> <div>UL</div> <div>UR</div> <div>LL</div> <div>LR</div> </div>	WILLIAMSPORT.UL	WILLIAMSPORT.UL.CLASFY1	JMWILLUL
	57x79		WILLIAMSPORT.UR	WILLIAMSPORT.UR.CLASFY	JMWILLUR
			WILLIAMSPORT.LL	WILLIAMSPORT.LL.CLASFY1	JMWILLLL
			WILLIAMSPORT.LR	WILLIAMSPORT.LR.CLASFY	JMWILLLR
16 - 32	HARRISBURG	<div> <div>UL</div> <div>UR</div> <div>LL</div> <div>LR</div> </div>	HARRISBURG.UL	HARRISBURG.UL.CLASFY2	JMHARRUL
	57x79		HARRISBURG.UR	HARRISBURG.UR.CLASFY	JMHARRUL
			HARRISBURG.LL	HARRISBURG.LL.CLASFY1	JMHARRLL
			HARRISBURG.LR	HARRISBURG.LR.CLASFY	JMHARRLR

TABLE B1 (contd.)

RAW-DATA SCENE NAME PIXEL SIZE IN METERS		SUB-SECTION DISTRIBUTION		TABLE B1 (contd.) RAW DATA SUB-SCENE NAME		CLASSIFIED SUB-SCENE NAME		STAT-FILE	
17 - 32	ALTOONA	UL	UR	ALTOONA.UL	ALTOONA.UL.CLASFY			JMALTOUL	
	57x79			ALTOONA.UR	ALTOONA.UR.CLASFY			JMALTOUR	
		LL	LR	ALTOONA.LL	ALTOONA.LL.CLASFY			JMALTOLL	
				ALTOONA.LR	ALTOONA.LR.CLASFY			JMALTOLR	
15 - 33	SALISBURY		UH	SALISBURY.UH	SALISBURY.UH.CLASFY			JMSALIUH	
	57x57			SALISBURY.LH	SALISBURY.LH.CLASFY			JMSALILH	
			LH						
16 - 33	FILE1	UL	UR	WASH.UL	WASH.UL.CLASFY			JMWASHUL	
	57x79			WASH.UR	WASH.UR.CLASFY			JMWASHUR	
		LL	LR	WASH.LL	WASH.LL.CLASFY			JMWASHLL	
				WASH.LR	WASH.LR.CLASFY			JMWASHLR	
17 - 33	FRONT.ROYAL	UL	UR	FRONT.ROYAL.UL	FRONT.ROYAL.UL.CLASFY			JMFRONUL	
	57x79			FRONT.ROYAL.UR	FRONT.ROYAL.UR.CLASFY			JMFRONUR	
		LL	LR	FRONT.ROYAL.LL	FRONT.ROYAL.LL.CLASFY1			JMFRONLL	
				FRONT.ROYAL.LR	FRONT.ROYAL.LR.CLASFY			JMFRONLR	

PATH-ROW	RAW-DATA SCENE NAME PIXEL SIZE IN METERS	SUB-SECTION DISTRIBUTION	TABLE B1 (contd.) RAW DATA SUB-SCENE NAME	CLASSIFIED SUB-SCENE NAME	STAT-FILE
15 - 34	NORFOLK	<div> <div>UL</div> <div>UR</div> <div>LH</div> </div>	NORFOLK.UL	NORFOLK.UL.CLASFY	JMNORFUL
	57x57		NORFOLK.UR	NORFOLK.UR.CLASFY	JMNORFUR
			NORFOLK.LH	NORFOLK.LH.CLASFY2	JMNORFLL
16 - 34	RICHMOND	<div> <div>UL</div> <div>UR</div> <div>LL</div> <div>LR</div> </div>	RICHMOND.UL	RICHMOND.UL.CLASFY	JMRICHUL
	57x79		RICHMOND.UR	RICHMOND.UR.CLASFY	JMRICHUR
			RICHMOND.LL	RICHMOND.LL.CLASFY	JMRICHLL
			RICHMOND.LR	RICHMOND.LR.CLASFY1	JMRICHLR
17 - 34	LYNCHBURG	<div> <div>LH</div> <div>RH</div> </div>	LYNCHBURG.LH	LYNCHBURG.LH.CLASFY1	JMLYNCLH
	57x57		LYNCHBURG.RH	LYNCHBURG.RH.CLASFY	JMLYNCRH
18 - 34	ROANOKE	<div> <div>RH</div> </div>	ROANOKE.RH	ROANOKE.RH.CLASFY	JMROANRH
	57x79				

CRITERIA FOR SELECTING LANDSAT SCENES

The criteria for Landsat scene selection were determined by the requirements of the Chesapeake Bay fluvial model. The land cover dataset needed to be a USGS Level I, present use, land cover classification. Within the agricultural class, minimum and conventional tillage as well as pasture land covers needed to be identified. A study was undertaken to determine the feasibility of developing two land cover datasets for the Chesapeake Bay Basin: a more detailed land cover dataset developed from a multitemporal analysis for areas with an estimated river transport time to the Bay of less than 5 days; and a less detailed dataset developed from a single date for all other areas. The multitemporal was to be done at ERRSAC by NVPDC personnel and the single data work by Kennedy Space Center (KSC). After meeting with Kennedy Space Center personnel, it was mutually agreed that KSC did not have the resources to participate in the project. Therefore, it was planned that a single land cover database for the entire Chesapeake Bay Basin would be developed at ERRSAC by NVPDC and that it would not use the multitemporal approach. After discussions with District Conservationists and Agriculture Extension Agents from Fauquier, Fairfax, Loudoun, and Prince William Counties in Virginia and Agricultural Engineers from the University of Maryland, it was decided that only Landsat scenes from 1977 to the present would adequately reflect present agricultural practices. To differentiate between minimum and conventional tillage practices, the Landsat scenes' date had to be after spring planting but before the crop cover reached 20%. To minimize the amount of undefined land cover, only Landsat scenes with a cloud cover of 10% or less were used.

Table B2 lists the Landsat scenes in possession of the Chesapeake Bay Program. "Used in study" denotes the scenes used in the development of the land cover database. "Quality" denotes the image quality on a scale of 1 to 8 for bands 4, 5, 6, and 7, respectively.

There are six areas--three in Virginia, one in Pennsylvania and two in New York--where there is not total coverage of Chesapeake Bay Basin by the Landsat scenes. In Virginia's George Washington National Forest near Back Creek Mountain, there is an area of approximately 250 square miles that is not covered. This area is over 95% forested, and it is not covered because the Front Royal and Roanoke Landsat scenes do not overlap. There are two small portions of the drainage basin south of Norfolk, Virginia that are not covered by the Norfolk Landsat scene. They are about 15 square miles each. One is west of the Dismal Swamp and south of Route 58; the other is east of Dismal Swamp and south of Great Bridge, Virginia. The missing area west of Dismal Swamp is about 80% forest, and the area east of the Dismal Swamp is predominately marsh. On the West Branch Susquehanna River south of Curwensville, Pa., there is an area of approximately 300 square miles which is 85% forested that is not covered by the Altoona Landsat scene. In New York State there are two areas which fall outside of the Williamsport Landsat scene. The first is an area of approximately 150 square miles that is west of Kenka Lake and north of Avoca; the second is 25 square miles in area and is east of Kenka Lake and north of Weston. Both areas are predominately agriculture. For each of the missing areas it was assumed that the ratio of land cover types within the missing areas was the same as that for the entire subbasin.

TABLE B2
EPA/CBP AVAILABLE LANDSAT CCT'S

<u>TAPE NUMBERS</u>	<u>PATH ROW</u>	<u>SCENE I.D.</u>	<u>DATE</u>	<u>CLOUD COVER</u>	<u>QUALITY</u>	<u>USED IN STUDY</u>
21	15-33	30422-15025	5-1-79	10%	8888	*
22	15-34	30422-15031	5-1-79	0%	8888	*
23	16-30	28321-44815	5-3-77	10%	8888	*
24	16-31	28141-44935	4-15-77	10%	8888	*
25	16-32	21192-14425	4-28-78	10%	5888	*
26		28681-44715	6-8-77	10%	8888	
27	16-33	21192-14432	4-28-78	10%	8888	*
28	16-34	28501-44855	5-21-77	10%	8888	*
29		21192-14434	4-28-78	0%	8888	
30	17-31	21193-14482	4-29-78	10%	8858	*
31	17-32	30082-15125	5-26-78	0%	8888	
32		28151-45545	4-16-77	0%	8888	
33	17-33	28151-45605	4-16-77	0%	5888	*
34		21229-14505	6-4-78	10%	8888	
35		30082-15131	5-26-78	10%	5888	
36	17-34	21589-15062	5-30-79	10%	8888	*
37	18-34	30101-15193	6-14-78	10%	8588	*

LAND COVER SIGNATURE DEVELOPMENT

An unsupervised classifier was the first step in developing land cover signatures for each subscene. Only spectral data from every other line and sample pixel (within a subscene) were used as input to the unsupervised classifier. The unsupervised classifier, using an iterative clustering algorithm, grouped the spectral data into 50 unique spectral classes. The statistics from the 50 classes (mean, variance, and covariance in the 4 spectral bands) were used as the land cover signatures and stored in a statfile. The entire subscene (every line and sample) was then classified by a "maximum likelihood" classifier using the signatures generated by the unsupervised classifier.

Thematic line printer maps were output for the various ground truth sites within each subscene. The line printer map in conjunction with the ground truth were used to assign each of the 50 spectral classes to one of the following land cover classes: undefined (clouds and shadows), forest, winter agriculture, conventional tillage, minimum tillage, pasture, water, marsh, urban, strip mine, and idle land.

If all the land cover classes were not adequately represented by the 50 spectral classes developed by the unsupervised classifier, a supervised approach was used to develop the missing land cover signature. The supervised signature development was done at ERRSAC and the typical procedure was:

1. The Landsat data corresponding to the ground truth site was displayed on a color cathode ray tube (CRT).
2. Training sites (locatable areas on a Landsat scene with distinct spectral features) for the missing land cover classes were selected

and their statistics calculated and appended to the existing statfile.

3. The subscene was reclassified using the updated statfile.
4. The resulting classified subscene was examined on the CRT and checked with ground truth.
5. If the new classification was not adequate, steps 2-4 were repeated.

When a satisfactory land cover classification was developed for all 36 subscenes, the data was overlaid with the geographic data and tabulated.

GEOGRAPHIC ENTRY OVERVIEW

In order to facilitate the registration of ground data to Landsat imagery, the Geographic Entry System (GES) was used. GES is an interactive system capable of entering, editing, and storing geographic information taken directly from a map surface. GES has no analytical capabilities. Its only purpose is to allow geographic information to be put into a data structure that is accessible to other programs such as IDIMS.

The GES program uses three storable entities as it acquires geographical information. They are points, lines, and polygons. Discrete points consist of a coordinate and a point name. Such points may be used as ground control points for use in generating registration transformations between ground data and digital imagery. Discrete lines consist of a series of coordinates. Discrete lines are useful for digitizing roads, pipelines, trails, and to a limited extent, contour lines. Polygons consist of lines that intersect at nodes called junction points. Polygons may be used to digitize any geographic boundary.

The GES program can also construct a latitude/longitude or UTM base grid. The grid facility is very useful for cell by cell stratification of data.

All digitized information in GES is done with reference to a "geoblock." A geoblock is a rectangular subsection of the earth's surface whose edges are oriented N-S and E-W.¹ The user defines the position and dimensions of the geoblock, and then the GES program creates an internal representation of the geoblock and superimposes a grid over it. The grid's

¹"Data Stratification and the Geographic Entry System: A User's Manual," ESL Inc. Technical Memo. ESL-TM 991, 1978.

individual cells are called internal units. As a result, ground resolution varies with the geoblocks's size. When the size of the geoblock increases, the ground resolution, as defined by the internal units, decreases. GES also recognizes three additional coordinate systems: latitude/longitude, UTM, and digitizer coordinates.

The data digitized in GES is stored in six different Multiprogramming Executive (MPE) files. They are: the geoblock directory, the overlay, the polygon, the line, the junction point, and the discrete point files. These six files exist for each geoblock, and the files are unique for that geoblock. Table B3 lists the geoblock name, MPE files and the information stored in them for the Chesapeake Bay Program.

TABLE B3
GES DATA STRUCTURE

GEOBLOCK NAME: WHITE

MPE FILES

INFORMATION STORED

ARCPBSBB

POLYGONS

CPCPBSBB

DISCRETE POINTS

JPCPBSBB

JUNCTION POINTS

LSCPBSBB

LINES

OVCPBSBB

OVERLAY

TXCPBSBB

TEXT

WHITE

GEOBLOCK DIRECTORY

GEOGRAPHIC DATA

All geographic data was digitized from nineteen 1:250,000 scale, USGS topographic maps. The following information was digitized from these base maps: river subbasin boundaries, state boundaries, populated area boundaries, contiguous boundaries of the Landsat images, and the control points used to transform the geographic data to the Landsat images. Table B4 lists the GES overlay number, its name, and the geographic data it contains. The following information on the GES overlays: the overlay number, the overlay name, the GES class, and the description of that class, is contained in a subsequent section entitled "Tape Catalog."

The river subbasins were divided into two overlays. Overlay 1 containing fifty-six subbasins covers the basins above the fall line, and overlay 2 containing twenty-nine subbasins covers the basins below the fall lines.

The first step in digitizing the subbasin boundaries on these two overlays was locating the USGS gaging stations on the maps. This was done using information the USGS provided on the gage's latitude and longitude coordinates and the description of the gage's location. From this point, the boundaries of the subbasins were hand drawn on the 1:250,000 scale maps. The subbasins were then digitized as polygons which are stored in GES overlays 1, "SUBBASIN," and 3, "COASTAL."

State boundaries in the basin for Delaware, Maryland, New York, Pennsylvania, Virginia and West Virginia were digitized from the base maps. The boundaries were digitized as polygons on overlay 5, "STATE." This information was not needed for the hydrologic tabulations, but was digitized for possible future use.

Populated areas below forty degrees north latitude which have relatively short travel times to the Bay, as highlighted on the base maps, plus populated areas on the Harrisonburg base map were digitized. The USGS criteria for defining populated areas on the USGS 1:250,000 scale maps is that any area large enough on this cartographic product with detectable housing or construction was a populated area. The purpose for digitizing these populated areas was to obtain data on the distribution of urban, suburban, and rural areas in the subbasins. The populated areas were digitized as polygons on GES overlay 6, "URBAN."

Due to the fact that adjacent Landsat images overlap between 20 and 30 percent, there is a problem of double counting the areas within the overlap. Double counting the area within the overlap can be prevented by merging the images together or dividing the images along a common boundary where the images overlap. Rather than merging the twelve Landsat images together, a costly and time-consuming task which in this case required too much data storage, it was decided that the most efficient method for correcting the problem of double counting the area of overlap would be by using contiguous boundaries. To do this, an accurate approximation of the area covered by each image was needed. Based on 9 x 9 inch hard copy prints of the images, the boundaries of each image were drawn on the base maps. Noting the overlap between the areas covered by the images, contiguous boundaries for the images were then drawn in the areas of overlap. Also, at the edge of the basin, the image boundaries were extended past the basin boundary. This insured the maximum coverage of the basin by the Landsat images. The outer boundaries drawn on the map contained the total basin.

The contiguous boundaries and the outer boundaries were then digitized as polygons on GES Overlay 2, "Images."

In order to generate a GES-to-Landsat transformation, landmarks that were identifiable on both the IDIMS digital display and the GES base maps were selected as control points. The control points were marked and labeled on the base maps and their line and sample values from the Landsat image were noted and saved in a file. A total of 570 points, more or less uniformly distributed throughout the basin, were chosen. The control points on the base maps were then digitized on the point overlay, overlay 4, "CONTROL."

TABLE B4
GEOGRAPHIC ENTRY SYSTEM
OVERLAYS

<u>OVERLAY NO.</u>	<u>NAME</u>	<u>DESCRIPTION</u>
1	Subbasin	Non-Tidal River Subbasins
2	Images	Contiguous Boundaries of the Landsat Images
3	Coastal	Tidal River Subbasins
4	Control	Control Points
5	State	State Boundary Lines
6	Urban	Populated Areas Highlighted on the USGS, 1:250,000 Scale Maps

REGISTRATION OF GEOGRAPHIC DATA

The general procedure for registering the geographic data to the Landsat scenes was as follows:

1. The Landsat scenes were displayed on a CRT and significant landmarks (ground control points) were located. The line and sample coordinates of the landmarks along with their identifying labels were stored in a mensuration file (a unique file for each Landsat scene). The location of the landmarks along with their identifying labels were marked on the 1:250,000 scale USGS topographic maps.

2. The ground control points were digitized off the 1:250,000 scale maps using GES software. The identifying labels and their coordinates (in internal units) were saved in overlay 4.

3. Using IDIMS software, a third order polynomial equation was developed (a unique equation for each Landsat scene) which converts GES internal unit coordinates to IDMS line and sample coordinates. The residuals from the transformation equations were all within ± 3 pixels.

4. Using the transformation equation, the geographic data was transferred into an IDIMS image format such that they had the same number of lines and samples as their corresponding Landsat scenes. For each Landsat scene, an image was created containing the Landsat scene boundaries (overlay 2). For Landsat scenes where the data was digitized, an image was created containing the urban boundaries (overlay 6).

[NOTE: The Landsat data was not transformed to a ground coordinate system (Latitude/Longitude, Universal Transverse Mercator, State Plane) because of increased computer time and storage limitations. The GES files will be

available for future users to do the transformations. See TECHNICAL MEMORANDUM "A Procedure for merging Landsat data with other geographic data using the Geographic Entry System (G.E.S.) and the Interactive Digital Image Manipulation Systems (IDIMS)" by Wayne A. Hallada, Computer Science Corporation, April 22, 1981)].

TABULATION OF LANDCOVER DATA

The landcover data was tabulated by river subbasin for each of the thirty-six subscenes. The general procedure for tabulating the land cover data was:

1. The classified subscene was overlaid by the image containing the Landsat scene boundaries. Only the portion of the subscene inside the Landsat scene boundary was used in the tabulation.
2. The classified subscene was then overlaid by the image containing urban boundaries. The subscene areas inside the urban boundaries were changed to either high, medium, or low density urban depending on their spectral characteristics.
3. The subscene was then overlaid by the image containing the river subbasin boundaries and the land cover types tabulated by subbasin.

LANDSAT ACCURACY ANALYSIS

The verification of the Landsat land cover data set followed two different procedures. The first procedure was to randomly select areas within the Chesapeake Bay drainage basin and compare the Landsat land cover statistics with statistics from photointerpreting color infrared photography. The second was to compare land cover statistics from Landsat with land cover statistics from various agencies in the Chesapeake Bay basin.

The general procedure for comparing the Landsat land cover statistics with the photointerpreted land cover statistics was:

1. The classified Landsat image was displayed on a CRT. An IDIMS function was run which randomly selects blocks whose area was selected by the operator from within the Landsat scene. The land cover statistics of the block were tabulated.
2. The positions of the blocks were located on the color infrared photography, a mylar overlay was placed on the photography and land cover types drawn and labeled. The blocks were labeled for geographic features near their location.
3. The mylar was then transferred to a digital planimeter and the area of each land cover calculated. These were compared with the values tabulated from the classified Landsat data.

The only requirement on the location of the randomly selected areas was that it could be identified on the color infrared photographs (which was the best ground truth available) on loan from Maryland State Planning. There was at least one randomly selected site in each of the Chesapeake Bay basin physiographic provinces. The Appalachian Plateau, Appalachian Ridge and

Valley, and the Blue Ridge each have one site. The Piedmont has two sites, and the Coastal Plain has three randomly selected areas. The randomly selected areas fell across three different Landsat scenes (Front Royal, Washington, Salisbury). Each of the sites was 50 x 50 pixels. For the Front Royal and Washington scenes, that corresponds to 4.3 square miles. For the Salisbury scene the area is 3.1 square miles.

Because the randomly selected areas were located on three different Landsat scenes, on different dates, and represent all 5 geographic provinces, it was decided that, when aggregated, their statistics would adequately represent the accuracy of the land cover over the entire basin.

There was some evidence to suggest that the randomly selected site near Loch Raven Reservoir should not be included in the accuracy analysis. The site, 10 miles north of the Baltimore beltway, was in a state of transition between agriculture land use and residential land use. There were indications on the aerial photography that many of the agricultural fields had been left idle. In one field a road network was in place for a subdivision development. If the fields had been left idle, their spectral characteristics would not be representative of the land cover type and therefore should not be included in the analysis. The photointerpreted land covers for Loch Raven Reservoir in winter agriculture and pasture were 2.2% and 41.44%, respectively. There was no other site that had such large discrepancies between these two land cover types. There were no indications that the classification errors were the result of physiographic influences. Indeed, another site, Liberty Reservoir which is only 15 miles from Loch Raven Reservoir, has a land cover classification that correlated well with the photointerpreted land cover.

Table B5 contains the Landsat land cover accuracy results. Lines A-H are the 8 randomly selected sites and their tabulation of land cover types. Line I is the sum of all 8 sites and Line J is the sum of 7 sites with line E (Loch Raven Reservoir) excluded. Line K lists the percent error for the lines I and J. Columns 1-5, 9, and 10 are the land cover types tabulated from the randomly selected sites. The value in column 1 (FOREST) includes Idle land. Columns 6-8 are different aggregations of the agriculture land covers. From inspection of line K, it can be seen that only columns 2, 5, and 9 (winter agriculture, pasture, and urban) are significantly effected by the deletion of Loch Raven Reservoir from the accuracy analysis. The change in percent error in winter agriculture from 50.3% to 3.43% and in pasture from -11.45% to +15.91% are reasonable. After visual inspection of the classified data and comparison of the classified data to other land cover data sets, it was determined that the percent error tabulated without Loch Raven Reservoir was more representative. The percent error in the urban classification is probably not representative of the error in urban classification basinwide. Most of the error in the urban classification is caused by Catoctin Mountain and Cumberland sites. In both cases, the urban areas were located in the shadows of mountains, which is not representative of urban areas basinwide. Visual inspection of the classified data and comparison of the classified data with other land use data sets also indicates that the urban area classification errors are less than the accuracy analysis indicates.

In addition to the randomly selected sites, the Landsat land cover data set was compared with land use data sets from various state and federal agencies. The following river basins were used in this comparison:

Potomac, James, York, Rappahannock, Patuxent, Gunpowder, Occoquan, Appomattox, and Susquehanna. The Landsat land cover data set was compared with the Environmental Protection Agency (EPA) Chesapeake Bay Program Historic Land Use data base. The EPA data base was compiled from Agricultural Census data (1978) and Timber Survey data (1975). Tables B6 - B9 show the comparisons for the Potomac, James, York, and Rappahannock river basins. For the Patuxent and Gunpowder river basins, the Landsat data set was compared with data from the Maryland Department of State Planning's Maryland Automated Geographic Information (MAGI) System. The MAGI's 1978 land use data set was developed from high-altitude color infrared photography with a minimum mapping area of 10 acres. Table B10 shows the comparison of the Landsat land cover data with MAGI land use for the Patuxent and Gunpowder river basins. For the Occoquan River Basin, the Landsat land cover data was compared with the land cover statistics planimetered from a 1979 1:48,000 scale land use map developed by the Northern Virginia Planning District Commission. Table B11 shows the comparison for the Occoquan River Basin. In the Appomattox River Basin, the Landsat land cover statistics were compared with land cover statistics from the Piedmont Planning District Commission and Forest Statistics for the South Piedmont of Virginia. This comparison is found in Table B12. Table B13 shows a comparison of the percent forest developed by the Landsat data base with percent forest figures developed by the Susquehanna River Basin Commission.

TABLE B5
LANDSAT ACCURACY ANALYSIS

	1	2	3	4	5	6	7	8	9	10
	FOREST	WINTER AG	MIN. TILL.	CONV. TILL.	PASTURE	TOTAL MIN. TILL. (2+3)	TOTAL TILL. (2+3+4)	TOTAL AG. (2+3+4+5)	URBAN	WATER
A	Liberty									
	Reservoir	23.93	13.66	30.95	1.80	28.20	44.61	74.61	1.22	0.24
	Area=2782 Acres	25.36	15.00	31.04	0.12	28.28	46.04	74.44	0.08	0.12
B	Catoctin									
	Mountain	81.19	3.26	1.34	---	7.06	4.60	11.66	7.13	---
	Area=2782 Acres	79.60	3.92	3.56	0.04	12.72	7.48	20.24	0.16	---
C	Cumberland									
	Photo	70.02	---	---	1.17	14.51	---	1.17	14.30	---
	Area=2782 Acres	75.52	1.76	2.76	0.12	18.48	4.52	23.12	1.32	0.04
D	Deep Creek									
	Lake	84.03	---	---	0.57	2.95	---	0.57	1.17	11.28
	Area=2782 Acres	82.12	1.00	2.80	0.20	2.64	3.80	6.64	1.24	10.00
E	Lock Raven									
	Reservoir	36.28	2.20	9.23	0.65	41.44	11.43	53.52	9.95	---
	Area=2782 Acres	38.72	19.52	10.48	1.52	18.92	30.00	50.44	10.84	---
F	Swan Creek									
	Photo	51.50	3.36	37.31	1.28	2.44	40.67	44.38	1.82	2.29
	Area=2782 Acres	47.64	1.16	33.60	5.96	8.96	34.76	49.68	0.56	2.12
G	Tolchester									
	Beech	20.38	1.07	25.11	2.98	5.98	26.18	35.14	0.95	43.59
	Area=2007 Acres	27.36	0.88	23.12	2.76	2.40	24.00	29.16	0.36	43.12
H	Langford									
	Photo	5.0	18.88	29.22	39.00	7.69	41.80	94.79	---	0.21
	Area=2007 Acres	8.2	17.16	25.04	46.00	3.52	42.20	91.72	0.08	---
I	TOTAL									
	Area=20,706 Acres	49.08	4.95	15.90	4.80	14.30	20.85	39.95	4.87	6.10
		50.33	7.44	15.98	5.80	12.66	23.42	41.88	1.95	5.84
J	TOTAL**									
	Area=17,924 Acres	51.06	5.38	16.89	5.45	10.09	22.27	37.81	4.09	7.05
		52.13	5.57	16.84	6.46	11.70	22.41	40.57	0.57	6.75
K	TOTAL*									
	Area=20,706 Acres	42.55	+ 50.3	+ 0.50	+20.83	-11.45	+10.97	+ 4.83	-59.96	- 4.26
		+2.10	+ 3.43	- 0.29	+18.52	+15.91	+ 0.63	+ 7.30	-86.04	- 4.31

* %ERROR= $\frac{(\text{Observed}-\text{Expected})}{\text{Expected}} \times 100$ Where: Observed=LANDSAT Land Use
 ** Tabulated without Lockraven Reservoir Expected=Photo Interpreted Land Use

TABLE B6

LAND COVER COMPARISON POTOMAC RIVER BASIN

LAND COVER	<u>POTOMAC ABOVE FALL-LINE</u>		<u>POTOMAC BELOW FALL-LINE</u>	
	LANDSAT	EPA/CPB*	LANDSAT	EPA/CPB*
PASTURE	18.42 %	18.32 %	15.90 %	7.64 %
CROP	16.35 %	16.53 %	15.23 %	14.59 %
FOREST	61.00 %	57.00 %	54.47 %	51.70 %
OTHER	4.23 %	8.15 %	14.40 %	26.07 %

* Environmental Protection Agency Chesapeake Bay Program Historic Land Use Database

TABLE B7

LAND COVER COMPARISON JAMES RIVER BASIN

LAND COVER	<u>JAMES ABOVE FALL-LINE</u>		<u>JAMES BELOW FALL-LINE</u>	
	LANDSAT	EPA/CPB*	LANDSAT	EPA/CPB*
PASTURE	14.62%	14.49%	10.81%	2.75%
CROP	12.19%	7.16%	14.64%	12.78%
FOREST	65.23%	74.21%	62.68%	61.52%
OTHER	7.96%	4.14%	11.87%	22.95%

* Environmental Protection Agency Chesapeake Bay Program Historic Land Use Database

TABLE P8
LAND COVER COMPARISON YORK RIVER BASIN

LAND COVER	<u>YORK ABOVE FALL-LINE</u>		<u>YORK BELOW FALL-LINE</u>	
	LANDSAT	EPA/CPB*	LANDSAT	EPA/CPB*
PASTURE	12.88 %	9.11 %	11.84 %	3.25 %
CROP	13.90 %	11.00 %	19.26 %	12.33 %
FOREST	72.80 %	69.70 %	68.82 %	71.59 %
OTHER	0.42 %	10.19 %	0.05 %	12.83 %

* Environmental Protection Agency Chesapeake Bay Program Historic Land Use Database

TABLE B9

LAND COVER COMPARISON RAPPAHANNOCK RIVER BASIN

LAND COVER	<u>RAPPAHANNOCK ABOVE FALL-LINE</u>		<u>RAPPAHANNOCK BELOW FALL-LINE</u>	
	LANDSAT	EPA/CPB*	LANDSAT	EPA/CPB*
PASTURE	26.21%	23.59%	15.1%	3.22%
CROP	12.08%	15.32%	21.64%	19.94%
FOREST	61.42%	55.23%	62.20%	65.96%
OTHER	0.29%	5.86%	1.06%	10.88%

* Environmental Protection Agency Chesapeake Bay Program Historic Land Use Database

TABLE B10

LAND COVER COMPARISON PATUXENT AND GUNPOWDER RIVER BASINS

	<u>PATUXENT</u>		<u>GUNPOWDER</u>	
	LANDSAT	MAGI*	LANDSAT	MAGI*
Forest	53%	48%	47%	41%
Agriculture	41%	38%	44%	48%
Urban	6%	9%		

*From Maryland Automated Geographic Information (MAGI), 1978 Dept. of State Planning

TABLE B11
LAND COVER COMPARISON OCCOQUAN RIVER BASIN

	LANDSAT	NVPDC*
Forest	62%	59%
Tilled Agriculture	14%	11%
Pasture	20%	22%
Urban	4%	8%

*Planimetered from a 1:48,000 scale Land Use Map NVPDC 1979

TABLE B12

LAND COVER COMPARISON APPOMATOX RIVER BASIN, VIRGINIA

	<u>LANDSAT*</u>	<u>PIEDMONT PLANNING DISTRICT COMMISSION**</u>	<u>FOREST PUBLICATION***</u>
Forest	69%	65%	72%
Pasture	18%	20%	---
Agriculture	12%	13%	---

* From Subbasin in Appomattox River Basin

** Average of Amelia and Prince Edward Counties

*** Average of Amelia and Prince Edward Counties from "Forest Statistics for the South Piedmont of Virginia" 1976

TABLE B13

LAND COVER COMPARISON SUSQUEHANNA RIVER BASIN

<u>ZONE</u>	<u>LANDSAT % FOREST</u>	<u>SRBC* % FOREST</u>	<u>AREA SQUARE MILES</u>
1	57	57	4771
2	53	54	2596
3	60	55	3700
4	77	80	6900
5	72	66	3404
6	44	40	5288
TOTAL	61	60	26600

<u>ZONE</u>	<u>NAME</u>
1	Susquehanna River, Upstream From Athens, Pa.
2	Chemung River
3	Susquehanna River, Sayre, Pa. to Sunbury, Pa.
4	West Branch Susquehanna River, Source to Mouth
5	Juniata River
6	Susquehanna, Sunbury, Pa. to Mouth (excluding Juniata River)

* From "Assessment of the Water Quality of Streams in the Susquehanna River Basin," Susquehanna River Basin Comm., January 1976

LANDSAT IMAGE INFORMATION

CHESAPEAKE BAY BASIN

The following sections contain information on the location of the Landsat imagery, the location of the subscene on the imagery, the land cover classification scheme, and the tape number where each Landsat image is stored. Table B14 provides the information needed to locate and access the classified images for each Landsat scene. It lists the Landsat image's path/row location, the name of the file containing the classified information by the subscene name, the location of the subscene on the images by the starting line, starting sample, number of lines and number of samples, the number of classes in each file, and the tape number where the information is stored. Table B15 lists the identification numbers for the land cover types. Tables B16 through B27, which use the land cover identification numbers, relate the land cover types to the subscene class numbers. These tables provide all the information needed to access the land cover data for the Chesapeake Bay Basin.

TABLE B14

PATH ROW	SUBSCENE NAME	LOCATION ON ORIGINAL IMAGE		NUMBER OF LINES	NUMBER OF SAMPLES	NUMBER OF CLASSES	TAPE NO.
		STARTING LINE	STARTING SAMPLE				
16-30	CORTLAND.LH.CLASFY	1100	1	1241	1500	48	1
	CORTLAND.RH.CLASFY	1100	1501	1241	1500	50	1
16-31	SCRANTON.UH.CLASFY	1	1	1170	3343	50	2
	SCRANTON.LH.CLASFY	1171	1	1170	3343	50	2
17-31	WILLIAMSPORT.UL. CLASFY1	1	1	1170	1716	49	3
	WILLIAMSPORT.UR. CLASFY	1	1717	1170	1717	50	3
	WILLIAMSPORT.LL. CLASFY1	1171	1	1170	1716	50	3
	WILLIAMSPORT.LR. CLASFY	1171	1717	1170	1717	50	3
16-32	HARRISBURG.UL.CLASFY2	1	1	1170	1718	51	4
	HARRISBURG.UR.CLASFY	1	1719	1170	1719	51	4
	HARRISBURG.LL.CLASFY1	1171	1	1170	1718	52	4
	HARRISBURG.LR.CLASFY	1171	1719	1170	1719	50	4
17-32	ALTOONA.UL.CLASFY	1	1	1170	1682	50	5
	ALTOONA.UR.CLASFY	1	1683	1170	1683	50	5
	ALTOONA.LL.CLASFY	1171	1	1170	1682	50	5
	ALTOONA.LR.CLASFY	1171	1683	1170	1683	52	5
15-33	SALISBURY.UH.CLASFY	1	441	1491	1936	55	6
	SALISBURY.LH.CLASFY	1492	441	1492	1936	50	6
16-33	WASH.UL.CLASFY	1	1	1170	1720	50	7
	WASH.UR.CLASFY	1	1721	1170	1721	50	7
	WASH.LL.CLASFY	1171	1	1170	1720	46	7
	WASH.LR.CLASFY	1171	1721	1170	1721	50	7
17-33	FRONT.ROYAL.UL.CLASFY	1	1	1170	1720	50	8
	FRONT.ROYAL.UR.CLASFY	1	1721	1170	1721	50	8
	FRONT.ROYAL.LL.CLASFY1	1171	1	1170	1720	51	8
	FRONT.ROYAL.LR.CLASFY	1171	1721	1170	1721	50	8
15-34	NORFOLK.UL.CLASFY	1	1	2100	1432	50	9
	NORFOLK.UR.CLASFY	1	1433	2100	1000	50	9
	NORFOLK.LH.CLASFY2	2101	1	883	2432	51	9
16-34	RICHMOND.UL.CLASFY	1	1	1170	1722	48	10
	RICHMOND.UR.CLASFY	1	1723	1170	1722	45	10
	RICHMOND.LL.CLASFY	1171	1	1170	1722	50	10
	RICHMOND.LR.CLASFY1	1171	1723	1170	1722	46	10
17-34	LYNCHBURG.LH.CLASFY1	1	1	2983	1798	50	11
	LYNCHBURG.RH.CLASFY	1	1799	2983	1798	50	11
18-34	ROANOKE.RH.CLASFY	1	1000	1350	2373	50	12

TABLE B15

IDENTIFICATION NUMBERS FOR LAND COVER TYPES

<u>NUMBER</u>	<u>LAND COVER TYPE</u>
1	Unclassified
2	Forest
3	Winter Agriculture
4	Conventional Tillage
5	Minimum Tillage
6	Pasture
7	Water
8	Marsh
9	Urban
10	Strip Mine
11	Idle

TABLE B16

LAND COVER TYPES BY SUBSCENE CLASSES

<u>CLASS NO.</u>	<u>LAND COVER TYPE</u>	
	<u>CORTLAND.LH.CLASFY</u>	<u>CORTLAND.RH.CLASFY</u>
1	1	1
2	6	6
3	2	2
4	5	5
5	3	6
6	4	4
7	2	6
8	5	6
9	3	2
10	6	6
11	2	6
12	2	2
13	6	6
14	6	6
15	6	2
16	7	2
17	6	3
18	5	6
19	2	2
20	9	5
21	2	2
22	5	5
23	2	6
24	2	2
25	6	6
26	6	6
27	2	2
28	2	2
29	6	2
30	6	2
31	2	2
32	1	7
33	6	6
34	2	6
35	5	2
36	2	5
37	5	2
38	2	4
39	2	2
40	3	2
41	6	6
42	2	6
43	6	2
44	6	2
45	2	6
46	7	5
47	6	2
48	2	7
49		6
50		6
51		
52		
53		

TABLE B17

LAND COVER TYPES BY SUBSCENE CLASSES

<u>CLASS NO.</u>	<u>LAND COVER TYPE</u>	
	<u>SCRANTON.UH.CLASFY</u>	<u>SCRANTON.LH.CLASFY</u>
1	4	4
2	2	2
3	3	6
4	2	2
5	5	4
6	2	2
7	5	5
8	2	2
9	3	3
10	2	2
11	2	6
12	2	2
13	6	6
14	2	2
15	2	2
16	7	2
17	6	3
18	2	6
19	6	6
20	2	2
21	5	5
22	2	2
23	5	5
24	2	2
25	3	3
26	2	2
27	2	2
28	2	2
29	5	5
30	9	9
31	5	2
32	7	7
33	4	4
34	2	2
35	6	3
36	2	2
37	5	5
38	2	5
39	5	2
40	2	3
41	3	2
42	2	2
43	2	2
44	2	6
45	6	2
46	7	2
47	6	5
48	2	2
49	6	6
50	2	2
51		
52	B-41	
53		

TABLE B18

LAND COVER TYPES BY SUBSCENE CLASSES

<u>CLASS NO.</u>	<u>WILLIAMSPORT. UL.CLASFY1</u>	<u>WILLIAMSPORT. UR.CLASFY</u>	<u>WILLIAMSPORT. LL.CLASFY1</u>	<u>WILLIAMSPORT. LR.CLASFY</u>
1	4	1	4	4
2	1	6	2	2
3	2	5	6	5
4	1	2	2	2
5	3	4	6	3
6	1	2	2	2
7	2	2	2	5
8	1	2	3	2
9	5	3	2	4
10	1	2	2	2
11	2	6	2	2
12	1	2	2	2
13	5	6	6	6
14	1	2	2	2
15	2	2	2	2
16	6	2	2	2
17	1	6	6	6
18	2	2	2	2
19	1	5	6	6
20	6	2	2	2
21	1	6	5	6
22	2	2	2	2
23	1	2	2	5
24	5	2	2	2
25	1	6	6	5
26	2	2	2	2
27	1	2	2	2
28	2	2	2	2
29	1	6	2	6
30	7	2	2	5
31	1	9	2	2
32	4	7	7	7
33	1	6	4	4
34	2	2	2	2
35	1	5	6	5
36	6	2	5	2
37	1	5	2	3
38	2	2	2	5
39	1	2	3	2
40	5	3	2	5
41	1	6	2	5
42	2	2	6	2
43	1	6	5	2
44	5	2	5	6
45	1	2	5	5
46	2	6	2	5
47	1	6	5	2
48	6	5	2	2
49	4	2	6	3
50		6	2	2
51				
52				
53				

TABLE B19

LAND COVER TYPES BY SUBSCENE CLASSES

<u>CLASS NO.</u>	<u>HARRISBURG. UL.CLASFY2</u>	<u>HARRISBURG. UR.CLASFY</u>	<u>HARRISBURG. LL.CLASFY1</u>	<u>HARRISBURG. LR.CLASFY</u>
1	4	4	5	4
2	2	2	3	6
3	5	5	2	4
4	2	2	4	2
5	3	3	2	3
6	2	2	6	5
7	6	6	2	6
8	2	2	6	7
9	6	6	5	6
10	2	2	6	2
11	5	5	2	5
12	2	2	5	2
13	6	6	2	3
14	2	2	6	2
15	2	2	2	5
16	7	7	1	7
17	5	5	5	6
18	2	2	3	2
19	5	5	2	5
20	2	2	4	2
21	3	3	2	3
22	9	9	6	2
23	6	6	2	2
24	2	2	6	7
25	6	6	5	6
26	2	2	3	2
27	5	5	2	5
28	2	2	5	8
29	6	6	2	6
30	2	2	2	2
31	5	5	7	2
32	7	7	4	7
33	4	4	2	4
34	2	2	3	2
35	5	5	2	4
36	3	3	5	2
37	5	5	2	3
38	6	6	6	5
39	2	2	2	5
40	6	6	6	7
41	2	2	5	6
42	5	5	6	2
43	3	3	2	5
44	2	2	6	7
45	5	5	2	6
46	7	7	6	2
47	5	5	2	5
48	2	2	4	7
49	5	5	2	5
50	2	2	1	2
51	10	10	2	
52			9	
53				

TABLE B20

LAND COVER TYPES BY SUBSCENE CLASSES

<u>CLASS NO.</u>	<u>ALTOONA. UL.CLASFY</u>	<u>ALTOONA. UR.CLASFY</u>	<u>ALTOONA. LL.CLASFY</u>	<u>ALTOONA. LR.CLASFY</u>
1	3	3	3	3
2	4	4	4	4
3	4	2	6	6
4	2	5	4	2
5	6	3	3	6
6	2	6	6	6
7	2	2	6	6
8	2	9	2	2
9	6	6	6	3
10	2	6	2	4
11	2	2	2	2
12	2	2	2	2
13	6	6	6	5
14	2	6	2	5
15	2	2	2	6
16	9	4	2	9
17	6	3	3	3
18	4	4	6	5
19	6	2	2	2
20	5	5	5	2
21	2	2	2	6
22	2	6	2	5
23	2	2	6	2
24	2	7	2	2
25	2	2	3	3
26	2	5	2	5
27	2	2	2	2
28	2	2	2	2
29	2	2	2	2
30	2	2	2	5
31	2	2	2	2
32	7	7	7	7
33	3	3	3	3
34	5	5	6	4
35	6	2	6	6
36	2	2	5	2
37	2	2	2	6
38	2	6	5	6
39	2	2	6	2
40	9	4	2	5
41	6	6	2	6
42	2	6	2	5
43	2	2	2	2
44	2	2	2	2
45	2	6	2	2
46	2	6	3	5
47	7	7	6	2
48	3	3	2	2
49	5	5	9	3
50	2	2	2	5
51				9
52		B-44		5
53				

TABLE B21

LAND COVER TYPES BY SUBSCENE CLASSES

<u>CLASS NO.</u>	<u>SALISBURY. UH.CLASFY</u>	<u>SALISBURY. LH.CLASFY</u>
1	4	4
2	5	9
3	3	3
4	7	7
5	3	6
6	2	2
7	2	2
8	7	7
9	5	5
10	2	2
11	2	2
12	7	7
13	5	4
14	7	2
15	2	2
16	7	7
17	4	4
18	9	2
19	3	3
20	7	7
21	5	4
22	2	7
23	5	5
24	7	5
25	5	2
26	2	2
27	2	7
28	7	5
29	5	7
30	2	2
31	2	4
32	7	2
33	4	3
34	2	7
35	3	6
36	7	7
37	6	2
38	2	5
39	2	2
40	5	2
41	2	4
42	2	7
43	5	2
44	7	4
45	2	2
46	4	2
47	2	7
48	2	6
49	6	7
50	2	2
51	2	
52	5	
53	2	

TABLE B22

LAND COVER TYPES BY SUBSCENE CLASSES

<u>CLASS NO.</u>	<u>WASH.UL. CLASFY</u>	<u>WASH.UR. CLASFY</u>	<u>WASH.LL. CLASFY</u>	<u>WASH.LR. CLASFY</u>
1	4	4	3	4
2	5	2	2	5
3	3	5	4	5
4	2	7	2	7
5	6	3	4	3
6	6	9	2	7
7	6	2	2	2
8	2	7	7	7
9	5	6	6	3
10	5	5	2	2
11	6	5	2	6
12	2	7	7	6
13	5	6	6	7
14	2	2	2	2
15	6	2	2	6
16	2	4	6	2
17	4	2	2	5
18	2	6	4	6
19	3	7	7	7
20	2	3	6	2
21	6	7	5	6
22	6	2	2	2
23	3	5	6	2
24	2	2	2	2
25	5	5	5	7
26	2	7	7	2
27	3	6	6	4
28	2	7	2	5
29	6	2	2	5
30	2	4	3	3
31	6	2	2	7
32	7	5	5	2
33	4	7	2	6
34	5	3	6	2
35	3	9	2	2
36	2	2	2	3
37	6	5	7	7
38	6	5	3	2
39	9	5	2	5
40	5	3	2	2
41	9	2	7	5
42	3	2	6	3
43	2	4	3	2
44	5	2	2	6
45	2	6	5	7
46	6	3	3	5
47	7	7		2
48	5	2		2
49	2	5		4
50	3	2		5
51				
52				
53				

LAND COVER TYPES BY SUBSCENE CLASSES

<u>CLASS NO.</u>	<u>FRONT. ROYAL. UL. CLASFY</u>	<u>FRONT. ROYAL. UR. CLASFY</u>	<u>FRONT. ROYAL. LL. CLASFY2</u>	<u>FRONT. ROYAL. LR. CLASFY</u>
1	6	6	3	3
2	2	2	2	2
3	6	4	4	4
4	2	2	2	2
5	4	6	4	4
6	2	2	2	2
7	2	6	5	6
8	2	2	2	2
9	6	6	6	6
10	2	5	2	2
11	2	5	6	6
12	2	2	2	2
13	6	3	6	6
14	2	2	2	2
15	2	5	2	6
16	2	2	2	7
17	3	3	6	3
18	2	2	2	2
19	5	4	5	5
20	2	2	2	2
21	6	6	6	6
22	2	2	2	2
23	2	2	5	2
24	2	2	2	2
25	3	3	6	3
26	2	5	2	2
27	2	5	2	5
28	2	6	2	2
29	2	2	6	6
30	9	2	2	2
31	7	2	5	2
32	3	7	2	7
33	2	3	3	3
34	2	2	2	2
35	2	4	5	5
36	5	2	2	6
37	2	6	5	5
38	2	2	2	6
39	2	6	2	2
40	6	2	3	6
41	6	6	6	2
42	6	5	3	6
43	2	5	2	2
44	3	2	3	3
45	2	6	5	2
46	2	2	2	2
47	5	5	6	2
48	2	2	2	3
49	5	3	3	2
50	6	4	2	5
51			7	
52				
53				

TABLE B24

LAND COVER TYPES BY SUBSCENE CLASSES

<u>CLASS NO.</u>	<u>NORFOLK. UL.CLASSFY</u>	<u>NORFOLK. UR.CLASSFY</u>	<u>NORFOLK. LH.CLASSFY2</u>
1	4	4	4
2	2	7	2
3	3	5	3
4	7	7	7
5	6	3	6
6	7	7	7
7	2	2	2
8	7	7	7
9	5	5	5
10	8	7	8
11	2	2	2
12	7	7	7
13	5	6	5
14	7	7	7
15	6	8	6
16	7	4	7
17	4	7	4
18	2	2	2
19	2	3	2
20	7	2	7
21	5	5	6
22	7	7	8
23	2	2	2
24	5	2	5
25	7	8	8
26	2	4	2
27	6	5	7
28	7	3	5
29	2	2	7
30	7	6	2
31	4	7	4
32	8	2	2
33	3	2	2
34	6	7	7
35	7	5	6
36	2	7	7
37	5	2	2
38	7	2	5
39	2	8	2
40	5	5	2
41	7	7	7
42	2	2	6
43	4	2	2
44	2	8	4
45	2	4	2
46	6	5	2
47	2	3	6
48	5	2	7
49	7	5	2
50	2	7	5
51			9
52		B-48	
53			

TABLE B25
LAND COVER TYPES BY SUBSCENE CLASSES

<u>CLASS NO.</u>	<u>RICHMOND. UL.CLASFY</u>	<u>RICHMOND. UR.CLASFY</u>	<u>RICHMOND. LL.CLASFY</u>	<u>RICHMOND. LR.CLASFY1</u>
1	4	4	1	4
2	6	6	5	6
3	3	2	3	2
4	2	2	2	2
5	6	5	6	5
6	5	5	5	5
7	9	2	2	2
8	5	4	2	4
9	6	2	4	2
10	3	3	6	3
11	2	7	6	7
12	5	5	2	5
13	2	2	5	2
14	2	2	2	2
15	7	4	2	4
16	4	6	9	6
17	2	2	1	2
18	3	7	6	7
19	2	6	2	6
20	6	5	2	9
21	2	2	6	2
22	5	7	9	7
23	2	5	2	5
24	5	2	2	2
25	2	2	4	2
26	2	7	2	7
27	2	5	2	5
28	6	2	2	2
29	2	2	6	2
30	2	4	2	4
31	7	6	2	6
32	4	2	7	2
33	2	5	1	5
34	3	6	5	6
35	2	2	3	2
36	6	4	2	4
37	5	3	5	3
38	2	7	5	7
39	2	5	2	5
40	5	2	6	2
41	2	2	6	2
42	2	4	2	4
43	5	2	2	2
44	2	2	5	2
45	7	7	2	7
46	5		2	9
47	2		2	
48	3		4	
49			5	
50			2	
51				
52				
53				

TABLE B26

LAND COVER TYPES BY SUBSCENE CLASSES

<u>CLASS NO.</u>	<u>LYNCHBURG. RH.CLASFY</u>	<u>LYNCHBURG. LH.CLASFY2</u>
1	1	3
2	2	2
3	3	2
4	5	6
5	5	4
6	5	4
7	2	5
8	5	5
9	4	2
10	2	2
11	2	2
12	2	2
13	6	2
14	2	2
15	2	2
16	5	5
17	2	2
18	3	6
19	6	2
20	6	5
21	6	6
22	2	5
23	2	6
24	4	2
25	6	2
26	2	2
27	2	2
28	6	2
29	2	2
30	6	2
31	7	2
32	2	7
33	3	3
34	5	2
35	5	2
36	5	6
37	2	6
38	2	5
39	4	6
40	2	2
41	2	2
42	2	2
43	6	2
44	2	2
45	2	2
46	2	2
47	1	2
48	2	2
49	2	6
50	2	2
51		
52		
53		

TABLE B27
LAND COVER TYPES BY SUBSCENE CLASSES

<u>CLASS NO.</u>	<u>ROANOKE.RH.CLASFY</u>
1	3
2	6
3	2
4	2
5	2
6	2
7	4
8	2
9	2
10	4
11	2
12	5
13	6
14	6
15	2
16	9
17	2
18	6
19	2
20	2
21	2
22	2
23	5
24	2
25	2
26	2
27	2
28	2
29	5
30	2
31	7
32	3
33	6
34	2
35	2
36	2
37	2
38	5
39	2
40	2
41	6
42	2
43	2
44	6
45	6
46	2
47	2
48	6
49	2
50	2
51	
52	
53	

TAPE CATALOG

All the Landsat land cover data and ancillary information is stored on twenty 9-track tapes. Tapes 1-12 contain the classified data, the Landsat edge boundary, the subbasin boundaries, and where available, the urban boundaries. Tapes 13-18 contain the Landsat scenes preprocessed by IDIMS software. Tapes 19 and 20 contain the mensuration files, statfiles, and the GES files.

The classified data (Tapes 1-12) is stored by subscene without the spectral classes being aggregated into land cover types. If the classified data is to be overlaid with the geographic data (river subbasins, urban areas, Landsat edge), the following procedure should be followed:

1. Each of the classified scenes should be loaded off the tape.
2. The spectral classes should be aggregated into land cover types using Tables B15 - B27.
3. The subscenes should be reunited or mosaiced together. They will now overlay the geographic, pixel for pixel.

Tables B28 - B30 list the data contained on each tape. Each file on the tape contains all the data for a subscene. Within each file are a given number of records. Each record is one scan-line or line of data in a subscene. Each record is a given number of bytes in length, and each byte is one pixel. If there is an odd number of pixels in a line, an extra pixel of intensity zero is added to make the number of pixels even.

The GES files for the Chesapeake Bay program which are stored on Tape 19 are found in Table B31. The GES files can only be used with GES and IDIMS software.

Tape 20 contains the files for mensuration and transformation. The mensuration files for each Landsat image are listed in Table B32. (The mensuration file for the Salisbury Image was lost because of tape errors.) The transformation file contains the third degree polynomial transformation equations for each Landsat scene and are prefixed by a six letter code listed in Table B33. The six letter code is used to identify and access the transformation file for each Landsat image. The mensuration and transformation files can only be used with GES and IDIMS software.

Tape 20 also contains the land cover spectral signature files (statfiles). A list of the statfiles are found in Table B34. The format of the statfiles is as follows:

1. There is 1 record for each spectral signature of class in the statfile. See Table B14 for the number of classes in each statfile.
2. Each record contains 168 words, each word is 16 bits. Figure B2 represents the makeup of the record in a statfile.

The Chesapeake Bay Basin Landsat data has been transferred to the University of Maryland Remote Sensing Systems Library (RSSL) for permanent storage. The RSSL will make copies of the tapes available at cost to interested parties. Contact the Department of Civil Engineering, University of Maryland, College Park, Maryland, for information.

TABLE B28

TAPE NUMBER/ DENSITY	SUBSCENE NAME	FILE NO.	NO. OF RECORDS	LENGTH OF RECORD (BYTES)	BYTES PER PIXEL
1 (6250)BPI	CORTLAND.LH.CLASFY	1	1241	1500	1
	CORTLAND.LH.CLASFY	2	1241	1500	1
	CORTLAND.EDGE	3	1241	3000	1
	CORTLAND.SUBBASIN	4	1241	3000	1
2 (6250)BPI	SCRANTON.UH.CLASFY	1	1170	3344	1
	SCRANTON.LH.CLASFY	2	1170	3344	1
	SCRANTON.EDGE	3	2340	3344	1
	SCRANTON.SUBBASIN	4	2340	3344	1
3 (6250)BPI	WILLIAMSPORT.UL.CLASFY1	1	1170	1716	1
	WILLIAMSPORT.UR.CLASFY	2	1170	1718	1
	WILLIAMSPORT.LL.CLASFY1	3	1170	1716	1
	WILLIAMSPORT.LR.CLASFY	4	1170	1718	1
	WILLIAMSPORT.EDGE	5	2340	3434	1
	WILLIAMSPORT.SUBBASIN	6	2340	3434	1
4 (6250)BPI	HARRISBURG.UL.CLASFY2	1	1170	1718	1
	HARRISBURG.UR.CLASFY	2	1170	1720	1
	HARRISBURG.LL.CLASFY1	3	1170	1718	1
	HARRISBURG.LR.CLASFY	4	1170	1720	1
	HARRISBURG.EDGE	5	2340	3438	1
	HARRISBURG.SUBBASIN	6	2340	3438	1
	HARRISBURG.URBAN	7	2340	3438	1
5 (6250)BPI	ALTOONA.UL.CLASFY	1	1170	1682	1
	ALTOONA.UR.CLASFY	2	1170	1684	1
	ALTOONA.LL.CLASFY	3	1170	1682	1
	ALTOONA.LR.CLASFY	4	1170	1684	1
	ALTOONA.EDGE	5	2340	3366	1
	ALTOONA.SUBBASIN	6	2340	3366	1
	ALTOONA.URBAN	7	2340	3366	1
6 (6250)BPI	SALISBURY.UH.CLASFY	1	1491	1936	1
	SALISBURY.LH.CLASFY	2	1492	1936	1
	SALISBURY.EDGE	3	2983	2376	1
	SALISBURY.SUBBASIN	4	2983	2376	1
	SALISBURY.URBAN	5	2983	2376	1
7 (6250)BPI	WASH.UL.CLASFY	1	1170	1720	1
	WASH.UR.CLASFY	2	1170	1722	1
	WASH.LL.CLASFY	3	1170	1720	1
	WASH.LR.CLASFY	4	1170	1722	1
	WASH.EDGE	5	2340	3442	1
	WASH.SUBBASIN	6	2340	3442	1
	WASH.URBAN	7	2340	3442	1

TABLE B29

TAPE NUMBER/ DENSITY	SUBSCENE NAME	FILE NO.	NO. OF RECORDS	LENGTH OF RECORD (BYTES)	BYTES PER PIXEL
8 (6250)BPI	FRONT.ROYAL.UL.CLASFY	1	1170	1720	1
	FRONT.ROYAL.UR.CLASFY	2	1170	1722	1
	FRONT.ROYAL.LL.CLASFY1	3	1170	1720	1
	FRONT.ROYAL.LR.CLASFY	4	1170	1722	1
	FRONT.ROYAL.EDGE	5	2340	3442	1
	FRONT.ROYAL.SUBBASIN	6	2340	3442	1
	FRONT.ROYAL.URBAN	7	2340	3442	1
9 (6250)BPI	NORFOLK.UL.CLASFY	1	2100	1432	1
	NORFOLK.UR.CLASFY	2	2100	1000	1
	NORFOLK.LH.CLASFY	3	883	2432	1
	NORFOLK.EDGE	4	2983	2432	1
	NORFOLK.SUBBASIN	5	2983	2432	1
	NORFOLK.URBAN	6	2983	2432	1
10 (6250)BPI	RICHMOND.UL.CLASFY	1	1170	1722	1
	RICHMOND.UR.CLASFY	2	1170	1722	1
	RICHMOND.LL.CLASFY	3	1170	1722	1
	RICHMOND.LR.CLASFY2	4	1170	1722	1
	RICHMOND.EDGE	5	2340	3444	1
	RICHMOND.SUBBASIN	6	2340	3444	1
	RICHMOND.URBAN	7	2340	3444	1
11 (6250)BPI	LYNCHBURG.LH.CLASFY1	1	2983	1798	1
	LYNCHBURG.RH.CLASFY	2	2983	1798	1
	LYNCHBURG.EDGE	3	2983	3596	1
	LYNCHBURG.SUBBASIN	4	2983	3596	1
	LYNCHBURG.URBAN	5	2983	3596	1
12 (6250)BPI	ROANOKE.RH.CLASFY	1	1350	2373	1
	ROANOKE.EDGE	2	1350	2373	1
	ROANOKE.SUBBASIN	3	1350	2373	1
	ROANOKE.URBAN	4	1350	2373	1
13 (1600)BPI	ROANOKE (RAW DATA BAND 4)	1	2340	3372	1
	ROANOKE (RAW DATA BAND 5)	2	2340	3372	1
	ROANOKE (RAW DATA BAND 6)	3	2340	3372	1
	ROANOKE (RAW DATA BAND 7)	4	2340	3372	1
14 (1600)BPI	CORTLAND (RAW DATA BAND 4)	1	2340	3358	1
	CORTLAND (RAW DATA BAND 5)	2	2340	3358	1
	CORTLAND (RAW DATA BAND 6)	3	2340	3358	1
	CORTLAND (RAW DATA BAND 7)	4	2340	3358	1

TABLE B30

TAPE NUMBER/ DENSITY	SUBSCENE NAME	FILE NO.	NO. OF RECORDS	LENGTH OF RECORD (BYTES)	BYTES PER PIXEL
15 (6250)BPI	FRONT.ROYAL(RAW DATA BAND 4)	1	2340	3442	1
	FRONT.ROYAL(RAW DATA BAND 5)	2	2340	3442	1
	FRONT.ROYAL(RAW DATA BAND 6)	3	2340	3442	1
	FRONT.ROYAL(RAW DATA BAND 7)	4	2340	3442	1
	HARRISBURG(RAW DATA BAND 4)	5	2340	3438	1
	HARRISBURG(RAW DATA BAND 5)	6	2340	3438	1
	HARRISBURG(RAW DATA BAND 6)	7	2340	3438	1
	HARRISBURG(RAW DATA BAND 7)	8	2340	3438	1
	CORTLAND.SB(RAW DATA BAND 4)	9	1241	3000	1
	CORTLAND.SB(RAW DATA BAND 5)	10	1241	3000	1
	CORTLAND.SB(RAW DATA BAND 6)	11	1241	3000	1
	CORTLAND.SB(RAW DATA BAND 7)	12	1241	3000	1
16 (6250)BPI	RICHMOND (RAW DATA BAND 4)	1	2340	3444	1
	RICHMOND (RAW DATA BAND 5)	2	2340	3444	1
	RICHMOND (RAW DATA BAND 6)	3	2340	3444	1
	RICHMOND (RAW DATA BAND 7)	4	2340	3444	1
	NORFOLK.SB(RAW DATA BAND 4)	5	2983	2432	1
	NORFOLK.SB(RAW DATA BAND 5)	6	2983	2432	1
	NORFOLK.SB(RAW DATA BAND 6)	7	2983	2432	1
	NORFOLK.SB(RAW DATA BAND 7)	8	2983	2432	1
	ROANOKE.RH(RAW DATA BAND 4)	9	1350	2373	1
	ROANOKE.RH(RAW DATA BAND 5)	10	1350	2373	1
	ROANOKE.RH(RAW DATA BAND 6)	11	1350	2373	1
	ROANOKE.RH(RAW DATA BAND 7)	12	1350	2373	1
17 (6250)BPI	SCRANTON (RAW DATA BAND 4)	1	2340	3434	1
	SCRANTON (RAW DATA BAND 5)	2	2340	3434	1
	SCRANTON (RAW DATA BAND 6)	3	2340	3434	1
	SCRANTON (RAW DATA BAND 7)	4	2340	3434	1
	WILLIAMSPORT(RAW DATA BAND4)	5	2340	3434	1
	WILLIAMSPORT(RAW DATA BAND5)	6	2340	3434	1
	WILLIAMSPORT(RAW DATA BAND6)	7	2340	3434	1
	WILLIAMSPORT(RAW DATA BAND7)	8	2340	3434	1
	WASH(FILE1) (RAW DATA BAND 4)	9	2340	3442	1
	WASH(FILE1) (RAW DATA BAND 5)	10	2340	3442	1
	WASH(FILE1) (RAW DATA BAND 6)	11	2340	3442	1
	WASH(FILE1) (RAW DATA BAND 7)	12	2340	3442	1
18 (6250)BPI	ALTOONA (RAW DATA BAND 4)	1	2340	3366	1
	ALTOONA (RAW DATA BAND 5)	2	2340	3366	1
	ALTOONA (RAW DATA BAND 6)	3	2340	3366	1
	ALTOONA (RAW DATA BAND 7)	4	2340	3366	1
19 (6250)	GIS FILES				
20 (6250)	MENSURATION AND STAT FILES				

TABLE B-31
GES MPE FILES

FILE NO.	FILE NAME	DATA DESCRIPTION
1	ARCPBSBB.WHITE.GIS	Polygons
4	CPCPBSBB.WHITE.GIS	Control Points
6	JPCPBSBB.WHITE.GIS	Junction points
9	LSCPBSBB.WHITE.GIS	Line segments
11	OVCPBSBB.WHITE.GIS	Overlay
13	TXCPBSBB.WHITE.GIS	Text
14	WHITE.WHITE.GIS	Geoblock

TABLE B-32
MENSURATION FILES

FILE NO.	FILE NAME	PATH/ROW	SCENE NAME
3	JMWMALTO.USERFILE.IDIMS	17-32	ALTOONA
4	JMWMCORT.USERFILE.IDIMS	16-30	CORTLAND
5	JMWMFRON.USERFILE.IDIMS	17-33	FRONT ROYAL
6	JMWMHARR.USERFILE.IDIMS	16-32	HARRISBURG
7	JMWMLYNC.USERFILE.IDIMS	17-34	LYNCHBURG
8	JMWMNORF.USERFILE.IDIMS	15-34	NORFOLK
9	JMWMRICH.USERFILE.IDIMS	16-34	RICHMOND
10	JMWMROAN.USERFILE.IDIMS	18-34	ROANOKE
11	JMWMSCRA.USERFILE.IDIMS	16-31	SCRANTON
13	JMWMWASH.USERFILE.IDIMS	16-33	WASHINGTON
14	JMWMWILL.USERFILE.IDIMS	17-31	WILLIAMSPORT

TABLE B-33

TRANSFORMATION FILES

FILE NO.	FILE NAME	CODE	PATH-ROW	SCENE NAME
12	JMWMTRNF.USERFILE.IDIMS	ALTOON	17-32	ALTOON
		NEWCOR	16-30	CORTLAND
		FRONTR	17-33	FRONT ROYAL
		HARRIS	16-32	HARRISBURG
		LYNCHB	17-34	LYNCHBURG
		NORFOL	15-34	NORFOLK
		RICHMO	16-34	RICHMOND
		NEWROA	18-34	ROANOKE
		SALISB	15-33	SALISBURY
		SCRANT	16-31	SCRANTON
		WASHIN	16-33	WASHINGTON
		WILLIA	17-31	WILLIAMSPORT

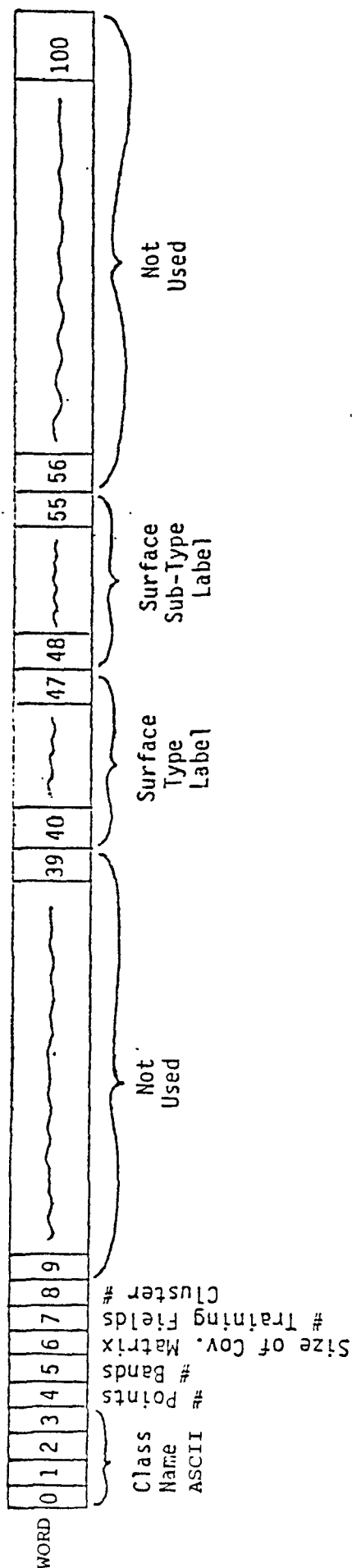
TABLE B-34
STATS FILES

FILE NO.	FILE NAME	PATH/ROW	SCENE NAME
16	JMALTOLL.STATS.IDIMS	17-32	ALTOONA.LL
17	JMALTOLR.STATS.IDIMS	17-32	ALTOONA.LR
18	JMALTOUL.STATS.IDIMS	17-32	ALTOONA.UL
19	JMALTOUR.STATS.IDIMS	17-32	ALTOONA.UR
20	JMCORTLH.STATS.IDIMS	16-30	CORTLAND.LH
21	JMCORTRH.STATS.IDIMS	16-30	CORTLAND.RH
22	JMFRONLL.STATS.IDIMS	17-33	FRONT.ROYAL.LL
23	JMFRONLR.STATS.IDIMS	17-33	FRONT.ROYAL.LR
24	JMFRONUL.STATS.IDIMS	17-33	FRONT.ROYAL.UL
25	JMFRONUR.STATS.IDIMS	17-33	FRONT.ROYAL.UR
26	JMHARRLL.STATS.IDIMS	16-32	HARRISBURG.LL
27	JMHARRLR.STATS.IDIMS	16-32	HARRISBURG.LR
28	JMHARRUL.STATS.IDIMS	16-32	HARRISBURG.UL
29	JMHARRUR.STATS.IDIMS	16-32	HARRISBURG.UR
30	JMLYNCLH.STATS.IDIMS	17-34	LYNCHBURG.LH
31	JMLYNCRH.STATS.IDIMS	17-34	LYNCHBURG.RH
32	JMNORFLH.STATS.IDIMS	15-34	NORFOLK.LH
33	JMNORFUL.STATS.IDIMS	15-34	NORFOLK.UL
34	JMNORFUR.STATS.IDIMS	15-34	NORFOLK.UR
35	JMRICHLL.STATS.IDIMS	16-34	RICHMOND.LL
36	JMRICHLR.STATS.IDIMS	16-34	RICHMOND.LR
37	JMRICHUL.STATS.IDIMS	16-34	RICHMOND.UL
38	JMRICHUR.STATS.IDIMS	16-34	RICHMOND.UR
39	JMROANRH.STATS.IDIMS	18-34	ROANOKE.RH
40	JMSALILH.STATS.IDIMS	15-33	SALISBURY.LH
41	JMSALIUH.STATS.IDIMS	15-33	SALISBURY.UH
42	JMSCRAUH.STATS.IDIMS	16-31	SCRANTON.LH
43	JMSCRAUH.STATS.IDIMS	16-31	SCRANTON.UH
44	JMWASHLL.STATS.IDIMS	16-33	WASHINGTON.LL
45	JMWASHLR.STATS.IDIMS	16-33	WASHINGTON.LR
46	JMWASHUL.STATS.IDIMS	16-33	WASHINGTON.UL
47	JMWASHUR.STATS.IDIMS	16-33	WASHINGTON.UR
48	JMWILLLL.STATS.IDIMS	17-31	WILLIAMSPORT.LL
49	JMWILLLR.STATS.IDIMS	17-31	WILLIAMSPORT.LR
50	JMWILLUL.STATS.IDIMS	17-31	WILLIAMSPORT.UL
51	JMWILLUR.STATS.IDIMS	17-31	WILLIAMSPORT.UR

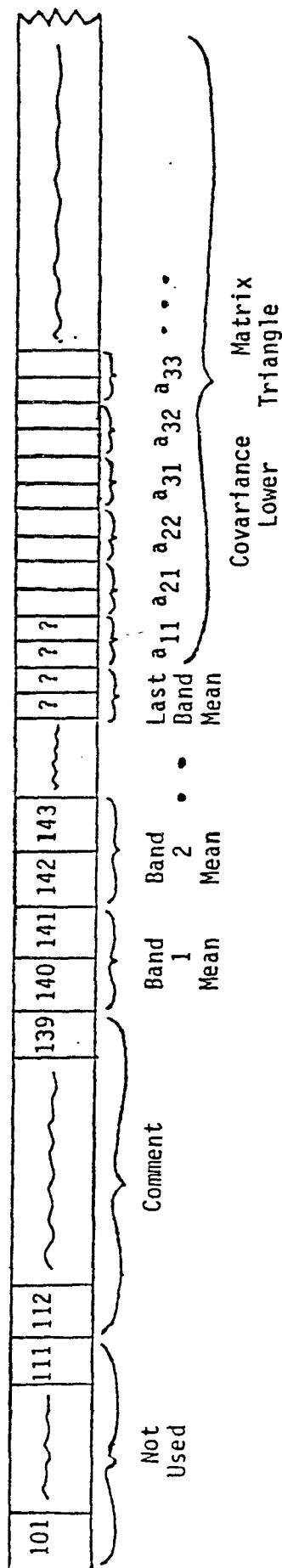
FIGURE B2

STATISTICS RECORD FORMAT

1 WORD = 2 BYTES



B-61



- Means and Covariance stored as reals (two words)

- Length of record in words

$$= 140 + 2 * (\text{word 6} + \text{word 7})$$

$$= 140 + (\# \text{ bands})^2 + 3 * (\# \text{ bands})$$

• Covariance Matrix:

$$\begin{pmatrix} a_{11} & a_{12} & a_{13} & \dots \\ a_{21} & a_{22} & a_{23} & \dots \\ a_{31} & a_{32} & a_{33} & \dots \\ \vdots & \vdots & \vdots & \ddots \end{pmatrix}$$

GEOGRAPHIC ENTRY SYSTEM

This section contains a list of the base maps and the GES overlay information needed to access the digitized geographical information. Table B35 lists the names of the 1:250,000 scale, USGS maps used for the GES base maps. Tables B36 through B41 list the GES classes and the geographic information contained in the classes for each overlay.

TABLE B35
GEOGRAPHIC ENTRY SYSTEM BASE MAPS
Scale: 1:250,000

MAP NAME	STATE
Wilmington	Del.
Washington	D. C.
Baltimore	Md.
Cumberland	Md.
Salisbury	Md.
Newark	N. J.
Binghamton	N. Y.
Elmira	N. Y.
Harrisburg	Pa.
Pittsburgh	Pa.
Scranton	Pa.
Warren	Pa.
Williamsport	Pa.
Charlottesville	Va.
Eastville	Va.
Norfolk	Va.
Richmond	Va.
Roanoke	Va.
Bluefield	W. Va.
Clarksburg	W. Va.

TABLE B36
GES OVERLAY NO. 1 -SUBBASIN

CLASS	DESCRIPTION OF CLASS
88	SUBBASIN 10
89	" 20
87	" 30
81, 83	" 40
74, 75	" 50
76, 85	" 60
79, 80	" 70
60, 78, 84	" 80
55	" 90
72, 73, 77	" 100
61, 82	" 110
66, 67	" 120, 130, 140, 150
32, 51, 52, 53	" 160
30	" 170
54, 56, 57	" 180
13, 29, 31, 34	" 190
33, 39	" 200
58, 59	" 210
38, 40	" 220
35, 36, 37	" 230
23	" 240
12, 22	" 250, 260
1, 2, 3, 5, 6	" 270
7, 8, 9	" 280
11	" 290
10	" 300, 310, 320

TABLE B37
GES OVERLAY NO. 2 IMAGE

CLASS	DESCRIPTION OF CLASS
1	ROANOKE LANDSAT IMAGE
2	LYNCHBURG LANDSAT IMAGE
3	RICHMOND LANDSAT IMAGE
4	NORFOLK LANDSAT IMAGE
5	FRONT ROYAL LANDSAT IMAGE
6	WASHINGTON LANDSAT IMAGE
7	SALISBURY LANDSAT IMAGE
8	ALTOONA LANDSAT IMAGE
9	HARRISBURG LANDSAT IMAGE
10	WILLIAMSPORT LANDSAT IMAGE
11	SCRANTON LANDSAT IMAGE
12	CORTLAND LANDSAT IMAGE

TABLE B38
GES OVERLAY NO. 3 COASTAL

CLASS	DESCRIPTION OF CLASS
69	LAND SEGMENT CLASS 1
42	LAND SEGMENT CLASS 5
65	LAND SEGMENT CLASS 6
19	LAND SEGMENT CLASS 8
17	LAND SEGMENT CLASS 9
68	LAND SEGMENT CLASS 11
47	ANACOSTIA
10	APPOMATTOX
64	BALTIMORE HARBOR
71	BOHEMIA
48	CHESTER
14	CHICKAHOMINY
44	CHOPTANK
25	ELIZABETH
20	GREAT WICOMICO
62	GUNPOWDER
15	JAMES
24	NANSEMOND
46	NANTICOKE
91	OCCOQUAN
63	PATAPSCO
41	PATUXENT
28	POCOMOKE
21	POTOMAC
18	RAPPAHANNOCK
90	SEVERN
49	WICOMICO
43	WYE
16	YORK

TABLE B39
GES OVERLAY NO. 4 CONTROL

CLASS	DESCRIPTION OF CLASS
1	BLUEFIELD MAP: PT 7, 8, 144, 145
2	ROANOKE MAP: PT 1-6, 10-49
3	RICHMOND MAP: PT 50-119, 131, 132
4	NORFOLK MAP: PT 120-130
5	EASTVILLE MAP: PT 133-143
6	CHARLOTTESVILLE MAP: PT 150, 151, 326, 330, 332-351
7	WASHINGTON MAP: PT 152-169, 180-241, 250, 251
8	SALISBURY MAP: PT 278-281, 290-297
9	WILMINGTON MAP: PT 276, 277, 288, 289, 431, 440
10	BALTIMORE MAP: PT 242-249, 252-275, 283-287, 299-303, 398, 400, 402, 405-408, 433-439
11	CUMBERLAND MAP: PT 304-325, 327, 329, 331, 395, 404
12	NEWARK MAP: PT 419-421, 430 HARRISBURG MAP: PT 358-368, 378-388, 396, 397, 399, 401, 413-415, 417, 418, 422-429
13	PITTSBURGH MAP: PT 354, 357, 370-374, 377, 389-394, 403
14	SCRANTON MAP: PT 491-496, 507-514, 528-531
15	WILLIAMSPORT MAP: PT 410-412, 416, 482, 484, 489, 497-506, 515-527, 532, 533, 548, 549, 551, 555-561, 565, 566, 568-570
16	WARREN MAP: PT 353, 355, 356, 552-554, 562-564, 567
17	BINGHAMTON MAP: PT 445-459, 465-473, 477, 478, 490
18	ELMIRA MAP: PT 441-444, 460-464, 474, 476, 479-481, 483, 485-488, 540-547, 550

TABLE B40
GES OVERLAY NO. 5 STATE

CLASS	DESCRIPTION OF CLASS
1	VIRGINIA
2	MARYLAND
3	DELAWARE
4	WEST VIRGINIA
5	ARLINGTON COUNTY, VIRGINIA
6	ALEXANDRIA CITY, VIRGINIA
7	FAIRFAX COUNTY, VIRGINIA
8	PRINCE WILLIAM COUNTY, VIRGINIA
9	LOUDOUN COUNTY, VIRGINIA
10	PENNSYLVANIA
11	NEW YORK

TABLE B41
GES OVERLAY NO. 6 URBAN

CLASS	DESCRIPTION OF CLASS
1	SALISBURY MAP EASTVILLE MAP NORFOLK MAP
2	RICHMOND MAP
3	ROANOKE MAP
5	BLUEFIELD MAP
6	WASHINGTON MAP
8	CHARLOTTESVILLE MAP
9	WILMINGTON MAP BALTIMORE MAP
10	CUMBERLAND MAP
11	HARRISBURG MAP

GROUND TRUTH

This section contains lists of aerial photography (Table B42) and USGS orthophoto quads (Table B43) used as ground truth for the Landsat study of the Chesapeake Bay basin.

TABLE B42

GROUND TRUTH: CHESAPEAKE BAY BASIN
AERIAL PHOTOGRAPHY

7 1/2' QUAD	STATE	AGENCY	DATE	SCALE	FORMAT	TYPE	USGS* PROJECT/NASA PHOTO CODE	I.D. NO.	ROLL	FRAME
Jamesville	N.Y.	NASAAM	750507	1:130,000	9x9 Paper	Color I/R	5750020854031			4031
Ithaca	N.Y.	NASAAM	750507	1:129,000	9x9 Paper	Color I/R	5750020854001			4001
Meadow Grounds	Pa.	NASAAM	740425	1:126,000	9x9 Paper	Color I/R	5740017038115			8115
Hanover	Pa.	NASAJS	770421	1:118,972	9x9 Paper	Color I/R	6356000200054			0054
York	Pa.	NASAJS	760907	1:126,928	9x9 Paper	Color I/R	6356000100039			0039
Williamsport	Pa.	NASAAM	740516	1:128,000	9x9 Paper	Color I/R	5740017628808			8808
Williamsburg	Pa.	NASAAM	740425	1:128,000	9x9 Paper	Color I/R	5740017038125			8125
Carlisle	Pa.	NASAAM	740516	1:128,000	9x9 Paper	Color I/R	5740017628799			8799
Meadow Ground	Pa.	USGS	770501	1: 80,000	9x9 Paper	B/W	VEHR*		1	240
Entriaken	Pa.	USGS	770501	1: 80,000	9x9 Paper	B/W	VEHR*		1	256
Williamsburg	Pa.	USGS	770501	1: 80,000	9x9 Paper	B/W	VEHR*		1	232
Holtwood	Pa.	USGS	761012	1: 80,000	9x9 Paper	B/W	VDUM*		1	105
Northumberland	Pa.	USGS	761012	1: 78,000	9x9 Paper	B/W	VDUM*		7	111
Towanda	Pa.	USGS	761012	1: 78,000	9x9 Paper	B/W	VDUM*		7	10
Harveys Lake	Pa.	USGS	761012	1: 78,000	9x9 Paper	B/W	VDUM*		1	78
Mifflinville	Pa.	USGS	761012	1: 78,000	9x9 Paper	B/W	VDUM*		1	156
Harrisburg	Pa.	USGS	761012	1: 78,000	9x9 Paper	B/W	VDUM*		7	125
Scottsville	Va.	NASAAM	731101	1:128,000	9x9 Paper	Color I/R	5730015315794			5794
Buckner	Va.	NASAAM	750508	1:129,000	9x9 Paper	Color I/R	5750020914122			4122
Mount Landing	Va.	JASAJS	770412	1:128,000	9x9 Paper	Color I/R	6346000100073			0073
Chesterfield	Va.	NASAAM	750508	1:129,000	9x9 Paper	Color I/R	5750020914135			4135
Wareneck	Va.	NASAAM	750508	1:127,000	9x9 Paper	Color I/R	5750020914185			4185
Toms Brook	Va.	USGS	770415	1: 80,000	9x9 Paper	B/W	VEHO*		1	54
Mineral	Va.	USGS	770415	1: 80,000	9x9 Paper	B/W	VEHO*		4	158
Lakeside Village	Va.	USGS	760321	1: 76,000	9x9 Paper	B/W	VOLP*		11	14
Ivor	Va.	USGS	780429	1: 80,000	9x9 Paper	B/W	VENB*		2	98
Toano	Va.	USGS	780429	1: 80,000	9x9 Paper	B/W	VENE*		2	92
Williamsburg	Va.	USGS	780429	1: 80,000	9x9 Paper	B/W	VENB*		2	50
Irvington	Va.	USGS	780429	1: 80,000	9x9 Paper	B/W	VENB*		3	84
Gladstone	Va.	USGS	770325	1: 80,000	9x9 Paper	B/W	VDLP*		6	11
Stonewall	Va.	USGS	770325	1: 80,000	9x9 Paper	B/W	VDLP*		11	29
Buchanan	Va.	USGS	770324	1: 78,000	18x18 Paper	B/W	VDUX*		5	18
Arnold Valley	Va.	USGS	770324	1: 78,000	18x18 Paper	B/W	VDUX*		4	28
Daleville	Va.	USGS	770324	1: 78,000	18x18 Paper	B/W	VDUX*		5	98
Roanoke	Va.	USGS	770324	1: 78,000	18x18 Paper	B/W	VDUX*		5	100
Lexington	Va.	USGS	770324	1: 78,000	18x18 Paper	B/W	VDUX*		3	128
Maryland has	Md.	NASAAM	770428	1:122,000	9x9 TRANS	Color I/R	----		--	----
Total Coverage	Md.	NASAAM	770512	1:122,000	9x9 TRANS.	Color I/R	----		--	----

TABLE B43
GROUND TRUTH: CHESAPEAKE BAY BASIN
ORTHOPHOTO QUADS
SCALE = 1:24,000

MAP NAME	STATE	MAP NAME	STATE
Barton	NY.	Beach	Va.
Binghamton West	NY.	Bentonville	Va.
Cortland	NY.	Bon Air	Va.
Endicott	NY.	Bowers Hill	Va.
Guilford	NY.	Charlottesville, East	Va.
Holmesville	NY.	Charlottesville, West	Va.
New Berlin North	NY.	Harrisonburg	Va.
New Berlin South	NY.	Hopewell	Va.
Norwich	NY.	Lake Drumond	Va.
Oxford	NY.	Luray	Va.
Pitcher	NY.	McKenney	Va.
Seeley Creek	NY.	Midlothian	Va.
Sherburne	NY.	New Kent	Va.
Spafford	NY.	Newport News North	Va.
Waverly	NY.	Petersburg	Va.
Altoona	Pa.	Prince George	Va.
Beech Creek	Pa.	Strasburg	Va.
Berwick	Pa.	Walkers	Va.
Black Moshannon	Pa.	Warfield	Va.
Crooked Creek	Pa.	Waynesboro East	Va.
Harveys Lake	Pa.	Waynesboro West	Va.
Howard	Pa.		
Julian	Pa.		
Kingston	Pa.		
Knoxville	Pa.		
Lopez	Pa.		
Mifflinetown	Pa.		
Millersburg	Pa.		
Phillipsburg	Pa.		
Ransom	Pa.		
Schellsburg	Pa.		
State College	Pa.		
Tamaqua	Pa.		



Chesapeake Bay basin
model final report
EJDD CB 00351